

Magnetic Resonance Imaging of Brain Development in Fetal Alcohol Spectrum Disorders

by

Sarah Christine Treit

A thesis submitted in partial fulfillment of the requirements for the degree of

Doctor of Philosophy

Centre for Neuroscience
University of Alberta

© Sarah Christine Treit, 2015

Abstract

Prenatal alcohol exposure has detrimental consequences on brain development, resulting in a wide range of physical, cognitive and behaviour deficits termed fetal alcohol spectrum disorders (FASD). Advanced magnetic resonance imaging (MRI) methods have identified numerous abnormalities of brain structure in groups of individuals with FASD compared to groups of healthy typically developing controls, including volume reductions and abnormalities of cortical thickness and white matter microstructure. Although informative, many previous studies have included limited sample sizes or narrow age ranges, precluding investigation of age-related changes or sex-differences in neurological abnormalities in this population. Moreover, few studies have investigated abnormalities with more than one imaging method in the same sample, needed to determine the relative magnitude of observed impairments. This thesis aims to address these limitations by using advanced imaging methods (high resolution T1-weighted and diffusion tensor imaging) to examine white matter microstructure, cortical thickness and brain volumes in a large cross sectional and longitudinal follow up dataset of individuals diagnosed with FASD. Data presented here uncover novel information about the developmental trajectories of children and adolescents with FASD, demonstrating delayed development of both cortical thickness and white matter microstructure but expected changes in brain volume with age. Cross sectional analysis reveals robust reductions of brain volume, smaller but consistent reductions of cortical thickness and few differences in white matter microstructure between groups. Sex differences are identified in the control group, as expected given known sexual dimorphism of brain structure, but appear to be attenuated in the FASD group. Males with FASD are shown to have greater structural brain impairment than females, despite similar performance on cognitive tests. In addition, novel information on correlations between head circumference (a widely used

diagnostic measure of neurological impairment in this population) and brain volume are presented, and implications for diagnosis are discussed. Overall this thesis provides independent evidence of altered brain structure in individuals with FASD, and uncovers novel information about sex differences, developmental trajectories, and brain-behaviour relationships that will help advance the development of medical and behavioural interventions for this population.

Preface

All of the research conducted for this thesis is part of a larger collaborative effort that includes the contributions of various co-authors. Portions of Chapter 3 appear in a book chapter as Treit S & Beaulieu C “Can FASD be Imaged?” Institute of Health Economics Consensus on the Legal Issues of Fetal Alcohol Spectrum Disorders (accepted for publication with Springer Inc). I conducted the literature review and was the primary author. Chapter 4 of this thesis has been published as Treit S, Lebel C, Baugh L, Rasmussen C, Andrew G, Beaulieu C (2013) “Longitudinal MRI Reveals Altered Trajectory of Brain Development during Childhood and Adolescence in Fetal Alcohol Spectrum Disorders” *Journal of Neuroscience* 33(24):10098-10109. Data collection was conducted by Catherine Lebel at the first scan and then by myself at the longitudinal follow up. I conducted all image and statistical analysis, created all figures and wrote the manuscript with the feedback and guidance of my co-authors. Chapter 5 of this thesis has been published as Treit S, Zhou D, Lebel C, Rasmussen C, Andrew G, Beaulieu C “Longitudinal MRI Reveals Impaired Cortical Thinning in Children and Adolescents Prenatally Exposed to Alcohol” *Human Brain Mapping* 35(9):4892-4903. Catherine Lebel collected data at scan 1; I collected longitudinal follow up data. Dongming Zhou performed image analysis, and both him and I performed statistical analysis. I wrote the manuscript with the feedback and guidance of my co-authors. Chapter 6 has not been previously published, but is currently under review for publication as Treit S, Zhou D, Chudley AE, Andrew G, Rasmussen C, Nikkel S, Samdup D, Hanlon-Dearman A, Loock C, Beaulieu C “Relationships between Head Circumference, Brain Volume and Cognition in Children with Prenatal Alcohol Exposure”. Data for this chapter was collected by myself at the University of Alberta (under a project funded by the Canadian Institutes of Health Research) and by the NeuroDevNet Investigators at the

University of Alberta, University of British Columbia, University of Manitoba and Queens University (under a project funded by the Network for Centres of Excellence). Image analysis was performed by myself and Dongming Zhou. I performed all statistical analysis, created all figures and wrote the manuscript. Chapter 7 is an original contribution to this thesis and has not been published elsewhere. Data for Chapter 7 was collected by myself (~120/140 subjects) and Catherine Lebel (~20/140 subjects). Image analysis was performed by myself and Dongming Zhou. I conducted all statistical analysis, created all figures and wrote the chapter. Ethics approval for all research conducted for this thesis was provided by the Health Research Ethics Board at the University of Alberta.

Acknowledgments

Funding for this work was provided by the Canadian Institutes of Health Research (CIHR) and the Networks of Centres of Excellence (NCE). Thank you to CIHR, the Women and Children's Health Research Institute (WCHRI), Alberta Innovates Health Solutions (AIHS) and the University of Alberta for providing me with salary support. A very special thank you to all of the volunteers who participated in this research—none of this work would have been possible without the time and efforts of many dedicated individuals and families.

I have many people to acknowledge for providing essential advice, guidance and help throughout my graduate degree. I would like to extend a huge thanks to all of my colleagues and co-authors in Biomedical Engineering—Catherine Lebel, Min Liu, Corey Baron, John Chen, and Dongming Zhou to name a few. Your expertise and guidance have helped to make much of this work possible. Thank you to Gail Andrew for your clinical expertise and help with recruitment, Lauren Baugh for countless hours of cognitive testing, and all of the FASD Lab for sharing your knowledge and insight. Thank you to my supervisory committee, and especially my supervisors Carmen Rasmussen and Christian Beaulieu for all of the feedback, mentorship and opportunities you have provided me with along the way.

Finally, I am grateful for the love and support of my friends and family. Thanks for being there for me when this journey was challenging, and for celebrating with me when it was rewarding. I am especially grateful to my mom and dad for playing double-duty as parents and impromptu academic advisors—your interest, enthusiasm and unwavering belief in my ability have helped me to get where I am today.

Table of Contents

Introduction	1
1 The Healthy Human Brain.....	2
1.1 Overview of Brain Structure and Function.....	2
1.1.1 Gross Anatomy and Organization.....	2
1.1.2 Micro to Macroscopic Brain Structure.....	3
1.2 Brain Development.....	8
1.2.1 First Trimester.....	8
1.2.2 Second and Third Trimester.....	10
1.2.3 Birth through Adolescence and Adulthood.....	12
2 Magnetic Resonance Imaging (MRI)	16
2.1 MRI Background and Basics.....	16
2.2 3D MPRAGE.....	19
2.2.1 Acquisition.....	19
2.2.2 Analysis Methods.....	19
2.3 Diffusion Tensor Imaging.....	22
2.3.1 Background and Acquisition.....	22
2.3.2 DTI Analysis Methods.....	28
2.3.3 Interpretations of parameters and changes with age.....	31

3	Fetal Alcohol Spectrum Disorder	34
3.1	Introduction & Diagnosis	34
3.2	Mechanisms of Alcohol Teratogenicity	36
3.3	Autopsy and Qualitative Brain Imaging	38
3.4	Quantitative Structural Brain Imaging in FASD	40
3.4.1	Volumetric Analysis in FASD	40
3.4.2	Cortical Development in FASD	44
3.4.3	Diffusion Tensor Imaging of White Matter in FASD	46
3.5	Links between Brain Structure and Clinical/Demographic Variables.....	48
3.5.1	Sex Differences	48
3.5.2	Behaviour and Cognition	49
3.5.3	Facial Dysmorphology	49
3.5.4	Alcohol Exposure Patterns	50
3.6	Summary and Thesis Objectives	51
	Research	55
4	Longitudinal Changes in Brain Volume and White Matter Microstructure in FASD	55
4.1	Introduction	56
4.2	Materials and Methods	58
4.2.1	Subjects	58

4.2.2	Cognitive Testing & Demographics.....	60
4.2.3	Image Acquisition	61
4.2.4	Tractography	62
4.2.5	Volume Analysis.....	63
4.2.6	Statistical Analysis	63
4.3	Results	65
4.3.1	Cognitive Testing	65
4.3.2	Brain Volumes.....	68
4.3.3	Tractography	70
4.3.4	Brain-Behaviour Relationships	76
4.4	Discussion.....	77
5	Longitudinal Cortical Development in FASD	84
5.1	Introduction	85
5.2	Materials and Methods	87
5.2.1	Participants.....	87
5.2.2	Cognitive Testing and Demographics.....	88
5.2.3	Image Acquisition	88
5.2.4	Image Processing and Statistics	89
5.2.5	Sub-Sample Comparison.....	90
5.3	Results	90

5.3.1	Demographic and Cognitive Scores	90
5.3.2	Brain Volume and Cortical Thickness Trajectories	93
5.3.3	Sub-Sample Comparisons	100
5.3.4	Relationship between Cortical Thickness and Cognition	100
5.4	Discussion.....	100
6	Head Circumference as a Proxy for Brain Volume and Cognition in FASD.....	108
6.1	Introduction	109
6.2	Methods	110
6.2.1	Participants	110
6.2.2	Image Acquisition and Analysis	111
6.2.3	Cognitive Testing	111
6.2.4	Normalization of Cognitive scores, HC and Brain Volume.....	112
6.2.5	Group Differences, Change with Age, and Correlations between HC, Brain Volume and Cognition.....	112
6.3	Results	113
6.3.1	Group Differences and Changes with Age.....	113
6.3.2	HC Correlations.....	118
6.3.3	PAE Participants with HC under 3 rd Percentile	118
6.4	Discussion.....	121

7 Relationships between DTI tractography, volumes and cortical thickness in FASD

126

7.1	Introduction	127
7.2	Materials and Methods	129
7.2.1	Subjects:	129
7.2.2	Demographic and Cognitive Data	130
7.2.3	Image Acquisition	131
7.2.4	DTI Tractography.....	131
7.2.5	Cortical Thickness.....	132
7.2.6	Brain Volumes.....	132
7.2.7	Statistical Analysis	133
7.3	Results	136
7.3.1	Cognitive and Demographic Data	136
7.3.2	Age Effects on FA, MD, Brain Volumes and Cortical Thickness	139
7.3.3	Sex Effects on FA, MD, Brain Volumes and Cortical Thickness.....	141
7.3.4	Group Differences and FASD Group Z Score Calculation.....	142
7.3.5	Hemispheric Asymmetry of FASD Z Scores	142
7.3.6	FASD group Z Score Rankings.....	152
7.3.7	FASD Z Score Correlation Analysis.....	155
7.4	Discussion.....	158

Summary & Conclusions	165
References	171
Appendix A: Diagnostic Terms under the FASD Umbrella	194
Appendix B: Studies of DTI in FASD	195
Appendix C: Studies of Brain Volume in FASD	197
Appendix D: Studies of Cortical Thickness in FASD	201
Appendix E: Automated DTI Tractography Pipeline	202
Appendix F: Cognitive Testing ‘Bloopers’	203

List of Tables

Table 4.2: Cognitive testing in FASD group.....	67
Table 4.3: Effects of age, group, and age-by-group interactions for brain volumes.	70
Table 4.4: Fractional anisotropy (FA) and mean diffusivity (MD) group and age effects between scans.	72
Table 5.1: Participant characteristics, demographic information and cognitive scores	92
Table 5.2: AAL regions with significant age-by-group interactions of cortical thickness between controls and FASD.....	97
Table 6.1: Subject Characteristics and Cognitive Test Scores	114
Table 7.1: Participant Demographic and Clinical Information	137
Table 7.2: Cognitive Test Scores in FASD and Controls	138
Table 7.3: Effects of Age, Sex and Group on Fractional Anisotropy.....	144
Table 7.4: Effects of Age, Sex and Group on Mean Diffusivity.....	145
Table 7.5: Effects of Age, Sex and Group on Brain Volumes	146
Table 7.6: Effects of Age, Sex and Group on Cortical Thickness in Frontal Regions.....	147
Table 7.7: Effects of Age, Sex and Group on Cortical Thickness in Parietal Regions	148
Table 7.8 Effect of Age, Sex and Group on Cortical Thickness in Temporal Regions.....	149
Table 7.9: Effects of Age, Sex and Group on Cortical Thickness of Occipital Regions.....	150
Table 7.10: Effect of Age, Sex and Group on Cortical Thickness of Limbic Areas	151

List of Figures

Figure 1.1: Overview of brain structure.....	7
Figure 1.2: Primary and secondary vesicles.....	10
Figure 1.3: Examples of age-related changes in brain structure.....	14
Figure 2.1:T1-weighted, T2-weighted and FLAIR images.....	18
Figure 2.2: Cortical thickness and volume segmentation pipelines.....	21
Figure 2.1: Stejskal-Tanner pulse sequence.....	23
Figure 2.2: Diffusion tensor ellipsoid.....	25
Figure 2.3: FA, MD, colourmaps and diffusion ellipsoids.....	28
Figure 3.1: FAS facial features.....	35
Figure 3.3: FAS Autopsy.....	38
Figure 3.4: FAS MRI case study.....	39
Figure 3.5: Brain volume studies of FASD.....	42
Figure 3.6: Volume studies of FASD that control for total brain volume/ICV.....	43
Figure 3.7: Cortical thickness studies of FASD.....	45
Figure 3.8: DTI studies of FASD.....	47
Figure 4.1: Age and time between scans by diagnosis.....	59
Figure 4.2: Changes in brain volumes with age.....	69
Figure 4.3: FA changes with age.....	73
Figure 4.4: MD changes with age.....	74
Figure 4.5: DTI age-by-group interactions.....	75
Figure 4.6: DTI-cognition correlations.....	77
Figure 4.7: IFO changes by diagnosis.....	79
Figure 5.1: Total mean thickness by group.....	94
Figure 5.2: Individual subject maps.....	95
Figure 5.3: Thinning patterns across the cortex.....	98
Figure 5.4 Age-by-group interactions:.....	99
Figure 6.1: Raw head circumference, brain volume and IQ by group and sex.....	115
Figure 6.2: Standardized head circumference, brain volume and IQ by group.....	117
Figure 6.3: Head circumference-brain volume correlations.....	120
Figure 7.1: Flowchart outlining statistical analysis plan.....	135
Figure 7.2: Examples of correlations with age.....	140
Figure 7.3: Z scores in the FASD group.....	153
Figure 7.4: Rank ordered FASD group Z scores in male (A) and females (B).....	154
Figure 7.5: FASD group Z score correlation matrix.....	156
Figure 7.6: Examples of partial correlations controlling for age.....	157

List of Symbols & Abbreviations

$\lambda_{//}$: parallel diffusivity	27
ΔFA: change in FA between scans	65
ΔMD: change in MD between scans	56
Δvolume: change in volume between scans	65
2D: two dimensional	30
3D: three dimensional	30
ADC: apparent diffusion coefficient	24
ADHD: attention deficit hyperactivity disorder	38
ALIC: anterior limb of the internal capsule	6
ARND: alcohol related neurobehavioural disorder	52
b0: non diffusion weighted image	26
B₀: main magnetic field	16
bCC: body of the corpus callosum	6
BRIEF: Behavioural Rating Inventory of Executive Function	61
CNS: central nervous system	4
CREVT: Comprehensive Receptive & Expressive Vocabulary Test	61
CSF: cerebrospinal fluid	14
CST: cortico-spinal tract	6
D: diffusion coefficient	24
DTI: diffusion tensor imaging	26
FA: fractional anisotropy	27

FAS: fetal alcohol syndrome	38
FASD: fetal alcohol spectrum disorders	1
FOV: field of view	62
gCC: genu of the corpus callosum	6
H¹: hydrogen	16
IFO: inferior fronto-occipital fasciculus	6
ILF: inferior longitudinal fasciculus	6
IQ: intelligence quotient	37
M₀: magnetization along the Z axis	17
MD: mean diffusivity	27
MPRAGE: magnetization-prepared rapid acquisition gradient echo	19
MRI: Magnetic Resonance Imaging	2
pFAS: partial fetal alcohol syndrome	52
RF: radiofrequency pulse	16
ROI: region of interest	30
sCC: splenium of the corpus callosum	6
SD: standard deviation	39
SFO: superior fronto-occipital fasciculus	6
SLF: superior longitudinal fasciculus	6
T1: longitudinal relaxation time	17
T2: transverse relaxation time	17
TE: echo time	18
TI: inversion time	62

TR: repetition time	18
UF: uncinate fasciculus	6
VBA: voxel-based analysis	30
WMTB-C: Working Memory Test Battery for Children	61
WRIT: Wide Range Intelligence Test	62
WRMT-R: Woodcock Reading Mastery Test-Revised	61
λ_{\perp}: perpendicular diffusivity	27
γ: gryomagnetic ratio	16

Introduction

Brain maturation is an intricate and dynamic process, characterized by progressive and regressive changes that begin just weeks after conception and continue into adulthood. Prenatal brain development is widely influenced by genetic and environmental factors, as well as their interactions, making it a time of both remarkably plasticity and vulnerability. Perturbations to this process can influence brain structure and function, resulting in lasting effects on cognition and behaviour across the lifespan.

Fetal alcohol spectrum disorders (FASD) describe the myriad of deficits that can arise from prenatal alcohol exposure. Animal models have demonstrated that alcohol directly crosses the placental barrier, causing measurable neurotoxic effects in the developing fetus. However, these studies have also demonstrated that the neurological outcomes associated with alcohol exposure in utero are complex and variable, depending on many factors including amount, frequency and timing of exposure, nutrition, genetics and so on. This is reflected by the enormous phenotypic variability observed in humans who were prenatally exposed to alcohol. Although individuals with FASD experience physical, cognitive, behavioural and emotional deficits, a brain imaging ‘biomarker’ for FASD remains elusive.

The aim of this thesis is to characterize brain structure and postnatal developmental trajectories in children, adolescents and adults with prenatal alcohol exposure. To this end, an introduction to healthy brain structure and development (Chapter 1), magnetic resonance imaging (MRI; Chapter 2), and fetal alcohol spectrum disorders (Chapter 3) are provided as background. In Chapters 4 and 5, I examine longitudinal changes in white matter and cortical grey matter in a cohort of children and adolescents with FASD who were scanned twice each

several years apart, revealing previously uncharacterized aspects of postnatal brain development in this population. The use of head circumference as a proxy for brain volume in FASD is examined in Chapter 6, providing commentary on the validity of this widely used diagnostic tool. Chapter 7 examines three imaging modalities (volumes, diffusion tensor imaging, and cortical thickness) in the same large cross-sectional cohort of individuals with FASD in order to determine the relative severity of deficits identified with each method and the relationships between them. Importantly, these data also identify sex differences in the degree of structural impairment in FASD. Following these research chapters, a brief discussion of the impact of these findings on our understanding of FASD is provided, along with a discussion of future directions in this field.

1 The Healthy Human Brain

1.1 Overview of Brain Structure and Function

1.1.1 Gross Anatomy and Organization

In its simplest division, the brain is composed of 3 major structures: the cerebellum, the brainstem (midbrain, pons, medulla) and the cerebrum. The cerebrum is in turn composed of the two cerebral hemispheres (containing the cerebral cortex, caudate, putamen, nucleus accumbens, globus pallidus, hippocampus, amygdala and the white matter pathways connecting them), and the diencephalon (thalamus, and hypothalamus). Each cerebral hemisphere is anatomically subdivided by major sulci into 4 bilateral lobes (Figure 1.1A), and connected via the corpus callosum. In addition to their anatomical division, the frontal, parietal, temporal, and occipital lobes bear numerous functional distinctions. Among other key areas, the occipital lobes contain the primary visual and visual association cortices; the temporal lobes contain primary auditory

cortex, Wernicke's area, and limbic structures associated with emotional processing and memory; the parietal lobes contain primary somatosensory cortex and numerous areas associated with language comprehension and spatial perception; and the frontal lobes contain primary motor, pre-motor and supplementary motor areas, Broca's area and the prefrontal cortex, which itself can be further subdivided into numerous areas associated with higher order cognitive processes and executive functioning. The brain is massively interconnected by white matter pathways, which link areas within and between the hemispheres, as well as with brain stem and deep grey matter nuclei, allowing for complex information processing through many organizational levels. Although some basic functions (e.g. visual processing) seem to be highly localized, complex behaviours and processes (e.g. emotional regulation, decision making, etc.) likely require integrated input from numerous areas, complicating the establishment of localized brain-behaviour relationships for higher order tasks.

1.1.2 Micro to Macroscopic Brain Structure

Neurons and glia comprise the two major cell types in the human brain, which contains an estimated 85 billion neurons, and several times more glia (Herculano-Houzel, 2009). Neurons have been classically regarded as the functional units of the brain (responsible for synaptic transmission), while glial cells primarily function as metabolic and mechanical support, but are gaining recognition for their role in cellular communication (Haydon, 2001; Perea and Araque, 2005; Theodosis et al., 2008). Unlike glia, neurons are post-mitotic cells that are almost exclusively produced before birth (with the exception of a few select brain regions), while glia can multiply throughout the lifespan (e.g. in response to injury). Glial sub-types are responsible for a wide range of essential processes including myelination (oligodendrocytes), formation of the blood-brain-barrier, extracellular ion buffering and metabolism (astrocytes), immunology

(microglia), production of cerebrospinal fluid (ependymal cells) as well as many key processes in development (radial glial cells).

A typical neuron is composed of a cell body (soma), dendrites (which form various configurations of branches off of the cell body and receive information from other neurons via synapses), a myelinated axon, and a number of axon terminals (synaptic boutons) which in turn synapse with the dendrites or cell bodies of other neurons (Figure 1.1B). However, numerous neuronal sub-types exist (pyramidal, granule, Purkinje, etc.), each with a characteristic structure. Neurons can be unipolar, bipolar, or multipolar, with axons that vary greatly in length, ranging from the short distances covered by cortical interneurons to the very long distances covered by projection neurons that originate in the cortex and synapse in the spinal cord.

The axon itself is comprised of an axonal plasma membrane (axolemma), actin microfilaments, microtubules, neurofilaments, micro-tubule associated proteins (which form cross bridges between neurofilaments and microtubules), and axonal cytoplasm (Figure 1.1B,F). Neurofilaments provide structure and are the primary determinants of axon diameter, whereas microtubules provide structure but are also responsible for protein transport within the axon. The dynamic state of microtubules and actin microfilaments allow the mature neuron to retract old processes and extend new ones.

The majority of axons in the central nervous system (CNS) are myelinated to increase conduction velocities of synaptic transmission (Figure 1.1B,F). Myelin is a membranous lipid-rich structure produced by oligodendrocytes in the CNS. The internodes of each axon are wrapped up to 160 times (Hildebrand et al., 1993), forming either compact or non-compact myelin which can be distinguished by the presence (or absence) of cytoplasm between the layers of the myelin membrane. In compact myelin the layers of the myelin membrane fuse together

and the cytoplasm between them is extruded. In both compact and non-compact myelin, lipid bilayers are also interleaved with extracellular water: both the cytoplasmic and extracellular water constitute “myelin water” that makes up 40% of the total weight of myelin, and is exploited with methods such as myelin water fraction imaging (Laule et al., 2007).

At a macroscopic level, myelinated axons and cell bodies are spatially and visually segregated in the brain, forming the basis for classifying brain tissue into “white” and “grey” matter (Figure 1.1C,E). Grey matter refers to areas primarily composed of cell bodies, dendrites, and glia, whereas white matter refers to areas primarily composed of myelinated axons (responsible for its white appearance appearance) as well as astrocytes, oligodendrocytes and microglia. Grey matter is found surrounding the outer surface of the brain (referred to as cortical grey matter), as well as in collections of cell bodies or ‘nuclei’ that are both anatomically and functionally distinct from their surrounding tissues (e.g. nuclei of the basal ganglia). The grey matter cortex is comprised of 6 horizontal layers (running parallel to the surface), each with a distinct neuronal cell type that can be distinguished with microscopy (Figure 1.1D). The cortex is also functionally organized into ‘cortical columns’, which run through the layers and perpendicular to the surface, with vertical interconnections between neurons. Unfortunately, this level of detail is not possible to discern with MRI, so we instead focus on visible divisions of the cortical mantle, typically subdivided according to Brodmann’s areas, gyral name, or functional area. Likewise, deep grey matter structures in the brain can be readily discerned with MRI, but high-field acquisition (beyond the methods applied in this thesis) is required to differentiate sub-nuclei, such as the hippocampal subfields or nuclei of the thalamus.

White matter is found throughout the brain and beneath the cortical surface (Figure 1.1C,E). White matter tracts (aka bundles, pathways, fasciculi) are frequently named by the

structures they connect (e.g. the fronto-occipital fasciculus, connecting aspects of the frontal and occipital lobes). Major white matter tracts can be grouped into i) projection fibres, projecting inferior-superior and vice versa, ii) commissural fibres, connecting structures in the right and left hemispheres, and iii) association fibres, connecting areas within the same hemisphere. Twelve major white matter tracts will be discussed in this thesis, including 2 projection tracts: the anterior limb of the internal capsule (ALIC) and corticospinal tracts (CST); 3 commissural tracts: the genu, body and splenium of the corpus callosum (gCC; bCC; sCC); and 5 association tracts: the cingulum (cing), inferior and superior longitudinal fasciculus (ILF; SLF), inferior and superior fronto-occipital fasciculus (IFO; SFO), and uncinata fasciculus (UF). With the exception of the corpus callosum, all of these tracts are bilateral.

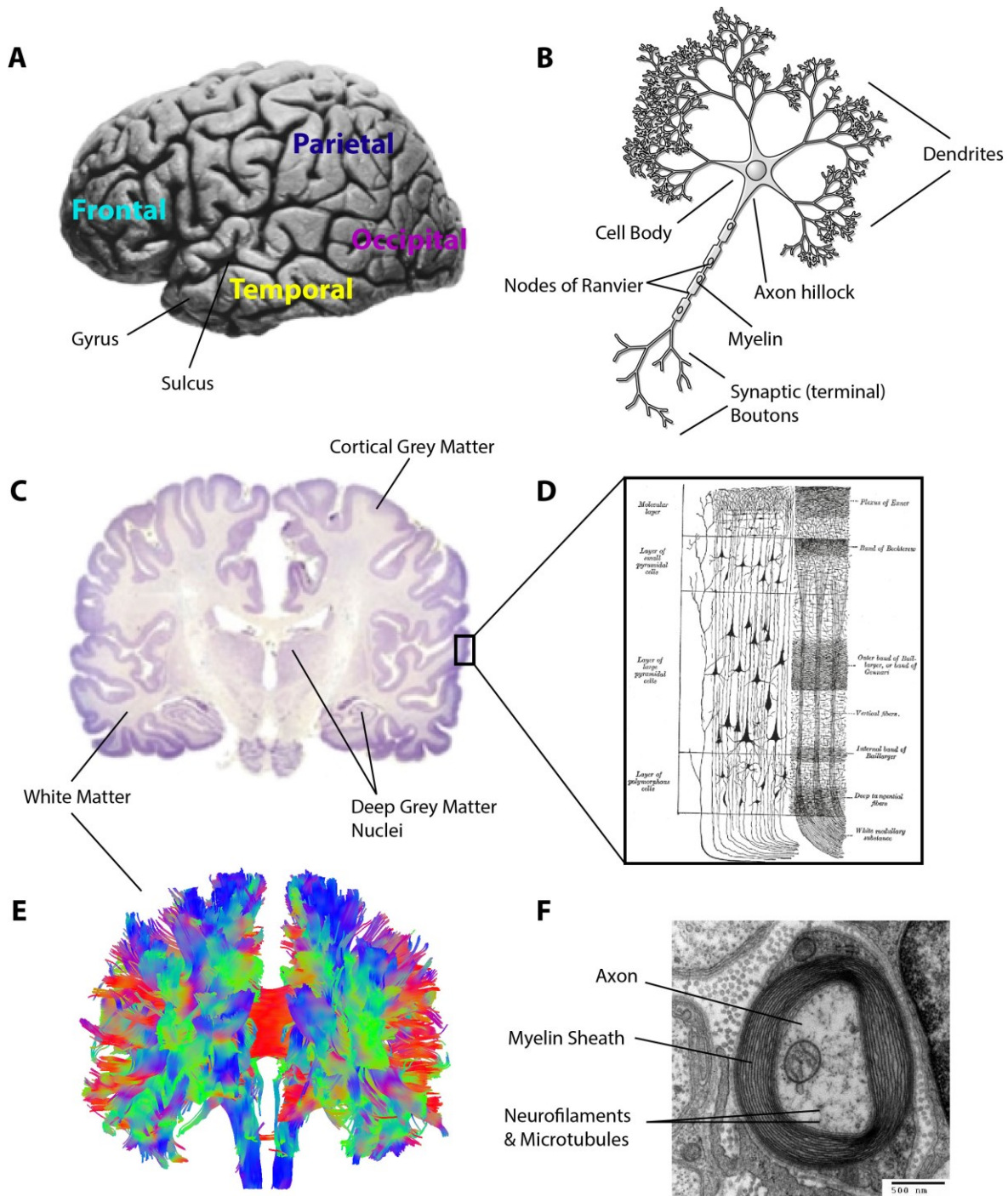


Figure 1.1: Overview of brain structure. Modified from WikimediaCommons (A,B,C,F; public domain) and Gray's Anatomy 20th edition (D; public domain) showing (A) a lateral view of the cerebral hemisphere, labelled by lobe; (B) a typical neuron; (C) histological section of the human brain (coronal view) showing grey and white matter (stained in purple and white, respectively); (D) an illustration of the laminar 6-layer structure of the cortex; (E) diffusion tensor imaging tractography of whole brain white matter in a 27 year old healthy female; (F) scanning electron microscopy of an axon (cross-section) showing several key structural components including myelin, microtubules, neurofilaments and mitochondria.

1.2 Brain Development

Just thirteen days after conception, the nervous system begins its journey of differentiation and development-- an amazingly complex and protracted process that continues well into adulthood. Although an in-depth review of fetal brain development is beyond the scope of this thesis (for further reading, see Stiles, 2008), an overview of major events is helpful for understanding the eventual structure and organization of the brain. Furthermore, identifying the potential for cumulative effects to arise from perturbations to any of these processes will help provide an appreciation for the enormous phenotypic variability that can stem from prenatal alcohol exposure.

1.2.1 First Trimester

During the 3rd week of development, neural progenitor (stem) cells differentiate from the epiblast through a process called gastrulation, and begin to align along the midline of the embryo in a zone known as the neural plate of the ectoderm. This alignment unfolds according to a complex and time-sensitive series of signalling mechanisms, such that the progenitor cells aligned closest to the rostral end are primed to differentiate into forebrain structures, and those closest to the caudal end are primed to become aspects of the hindbrain and spinal cord (a process called primitive patterning).

During the 4th week, two ridges emerge along the length of the neural plate, rise up and fold inward to form the neural tube. Closing of the neural tube begins in the centre, proceeding outward to the rostral and caudal ends. Errors in neural tube closure produce distinct 'neural tube defects' including spina bifida (failed closure of the caudal end) or anencephaly (failed closure of the rostral end) (Detrait et al., 2005). Upon completion of neural tube closure, the neural progenitor cells form a single layer lining the inside of the hollow centre of neural tube (which

eventually becomes the ventricular system of the brain) referred to as the ventricular zone. Three ‘bulges’ appear at the rostral end of the embryo, known as the primary vesicles: the prosencephalon (forebrain), mesencephalon (midbrain) and rhombencephalon (hindbrain) (Figure 1.2A).

Meanwhile, neural progenitor cells undergo symmetric mitotic division from weeks 3-6, greatly increasing the pool of progenitor cells available for neuron production. Beginning on day 42 (week 5), this mitotic division of neural progenitors shifts from symmetrical to asymmetrical: each division now produces one neural progenitor cell, and one neuron (Wodarz and Huttner, 2003). This process continues at unfathomable rates, producing over 150 *billion* neurons by just 12 weeks post-conception (Bayer et al., 1993). During this time, precise concentration gradients of signalling molecules induce progenitor cells to produce neurons for specific cortical areas, in a process known as embryonic patterning. Experimental manipulation of these concentration gradients can change the relative size and organization of downstream cortical areas (Bishop et al., 2000). Recall that this elaborate system of embryonic patterning is applied to cells that arose from precursor cells which themselves underwent primitive patterning to align along the midline of the neural crest, thus requiring cumulative processes for correct neural organization.

Toward the end of the embryonic period (week 7-8), the prosencephalon and rhombencephalon further divide to form 5 secondary vesicles (telencephalon, diencephalon, mesencephalon, metencephalon and myelencephalon), providing a basis for the eventual organization of brain structure that is evident at birth (Figure 1.2B). It is also relevant to note that in addition to forming the forebrain, cells in the caudal aspects of the prosencephalon go on to produce the eyes and midline facial features; thus injury during the patterning of these cells can produce both midline brain and facial abnormalities (Sulik et al., 1988).

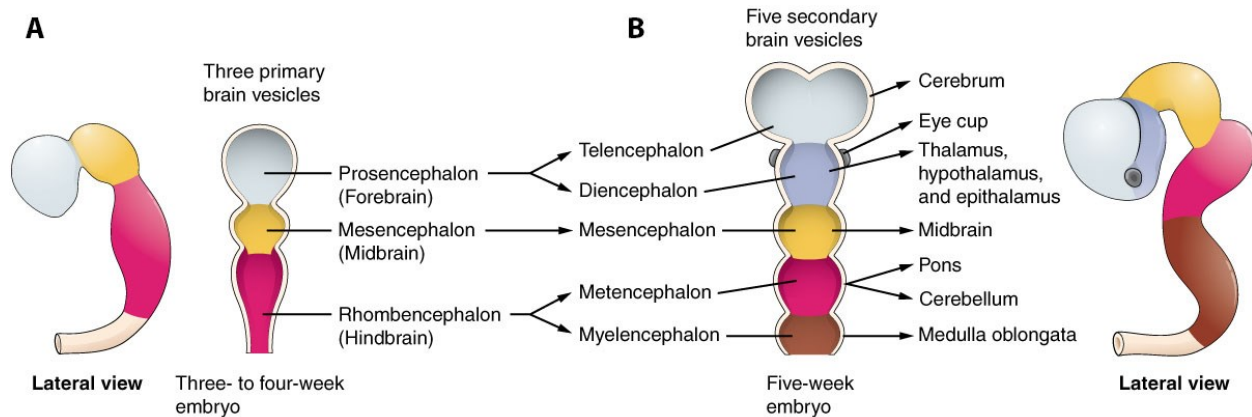


Figure 1.2: Primary and secondary vesicles. Adapted from WikimediaCommons (public domain), illustrating the emerging primary (A) and secondary vesicles (B), and their eventual structures. Complex patterning of both neural progenitor cells and neurons prior to migration and differentiation is required in order to correctly produce the characteristic structure of the brain.

As neurons are produced from week 6-12, they begin to migrate to their final locations and differentiate into their final neuronal cell type (e.g. pyramidal cells, interneurons etc.)—a process that continues until birth. The size of the telencephalon grows rapidly, folding over the diencephalon, and the embryonic nervous system begins to resemble the gross morphometry of the adult brain. Just before the end of the 1st trimester the longitudinal fissure begins to form, dividing the telencephalon into two hemispheres.

1.2.2 Second and Third Trimester

Although neuron production is now complete, migration and differentiation continue through the second and third trimesters. Neurons produced in the ventricular zone (located now in the centre of the brain), migrate radially to the neocortex, generally following an ‘inside-out’ sequence, such that the earliest migrating neurons form the deepest layers of the cortex and later migrating neurons sequentially form the more superior layers (with the exception of the transient pre-plate, not present in adult cortex). Upon reaching its final destination, each neuron then

begins to grow axonal and dendritic processes to form synaptic connections with neighboring cells. Each sprouting axon forms a growth cone, which extends from the cell body, sampling the local environment and guiding the elongating axon to its target by following signalling molecules released from target neurons. Precise signalling of these axons is needed to correctly form the major white matter pathways of the brain. Once they have reached their target, each axon synapses with their target neurons, starting a massive wave of ensuing synaptogenesis that dramatically increases the number of connections in the brain by several orders of magnitude, continuing into the second decade of life. Myelination of these axons then begins at week 16, and is at least partially promoted by axonal electrical activity established from these synaptic connections (Wake et al., 2011).

In addition to the many progressive cellular and morphological events, it is important to consider several major regressive events that occur during this time. The first is apoptosis (programmed cell death) which occurs in massive populations of neurons during prenatal development, resulting in the striking loss of ~50% of neurons in the brain (Gordon, 1995). Prenatal apoptosis is partly regulated by competition for neurotrophic factors produced by neuronal targets, the basis for one possible mechanism by which the most efficient connections increase their likelihood of survival. The second regressive event is axonal loss. Migrating axons must receive signalling molecules from their target cells and compete for growth factors in order to successfully form synaptic connections. Axons that do not reach the correct target are retracted by the cell body and eliminated by macrophages (Innocenti et al., 1983). Likewise, up to 50% of oligodendrocytes die during development, which is thought to follow axonal loss as a result of lost communication from axons needed to survive (McTigue and Tripathi, 2008). These regressive changes are thought to be a planned/normal method of refining neural networks, but

some aspects (e.g. cell death) have also been proposed as mechanisms to correct errors in neuronal production or migration (Buss and Oppenheim, 2004).

Stemming from these massive cellular changes, numerous visible morphological changes also occur in the 2nd and 3rd trimesters, including dramatic increases in overall size (doubling in 3rd trimester), gyrification of the cortical surface (Figure 1.3A), and emergence of major white matter tracts. Primary sulci (central sulcus, sylvian fissure, etc) form during weeks 13-26, followed by secondary sulci from week 30-35, and tertiary sulci from week 36 to after birth. Major white matter tracts begin to take form in weeks 8-12, including the anterior commissure, the optic chiasm, and the internal capsule, followed by the corpus callosum from weeks 12-16. Myelination begins at week 16 and proceeds in a caudal-rostral pattern starting in the spinal cord, continuing well past birth.

1.2.3 Birth through Adolescence and Adulthood

Postnatal development is marked by substantial morphological, cellular and neurochemical change. The total size of the brain increases rapidly in the first few years of life, reaching a 95% of its maximal size by about age 6 (Giedd et al., 1999). However, the proportion of grey and white matter volumes and their microstructural properties continue to mature into adulthood. Unlike neurogenesis, proliferation of glial cells continues well after birth, and for some glial sub-types, persists across the lifespan. Likewise, glial apoptosis follows a protracted post-natal time course. These shifted neural versus glial trajectories may in part allow for drastic changes in neuronal function (e.g. through myelination) to continue throughout development, despite the fact that neuronal production is largely complete.

Myelination proceeds rapidly for the first 2 years of life, continuing at slower rates into adulthood (Yakovlev and Lecours, 1967). In addition to myelin, oligodendrocytes have been

shown to produce trophic factors that influence axon diameter and integrity and maintain neuronal survival throughout childhood (McTigue and Tripathi, 2008). As a result of these processes, the total volume of white matter increases rapidly during childhood (Figure 1.3B), slowing and reaching a peak in adulthood (Giedd et al., 1999; Lebel and Beaulieu, 2011). Likewise, microstructural changes in white matter (as measured through diffusion tensor imaging) occur most rapidly during childhood, slowing and then peaking at various times throughout early to mid-adulthood varying by tract (Lebel and Beaulieu, 2011; Lebel et al., 2012a; Figure 1.3C).

Synaptogenesis continues rapidly throughout the post-natal period, resulting in widespread over-production of connections throughout the brain. In most brain areas, the density of these synaptic connections peaks in mid childhood at roughly double the number observed in the adult brain, and then slowly declines through a process of synaptic pruning from around 7-16 years (Huttenlocher, 1979; Huttenlocher et al., 1982; Innocenti and Price, 2005). Both competition for trophic factors and electrical activity are thought to modulate the stability of these connections. These cellular changes likely underlie decreasing grey matter volume, density, and thickness observed from childhood to adolescence on MRI (Gogtay et al., 2004; Zhou et al., 2015; Figure 1.3D). In addition, cortical changes in gyrification and asymmetry (White et al., 2010; Zhou et al., 2013) are observed during this time period, reflecting refinement of surface morphology.

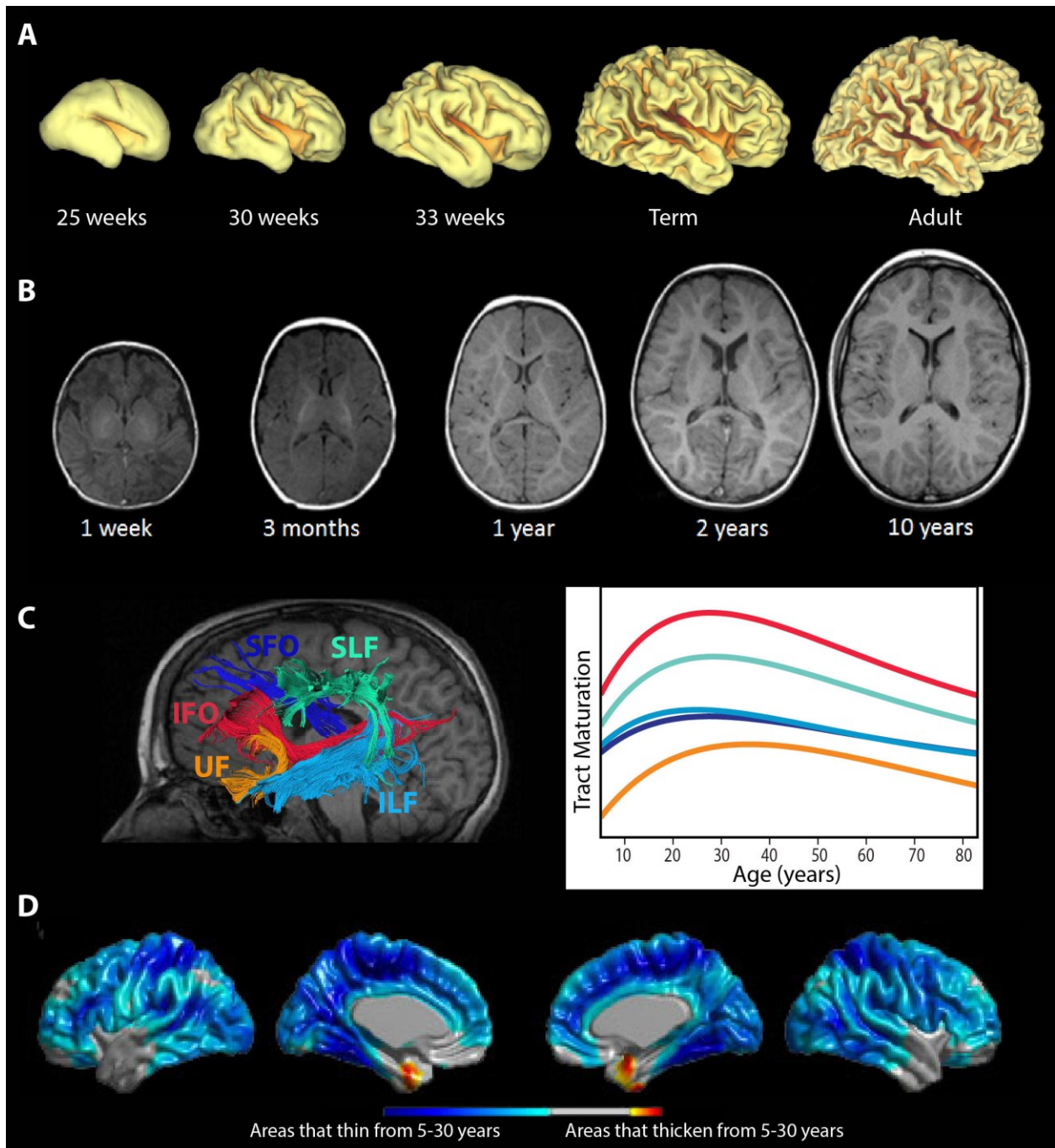


Figure 1.3: Examples of age-related changes in brain structure. Adapted from WikiCommons (A;B, Public Domain) and original figures (C;D) created (with permission) using data from Lebel et al 2012 Neuroimage, and Zhou et al Neuroimage 2015. A) shows increasing complexity of cortical gyrfication from week 25 in utero to adulthood B) MRI showing visible increases in white matter in the first 10 years of life, C) showing the trajectory of microstructural changes in white matter that peak in the 20s-30s, varying by tract, and D) areas of the cortex shown to thin from 5-30 years of age.

In addition to pruning in the cortex, loss of neuronal density and massive changes in neurochemistry has been observed in the striatum during adolescence in rhesus monkeys (Martin and Cork, 2014). In humans, volume changes are observed in deep grey matter structures during development, including volume loss in the caudate and putamen, and concomitant increases in hippocampus and amygdala volume during adolescence (Toga et al., 2006). These volume changes appear to be at least somewhat influenced by puberty, and may be associated with androgen receptor density in each respective structure (Goddings et al., 2014).

Structural changes are accompanied by neurochemical changes in both childhood and adolescence. Animal models have suggested that neurotransmitter systems are overproduced and undergo receptor pruning during development (Kilb, 2012; Lidow et al., 1991), particularly for excitatory neurotransmitters, resulting in less excitatory stimulation of the cortex. Less is known about neurotransmitter system development in humans, though changes in receptor density have been observed from childhood to adulthood in histology studies (Montague et al., 1999). Hormonal changes associated with puberty are also thought to influence the progression of brain development (Sisk and Zehr, 2005), which may in part underlie the acceleration of some development changes observed during adolescence (e.g. Zhou et al., 2015).

In addition to unique time courses, many of these processes follow spatially dependent developmental patterns. For example, cortical thinning and myelination are observed to generally follow an posterior to anterior and medial to lateral pattern (Toga et al., 2006). Although the overall pattern and timing of these processes is relatively prescribed, they are also thought to be largely experience-dependent processes. Moreover, deviations in these processes are commonly observed in children with developmental disabilities and neuropsychiatric disorders (Marsh et al., 2008; Rice and Barone, 2000).

2 Magnetic Resonance Imaging (MRI)

2.1 MRI Background and Basics

MRI takes advantage of the nuclear properties of hydrogen (^1H), found in water molecules abundant in all tissues in the body. Hydrogen nuclei have intrinsic angular momentum (spin), and can be thought of as randomly oriented spinning magnetic dipoles that collectively have a vector sum of zero. When placed in an external magnetic field (such as the B_0 field of an MRI scanner), these hydrogen dipoles begin to align with the long axis of the MRI in either a parallel or anti-parallel orientation with respect to B_0 , precessing at the Larmor frequency (Equation 2.1), which is proportionate to the strength of the magnetic field and gyromagnetic ratio (γ) of the nuclei (for H^1 42.58 MHz T^{-1}). At equilibrium, slightly more protons exist in the parallel (lower energy state) than anti-parallel (higher energy state) alignment, creating a net magnetic moment along the axis of B_0 (a.k.a longitudinal magnetization along the Z axis). If a radiofrequency (RF) excitation pulse at the Larmor frequency (ω_0) of the precessing protons is then applied perpendicular to B_0 , the magnetization vector will be tipped by the B_1 field.

$$\text{Equation 2.1} \quad \omega_0 = \gamma B_0 \text{ (Larmor Equation)}$$

This is achieved by a transfer of energy from the RF pulse to the protons which causes i) some spins to change to the higher energy (spin-down) state, thus weakening the longitudinal magnetization vector, and ii) all of the spins to align and precess in phase, which causes the perpendicular portion of each vector to sum instead of cancel, thus ‘tipping’ the magnetization vector into the transverse plane.

Once the RF pulse is turned off, the magnetization vector returns to M_0 through a process called ‘relaxation’, following two distinct time courses. Longitudinal, or T1 relaxation describes the elongation of the longitudinal magnetization vector as protons begin to return to the lower

energy equilibrium state, re-emitting energy into their surroundings (spin-lattice). Transverse or T2 relaxation describes the reduction of the transverse magnetization vector as the spins lose phase coherence due to magnetic field inhomogeneities and the influence of neighbouring nuclei (spin-spin interactions). Thus, T1 and T2 relaxation occur simultaneously, but through independent mechanisms. Longitudinal magnetization increases with time after the RF pulse is turned off, and the time it takes for the longitudinal magnetization vector to return to 67% of its original value is termed the longitudinal relaxation time T1. Transverse magnetization decreases with time after the RF pulse is turned off, and the time it takes the transverse magnetization vector to reach 37% of its original (maximum) value is termed T2 relaxation time. The rotating transverse magnetic moment induces an electric current in an antenna (i.e. RF coil). The signal produced is called the Free Induction Decay, which reduces as the transverse magnetic vector dephases.

Given that T1 and T2 depend on molecular interactions and the presence of macromolecules, both differ by tissue composition, forming the basis for tissue contrast (e.g. between grey and white matter). Relaxation times also change in pathological tissue, which makes tumours, strokes and other drastic changes in tissue composition visible on MRI. CSF has the longest T1 and T2 times in the brain, followed by grey matter. White matter has the shortest T1 and T2 times because it is lipid rich, iron-rich (in oligodendrocytes) and has less free water.

By varying the magnetic field (through the use of gradient coils), the ‘flip’ angle of the RF pulse, the time between successive RF pulses (repetition time; TR), and the time between the RF pulse and subsequent measurement of signal (echo time; TE), it is possible to produce a variety of MR image contrasts (Figure 2.1). The signal produced can be ‘weighted’ by the T1, T2, diffusion, or proton density properties of the tissue being imaged, though the signal will

almost always be at least somewhat influenced by all of these factors. For example, shorter TRs allow some tissues to regain T1 fully while others regain it only partly (e.g. brain versus CSF)—changing the signal intensity of tissues relative to each other, allowing us to visually distinguish them. A pulse sequence that induces differences in signal intensity between tissues (tissue contrast) primarily from their relative differences in T1 is called a T1-weighted image (e.g. 2.1A). A longer TE allows for more differentiation in T2 curves (and thus greater T2 contrast) but the longer the TE the more total signal is lost. An image with contrast that is produced based on differences in T2 between tissues is called a T2-weighted image (Figure 2.1B). Fluid attenuated inversion recovery (FLAIR; Figure 2.1C) sequences suppress signal from CSF, and are particularly useful for identifying periventricular lesions. These three sequences are commonly used in both clinical practice and research, though other contrasts (such as diffusion weighting) can also be produced.

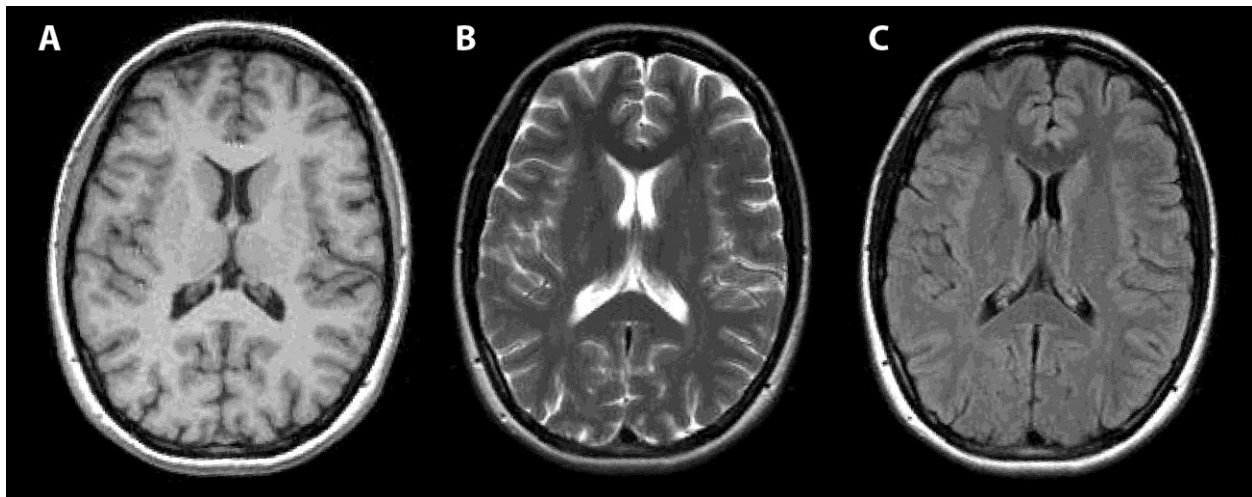


Figure 2.1: T1-weighted, T2-weighted and FLAIR images. Example of T1-weighted (A), T2-weighted (B) and fluid-attenuated inversion-recovery (FLAIR; C) images of the same 27 year old female control.

2.2 3D MPRAGE

2.2.1 Acquisition

3D Magnetization-Prepared Rapid Gradient Echo (MPRAGE) uses an initial 180° inversion RF pulse (inverting the magnetization vector into the $-Z$ plane), followed by a gradient echo sequence to produce T1 weighted images (e.g. Figure 2.1A). This sequence is chosen for its ability to produce high signal, high resolution ($1 \times 1 \times 1 \text{mm}^3$) images with good contrast between grey matter, white matter and CSF in a relatively short amount of time (~ 4 minutes for a whole brain acquisition here).

2.2.2 Analysis Methods

T1-weighted MPRAGE sequences produce high-resolution images with excellent grey matter-white matter contrast, well suited for quantitative analysis methods. Many types of quantitative analysis can be achieved from the same set of images, including voxel based-morphometry, volume, cortical thickness, surface area and gyrification index, texture analysis, shape analysis etc. Volume and cortical thickness analysis will be discussed here.

In essence, volume analysis is carried out by assigning each voxel in the brain a neuroanatomical label (e.g. white matter, hippocampus, CSF, etc), and then summing the voxels of each label type to produce a 3D volume for a given structure. This can be done manually (by delineating the borders of the structure on successive 2D slices and calculating the volume) or through various automated segmentation pipelines such as FreeSurfer-- the method used in this thesis. In short, FreeSurfer assigns each voxel in the brain an anatomical label based on probabilistic information from an atlas of 39 manually-traced subjects, and a set of algorithmic 'rules' about global position, local positioning (i.e. the amygdala is always anterior to the

hippocampus), and the signal intensity of each voxel (Fischl et al., 2002). With this information, an anatomically labelled map is produced (Figure 2.2) and the volume of each structure is computed, allowing statistical comparison of specific volumes across large numbers of subjects.

Cortical thickness relies on surface-based (rather than voxel-based) segmentation to calculate the distance between the pial cortical border and the grey matter white matter border, across thousands of points along the cortical surface. This can be achieved with several automated pipelines, including FreeSurfer (Fischl and Dale, 2000) and CIVET (Kim et al., 2005). CIVET was used to process cortical thickness data in this thesis, to be briefly described here. First, native space images are normalized to the ICBM-152 template, and classified into grey matter, white matter and CSF. The grey matter-white matter boundary is then extracted, and a triangular mesh of this surface is created and smoothed based on T1 intensity gradients. This surface is then expanded to the grey matter-extra cortical CSF border to extract the pial surface. Cortical thickness is measured by calculating the distance (in mm) between corresponding vertices on each surfaces at 40,962 vertices per hemisphere in native space, and then interpolated onto the ICBM-152 surface template for visualization and parcellation into lobes or automated anatomical labelling (AAL) regions (Tzourio-Mazoyer et al., 2002) (Figure 2.2).

Both volume segmentation and cortical thickness pipelines are fully automated, which provides the advantage of saving time (manual segmentation of brain volumes can take weeks per subject) and importantly is user-independent and highly reproducible. However, neither method is totally error-free, so accuracy of segmentation must be ensured by visually inspecting data outputs prior to statistical analysis.

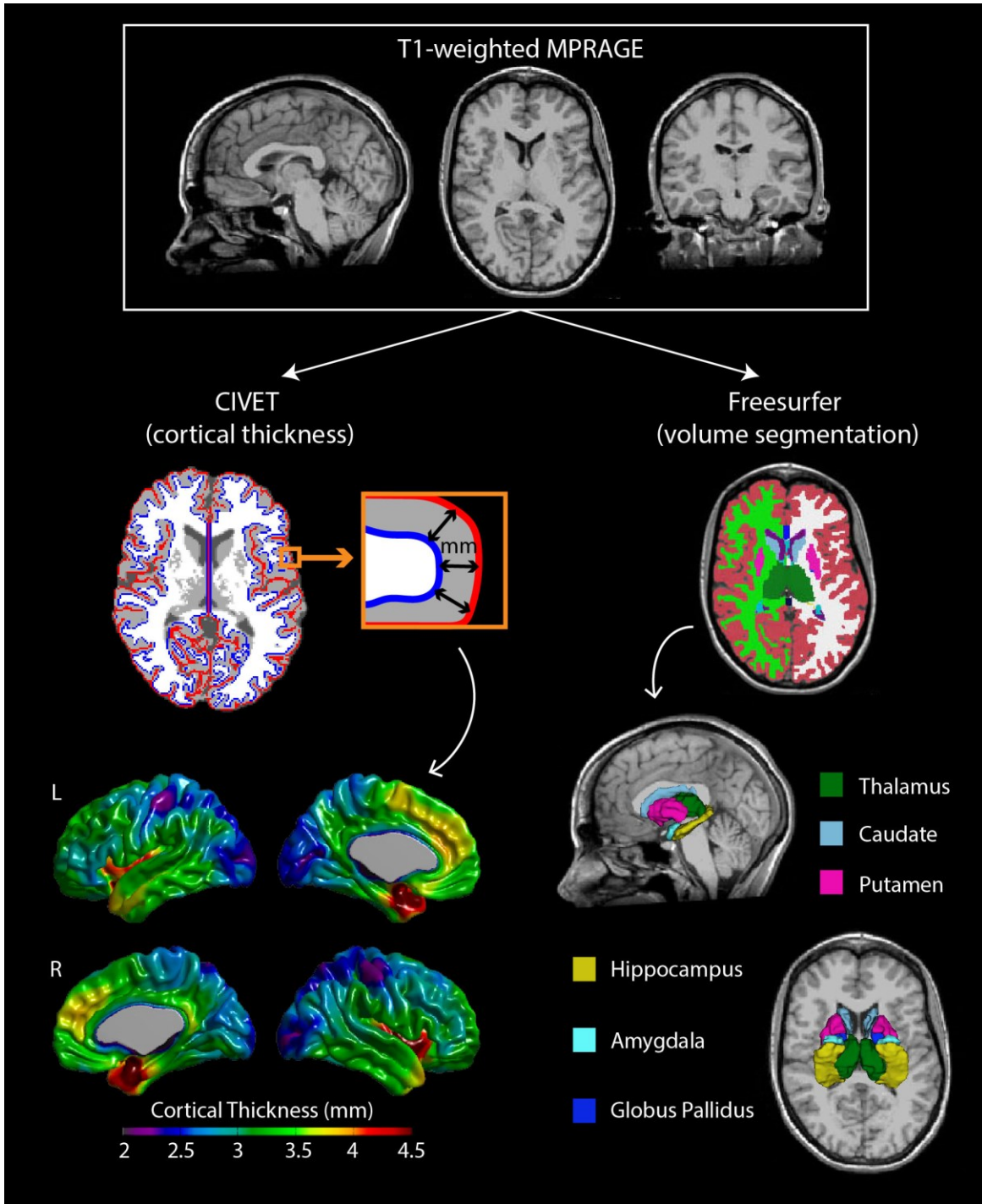


Figure 2.2: Cortical thickness and volume segmentation pipelines. Schematic of cortical thickness and volume segmentation for a 34 year old female control. CIVET extracts the white-matter grey matter surface (blue) and the pial cortical surface (red), and calculates the distance between them along $\sim 80,000$ points on the cortical mantle. These values are then projected onto the surface template to produce a cortical thickness map (bottom left). Freesurfer assigns neuroanatomical labels to each voxel in the brain, allowing for 3D reconstruction and volume calculation, e.g. of deep grey matter structures (bottom right).

2.3 Diffusion Tensor Imaging

2.3.1 Background and Acquisition

Diffusion describes the constant random motion of molecules in fluid, first observed by Robert Brown (Brown, 1828) and later described by Albert Einstein (Einstein, 1905). In a medium with no concentration gradient, a diffusing molecule will travel a distance of:

Equation 2.2: $\langle r \rangle = \sqrt{2Dt}$

in one dimension, where D is the diffusion coefficient of the substance and the measurement is made in time t . Diffusion tensor imaging takes advantage of the Brownian motion of water molecules in the brain to infer information about tissue microstructure at a level of detail that is not possible with conventional methods (Basser et al., 1994). Due to the inherently random nature of diffusion, water molecules have an equal probability of diffusing in any direction in an unrestricted space (e.g. CSF): this pattern is termed isotropic diffusion. However, in an environment with geometric barriers, diffusion becomes directional, or anisotropic. This becomes most apparent in white matter, where water molecules are able to travel relatively unhindered along the length of the axon, but perpendicular motion is restricted by membranes, myelin, and other cellular components. Thus, by measuring properties of diffusion in the brain we are able to infer information about the environment in which diffusion is occurring.

When a magnetic field gradient is applied in an MR experiment, spins in different spatial locations experience different magnetic field strengths, and thus precess at a different frequency according to the Larmour equation. Diffusion that occurs in the direction of an applied gradient therefore causes signal loss, given that spins move out of the local field they started in and thus start to resonate at different frequencies, producing different MR signals. By measuring this

signal loss in multiple orientations, we can infer information about the underlying spatial pattern of diffusion during the measurement time. This was first achieved with the pulsed spin echo sequence (Stejskal and Tanner, 1965), which uses two equal diffusion-sensitizing gradients on either side of a 180° refocusing pulse (Figure 2.1).

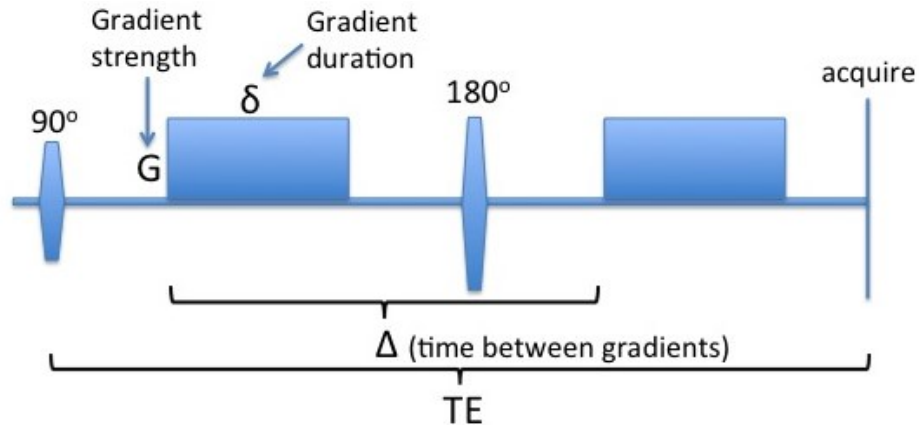


Figure 2.1: Stejskal-Tanner pulse sequence. This pulse sequence achieves diffusion weighting by pairing symmetric gradients on either side of a 180° refocusing pulse (imaging gradients not shown).

In a spin-echo sequence, a refocussing pulse is typically applied with the intention of reversing signal loss from dephasing of spins (T_2 decay); however, this only reverses the phase of the spins but does not change their frequency. Spins that do not move in the direction of the gradients will experience the same environment between the two gradients, and will be completely refocused by the 180° pulse and the 2nd gradient. However, spins that move in the direction of the gradient will experience different local magnetic fields and will not be refocused, resulting in signal loss from both diffusion and T_2 decay. Given that T_2 decay stays the same with and without diffusion encoding if TE is kept constant, signal loss from diffusion in the

direction of the applied gradients can be quantified according to equation 2.3, simplified to equation 2.4:

$$\text{Equation 2.3: } \frac{S}{S_0} = e^{-\gamma^2 G^2 \delta^2 \left(\Delta - \frac{\delta}{3}\right) ADC}$$

$$\text{Equation 2.4 } \frac{S}{S_0} = e^{-bADC}$$

According to this equation, the higher the apparent diffusion coefficient (ADC) of the tissue or the b-value of the acquisition (i.e. the sensitivity of a diffusion encoding gradient), the more signal loss. Increasing the b-value (e.g. by increasing G, δ , or Δ , thus increasing the gradient strength or diffusion time) makes the measurement sensitive to even smaller diffusion distances. However, the scanner limits G, and increasing δ or Δ must be balanced by signal loss from increased T2 relaxation.

Diffusion weighted imaging in this thesis is acquired with single-shot echo-planar imaging (SS-EPI). This method acquires all of k -space in a single-shot (compared to acquiring a small fraction of k -space with each excitation), allowing for very rapid acquisition of multiple volumes of diffusion weighted images (i.e. in multiple directions and at multiple b-values per slice-- discussed below) within a reasonable total scan time (~6 minutes). Although this approach mitigates effects of bulk motion induced phase changes between shots and makes the total acquisition time very fast, the duration of k -space readout is actually longer than for multi-shot methods, making SS-EPI more sensitive to artifacts from distortions, signal dropout, blurring etc. than other methods. As such, corrections for some of these artifacts are often applied in post-processing.

An MRI scanner has gradients in the X, Y, and Z axes, so by combining these gradients we can acquire diffusion weighted images along any orientation. Two images must be acquired

to calculate ADC: one that is diffusion weighted (usually $b=1000 \text{ s/mm}^2$), and one that is non-diffusion weighted ($b=0 \text{ s/mm}^2$; b_0). ADC measurements of tissues are directionally dependent—i.e. ADC measured with a gradient oriented parallel to a nerve fibre will be much higher than if measured with a gradient oriented perpendicular to it. Purposefully orienting the gradients parallel and perpendicular to the structure in question is achievable ex-vivo, but in order to model unknown tissue orientations (as is the case with living brain) we require a more complex model, such as the diffusion tensor.

The diffusion tensor models 3D diffusion as an ellipsoid, which is mathematically represented by a symmetric 3x3 matrix with 6 unique elements. Thus, diffusion tensor imaging (DTI) acquisition requires diffusion encoding along a minimum of 6 non-collinear directions, in addition to at least one non-diffusion weighted ($b=0 \text{ s/mm}^2$) image.

$$D = \begin{bmatrix} D_{xx} & D_{xy} & D_{xz} \\ D_{yx} & D_{yy} & D_{yz} \\ D_{zx} & D_{zy} & D_{zz} \end{bmatrix}$$

Once these are acquired the tensor can be diagonalized to calculate the 3 eigenvalues ($\lambda_1, \lambda_2, \lambda_3$), representing diffusivity along the major axes of the diffusion ellipsoid.

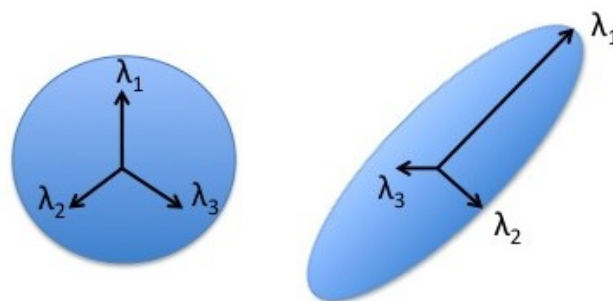


Figure 2.2: Diffusion tensor ellipsoid Diffusion tensor ellipsoids for isotropic diffusion (left and anisotropic diffusion (right). In the elongated ellipse it is clear that λ_1 is much greater than λ_2 or λ_3 .

The relative magnitudes of each eigenvalue can provide useful quantitative information about the shape of the tensor, which can be used to infer information about the underlying microstructure. Several metrics are typically described from a DTI measurement: mean diffusivity (MD), fractional anisotropy (FA), parallel (λ_{\parallel}) and perpendicular (λ_{\perp}) diffusivity. Mean diffusivity describes the average magnitude diffusion, irrespective of direction and is described by the mean of the three eigenvalues.

$$\text{Equation 2.5} \quad MD = \frac{\lambda_1 + \lambda_2 + \lambda_3}{3}$$

Conversely, fractional anisotropy is a normalized measure of the variance between the eigenvalues, and describes the degree of anisotropy. FA ranges from 0-1 and is rotationally invariant.

$$\text{Equation 2.6} \quad FA = \frac{\sqrt{3}}{2} \sqrt{\frac{(\lambda_1 - MD)^2 + (\lambda_2 - MD)^2 + (\lambda_3 - MD)^2}{\lambda_1^2 + \lambda_2^2 + \lambda_3^2}}$$

Parallel diffusivity (λ_{\parallel}) is simply the first eigenvalue, describing diffusion along the long axis of the ellipse, whereas perpendicular (λ_{\perp}) diffusivity is equal the mean of the 2nd and 3rd eigenvalues, and thus describes diffusion perpendicular to the long axis of the ellipse.

$$\text{Equation 2.7} \quad \lambda_{\parallel} = \lambda_1$$

$$\text{Equation 2.8} \quad \lambda_{\perp} = \frac{\lambda_2 + \lambda_3}{2}$$

The tensor is solved for every voxel in the brain, allowing the construction of anatomical ‘maps’ of each of these parameters (Figure 2.3A,B). In addition to eigenvalues, the eigenvectors of the tensor ellipsoid, which represent the orientation of the principle axes of the diffusion ellipsoid

$(\epsilon_1, \epsilon_2, \epsilon_3)$, can provide valuable information about fibre orientation that become crucial for tractography analysis. The primary eigenvector is the eigenvector associated with the largest eigenvalue, and is combined with measures of anisotropy to produce DTI colourmaps in which directional information is represented by colour (typically red for left-right, blue for inferior-superior, and green for anterior-posterior), and anisotropy is represented by intensity (Figure 2.3C). Diffusion ellipsoids can also be represented at each voxel (Figure 2.3D), and tractography can be performed from these maps (Figure 2.3E) to be discussed further below.

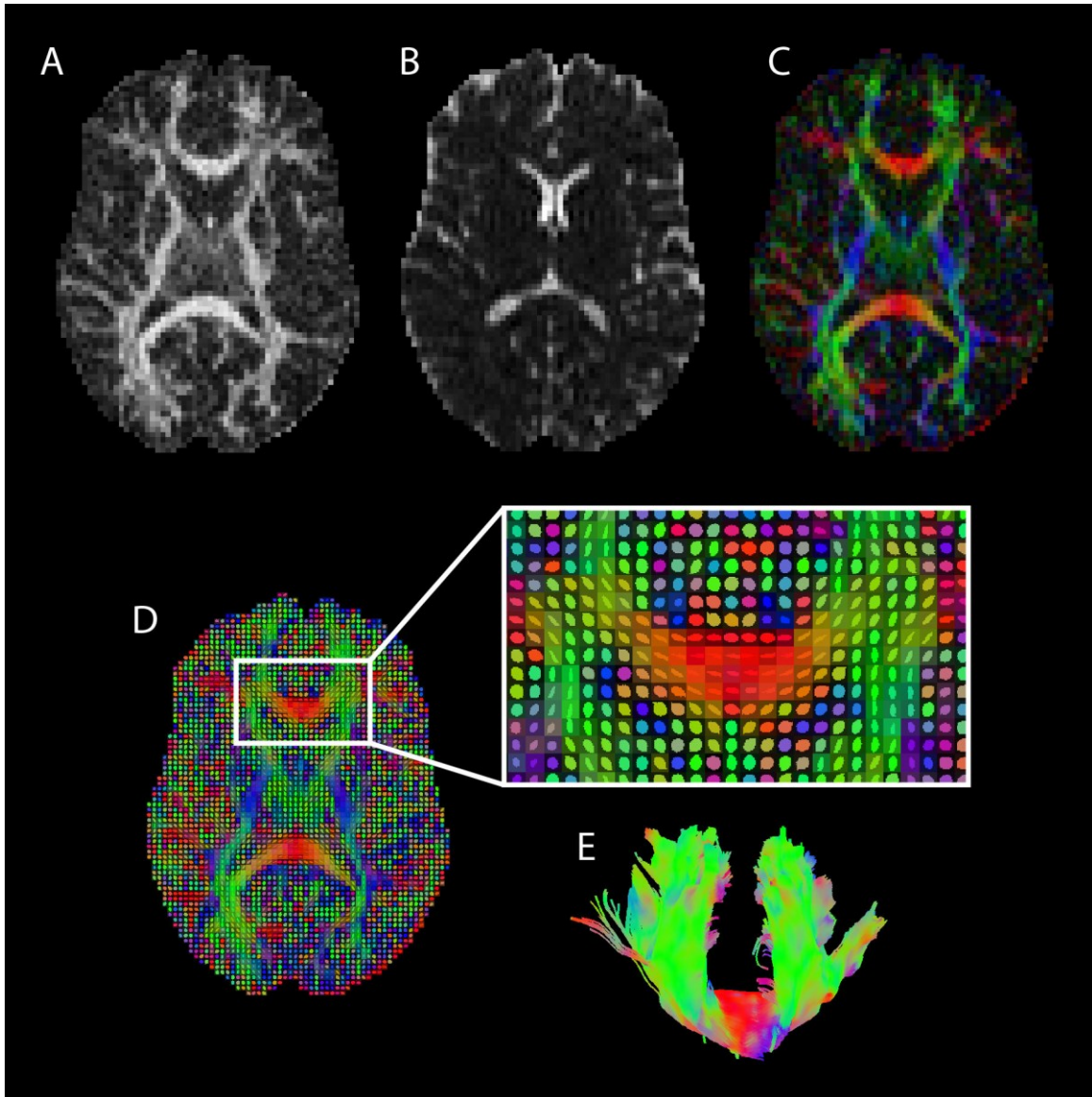


Figure 2.3: FA, MD, colourmaps and diffusion ellipsoids An FA map (A), MD map (B) and Colourmap (C) are shown for the same adult female. (D) shows the diffusion ellipsoids for an axial slice; zoomed in portion shows a uniform directional pattern of ellipoids and a strong left-right orientation organization in the corpus callosum. (E) tractography reconstruction of this same area of the anterior corpus callosum.

2.3.2 DTI Analysis Methods

There are numerous ways to analyze DTI data, each with advantages and pitfalls. For the sake of brevity, only 3 basic approaches will be described here, but numerous other methods are available.

First, scalar maps (FA, MD etc.) can be analyzed using region-of-interest (ROI) analysis, whereby the user simply defines an area of interest and then takes the average of a given parameter (e.g. of FA) across all of the voxels in that 2D area, comparing the values across groups of subjects. Although straight-forward, precise, and intuitive, this approach can be both time consuming and highly user-dependent. ROI placement requires a-priori knowledge of the location of interest (excluding discovery of differences in other areas), and is not immune to anatomical and acquisition related variability (e.g. orientation of the slice) between subjects. Moreover, it only queries a small portion of the actual structure (e.g. the midline of the corpus callosum) and leaves out valuable information about the much larger 3D tract. Nonetheless, with a well-trained user this approach can be highly reproducible, ensuring comparison of the same structure or even number of voxels between subjects.

Voxel-based analysis (VBA) can overcome some of these limitations of ROI analysis by systematically comparing all of the white matter voxels in the brain between groups of subjects, without requiring any a-priori hypothesis about areas of interest. In addition to group differences, voxel-based approaches can be used to establish correlations with other variables, such as age or clinical/cognitive measures. However, the main challenge of this approach is accurate normalization of the images into template-space, required to ensure that the voxels being compared are indeed in the same anatomical location across subjects. In addition, although this approach is in some ways very user independent, there are a large number of analysis parameters (e.g. size of smoothing kernel) and statistical considerations (e.g. minimum number of contiguous voxels) with no clear consensus in the literature, which can substantially change results, making comparisons across studies challenging.

Lastly, 3D reconstruction of white matter tracts can be achieved through the use of tractography algorithms. In short, a region of interest ('seed') is drawn around an area of white matter, and an algorithm is applied to follow the primary diffusion vector voxel-to-voxel according to a prescribed set of rules, producing streamline representations of the connections between various brain areas. For example, one could draw a 'seed' and a 'target' (aka 'and') ROI, requiring that the streamlines produced must pass through both regions, as well as a 'not' ROI, ensuring that streamlines do not pass through that region to increase the likelihood of delineating the tract of interest while eliminating spurious connections. The algorithm applies several rules, including an FA threshold (typically set to ~ 0.2) to prevent propagation through grey matter areas, and an angle threshold (set specifically for each tract) to prevent unlikely turns. Once a tract is reconstructed, measures of FA, MD, parallel and perpendicular diffusivity can be produced for the whole tract. This approach has the advantage of analyzing the entire structure in question, can be performed in native space without normalization of the images, and is typically more accommodating of anatomical variability between subjects. However, tractography algorithms can run into challenges in areas of crossing fibres, diverging fibres or 'kissing' fibres, where the primary diffusion direction can be difficult to determine, thus leading the streamline in a spurious direction or stopping tractography due to low anisotropy. Moreover, tractography follows the overall assumption that fibre orientation is in alignment with the orientation of maximal diffusion, which is impossible to confirm in-vivo. These limitations are influenced not only by the tracking algorithm, but also acquisition parameters—e.g. larger voxels are more likely to contain multiple fibre orientations. In addition, averaging all of the voxels in a tract can mask regional differences or abnormalities that are concentrated into discrete anatomical locations. Numerous advances have helped to overcome these limitations, including

more sophisticated tractography algorithms, and along-the-tract analysis. Finally, placement of each ROI presents yet another limitation, and must be carefully chosen to accurately and reproducibly delineate the white matter tract in question. Although there are a number of atlases available to guide ROI placement (Catani and Thiebaut de Schotten, 2008; Nowinski et al., 2012; Oishi et al., 2008; Wakana et al., 2004) some groups of tracts remain challenging to differentiate from each other (e.g. the corticospinal and corticobulbar tracts), while there also remains controversy in the literature about the geometry and spread of some tracts and even the existence of others (Forkel et al., 2014; Schmahmann and Pandya, 2007). Nonetheless, deterministic tractography remains a robust approach for studying white matter abnormalities, particularly in large well-defined white matter tracts such as the ones described in this thesis.

2.3.3 Interpretations of parameters and changes with age

Although diffusion parameters are commonly thought of as measures of myelin, it is important to keep in mind that numerous cellular components contribute to anisotropy. Indeed, experimental models have demonstrated anisotropy in naturally unmyelinated axons (Beaulieu and Allen, 1994) as well as in axons prior to myelination (e.g. in-utero; Kasprian et al., 2008), confirming that other aspects of the axonal structure must contribute to anisotropy. Experiments in giant squid axons and garfish nerves demonstrated that microtubules and neurofilaments make only a minor contribution to diffusion anisotropy, but that axonal membranes impose significant barriers to diffusion (Beaulieu and Allen, 1994). Thus, in addition to myelin, the density of axonal packing and coherence of axon orientation are all important contributors to anisotropy.

As such, FA changes markedly from grey (ranging from around 0.2-0.4) to white matter, and varies widely between tracts (~0.45-0.85); whereas MD is fairly stable across brain tissues beyond the neonatal period, with similar values in grey and white matter but higher values in

CSF. The differences in FA values between tracts can be attributed to differences in myelination (proportion of myelinated fibres and thickness of myelin), axon diameter, packing, cohesion of orientation, etc, but not to any one factor as these tend to covary together throughout the brain. For example, monkey studies indicate that posterior regions of the corpus callosum have the widest diameter axons and greater proportion of myelinated axons in contrast to anterior portions (Lamantia and Rakic, 1990), confirming that multiple factors vary regionally even within a single tract. As a result, it is essential to compare the same tract/area between groups of subjects of similar ages (or within groups over time), in which case differences or changes in FA and MD can provide valuable insight into underlying microstructure.

When studying patient groups, it is common to observe reduced FA and elevated MD relative to controls. However, there are also numerous situations in which change in FA or MD is observed in isolation-- for example, acute stroke showing a ~40% drop in MD with no change in FA as a result of similar reductions of all 3 eigenvalues (λ_1 , λ_2 and λ_3), or Wallerian degeneration, where decreases in parallel diffusivity are offset by increases of perpendicular diffusivity, yielding reduced FA with no change of MD (Beaulieu et al., 1996). As such, the biological factors driving change in FA and MD are best appreciated by investigation of the eigenvalues of the diffusion tensor. Animal models indicate that perpendicular diffusivity is sensitive to changes in myelination, whereas parallel diffusivity is sensitive to axonal degradation (Song et al., 2003; Song et al., 2002), further suggesting that these diffusion metrics provide unique and useful additions to interpreting changes in FA and MD.

Although the expectation is that reduced FA/ parallel diffusivity and elevated MD/ perpendicular diffusivity reflect “abnormal” tissues, counter-intuitive changes are sometimes observed, and can be difficult to interpret. There are many such examples in the literature,

including increased FA of the SLF associated with worse visuospatial performance in Williams Syndrome (Hoeft et al., 2007), and reduced perpendicular diffusivity of corpus callosum associated with worse phonological skill in healthy children, which the authors suggest may reflect fewer but larger axons in skill readers or differences in membrane permeability (Dougherty et al., 2007).

In addition to changes with injury or disease, diffusion parameters also change in a characteristic pattern with age, providing a non-invasive measures of development that are central to this thesis. Diffusion MRI has been used to characterize white matter development as early as 28-30 weeks gestation in pre-term infants (Huppi et al., 1998) all the way across the lifespan to 85 years of age (Lebel et al., 2012a). This work has revealed a general pattern of decreasing MD and increasing FA, thought to reflect decreasing tissue water content and increasing complexity of white matter structure with age (including the onset of myelination). These changes are observed to continue well into the 2nd and even 3rd decades of life, varying regionally throughout the brain (Lebel et al., 2008b), after which an inversion is observed, and FA decreases while MD increases with age, presumably reflecting subtle degenerative processes in the brain. Importantly, FA and MD follow distinct trajectories in healthy development, reaching maxima/minima at different ages even within the same tract (Lebel and Beaulieu, 2011; Lebel et al., 2008b).

3 Fetal Alcohol Spectrum Disorder¹

3.1 Introduction & Diagnosis

Fetal Alcohol Spectrum Disorder (FASD) describes a range of physical, behavioural, emotional and cognitive deficits stemming from pre-natal alcohol exposure. FASD has a startling estimated prevalence of ~1 in 100 live births in Canada each year, and represents a leading cause of preventable intellectual disability (Health Canada, 2006; Chudley et al., 2005; Canadian Pediatric Society, 2002). A large body of research has demonstrated that individuals with FASD experience impairments in many domains of cognition, including general intellectual ability, attention and processing speed, language, numerical processing and mathematical skill, as well as learning and memory (Kodituwakku, 2007). Executive functioning (defined as goal oriented skills including planning, set shifting, inhibition, and working memory) is also impaired, in addition to behavioural impairments such as impulsivity and difficulties with adaptive behaviour and emotional regulation (Kodituwakku, 2007). Beyond impairments in cognition and behaviour, individuals with FASD often experience a myriad of adverse outcomes, such as delinquency, substance abuse, disrupted school experience, and psychopathology (Streissguth et al., 2004). Many of these issues may in part stem from primary deficits (i.e. learning disabilities) but it is likely that they are also influenced by other environmental and biological factors which may include altered postnatal brain development.

Fetal alcohol syndrome (FAS), first described in the 1970s (Jones and Smith, 1973), is characterized by growth restriction, the presence of cardinal facial abnormalities (short palpebral fissures, smooth philtrum and thin upper lip, Figure 3.1) and evidence of CNS damage (Astley and Clarren, 2000). Animal models have demonstrated that facial dysmorphology results from

¹ Portions of this chapter have been published. Treit & Beaulieu. Can FASD be Imaged? In: IHE Consensus on the Legal Issues of FASD. Under review with Springer Inc.

alcohol exposure during a critical period during the first trimester (Sulik et al., 1981), and as such it is possible for heavily exposed individuals to lack facial features, and for less severely affected children to display facial features. Subtypes of FASD that present in the absence of physical features or facial dysmorphology are estimated to occur up to 8 times more often than cases of full FAS (Astley, 2006) and are characterized by similar cognitive impairments and adverse outcomes (Mattson et al., 1998), further highlighting the need for neurological investigation of the full spectrum of affected individuals.

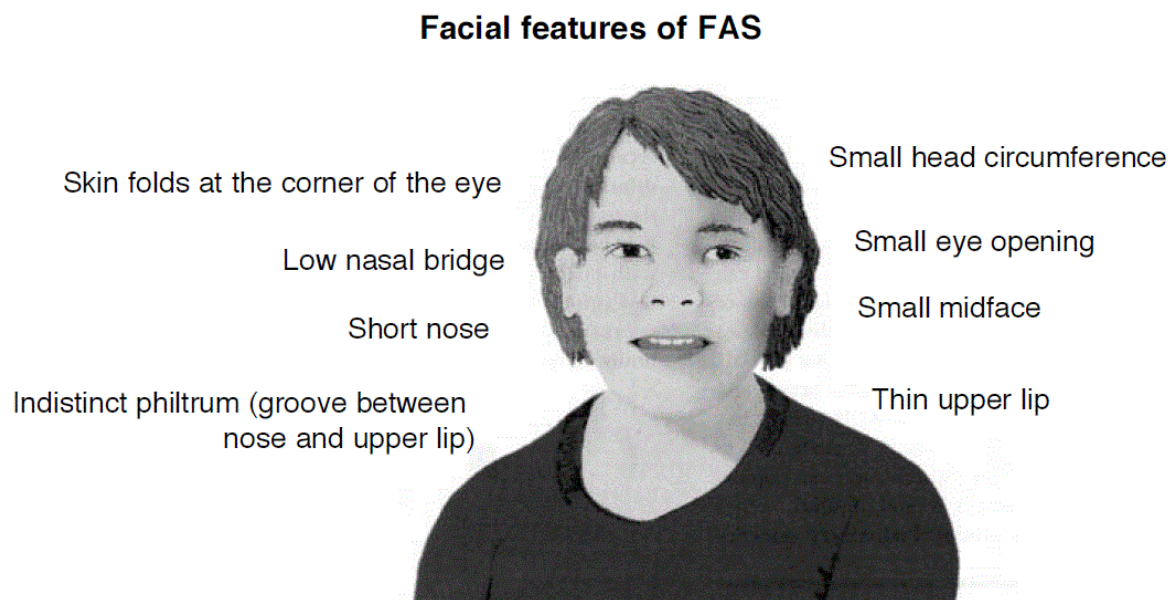


Figure 3.1: FAS facial features. Illustration adapted from NIH/National Institute on Alcohol Abuse and Alcoholism [Public domain], via Wikimedia Commons, showing the cardinal facial features associated with fetal alcohol syndrome.

The Glenrose FASD Diagnostic Clinic (the primary recruitment source of participants with FASD in this thesis) requires physician referral and confirmation of alcohol exposure (through birth records, child and youth services documentation, birth mother report, or other reliable sources) prior to assessment in the clinic. Assessment is then conducted by a multi-

disciplinary team (psychologist, speech-language pathologist, occupational therapist, social worker and developmental pediatrician) who evaluate information gathered from standardized testing, rating scales, clinical observation, interviews, photographic analysis, and information from families, teachers, social workers, referring physicians, birth records and medical chart review. Diagnoses are made according to the Canadian Guidelines (Chudley et al., 2005) and the 4-digit code (Astley, 2004), which classifies children using a Likert scale in each of 4 key categories: growth restriction, facial dysmorphology, brain dysfunction, and alcohol exposure. The Canadian Guidelines attempt to harmonize the 4-digit code with the Institute of Medicine FASD guidelines (Hoyme et al., 2005), which rely heavily on facial features and physical anomalies associated with alcohol exposure and place less emphasis on neurocognitive dysfunction given that it is not specific to prenatal alcohol exposure. The Canadian Guidelines further stress differential diagnosis with review of available genetic information, pre- and post-natal confounding factors (e.g. trauma), and by assessing neurobehavioural features across 9 domains: hard and soft neurological signs, brain structure, cognition, communication, academic achievement, memory, executive functioning, attention, and adaptive behaviour, at least 3 of which must be impaired (>2 standard deviations (SD) below population norm) for a diagnosis to be considered. However, given the lack of a brain imaging ‘biomarker’ for FASD (discussed further below), MRI is not typically used in diagnostic assessment, and measures of ‘CNS impairment’ are largely indirect. Head circumference is one measure of CNS impairment used in all 3 diagnostic systems, and is discussed in detail in Chapter 7.

3.2 Mechanisms of Alcohol Teratogenicity

Alcohol is a potent teratogen that directly crosses the placental barrier, enters the fetal bloodstream and impairs brain development through a number of mechanisms (for review, see

Goodlett et al., 2005). Animal models of pre-natal alcohol exposure have demonstrated alcohol-induced hypoxia (Mitchell et al., 1998); oxidative stress (Ornoy, 2007; Pollard, 2007); disruption of growth factor signalling (Feng et al., 2005; Miller, 2003); disturbance of neurogenesis and or gliogenesis in the neocortex (Miller and Robertson, 1993), cerebellum (Shetty and Phillips, 1992) and hippocampus (Redila et al., 2006); increased neuronal apoptosis and cell death (Bonthius and West, 1990; Ikonomidou et al., 2000; Olney et al., 2000); abnormal proliferation and migration of cortical neurons and decreased myelination (Miller, 1986; Ozer et al., 2000); as well as numerous neurochemical and metabolic disruptions (Glavas et al., 2007; Guo et al., 2011; Honse et al., 2003; Hughes et al., 2001). The wide spectrum of behavioural and cognitive outcomes observed depend on characteristics of alcohol exposure itself, such as timing (when during pregnancy), frequency (how often) and quantity (how much), but is also mediated by a host of other prenatal factors including maternal nutrition, genetics and stress (Guerra et al., 2009). Indeed, both animal models and human dizygotic twin studies have demonstrated phenotypic variability even with identical amounts and patterns of prenatal alcohol exposure (Chen et al., 2011; Christoffel and Salafsky, 1975; Streissguth and Dehaene, 1993), further emphasizing the complexity of gene-environment interactions. Moreover, alcohol-related brain damage observed in childhood must be considered in the context of a dynamically changing brain that's developmental trajectory that is influenced by additional genetic and environmental factors. The following sections will describe attempts to characterize a specific set of alcohol-related brain anomalies in humans, in a collective attempt to establish a 'brain biomarker' for FASD, thus far eluded by the enormous neurological variability observed despite obvious abnormalities of behaviour and cognition in this population.

3.3 Autopsy and Qualitative Brain Imaging

The effects of prenatal alcohol exposure on human brain structure were first described in autopsy studies, such as in Figure 3.3 which compares the brain of a previously healthy 6 week old (A) with the brain of a 6 week old who had been heavily exposed to alcohol in utero (B) (Clarren et al., 1978). Autopsy of the alcohol-exposed brain revealed severe microencephaly (small brain), heterotopias (i.e. grey matter clusters in white matter), hydrocephalous, and agenesis of the corpus callosum. Other similar studies have confirmed extreme abnormalities including microcephaly, ventriculomegaly, small cerebellum and agenesis of the corpus callosum (Clarren et al., 1978; Jones and Smith, 1973; Peiffer et al., 1979). Although autopsy studies undoubtedly provide a wealth of detailed histological information, they only represent the most severely affected individuals who die in infancy or childhood, and as such do not generalize well to the much larger population living with FASD.

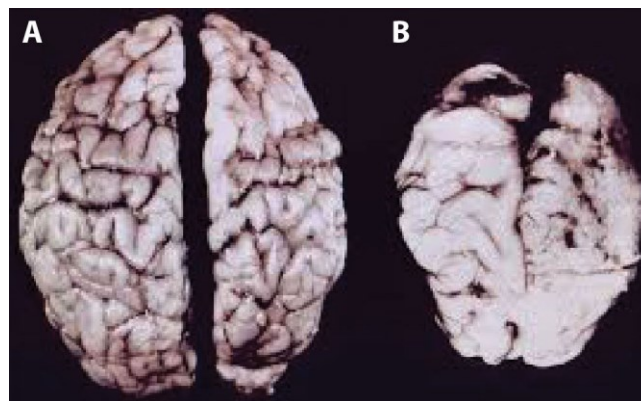


Figure 3.3: FAS Autopsy. Image courtesy of Sterling Clarren, showing the brain of a previously healthy 6 week old baby (A) and the brain of a 6 week old baby who had FAS (B). Although striking, this level of severity is not representative of the general population with FASD.

Insights into the living human brain are afforded by non-invasive imaging technology such as MRI. Most clinical MRI studies involve qualitative visual assessment of the images, which are evaluated for gross structural abnormalities or lesions. Figure 3.4 provides an example (albeit at the extreme end) of one such case study, showing the brain of a 9 year old female with FAS who had complete agenesis of the corpus callosum as well as holoprosencephaly, a birth defect in which the forebrain fails to divide into the two hemispheres (Riley et al., 1995). This and other similar MRI studies have provided in-vivo evidence of the potential for visible abnormalities in the brain associated with FASD, including microencephaly, agenesis or hypoplasia of the corpus callosum, cavum septum pellucidum and cavum vergae, ventriculomegaly, cortical, cerebellar and hippocampal atrophy, delayed myelination and polymicroglia (Autti-Ramo et al., 2002; Johnson et al., 1996; Narberhaus et al., 2004; Reinhardt et al., 2010; Riikonen et al., 1999; Swayze et al., 1997). It should be noted that the majority of subjects in these case studies had diagnoses of FAS, and many had very heavy exposure (e.g. >12 drinks/week throughout pregnancy; Riikonen et al., 1999).

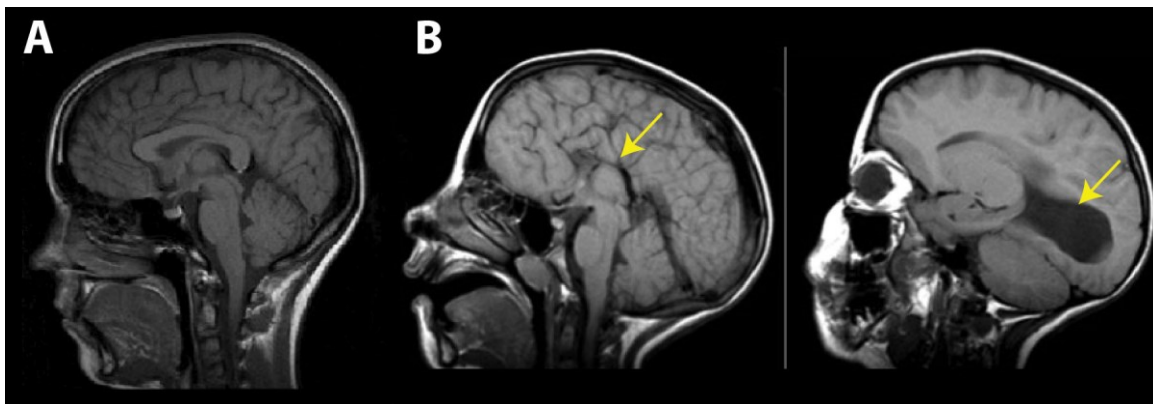


Figure 3.4: FAS MRI case study Adapted from Riley et al ACER 1995. A) shows a mid-sagittal MRI of a healthy subject, B) shows a mid and parasagittal slice from the MRI of a 9 year old female with FAS, showing complete absence of the corpus callosum, as well as abnormal formation of the ventricular system.

While gross abnormalities demonstrate the extreme end of alcohol teratogenesis in living subjects, these findings do not represent the norm in FASD. Indeed, one study of 65 participants across the full spectrum of FASD found that only 6 (~9%) had abnormalities evident on MRI through visual inspection by a radiologist (Astley et al., 2009a). Likewise, another study of 19 individuals with FAS found radiological abnormalities in only one subject (Clark et al., 2000), suggesting that ‘visible’ injury is not typical of this population (even among those with the most ‘severe’ diagnosis) despite obvious cognitive and behavioural impairments. Instead, conventional qualitative imaging likely *underestimates* the degree of brain damage in alcohol exposed individuals, highlighting the need for advanced, and importantly, quantitative imaging methods.

3.4 Quantitative Structural Brain Imaging in FASD

Advanced structural imaging typically relies on quantitative measurements (e.g. calculating the size of a structure), which are statistically compared between groups of subjects, rather than qualitative examination of a single individual. Examples from studies of brain volumes, shape analysis, cortical thickness and white matter microstructure will be discussed to highlight the strengths and weaknesses of using advanced quantitative structural MRI to further understand the brain abnormalities associated with FASD.

3.4.1 Volumetric Analysis in FASD

Recall that total brain volume increases in early childhood, reaching 95% of its maximum volume by about age 5 years, while progressive and regressive changes in the white and grey matter continue into adulthood. Brain volume varies considerably from person to person and is on average ~8-10% larger in males than females, loosely correlating with body size (Cosgrove et al., 2007). In the general population, this difference in size does not hold a one-to-one

relationship with performance (e.g. only small or inconsistent differences in IQ are found between males and females) though weak correlations between brain volume and intelligence have been demonstrated, suggesting that structural volume variability holds some relevance to function (Witelson et al., 2006).

Reduced brain volume seems to be one of the most robust findings in brain imaging of FASD, with many studies reporting ~10-15% reductions relative to control groups (e.g. Astley et al., 2009a; Cortese et al., 2006). This appears to hold even in samples where most participants do not have facial dysmorphology or growth delays (e.g. Lebel et al., 2008a), suggesting that alcohol has a disproportionate effect on the nervous system. In addition to global reductions of total brain volume, reductions in white matter, cortical grey matter, cerebellar, and sub-cortical volumes are also commonly reported, and persist in adult samples (for review, see Lebel et al., 2011; Nunez et al., 2011; Figure 3.5). White and grey matter volume reductions are similar in magnitude and seem to be more commonly reported in frontal, parietal and temporal regions, with relative sparing of the occipital lobes.

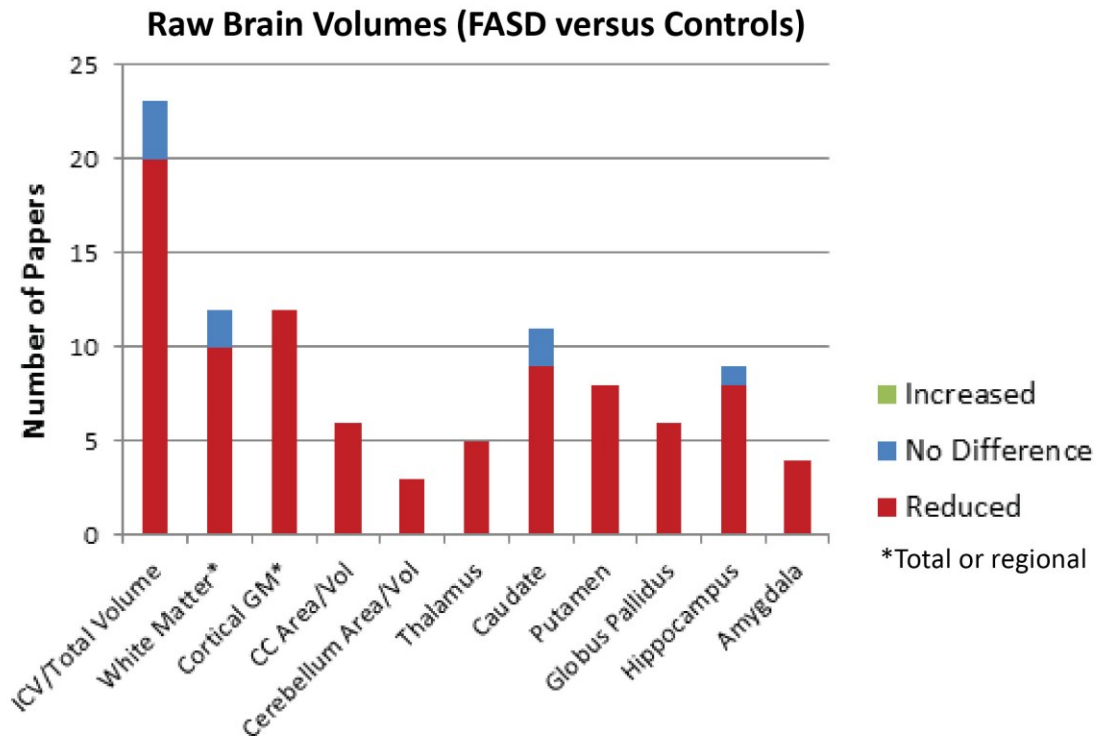


Figure 3.5: Brain volume studies of FASD. Summary of raw brain volume findings papers published as of March 2015. Only quantitative comparisons between groups are included (i.e. case reports of microcephaly are excluded). It is clear that the vast majority of papers report reduced volumes in FASD, with very few reporting no group difference, and none reporting larger volumes. See Appendix C for a more detailed table of this literature review.

Some studies report disproportionate reductions in certain regions (that remain significant after controlling for total brain volume), including the frontal lobes and caudate nucleus (Archibald et al., 2001; Astley et al., 2009a; Cortese et al., 2006; Nardelli et al., 2011; Figure 3.6), suggesting that these areas may be particularly susceptible to damage. However, these results are less consistent in many regions, and a large number of studies have reported reductions that scale with the global reduction of total brain volume (Figure 3.6).

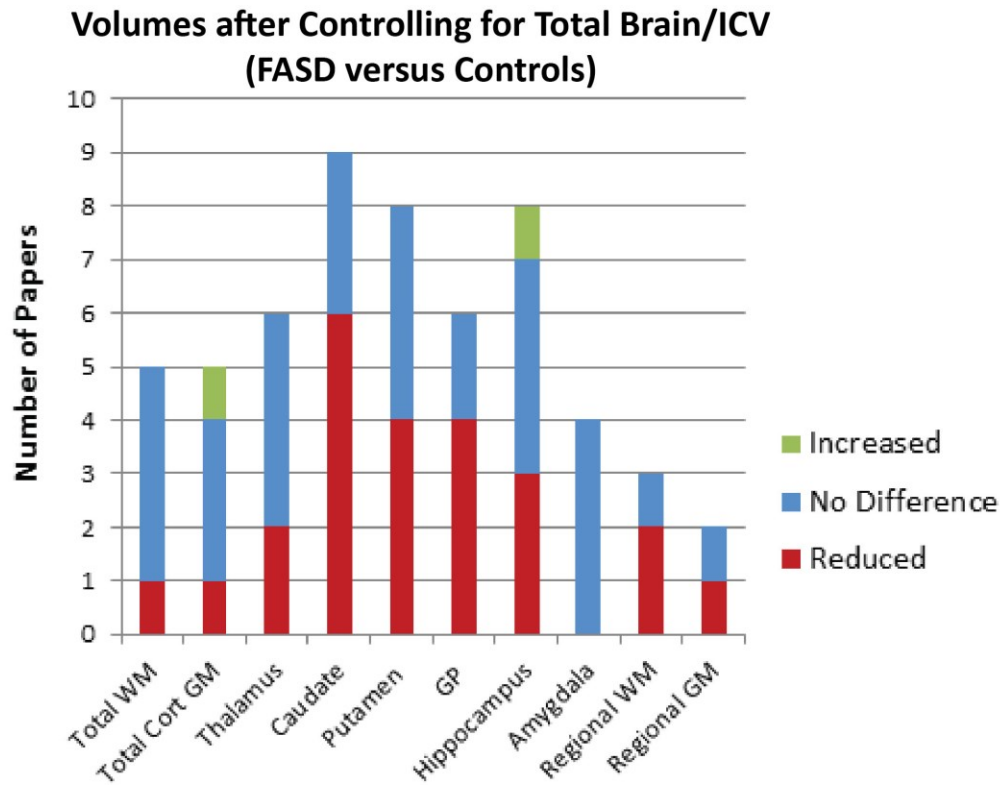


Figure 3.6: Volume studies of FASD that control for total brain volume/ICV. Summary of volume differences between FASD and control subjects after correcting for total brain volume or intracranial volume (either statistically or as a calculated ratio), from a literature review of published papers as of March 2015. Note that the number of papers does not match Figure 3.4 as many studies did not report corrected volumes. Many studies report regional volume reductions on par with reductions of total volume, resulting in no group difference (blue here). Nonetheless, several papers have reported significant reductions after correction, e.g. for caudate volume in 6/9 papers, versus 0/4 for the amygdala, suggesting that some areas of the brain may be disproportionately affected by prenatal alcohol exposure.

In addition to static differences, a recent longitudinal follow-up study found that adolescents with FASD underwent less developmental change in cortical grey matter volume with age (Lebel et al., 2012b), suggesting that prenatal alcohol exposure may also affect downstream developmental mechanisms years beyond when the injury was initiated in utero. See Appendix C for a list of volumetric studies of FASD and a summary of their findings.

In addition to volume deficits, morphology studies have reported displacement and/or greater variability in shape of the corpus callosum (Bookstein et al., 2001; Bookstein et al., 2002b; Sowell et al., 2001) frontal lobes (Sowell et al., 2002a), caudate, hippocampus (Joseph et al., 2014) and cerebellum (Bookstein et al., 2006; O'Hare et al., 2005); as well as reduced cortical asymmetry (Sowell et al., 2002b) in individuals with FASD relative to controls. These findings suggest that in addition to brain size, global aspects of structural organization are impaired in individuals with prenatal alcohol exposure.

3.4.2 Cortical Development in FASD

Beyond volume, analysis of the cortex can be subdivided to examine cortical thickness, surface area and gyrification index, as well as sulcal width and depth. These parameters follow distinct developmental trajectories both prenatally (Rakic, 1995) and post-natally, and appear to be under unique genetic influences (Raznahan et al., 2011). Studying these aspects of the cortex independently may provide clues to the cellular mechanisms underlying the global cortical abnormalities observed in FASD.

Studies of cortical thickness in FASD have yielded conflicting results, with findings of increased thickness (Fernandez-Jaen et al., 2011; Sowell et al., 2008b; Yang et al., 2011), decreased thickness (Gautam et al., 2014; Zhou et al., 2011), or no difference (Rajaprakash et al., 2014; Wozniak et al., 2013) in participants with FASD compared to controls (Figure 3.7).

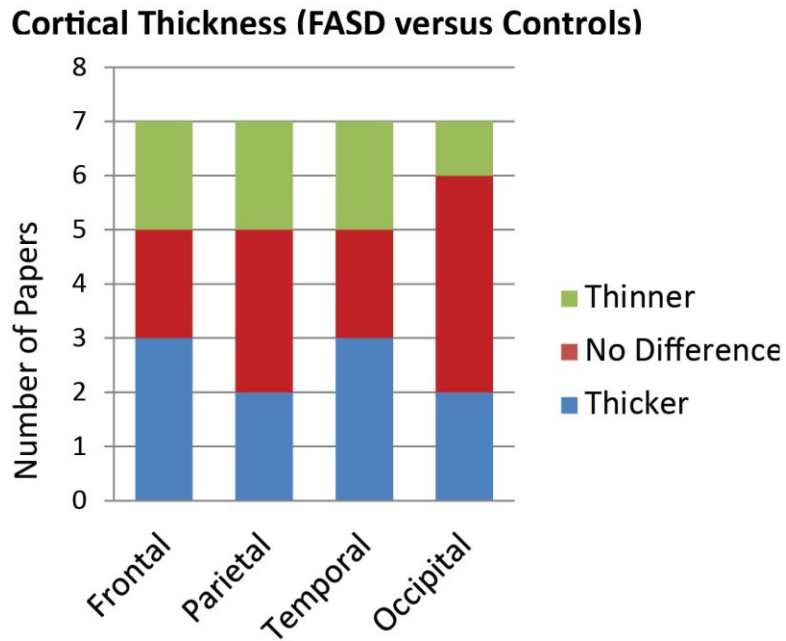


Figure 3.7: Cortical thickness studies of FASD. Cortical thickness differences between FASD and control participants from a literature review of published papers as of March 2015. It is evident that cortical thickness findings have been inconsistent across studies, with some finding regional increases in thickness, while others find no change or regional decreases in thickness in FASD subjects relative to controls. See Appendix D for further details.

These contradictory findings may stem from differences in patient population (e.g. proportion of subjects with FAS, ADHD co-morbidity, medication status and other factors that influence cortical thickness), but may also result from differences in the unique image processing methods between these studies. In particular, the pipelines used to calculate cortical thickness differ in their extraction of the pial-cortical surface, which is highly influenced by partial volume effects that may differ between groups given recent evidence of sulcal width and cortical folding abnormalities in FASD (De Guio et al., 2014). In addition, discrepancies between studies may also be influenced by age-related differences, given that cortical thickness declines with age. There is growing evidence that change in thickness over time (age-related development) may be a more sensitive metric than the absolute value of cortical thickness at a single time-point (Shaw

et al., 2008), lending support for longitudinal data collection, such as that discussed in Chapter 5 of this thesis.

In addition to cortical thickness abnormalities, two recent studies have found reduced surface area in bilateral frontal, temporal and right occipital regions (Rajaprakash et al., 2014), as well as reduced cortical folding complexity and increased space between cortical folds (sulcal width) in participants who were prenatally exposed to alcohol (De Guio et al., 2014). Despite discrepancies between studies, this body of work collectively suggests aberrant cortical development and organization in FASD, discussed further in Chapter 5.

3.4.3 Diffusion Tensor Imaging of White Matter in FASD

At the start of this thesis (in 2010) there were seven published DTI studies examining group differences between individuals with FASD/heavy prenatal alcohol exposure versus healthy controls (Fryer et al., 2009; Lebel et al., 2008a; Li et al., 2009; Ma et al., 2005; Sowell et al., 2008a; Wozniak et al., 2006; Wozniak et al., 2009). Collectively, these studies revealed a variety of white matter abnormalities in areas including the corpus callosum, cingulum, uncinate fasciculus, corticospinal tracts, superior and inferior longitudinal fasciculus, and inferior fronto-occipital fasciculus; albeit with large variations between studies. Since that time three more DTI studies comparing individuals with FASD to healthy controls have been published, finding group differences in the splenium (Paolozza et al., 2014), cerebellar peduncles (Spottiswoode et al., 2011), and in widespread white matter areas of newborns (Taylor et al., 2015)—see Figure 3.8. Note that other several other DTI studies comparing diffusion metrics to cognitive measures within alcohol-exposed samples have been published (e.g. Green et al., 2013; Lebel et al., 2010), but are omitted here given that they do not include group comparison to a control sample.

Group Differences in DTI Parameters by Tract

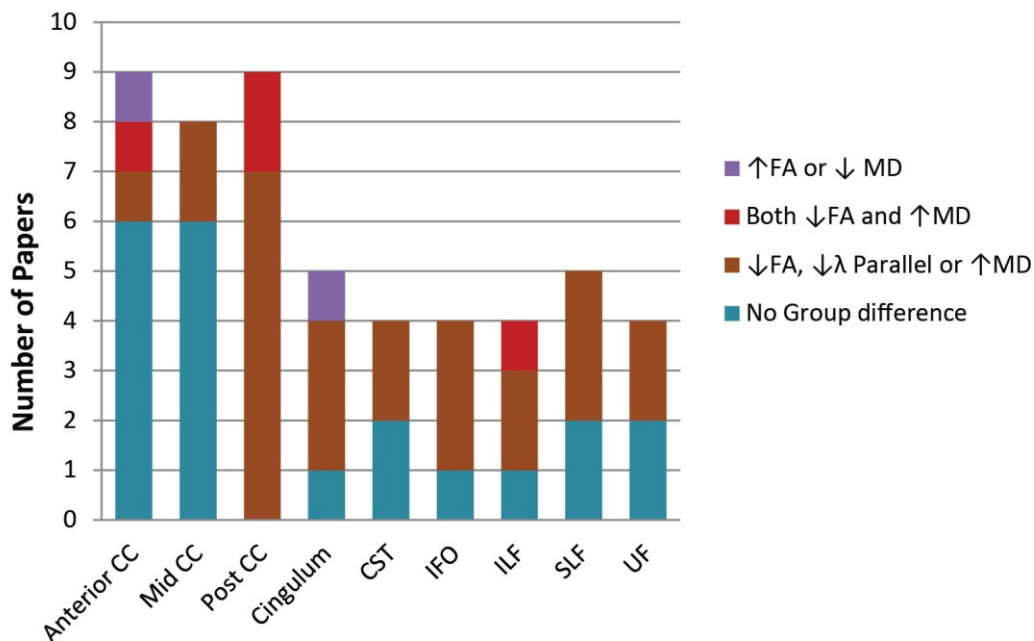


Figure 3.8: DTI studies of FASD. Literature review of DTI findings in major white matter tracts, as of March 2015. Note that several areas (e.g. cerebellar peduncle) are not included here due to limited number of papers. It is evident that findings are inconsistent for many tracts, with a substantial proportion of papers finding no group difference between FASD and controls. Moreover, the majority of significant differences have been in one parameter (e.g. FA or MD), with only a few select regions showing differences in both FA and MD, and a minority finding counter-intuitive changes (e.g. higher FA in the FASD group; purple). However, group differences in the posterior portion of the corpus callosum including reduced FA, elevated MD or both, appears to be a robust finding across studies. CC=corpus callosum, CST=corticospinal tract, IFO=inferior fronto-occipital fasciculus, ILF=inferior longitudinal fasciculus, SLF=superior longitudinal fasciculus, UF=uncinated fasciculus.

Although these results suggest widespread (but inconsistent) diffusion abnormalities in association with prenatal alcohol exposure, it is important to note that a variety of analysis methods, age distributions, clinical populations and target areas complicate their comparison, and may even underlie variable findings within the same tract/area (see Appendix B for further details). Four of the previous papers only examined differences in the corpus callosum, which confirms previous assertions of midline abnormalities (Bookstein et al., 2002a) but excludes the possibility of uncovering abnormalities in other brain areas. Another important limitation to

consider is that most previous work has included limited sample size over narrow age ranges, limiting conclusions about changes in these parameters with age in FASD, and no previous studies have examined sex differences; discussed further in Chapters 4 and 7.

3.5 Links between Brain Structure and Clinical/Demographic Variables

Identifying structural brain damage in subjects with FASD is an important step towards better understanding the effects of prenatal alcohol exposure on the brain, but it is also essential to establish how these findings relate to the variability in clinical presentation observed in FASD. With a better understanding of the relationship between alcohol exposure, physical dysmorphology, cognition and brain structure, brain imaging could become a useful tool for predicting outcomes and guiding interventions for affected individuals.

3.5.1 Sex Differences

Only a handful of studies have examined sex differences in brain structure in FASD, often due to limited sample sizes. Instead most studies include sex as a covariate in statistical analysis, given its known effects on brain volume among other measures (Giedd et al., 2012). Of those that have examine the effects of sex, most have found greater differences among males (FASD versus control) than females, and/or fewer sex differences within the FASD than control group (Chen et al., 2012; Dudek et al., 2014; Nardelli et al., 2011). Likewise, a longitudinal study of cortical volume found select regions with sex-age-group interactions where growth trajectories differed more between males (FASD versus control) than females (Lebel et al., 2012b). Although limited, these studies suggest that either males with FASD are more susceptible to brain volume abnormalities, or that sex effects (driven largely by genetic and hormonal factors) are not as robust in children with prenatal alcohol exposure. Interestingly,

there is not strong evidence to suggest that females with FASD are less cognitively impaired than males.

3.5.2 Behaviour and Cognition

A number of studies have found correlations between quantitative MRI parameters and performance on standardized cognitive or behavioural tasks in FASD, suggesting that observed structural brain abnormalities are functionally relevant. For example, in groups of prenatal alcohol-exposed subjects, quantitative measures of brain structure have been correlated with IQ (Roussotte et al., 2011), verbal learning (Sowell et al., 2001), executive functioning (Bookstein et al., 2002b), verbal recall (Coles et al., 2011a), mathematical skill (Lebel et al., 2010) and attention (Bjorkquist et al., 2010), among others. However, many other studies have failed to demonstrate any significant correlations between brain structure and cognitive performance (e.g. Autti-Ramo et al., 2002; Nardelli et al., 2011) again highlighting the complex relationship between brain structure and function/behaviour.

3.5.3 Facial Dysmorphology

Animal models have demonstrated that alcohol-related facial dysmorphology results from alcohol exposure in the equivalent of the 3rd and 4th weeks of pregnancy in humans, during which precursor cells migrate and divide to form the midline facial features as well as the forebrain (Sulik, 2005). The timeline and overlapping lineage of the development of the face and brain has led to interest in associating facial dysmorphology with brain structure in FASD. Astley et al. (2009a) explored this relationship by stratifying brain volume outcomes by diagnostic category, given that FAS and partial FAS (pFAS) require facial dysmorphology while the remaining diagnoses under the FASD umbrella do not. They found progressively greater reductions in total brain volume and frontal lobe volume with more dysmorphic diagnoses (i.e.

brain volume progressively decreased from Control to non-dysmorphic to pFAS to FAS groups). Likewise, Archibald et al. (2001) found reductions in brain volumes that were only significant among children with FAS/pFAS, but not alcohol related neurobehavioural disorder (ARND). Although intriguing, diagnoses of FAS and pFAS also require growth delays and severe central nervous system damage (as assessed by cognitive testing), so correlations are difficult to interpret. However, other studies have shown more specific relationships, such as correlations between reduced deep grey matter (Roussotte et al., 2011) or cortical volumes (Yang et al., 2011) with increased lipometer score (thinnest upper lip and flattest philtrum) and shorter palpebral fissure length (width of the eye opening). Moreover, Lebel et al. (2012b) found that children who underwent the least cortical volume development with age also had the highest lipometer scores, suggesting that links between the face and brain development may be relevant beyond the initial in utero period. Although correlations between facial dysmorphology and brain structure may provide clues about development and are of scientific interest, facial dysmorphology is only evident in ~10% of individuals with FASD (May et al., 2009), limiting the clinical utility of these relationships.

3.5.4 Alcohol Exposure Patterns

There is significant scientific and public interest in associating the degree of structural abnormality in the brain with the amount of alcohol exposure in utero. However, like all outcomes in FASD, this relationship is not straightforward, despite animal model evidence of robust teratogenic effects (e.g. cell death) even from a single binge exposure (Farber et al., 2010; Idrus and Napper, 2012). Nonetheless, some correlations have been established in human imaging studies. For example, Astley et al. (2009a) found that greater frequency of exposures (average number of drinking days per week) correlated with smaller hippocampal and mid-

sagittal volume, as well as shorter corpus callosum length, and that greater maximal number of drinks per occasion correlated with smaller frontal lobe, caudate and hippocampus volume among adolescents with FASD. Dose-dependent reductions of grey matter volume of the cingulate gyrus, bilateral middle frontal gyri, middle temporal gyrus and caudate have also been shown in adults who were prenatally exposed to low-moderate amounts of alcohol (Eckstrand et al., 2012). In addition, a longitudinal study found that reduced cortical development with age during adolescence correlated with a greater number of drinks per week during pregnancy (Lebel et al., 2012b). Although informative, variability in these findings has challenged efforts to establish a consistent set of brain abnormalities associated with a given amount of exposure in utero. Moreover, it is often very difficult to obtain accurate and detailed accounts of exposure history, particularly given that most participants live in foster or adoptive families and are recruited into research studies many years after birth. Prospective research studies in humans (which recruit women during pregnancy) are a key step toward collecting detailed and accurate exposure histories, as well as other valuable information about socio-economic factors and environmental variables that may impact later developmental outcomes (Jacobson and Jacobson, 1996).

3.6 Summary and Thesis Objectives

MRI has provided many valuable insights into prenatal alcohol-related brain damage in humans, including robust reductions in brain volume, abnormalities in the shape of the corpus callosum, thickness, surface area and folding of the cortex, and widespread abnormalities in white matter microstructure. One of the most salient features of this body of quantitative neuroimaging research is the ability to detect group differences in brain structure even in the absence of visible abnormalities in the brain, in keeping with the severe cognitive and

behavioural abnormalities observed in this FASD population. Given that these metrics are not used in diagnosis of FASD, this work has also provided objective, independent evidence associating prenatal alcohol exposure with brain damage in humans. However, several important limitations of previous findings should be noted, and underscore the need for continued research in this area, forming the motivation for much of the contents of this thesis.

At the onset of my graduate program, there were no longitudinal MRI studies of FASD, and the majority of cross sectional MRI studies of FASD had small sample sizes and/or narrow age ranges. Longitudinal imaging has the power to capture change with age within subjects, mitigating inter-subject variability and age-related sample bias. Establishing trajectories of brain development in FASD is imperative for understanding the influence of prenatal alcohol exposure on continued postnatal development, and may help to explain worsening of cognitive and behavioural symptoms during adolescence. Chapters 4 and 5 discuss longitudinal studies of DTI and cortical thickness, respectively, and are the first published studies using these methods in FASD.

As discussed in previous sections, MRI is not used routinely in the diagnosis of FASD given that clinical imaging typically yields non-significant findings. As a result, clinicians rely on other measures of neurological impairment, including cognitive testing, head circumference, and hard and soft neurological signs. However, little is known about how accurately these clinical measures predict structural brain damage. The relationship between head circumference and brain volume, for example, has been explored in healthy populations but has not yet been directly examined in children with prenatal alcohol exposure. Chapter 6 examines this relationship, with the aims of informing the clinical use of head circumference in this population,

and determining if MRI provides duplicative or additive information about the level of impairment than what can be garnered from these simpler measures.

Although a variety of studies have demonstrated abnormalities in diffusion parameters, volume and cortical thickness, none have reported on all 3 modalities in the same sample, challenging comparison between these modalities within-subjects. Examination of all 3 modalities in the same sample is needed to provide a more objective measure of severity of abnormalities observed with each method—e.g. is caudate volume more or less affected than the white matter microstructure, as well as the relationship between them—e.g. is a subject with a very small caudate more likely to have more severe white matter microstructure abnormalities? In addition, the vast majority of previous MRI studies of FASD have pooled males and females, often including sex as a statistical covariate. Sex differences in brain structure have been well established in healthy populations, and may be of particular interest for developmental disabilities which often differ in prevalence rate and symptom profile between boys and girls. Some of these limitations are addressed in Chapter 7 with a large cross sectional study of children, adolescents and adults with FASD.

Advanced brain imaging, including the work presented in this thesis, will help to provide a more complete understanding of the teratogenic effects of alcohol in living subjects. A clearer picture of the pattern of associated deficits in brain structure, and importantly, the developmental trajectories of these deficits with age is needed to better define the neurological ‘profile’ of individuals with FASD, with the eventual goal of establishing an imaging biomarker for this disorder, which would greatly aid differential diagnosis, particularly in cases when prenatal history is unclear and/or other forms of acquired brain injury need to be ruled out. Importantly, an understanding of brain structure and development is needed to tailor medical interventions for

this population, which often focus on co-morbidities (e.g. stimulant medications for attentional symptoms) and treatment of adverse behavioural issues (e.g. with use of atypical antipsychotics) rather than targeting primary impairments specific to FASD. A better understanding of brain development in this population is an essential precursor to evaluating the impact of medication use during critical periods of development in children who were prenatally exposed to alcohol. Lastly, advanced imaging methods also have the potential to predict outcomes and track neuro-cognitive and behavioural interventions for this population, needed to optimize outcomes for individuals with FASD, their families and communities.

Research

4 Longitudinal Changes in Brain Volume and White Matter Microstructure in FASD²

Abstract

Diffusion tensor imaging (DTI) of brain development in fetal alcohol spectrum disorders (FASD) has revealed structural abnormalities, but studies have been limited by the use of cross-sectional designs. Longitudinal scans can provide key insights into trajectories of neurodevelopment within individuals with this common developmental disorder. Here we evaluate serial DTI and T1-weighted volumetric MRI in a human sample of 17 participants with FASD and 27 controls aged 5-15 years who underwent 2 to 3 scans each, ~2-4 years apart (92 scans total). Increases of fractional anisotropy (FA) and decreases of mean diffusivity (MD) were observed between scans for both groups, in keeping with changes expected of typical development, but mixed-models analysis revealed significant age-by-group interactions for 3 major white matter tracts: superior longitudinal fasciculus (SLF) and superior and inferior fronto-occipital fasciculus (SFO, IFO). These findings indicate altered developmental progression in these frontal-association tracts, with the FASD group notably showing greater reduction of MD between scans. Δ MD is shown to correlate with reading and receptive vocabulary in the FASD group, with steeper decreases of MD in the SFO and SLF between scans correlating with greater

² A version of this chapter has been published. Treit S, Lebel C, Baugh L, Rasmussen C, Andrew G, Beaulieu C. (2013) Longitudinal MRI Reveals Altered Trajectory of Brain Development during Childhood and Adolescence in Fetal Alcohol Spectrum Disorders. *Journal of Neuroscience*. 33(24): 10098-10109

improvement in language scores. Volumetric analysis revealed reduced total brain, white, cortical grey and deep grey matter volumes and fewer significant age-related volume increases in the FASD group, although age-by-group interactions were not significant. Longitudinal DTI indicates delayed white matter development during childhood and adolescence in FASD, which may underlie persistent or worsening behavioural and cognitive deficits during this critical period.

4.1 Introduction

Fetal alcohol spectrum disorders (FASD) describe a range of physical, cognitive and behavioural deficits stemming from prenatal alcohol exposure. Despite increased awareness of the teratogenic effects of alcohol since their recognition in the 1970s, FASDs have an estimated prevalence of ~1 in 100 and represent the leading cause of preventable developmental disability in North America (May and Gossage, 2001; May et al., 2009). Alcohol negatively impacts the developing brain through numerous mechanisms including altered gene transcription, neuronal proliferation and migration errors, oxidative stress, hypoxia and cell death (for review, see Goodlett et al., 2005). Resulting impairments vary widely between individuals, depending on timing and quantity of exposure and the likely interaction of a host of environmental and genetic factors. Although physical and medical complications vary, neurobehavioural deficits are characteristic of the entire spectrum of FASD, and are considered to be the most functionally debilitating (Mattson et al., 1998).

Advanced brain imaging studies of FASD have revealed abnormalities in brain volume, microstructure, cortical thickness, metabolism, and functional activation (for review, see Roussotte et al., 2010). One of the most robust findings is reduced brain volume, with many studies reporting reduced total brain, grey and white matter as well as numerous deep grey matter

volumes, with some reductions persisting after controlling for total brain volume (Astley et al., 2009a; Lebel et al., 2011). Diffusion tensor imaging (DTI) studies of children with FASD have revealed microstructural abnormalities in the corpus callosum, cingulum, cortico-spinal tracts, cerebellar peduncles, and a number of association fibres (Fryer et al., 2009; Lebel et al., 2008a; Sowell et al., 2008a; Spottiswoode et al., 2011; Wozniak et al., 2006; Wozniak et al., 2009). Brain volume (Coles et al., 2011b) and DTI abnormalities (Li et al., 2009; Ma et al., 2005) also persist in adult subjects with FASD. Although DTI studies have greatly advanced our understanding of brain pathology in FASD, they have all been cross-sectional in design, limiting conclusions about brain development.

Longitudinal studies of healthy development have confirmed increases of white matter, decreases of cortical grey matter and various changes to deep grey matter volumes during childhood and adolescence (Giedd et al., 1999; Lenroot et al., 2007), in concert with underlying progressive and regressive cellular events. Likewise, increases of fractional anisotropy (FA) and reductions of mean diffusivity (MD) of white matter have been observed in longitudinal DTI studies of healthy children and adolescents (Bava et al., 2010; Giorgio et al., 2010; Lebel and Beaulieu, 2011), and are presumed to reflect reduced water content, increased myelination and/or increased coherence/packing of axons within white matter tracts. One recent longitudinal volume study has shown altered trajectories of cortical volume growth in FASD, but did not include DTI (Lebel et al., 2012). In order to better understand how brain abnormalities evolve during these key developmental periods of behavioural and cognitive progression, this study aims to examine for the first time within-subject longitudinal changes in white matter DTI parameters in FASD during childhood and adolescence.

4.2 Materials and Methods

4.2.1 Subjects

Participants were 17 children with FASD (11 males, 6 females; 5.4-11.8 years of age at first scan) and 27 control participants (15 males, 12 females; 5.7-11.1 years of age at first scan); all scanned 1.8-4.2 years apart (Figure 1, Table 1). Fourteen of 17 FASD scan 1 data were included in our cross-sectional DTI study (Lebel et al., 2008a), 9 of these 14 were also included in our cross-sectional deep grey matter volumetric study (Nardelli et al., 2011), and all control participant scans were a subset from our previous longitudinal study of healthy brain development (Lebel and Beaulieu, 2011). A total of 92 scans were collected: 15 subjects with FASD and 25 controls with 2 scans each; 2 subjects with FASD and 2 controls with 3 scans each. FASD participants were recruited from a hospital FASD diagnostic clinic, had confirmed prenatal alcohol exposure and were previously medically diagnosed with an alcohol related disorder falling under the FASD umbrella in accordance with the Canadian Guidelines for diagnosis of FASD (Chudley et al., 2005) and the 4-digit code (Astley, 2004). In addition, two subjects with FASD were recruited from a community clinic and were diagnosed under the Institute of Medicine guidelines (Hoyme et al., 2005). Two subjects had a diagnosis of fetal alcohol syndrome (FAS), 3 partial FAS (pFAS), 3 static encephalopathy alcohol exposed (SE:AE), 7 neurobehavioural disorder alcohol exposed (NBD:AE), 1 alcohol related neurobehavioural disorder (ARND) and 1 FASD that was not further specified. Given the small number of subjects, all sub-diagnoses were collapsed to form one “FASD” group for statistical analysis, but are represented separately in several figures. Control subjects were screened for psychiatric and neurological impairments, as well as contraindications to MRI. In addition, control subjects' caregivers were contacted retrospectively (at the time of data analysis for this

paper) and asked to estimate in-utero alcohol exposure for their child. Of the 21 control subject caregivers who were reached, 14/21 reported no exposure, 2/21 unknown, and 5/21 reported minimal alcohol exposure (range: 1-3 drinks; average of 2 drinks total during pregnancy). Written informed consent was obtained from all participants' parent/legal guardian, and written assent was collected from all participants prior to study procedures. This study was approved by the Health Research Ethics Board at the University of Alberta.

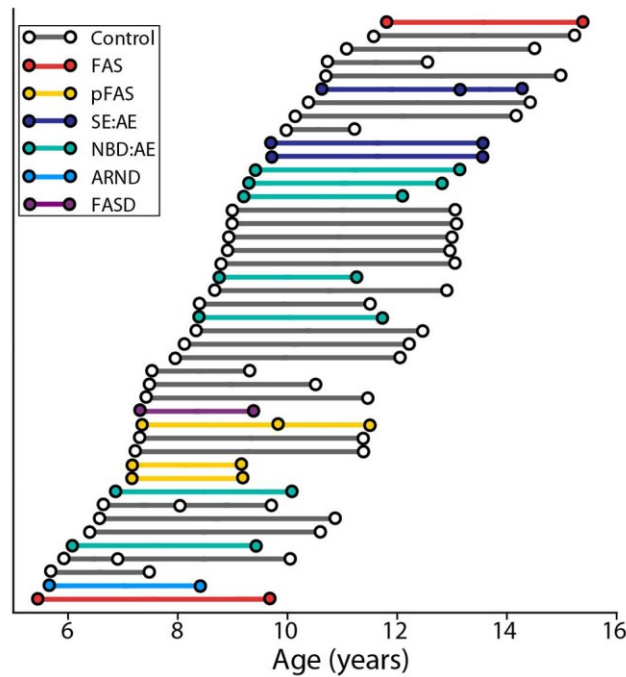


Figure 4.1: Age and time between scans by diagnosis. Circles represent each scan, connecting lines represents the time between scans for each participant, and colours indicate diagnostic subgroups under the FASD umbrella versus controls (shown in grey). 40 participants had 2 scans each and 4 participants had 3 scans each for a total of 92 scans, ~2-4 years apart.

Table 4.1: Participant characteristics and demographics for FASD and control groups

Participant Characteristics:		FASD (n=17)	Control (n=27)	p-value^c
Mean age 1 st scan (years):		8.2 ± 1.8 (5.4-11.8)	8.5 ± 1.6 (5.7-11.6)	ns
Mean age last scan (years):		11.4 ± 2.1 (8.4-15.3)	12.0 ± 1.8 (7.4-15.2)	ns
Mean time between scans (years):		3.2 ± 0.7 (2.0-4.2)	3.6 ± 0.9 (1.2-4.2)	ns
N males (%):		11 (65%)	15 (56%)	ns
N right handed (%):		13 (76%)	26 (96%)	0.046
Demographics:		FASD (n=16)	Control (n=21)^a	p-value
Ethnicity:	Caucasian	8 (47%)	20 (95%)	0.001
	Aboriginal	8 (53%)	0 (0%)	<0.001
	Other	0 (0%)	1 (5%)	ns
Median annual household income:		\$76,000 to \$100,000	\$76,000 to 100,000	ns
Caregiver status:	Biological parent(s)	0 (0%)	21 (100%)	<0.001
	Adopted	9 (53%)	0 (0%)	<0.001
	Foster	4 (29%)	0 (0%)	0.017
	Biological Relative	3 (18%)	0 (0%)	0.41
Mean number of foster care placements per child:		1.4	0.0	<0.001
Co-morbidities:	ADHD	11 (65%)	1 (5%) ^b	<0.001
	Oppositional Defiant Disorder			0.017
	Anxiety	4 (24%)	0 (0%)	
	Other	5 (29%)	0 (0%)	0.007
		6 (35%)	0 (0%)	0.002
Psychoactive medications:	Atypical Antipsychotic	11 (65%)	0 (0%)	<0.001
	Psycho-stimulant	10 (59%)	0 (0%)	<0.001
	Antidepressant	5 (29%)	0 (0%)	0.007
	Other	3 (18%)	0 (0%)	0.043
Average number per subject:		1.9	0	<0.001

^a Demographics information was collected at the second scan for FASD group but retrospectively by phone questionnaire for controls; demographic data was not collected for one FASD subject, and 6 control subjects were lost to follow up or did not return phone calls.

^b Parent-reported (diagnosis not confirmed); not medicated at time of MRI.

^c Group differences in categorical variables (e.g. sex) assessed with Mann-Whitney U; continuous variables (e.g. age) tested with independent sample t-test (at p<0.05)

4.2.2 Cognitive Testing & Demographics

Participants with FASD underwent approximately 1.5 hours of cognitive testing at each scan, administered by a trained research assistant. The test battery included the Woodcock Johnson Quantitative Concepts 18A&B (mathematics), Woodcock Reading Mastery Test-Revised (WRMT-R) Word ID, Comprehensive Expressive and Receptive Vocabulary Test (CREVT), Working Memory Test Battery for Children (WMTB-C), Behaviour Rating Inventory of Executive Function (BRIEF) parent form, and NEPSY/II (auditory attention and response set; memory for names, narrative memory; arrows). The NEPSY I was administered at scan 1 but

subsequently updated to NESPY II by scan 2; therefore only sub-tests that did not change in the new edition are included here. In addition, 9 participants in the FASD group were administered the Wide Range Intelligence Test (WRIT) at scan 2. Given that control data were previously collected for a study of healthy development, control subjects did not undergo a full battery of cognitive testing, but were administered WRMT-R Word ID at each scan. Demographic information (Table 1) was collected via questionnaire given to participants' caregivers at scan 2 for the FASD group, and retrospectively by phone interview for controls.

4.2.3 Image Acquisition

All data at both time-points were acquired using identical methods, hardware and sequence parameters on the same 1.5T Siemens Sonata MRI scanner. Scans included DTI, T1-weighted, T2-weighted, fluid-attenuated inversion recovery (FLAIR), and FLAIR-DTI (not used here) for a total scan time of ~26 minutes. DTI was acquired using a dual spin-echo, single shot echo-planar imaging sequence with: 40 3 mm axial-oblique slices with no inter-slice gap; TR=6400 ms; TE=88 ms; 6 non-collinear diffusion sensitizing gradient directions with $b=1000 \text{ s/mm}^2$; 8 averages; FOV=220x220 mm^2 ; matrix of 128x128 with 75% phase partial Fourier zero-filled to 256x256 for a total acquisition time of 6:06 minutes. T1-weighted images for volume analysis were acquired using a high resolution ($1 \times 1 \times 1 \text{ mm}^3$) MPRAGE sequence with: TR=1870 ms, TE=4.38 ms, TI=1100 ms for a total acquisition of 4:29 minutes. Three FASD and 2 control participants at scan 1, and 1 (different) control at scan 2 are missing MPRAGE data because they were either unable to tolerate the full length of scan, or moved too much to obtain adequate data. In addition, 3 FASD and 6 control MPRAGE data were acquired without including the top of cortex at scan 1, and were therefore excluded from volume analysis, leaving 11 FASD and 18 control subjects. By necessity, all subjects included here had successful DTI at both scans.

4.2.4 Tractography

A semi-automated tractography method (described previously in Lebel et al., 2008b) was used to delineate 11 major white matter tracts for each scan. Subject images were normalized to a template using a non-affine transformation, saving warping parameters for each subject. Seed, target and exclusion regions were drawn on the template according to a priori information on tract location (Wakana et al., 2004), and then applied to each subject's native colourmap using an inverse of their normalization parameters, such that the same seed, target and exclusion regions were applied to all subjects. White matter tracts included the genu (gCC), body (bCC), and splenium (sCC) of the corpus callosum, the anterior limb of the internal capsule (ALIC), corticospinal tracts (CST), superior and inferior longitudinal fasciculus (SLF; ILF), superior and inferior fronto-occipital fasciculus (SFO; IFO), cingulum, and uncinate fasciculus (UF). Tractography was carried out in native space for each subject, using a deterministic streamline method in ExploreDTI (Leemans et al., 2009), and fibres in the left and right hemisphere were measured separately at this stage for all tracts except the corpus callosum. A minimum FA threshold of 0.25 was used to initiate and continue tracking, and an angle threshold of 60° was set for the UF and SLF and 30° for all other tracts. Deterministic tractography robustly reconstructs major white matter tracts, but can lead to errors in areas with crossing fibres (e.g. the intersection of the corpus callosum and cortico-spinal tracts) where intersecting fibres within a voxel can make it difficult to determine a primary diffusion orientation, artificially lowering FA and in some cases terminating tracking. All tracts were manually inspected for consistency with known anatomy. Minor manual modifications were made to approximately 20% of tracts to exclude spurious fibres. Adequate tracking was not achieved in 3% of tracts (e.g. very small number of streamlines), and these were excluded from the analysis. Fractional anisotropy (FA)

and mean diffusivity (MD) were measured for each tract by averaging all voxels of a tract, counting each voxel only once (i.e. FA/MD in a given voxel was not weighted by number of streamlines). Similarly, parallel ($\lambda_{//}=\lambda_1$) and perpendicular ($\lambda_{\perp}=(\lambda_2+\lambda_3)/2$) diffusivities were calculated for each tract. FA or MD of left and right counterparts of all bilateral tracts were significantly correlated (i.e. left FA versus right FA, left MD versus right MD, R values ranging from 0.31-0.88, mean 0.69; $p<0.001$ to $p=0.003$), so in order to reduce the number of multiple-comparisons and streamline the data presentation, diffusion parameters of corresponding left and right tracts were averaged prior to statistical analysis.

4.2.5 Volume Analysis

T1-weighted MPRAGE images were processed using Freesurfer version 4.1.0 (Anthinoula A. Martinos Center for Biomedical Imaging, Charlestown M.A). An automated processing pipeline (Fischl et al., 2002) was used to extract volumes for total brain (excluding cerebrospinal fluid and cerebellum), white matter, cortical grey matter, as well as bilateral hippocampus, amygdala, thalamus, caudate, putamen, and globus pallidus. All segmentations were visually inspected for accuracy. Corresponding left and right deep grey matter structure volumes were significantly correlated ($R=0.83-0.94$; mean 0.90 $p<0.001$ for all structures) so left and right counterparts of bilateral structures were averaged prior to statistical analysis to reduce multiple comparisons.

4.2.6 Statistical Analysis

One-sample t-tests were used to compare cognitive test standard scores with population norms (standard score of 100 for all tests except NEPSY scaled score of 10 and BRIEF T scores of 50). Paired-sample t-tests were used to determine if there was a change in standard score from scan 1 to scan 2 for each test (at $p<0.05$).

The effect of age, group, and age-by-group interactions of FA, MD and volumes were assessed using a linear mixed-model with the following equation: *Dependent variable (DTI parameter or volume) = Intercept + A*age + B*group + C*sex + D*age x group + residual.* This statistical approach was chosen for its ability to handle datasets with repeated measures and varying intervals between measurements. For tractography analysis, a main effect of sex on FA or MD was only significant ($p < 0.05$) for FA of the ALIC ($p = 0.001$) and SLF ($p = 0.031$) and both FA and MD of the genu ($p = 0.004$ and $p = 0.015$, respectively); therefore, sex was subsequently removed from the model before testing age-by-group interactions for all other tracts. A main effect of sex on volume was significant ($p < 0.05$) for all structures and therefore included in the model for all volumetric analyses. Significant age-by group interactions ($p < 0.05$) of DTI parameters were followed up with two additional analyses: i) parallel and perpendicular diffusivities were tested using the same model to help determine underlying factors driving FA and MD changes, and ii) the relationship between brain development and cognition was tested using partial correlations of Δ FA or Δ MD (see calculation below) and Δ raw cognitive scores ($\text{raw score}_2 - \text{raw score}_1$), controlling for mean age and time between scans. Partial correlations were also used to test the relationship between Δ volume and Δ raw cognitive score for total brain volume, white matter, cortical grey matter, and all deep grey matter structures, controlling for mean age and time between scans.

In addition to mixed-models analysis, Δ FA, Δ MD and Δ volume values were determined for each subject by subtracting their value at scan 1 from scan 2 for each tract or volume. For subjects with 3 scans, a best fit line was determined and the value at scan 1 on the line was subtracted from the value at scan 3. A reliability study of 5 healthy adult subjects scanned 10 times each over a one week period (50 scans total) was performed to determine a measure of

within-subject inter-scan variability (i.e. test re-test variability independent of development). This sub-study was performed using identical DTI and MPRAGE protocols on the same scanner, as well as the same volume segmentation and tractography methods as described above. Within-subject standard deviations were calculated for FA and MD of each of the 11 tracts and multiple brain volumes, and then averaged across the 5 subjects to produce a mean standard deviation for each tract or structure. These mean standard deviation values were then used as change cut-offs for Δ FA, Δ MD and Δ volume values of FASD and control participants to determine the frequency of participants with increases (> 1 SD), decreases (> 1 SD) or no change (≤ 1 SD) between scans for each group. Significant differences in the proportion of subjects in each group with increases, decreases, or no change in diffusion parameters or volumes between scans were assessed using Chi Squared analysis (at $p < 0.05$).

4.3 Results

4.3.1 Cognitive Testing

The FASD group performed significantly below population norm ($p < 0.05$) on all cognitive measures at both time points, with the exception of NEPSY Memory for Names at scan 1, and WRMT-R Word ID (reading), NEPSY II Arrows (visuo-spatial) and Response Set (set shifting) at scan 2 (Table 4.2). FASD group raw score values increased on all subtests between time-points, though paired-sample t-tests did not reveal significant changes in standard scores between scans, suggesting persistent delays relative to population norms that were not mitigated nor exacerbated with age. Results of the WRIT collected at time 2 indicate that on average the FASD group was not significantly impaired on IQ, with a mean general IQ standard score of 99 ± 15 ; however, IQ was only tested in 53% (9/17) of these subjects. Control group Word ID standard scores were significantly above the population norm of 100 at both scans (mean

standard scores of 113 ± 14 at scan 1 and 111 ± 12 at scan 2), but did not show significant standard score change between scans on paired sample t-tests (i.e. they performed above average but changed at a rate on par with population norms).

Table 4.2: Cognitive testing in FASD group showing below average standard scores (age normalized) in most tests, but no significant differences in standard scores between longitudinal scans.

Cognitive Test	Sub-test/Domain	Category	Scan	N (of 17)	Mean Standard Score \pm SD	Standard Score Range	One sample t-test ^a p-value	
WMTB-C	Digit Recall	Working Memory	1	16	86 \pm 13	60-111	0.001	
			2	17	88 \pm 14	52-117	0.002	
	Block Recall	1	16	83 \pm 16	57-108	0.001		
		2	17	83 \pm 15	59-110	<0.001		
WJ	Quantitative Concepts 18A&B	Mathematics	1	16	90 \pm 16	62-115	0.019	
			2	15	90 \pm 10	70-107	0.002	
CREVT	Receptive	Vocabulary	1	16	91 \pm 7	75-102	<0.001	
			2	16	92 \pm 8	74-102	0.001	
	Expressive	1	16	84 \pm 16	63-112	0.001		
		2	16	82 \pm 14	57-107	<0.001		
	Composite	1	16	85 \pm 11	68-106	<0.001		
2		16	84 \pm 12	62-102	<0.001			
WRMT-R	Word ID	Reading	1	17	93 \pm 10	75-109	0.011	
			2	17	92 \pm 17	52-134	0.083	
NEPSY I/II	Arrows	Visuo-spatial	1	12	7.9 \pm 2.9	2-12	0.030	
			2	15	10.2 \pm 2.8	5-15	0.787	
	Auditory Attention (AA) and Response Set (RS)	AA	Attention & vigilance	1	14	5.3 \pm 4.0	1-13	0.001
				2	14	7.4 \pm 3.2	1-12	0.010
	AA vs. RS	RS	Inhibition & set-shifting	1	11	6.1 \pm 3.7	2-14	0.005
				2	14	8.6 \pm 3.0	1-13	0.109
	Memory for Names	AA vs. RS	Executive Function	1	11	7.5 \pm 3.3	4-13	0.030
				2	14	9.4 \pm 3.0	2-13	0.434
Memory for Names	Memory	1	12	8.3 \pm 3.8	3-15	0.134		
		2	14	6.9 \pm 2.9	3-12	0.001		
BRIEF parent form	Behavioural Regulation Index (BRI)	1	15	75 \pm 13	40-94	<0.001		
		2	16	79 \pm 12	50-97	<0.001		
	Metacognition Index (MI)	1	15	71 \pm 7	53-81	<0.001		
		2	16	72 \pm 7	55-84	<0.001		
	Global Executive Composite (GEC)	1	15	74 \pm 9	48-83	<0.001		
2		16	76 \pm 9	53-92	<0.001			
WRIT	Verbal IQ		2 ^b	9	94 \pm 14	75-118	0.255	
	Visual IQ		2 ^b	9	103 \pm 15	78-122	0.572	
	General IQ		2 ^b	9	99 \pm 15	75-116	0.789	

^aPopulation norm mean standard scores used as test value for one-sample t tests: 100 for all tests except NEPSY I/II (mean scaled score = 10), and BRIEF (mean T score = 50)

^bThe WRIT was only collected at Scan 2.

4.3.2 Brain Volumes

A significant effect of group ($p < 0.001$) on volume was found for all structures measured (whole brain, white matter, cortical grey matter, as well as thalamus, caudate, putamen, globus pallidus, hippocampus and amygdala), with 7-18% reductions observed in the FASD group compared to controls (Table 4.3, Figure 4.2). When total brain volume was added as a covariate, cortical grey matter ($p = 0.007$), white matter ($p = 0.036$), thalamus ($p = 0.007$), putamen ($p = 0.040$) and globus pallidus ($p = 0.007$) volumes remained significantly reduced in the FASD group.

Significant age-related increases of total brain ($p = 0.008$, 2%), white matter ($p < 0.001$, 10%), globus pallidus ($p = 0.046$, 1%), and amygdala ($p = 0.036$, 3%) volumes were found in the control but not FASD group. The only significant effect of age on volume found in the FASD group was cortical grey matter ($p = 0.042$, -4%) (Table 4.3). Despite these differences, mixed models analysis did not reveal significant age-by-group interactions. Likewise, Chi squared analysis did not reveal significant differences between the FASD and control groups in the proportion of subjects who underwent increases, no change, or decreases in volume between scans (Figure 4.2).

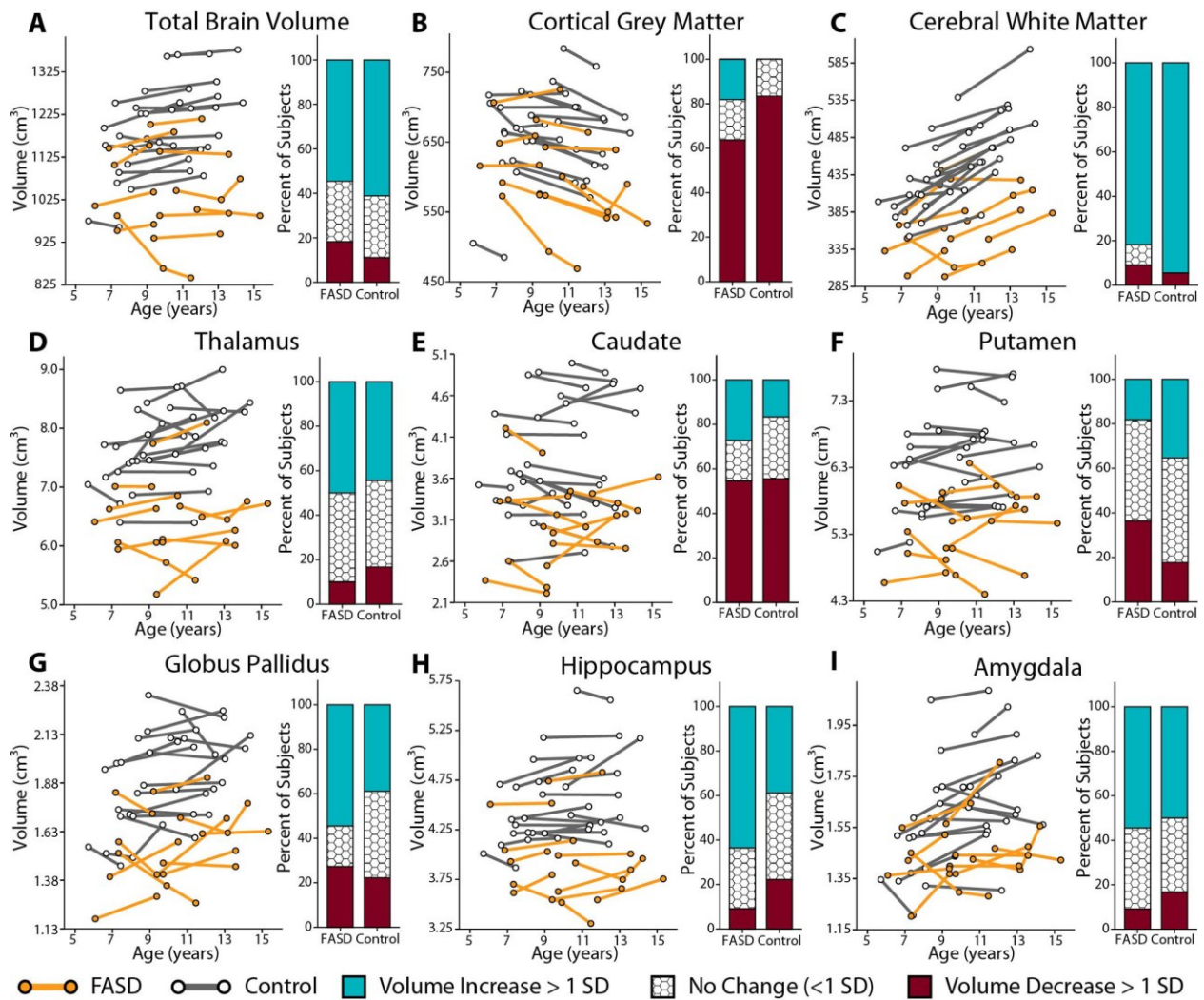


Figure 4.2: Changes in brain volumes with age. Changes in brain volume between scans for FASD (n=11) and control subjects (n=18). Significant group differences were found for all volumes ($p < 0.001$), with the FASD group having smaller volumes than controls. After adding total brain volume as a covariate, cortical grey matter ($p = 0.007$), white matter ($p = 0.036$), thalamus ($p = 0.007$), putamen ($p = 0.040$) and globus pallidus ($p = 0.007$) volumes remained significant. Age-by-group interactions in volume growth were not found, indicating similar trajectories of growth between groups, though there were significant effects of age in the control but not FASD group for some structures (Table 4.3).

Table 4.3: Effects of age, group, and age-by-group interactions for brain volumes. The FASD group shows smaller volumes for all structures, with many reductions persisting after controlling for total brain volume. Significant effects of age are found in several structures in the control but not FASD group, though age-by-group interactions are not significant (ns).

Structure	Group Differences			Longitudinal Changes				
	Main effect of group	% reduction (FASD < Control)	FASD (n=11)		Control (n=18)		Age-by-group interaction	
	<i>total brain volume controlled</i>		Age effect p-value	% change	Age effect p-value	% change		
Total Brain	<0.001	n/a	-11%	ns	0.1%	0.008	1.5%	ns
Cortical Grey Matter	<0.001	0.007	-16% ^a	0.042	-3.8%	ns	-3.7%	ns
White Matter	<0.001	0.036	-7% ^a	ns	6.9%	<0.001	9.8%	ns
Thalamus	<0.001	0.007	-14% ^a	ns	2.4%	ns	-2.1%	ns
Caudate	<0.001	ns	-18% ^a	ns	-1.0%	ns	-2.3%	ns
Putamen	<0.001	0.040	-15% ^a	ns	-2.0%	ns	1.2%	ns
Globus Pallidus	<0.001	0.007	-15% ^a	ns	2.4%	0.046	1.4%	ns
Hippocampus	<0.001	ns	-12% ^a	ns	1.6%	ns	1.1%	ns
Amygdala	<0.001	ns	-10% ^a	ns	4.2%	0.036	3.1%	ns

^aVolume reduction not corrected for total brain volume.

4.3.3 Tractography

Significant main effects of group indicate lower FA of the SFO ($p=0.015$) and MD of the genu ($p=0.044$) in the FASD group compared to controls (Table 4.4). When separated by scan, MD of the UF was lower in FASD than controls at scan 2 but not scan 1.

Significant age-related increases of FA ($p<0.05$) were found in 8/11 tracts in the FASD group and 11/11 tracts in the control group (Table 4.4, Figure 4.3). The ILF, UF and bCC did not show significant effects of age in the FASD group. Likewise, significant age-related decreases of MD ($p<0.05$) were found in 9/11 and 7/11 white matter tracts in FASD and control groups, respectively (Table 4.4, Figure 4.4); with the exception of SFO and CST in both groups and bCC and IFO in the control group.

Mixed-models analysis revealed 3 significant age-by-group interactions: MD of the SFO ($p=0.038$), IFO ($p=0.011$) and SLF ($p=0.034$) (Figure 4.5). In all 3 tracts, MD decreased more between scans in the FASD than control group. Further analysis of λ_{\perp} and $\lambda_{//}$ in these tracts revealed age-by-group interactions of λ_{\perp} for the SFO ($p=0.027$) and IFO ($p=0.030$), with λ_{\perp} decreasing more steeply in the FASD group in both tracts. No interactions were observed for λ_{\perp} or $\lambda_{//}$ of the SLF.

Chi squared analysis of the proportion of subjects with increases/decreases/no change in either FA or MD between scans revealed significant group differences in MD of the IFO and UF ($p=0.046$; 0.003 , respectively) and FA of the genu ($p=0.011$) (Figure 4.5). For the IFO and UF, more subjects in the FASD group underwent decreases of MD between scans and more controls showed no change between scans; for the genu most control subjects underwent no change or FA increases between scans, whereas more FASD participants underwent FA decreases between scans.

Table 4.4: Fractional anisotropy (FA) and mean diffusivity (MD) group and age effects between scans. Age parameters are significant for most tracts in both FASD (n=17) and control subjects (n=27). Three tracts (IFO, SFO, SLF) show significant age-by-group interactions suggesting different trajectories of MD change between groups.

Tract	Fractional Anisotropy (FA)						Mean Diffusivity (MD) mm ² /s x10 ⁻³					
	Group Main effect	FASD		Control		Age x group interaction	Group Main effect	FASD		Control		Age x group interaction
		Age effect value	% p- change	Age effect p-value	% change			Age effect p-value	Age effect value	% p- change	Age effect p-value	
bCC	ns	ns	1.6%	0.017	1.8%	ns	ns	0.031	-2.6%	ns	-1.6%	ns
gCC	ns	0.049	2.2%	<0.001	2.5%	ns	0.044	0.005	-1.9%	0.041	-1.6%	ns
sCC	ns	0.008	2.5%	0.002	2.7%	ns	ns	<0.001	-3.9%	<0.001	-3.3%	ns
ALIC	ns	<0.001	3.6%	<0.001	5.2%	ns	ns	<0.001	-3.8%	<0.001	-2.6%	ns
CST	ns	<0.001	2.8%	<0.001	4.7%	ns	ns	ns	-0.2%	ns	-1.3%	ns
Cingulum	ns	0.004	3.1%	<0.001	4.3%	ns	ns	<0.001	-3.4%	<0.001	-2.5%	ns
IFO	ns	<0.001	5.3%	<0.001	3.9%	ns	ns	<0.001	-3.3%	ns	-1.2%	0.011
ILF	ns	ns	2.1%	0.005	2.9%	ns	ns	<0.001	-3.4%	<0.001	-2.2%	ns
SFO	0.015	0.001	4.1%	0.001	2.9%	ns	ns	ns	-1.9%	ns	-0.7%	0.038
SLF	ns	0.006	3.3%	<0.001	3.9%	ns	ns	<0.001	-3.7%	<0.001	-2.4%	0.034
UF	ns	ns	1.9%	0.001	3.0%	ns	ns	<0.001	-3.0%	0.004	-1.7%	ns

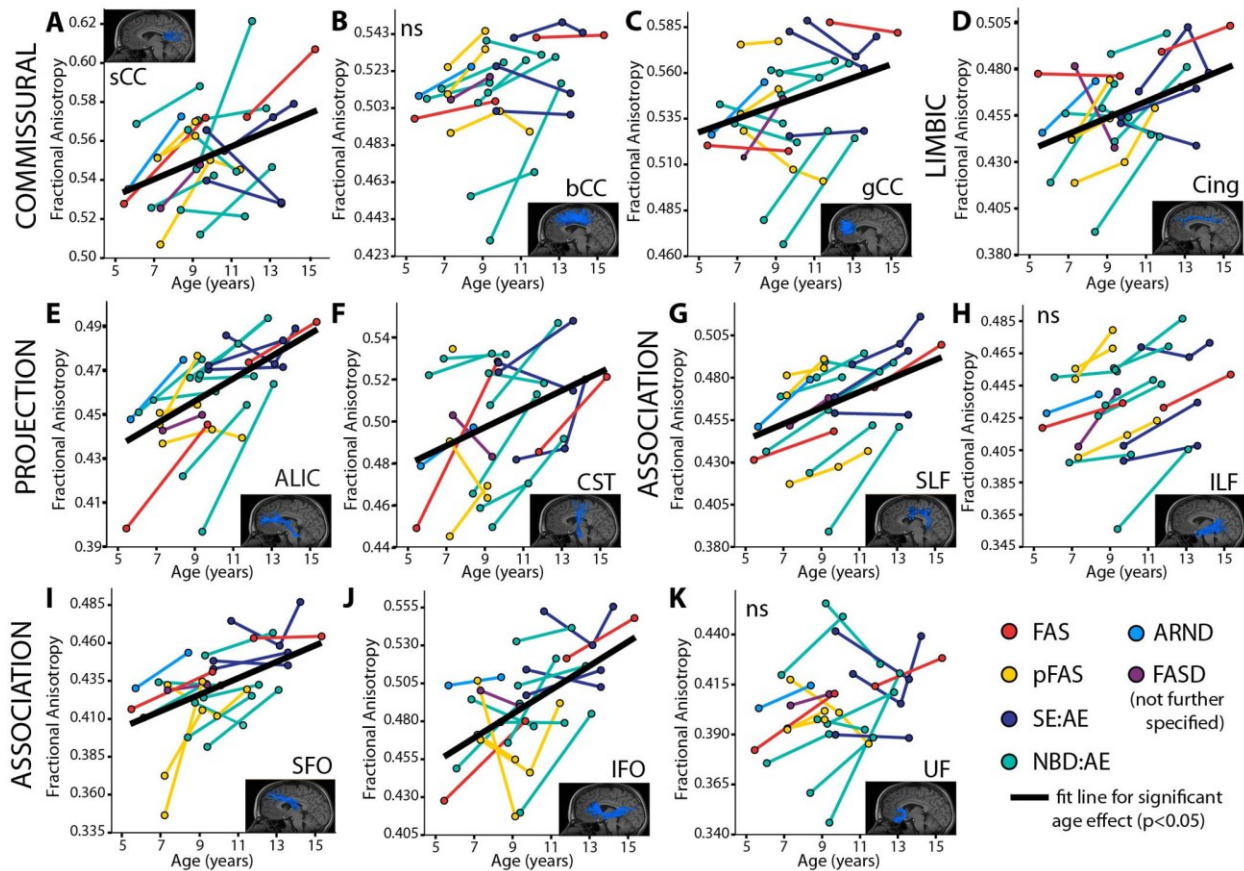
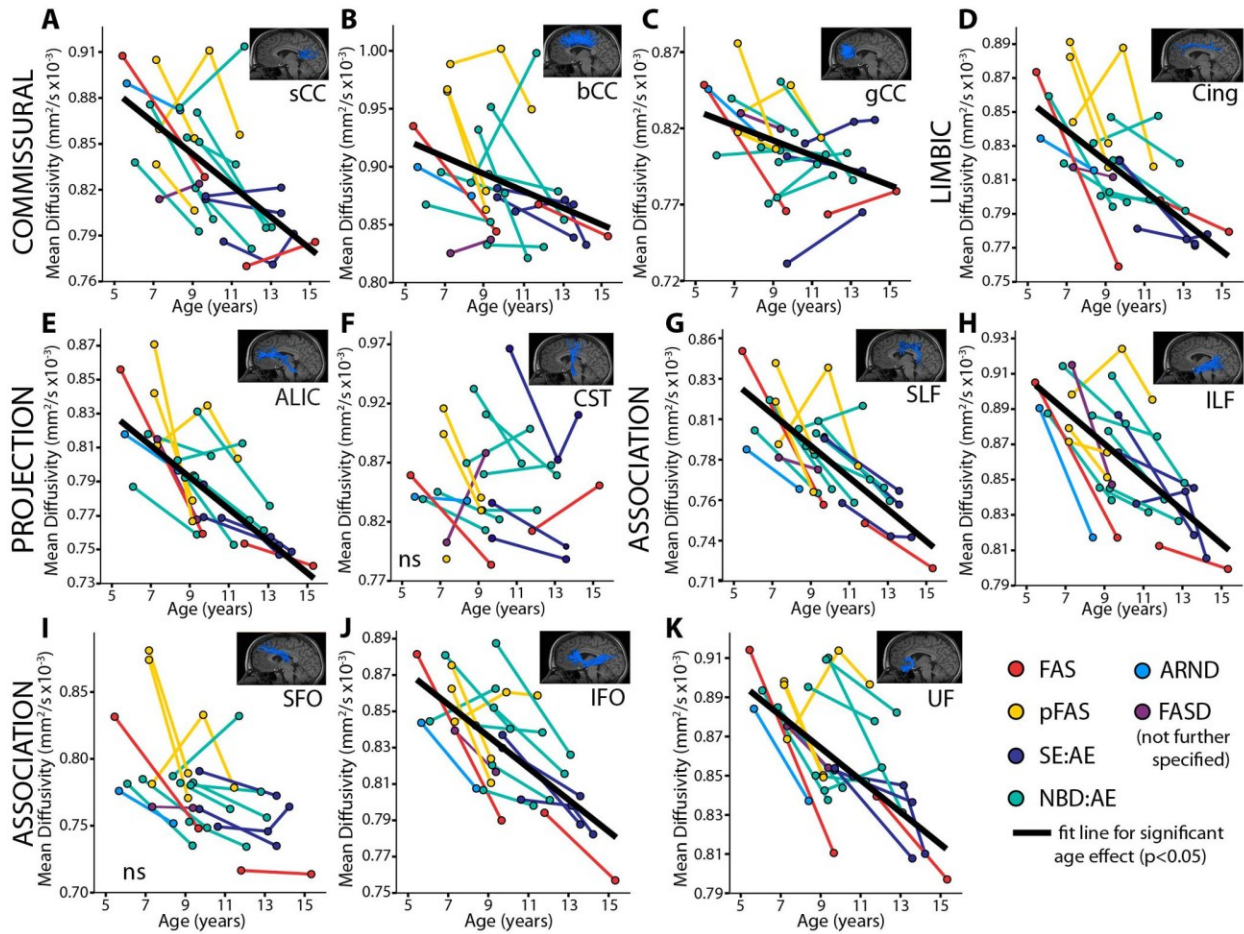


Figure 4.3: FA changes with age. Fractional Anisotropy (FA) of 11 major white matter tracts (A-K) in the FASD group (n=17); colours indicate diagnostic categories under the FASD umbrella. Mixed-models analysis shows 8/11 tracts had age-related increases of FA (as shown by best fit lines) with the exception of the body of the corpus callosum (B), inferior longitudinal fasciculus (H), and uncinate fasciculus (K). Increases of FA are expected over this age range in typical development.



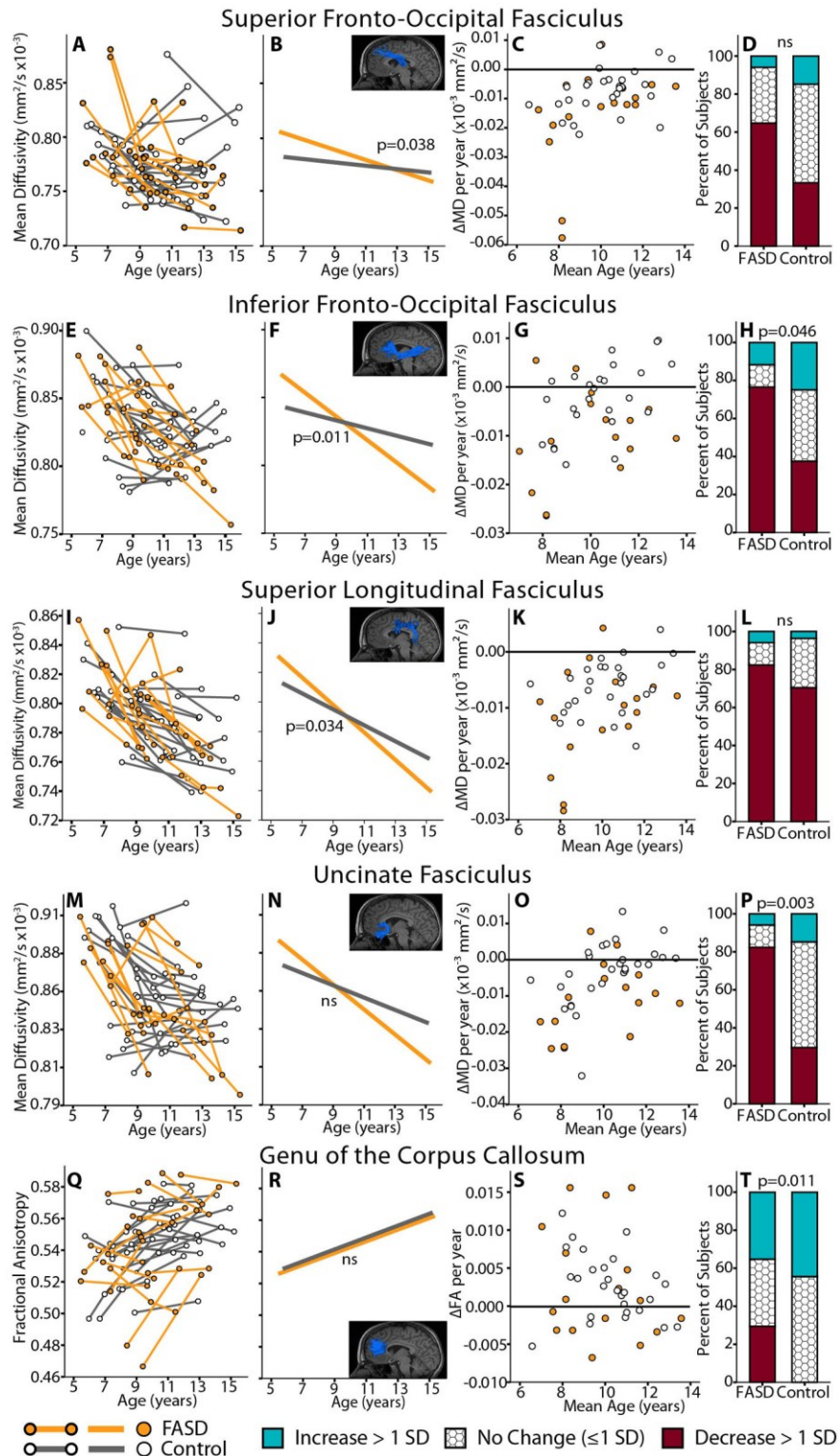


Figure 4.5: DTI age-by-group interactions. Trajectory differences of diffusion parameters (MD or FA) with age between FASD ($n=17$) and control ($n=27$) groups. Only tracts with significant age-by-group interaction in mixed-models, or significant difference in Chi Squared analysis are shown. Notably, all 5 tracts form frontal connections. For each tract, individual

subject trajectories are shown by group in the first column (FASD orange; controls grey), followed by interaction fit lines from mixed models analysis indicating age-by-group interactions, ΔMD or $\Delta FA/year$ ($(MD_2 \text{ or } FA_2) - (MD_1 \text{ or } FA_1)/\text{time between scans}$) by group, and finally bar graphs indicating the proportion of subjects in each group who underwent increases, decreases, or no change in MD or FA between scans (as determined by our established standard deviations for each tract—see Methods). The FASD group shows greater reductions of MD between time points than controls in the top four tracts, whereas the fifth tract (genu) shows more FASD participants with decreases of FA between scans than controls.

4.3.4 Brain-Behaviour Relationships

Three significant correlations between change in MD and change in cognitive score between scans were found after correcting both variables for mean age and time between scans (Figure 4.6). ΔMD in the SLF and SFO negatively correlated with $\Delta WRMT-R$ Word ID scores in the FASD group ($p=0.003$ and $p=0.001$, respectively), such that greater reductions of MD corresponded to larger gains in reading performance between scans. Equivalent Word ID correlations were not observed in the control group. In addition, ΔMD in the SFO negatively correlated with $\Delta CREVT$ receptive vocabulary ($p=0.028$) in the FASD group, where subjects with the greatest reductions in MD had the largest gains in receptive vocabulary score between scans (note CREVT was not administered to controls). There were no significant correlations between change in cognition and change in volumes.

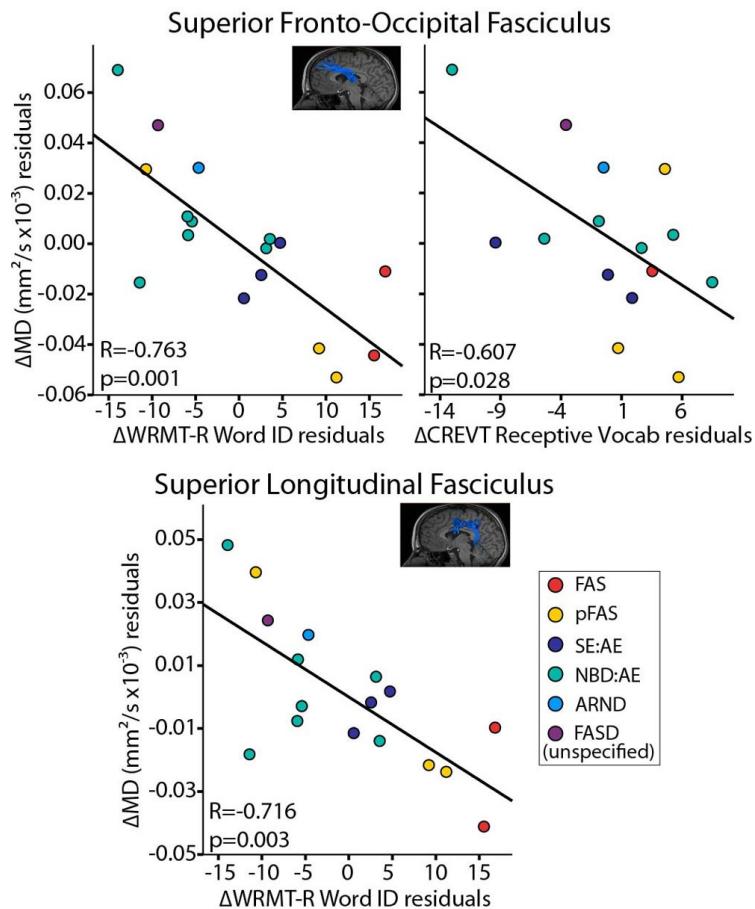


Figure 4.6: DTI-cognition correlations. DTI parameter cognitive correlations in the FASD group (n=17). Graphs show Δ mean diffusivity plotted against Δ cognitive scores (after correcting both variables for mean age and time between scans). Reductions of MD in the superior longitudinal fasciculus and superior fronto-occipital fasciculus significantly correlated with increases in performance on a word reading test (Word ID). In addition, decreases of MD in the superior fronto-occipital fasciculus correlated with increases in performance on receptive vocabulary (CREVT). Corresponding correlations of Δ MD with Δ WRMT-R Word ID were not observed in the control group.

4.4 Discussion

This study reports the first longitudinal DTI investigation of FASD, finding regional differences in brain development compared to healthy controls. Age related increases of FA and decreases of MD between scans were observed for most white matter tracts in the FASD group, in agreement with typical brain development; however, significant age-by-group interactions

indicate differences in the rate of change between groups for 3 of 5 major association fibres: superior fronto-occipital, superior longitudinal, and inferior fronto-occipital fasciculi. Altered trajectories of neurodevelopment during this critical 5-15 year old period, particularly in frontal lobe connections, may further compound existing deficits and contribute to high rates of secondary disabilities that emerge during adolescence in FASD (Streissguth et al., 1991).

Cross-sectional DTI studies show group differences of FA and MD in numerous white matter tracts among individuals with pre-natal alcohol exposure relative to controls (for review, see Wozniak and Muetzel, 2011). Our longitudinal analysis demonstrates relatively greater change (steeper decreases) of MD with age in the FASD group for the SFO, IFO and SLF; changes typical of earlier childhood in healthy subjects (Lebel and Beaulieu, 2011). Greater reductions of MD may reflect delayed compensation or more step-wise progression of underlying cellular events than expected of healthy development. For example, pre-natal alcohol exposure has been shown to reduce myelination in animal models (Ozer et al., 2000; Phillips, 1989). Age-by-group interactions of λ_{\perp} in the IFO and SFO (with greater decreases between scans in the FASD group) suggest delayed myelination as a possible mechanism underlying greater MD decreases in these tracts, in keeping with Shiverer mice studies linking increased myelination with reductions of both λ_{\perp} and MD (Nair et al., 2005; Song et al., 2002).

Interestingly, a post-hoc comparison of Δ MD between the 'more severe' (FAS, pFAS, SE:AE) versus 'less severe' (NBD:AE, ARND, FASD not further specified) FASD diagnoses and controls revealed a pattern in the IFO whereby the more severe group underwent the largest changes, followed by the less severe FASD group, and then controls (Figure 4.7). A similar trend was observed in the SFO, SLF and UF (data not shown) despite comparable cognitive profiles (at the time of study participation) between 'more' versus 'less severe' sub-groups (scan 1: reading

92 ± 13 versus 94 ± 8, math 91 ± 16 versus 89 ± 17, scan 2: reading 97 ± 6 versus 88 ± 22, math 90 ± 7 versus 89 ± 13, IQ 99 ± 15 versus 98 ± 15). Of note, a diagnosis of FAS or pFAS requires the presence of characteristic facial dysmorphology, which is associated with alcohol exposure during a critical period in the first trimester (Sulik et al., 1981) and has been correlated with structural brain abnormalities (Astley et al., 2009a; Lebel et al., 2012b; Roussotte et al., 2011). Children with ‘more severe’ diagnoses in this study appear to undergo the largest diffusion changes across this age range, which may relate to timing of gestational exposure or degree of initial injury, among other variables.

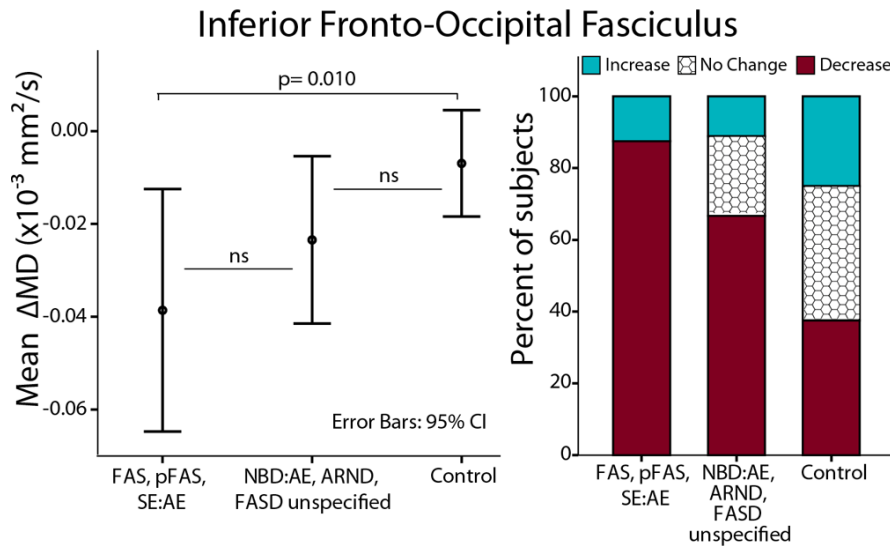


Figure 4.7: IFO changes by diagnosis. Change in mean diffusivity of the IFO between scans by diagnostic sub-group. Relatively greater ΔMD between scans is observed in the ‘more severe’ diagnostic categories (FAS, pFAS, SE:AE, n=8) followed by ‘less severe’ (NBD:AE, ARND, FASD unspecified, n=9) and finally controls (n=27), despite similar mean ages (10.3 ± 2.3 ; 9.4 ± 1.5 ; 10.3 ± 1.7), mean years between scans (3.4 ± 0.9 ; 3.0 ± 0.5 ; 3.6 ± 0.9) mean reading standard scores (95 ± 10 ; 91 ± 15 ; 112 ± 13) and math scores (91 ± 12 ; 89 ± 15 ; n/a) among these three groups, respectively.

All five of the tracts with either significant age-by-group interactions or Chi squared differences in the proportion of subjects with ΔFA or ΔMD (i.e. SLF, SFO, IFO, UF and genu,

Figure 5) form frontal lobe connections as part of their anatomical course. Frontal lobe abnormalities are reported in FASD (for review, see Norman et al., 2009), and may relate to impaired decision making. The frontal lobes undergo protracted maturation in healthy development (Giedd et al., 1999; Jernigan and Tallal, 1990; Pfefferbaum et al., 1994; Reiss et al., 1996), with frontal association fibres showing continued development into early adulthood according to longitudinal DTI (Lebel and Beaulieu, 2011), leaving them susceptible to environmental influence and epigenetic changes that may play a role in abnormal adolescent brain development in FASD.

This FASD group was impaired on a number of academic and executive functioning domains at both time points, despite average IQ scores (measured in 53% of the FASD sample). Longitudinal increases in raw cognitive scores (albeit without changes in age-corrected standard scores) suggest that the FASD group made cognitive gains at a typical rate with age, while still performing below average. Negative correlations of Δ MD in the SLF with increased gains in Word ID score fit with the putative role of this tract in language functioning (Brauer et al., 2011; Hoeft et al., 2011; Steinbrink et al., 2008), but have not been previously demonstrated in FASD. Correlations between Δ MD in the SFO with both increased reading and receptive vocabulary score also suggest a role for this tract in language development. Correlations with cognitive improvement provide evidence that steep decreases of MD in these tracts are functionally relevant in FASD; it is notable that SFO and SLF are the last association tracts to reach an MD plateau in healthy development (Lebel et al., 2008b) and thus may be even further delayed in FASD.

Given that microcephaly is a hallmark feature used to diagnose FASD, it is not surprising that smaller brain volumes are noted in almost every structural MRI study including this one. Of

note, the largest group difference was observed in the caudate (18% reduction in FASD), in agreement with 2 recent studies showing ~20% reductions of caudate volume (Astley et al., 2009b; Fryer et al., 2012); though these studies also demonstrate correlations with neurocognitive scores (Fryer et al., 2012) and diagnosis severity (Astley et al., 2009b). Reductions in cortical grey matter, white matter, thalamus, globus pallidus, and putamen volumes in this study remained significant after controlling for total brain volume, and have also been reported as disproportionately reduced in other samples (Archibald et al., 2001; Roussotte et al., 2011). Age-related increases in total brain, white matter, globus pallidus and amygdala volumes were observed in the control group in agreement with typical development (Brain Development Cooperative Group, 2011; Giedd et al., 1999; Giedd et al., 1997; Lenroot et al., 2007), but lack of significant age effects in the FASD group suggests delayed growth (though note age-by-group interactions were not significant). Nonetheless, persistent volume reductions compared to controls at both scans confirm that volume reductions are not mitigated during development. A recent longitudinal study of cortical volume development in 70 subjects with pre-natal alcohol exposure found reduced cortical plasticity (Lebel et al., 2012b), revealing age-by-group interactions of volume trajectory with alcohol-exposed participants showing flatter developmental curves than controls. Notably, smaller volume changes between scans were associated with lower IQ and greater facial dysmorphology at scan 1.

Many children with FASD experience both prenatal alcohol exposure and adverse post-natal environments, in some cases including abuse, neglect and multiple home placements, which likely compound alcohol-related brain abnormalities and may even act through independent mechanisms (McCrory et al., 2010; Streissguth et al., 2004). In addition to often unknown variability in the degree and timing of pre-natal alcohol exposure, these other adverse

life experiences complicate associations between prenatal alcohol exposure and adolescent brain development in human studies (as opposed to well controlled pre-clinical animal models). This study only included children in currently stable home placements (those who had moved placements between scans could not be located for follow up) and required participants to tolerate the MRI scanner and provide adequate data at least twice, potentially excluding more severely affected children. We found no difference between groups on annual household income or primary caregiver education, suggesting roughly matched socioeconomic status at the time of MRI study participation; however, we cannot rule out the influence of numerous other possible disparities, including adverse early life experience, poly-substance exposures, and unknown genetic factors that could influence sensitivity to alcohol-induced brain injury (Warren and Li, 2005). Ethnicity was not balanced between groups in this study, which may also confer systematic genetic differences, though brain volume reductions of our sample are on par with those of larger more ethnically diverse samples (Astley et al., 2009a). Finally, the relatively small sample size of this study required that we approximate a linear fit to the data despite converging evidence that development is non-linear (Giedd et al., 1999; Lebel et al., 2008b), and combining left and right tracts may have masked hemispheric asymmetries. Nonetheless, the longitudinal design of this study overcomes many limitations of previous studies, as it identifies changes within individuals, increasing power and reducing the effects of subject variation. Future studies should aim to test trajectory differences between FASD diagnostic sub-groups as well as other environmental and subject variables including ethnicity, age at diagnosis, history of abuse and home stability.

In this novel longitudinal DTI study over the ages of 5-15 years, participants with FASD demonstrated increases of FA and reductions of MD associated with typical white matter

development, albeit with regional differences in rate and magnitude. Steeper decreases of MD in three frontal association tracts in FASD may reflect delayed white matter development, but may also suggest compensatory plasticity. Participants with FASD had persistently smaller brain volumes than controls, confirming that these reductions are not mitigated nor exacerbated during development. Observed deviations from the typical trajectory of neurodevelopment during childhood and adolescence may underlie secondary deficits that emerge during this critical period.

5 Longitudinal Cortical Development in FASD³

Abstract

Brain imaging studies suggest that cortical thickness decreases during childhood and adolescence, in concert with underlying structural and synaptic changes required for cognitive maturation and regional specialization of function. Abnormalities of this protracted developmental process may provide key insights into the cognitive and behavioural deficits that emerge in individuals with fetal alcohol spectrum disorders (FASD). Several studies have demonstrated cortical thickness differences in children and adolescents who were prenatally exposed to alcohol, though all have been cross-sectional, limiting conclusions about cortical development. In this study we analyze serially collected T1-weighted MRI from 11 children with FASD and 21 controls, scanned twice each ~2-4 years apart. Mixed-models analysis of cortical thickness measurements revealed age-by-group interactions in cortical thinning, with FASD participants undergoing less developmental thinning than controls across many regions of the cortex, particularly in medial frontal and parietal areas. These results provide further longitudinal evidence in humans that prenatal alcohol exposure is associated with altered patterns of brain development that persist during childhood and adolescence.

³ A version of this chapter has been published. Treit S, Zhou D, Lebel C, Rasmussen C, Andrew G, Beaulieu C (2014). Longitudinal MRI Reveals Impaired Cortical Thinning in Children and Adolescents Prenatally Exposed to Alcohol. *Human Brain Mapping* 35(9):4892-4903.

5.1 Introduction

Cortical brain maturation is a dynamic process, marked by widespread progressive and regressive change during the course of human development. This process begins prenatally with massive proliferation and migration of neurons countered by ensuing waves of apoptosis, continues both pre and post-natally with the projection of axons and establishment of new synapses, and culminates in adolescence and thereafter with the subsequent pruning of these synaptic connections to refine neural networks. Cortical thickness, defined as the distance between the pial-cortical and grey matter-white matter borders on MRI scans, is a widely studied *in-vivo* measure of cortical morphology that has been reported to undergo an inverted U shaped trajectory in childhood and is presumed to follow in concert with these critical cellular transitions (Raznahan et al., 2011). Longitudinal studies of healthy development suggest that cortical thinning accelerates during adolescence (Shaw et al., 2008) and correlates with cognitive performance (Shaw et al., 2006a; Sowell et al., 2004), which may reflect regional specialization of cognition during development. Although genetic influence on cortical development has been demonstrated (Raznahan et al., 2012; van Soelen et al., 2012), less is known about the extent to which this pattern of adolescent cortical maturation may be disrupted by specific environmental teratogens, such as prenatal alcohol exposure.

Prenatal alcohol exposure damages the developing fetal brain via numerous mechanisms, including neuronal proliferation and migration errors, transcription factor down-regulation, hypoxia and cell death (Goodlett et al., 2005), which can result in a range of physical, cognitive and behavioural deficits known as fetal alcohol spectrum disorders (FASD). With an estimated prevalence of 1 in 100, FASD is the leading cause of preventable developmental disability in North America (May and Gossage, 2001; May et al., 2009). In addition to primary deficits such

as impaired learning, memory and executive functioning, individuals with FASD have high rates of secondary deficits (trouble with the law, substance abuse, etc.) (Streissguth et al., 2004), which have detrimental consequences for individuals, families and society. Longitudinal studies of white matter development (Treit et al., 2013) and cortical volume (Lebel et al., 2012b) in children with prenatal alcohol exposure have revealed altered trajectories of maturation during adolescence, further suggesting that key postnatal developmental processes may also be disrupted in alcohol-exposed children.

Four published cross-sectional studies have investigated cortical thickness in children with prenatal alcohol exposure, with three finding increased cortical thickness (Fernandez-Jaen et al., 2011; Sowell et al., 2008b; Yang et al., 2011) and one finding reduced cortical thickness (Zhou et al., 2011) relative to typically developing controls. One of these studies found both increased thickness and positive correlations with cognitive scores in the FASD group (whereby thinner cortex related to poorer performance on verbal recall and memory scores) (Sowell et al., 2008b), further complicating interpretation of these contrasting results. Moreover, the influence of other postnatal developmental processes (e.g. synaptic pruning, myelination) on the evolution of these observations must be considered, and may partially explain conflicting observations between these cross-sectional studies.

The purpose of the present study is to elucidate the developmental trajectory of cortical thinning in children and adolescents with FASD in order to further characterize patterns of brain development during this critical period.

5.2 Materials and Methods

5.2.1 Participants

Eleven children with FASD (four females and seven males, scanned at ages ranging from 6.1-15.4 years of age) and 21 controls (10 females and 11 males, ranging from 5.7-14.4 years) underwent two MRI scans each, 2-4 years apart, for a total of 64 scans (Table 1). Participants with FASD were recruited from a hospital FASD diagnostic clinic, had confirmed prenatal alcohol exposure and were previously medically diagnosed with an alcohol related disorder falling under the FASD umbrella using the 4-digit code (Astley, 2004) in accordance with the Canadian Guidelines for diagnosis of FASD (Chudley et al., 2005). Assessments were conducted by a multi-disciplinary team (psychologist, speech language pathologist, occupational therapist, social worker and pediatrician), who carefully reviewed evidence from standardized testing, clinical interview, medical chart review, physical exam, etc in order to assess each child in 4 major domains: growth deficiency, facial dysmorphology, central nervous system dysfunction and alcohol exposure, with careful consideration of pre and post-natal factors in the differential diagnosis of an FASD. One subject had a diagnosis of fetal alcohol syndrome, three had partial FAS, two had static encephalopathy alcohol exposed, four had neurobehavioural disorder alcohol exposed, and one had FASD that was not further specified. Given the small number of subjects, all sub-diagnoses were collapsed to form one “FASD” group for statistical analysis. Control subjects were screened for psychiatric and neurological impairments, as well as contraindications to MRI. All FASD subjects and 19/21 control subjects were included in our previous longitudinal diffusion tensor imaging study (Treit et al., 2013); though note that fewer subjects are included here due to MPRAGE image quality issues. Nine of 11 FASD subjects had scan one data that was included in both Lebel et al (2008a) and Zhou et al (2011), two FASD subjects had

scan 1 data included in Zhou et al 2011 but not Lebel et al 2008, and all control participant scans were from Lebel and Beaulieu's previous study of healthy longitudinal white matter development (Lebel and Beaulieu, 2011). Written informed consent was obtained from each participant's parent/legal guardian, and written assent was collected from all participants prior to study procedures. This study was approved by the Health Research Ethics Board at the University of Alberta.

5.2.2 Cognitive Testing and Demographics

Both the FASD and control participants were administered the Woodcock Reading Mastery-Revised (WRMT-R) Word ID at both scans. In addition, the FASD group (but not controls) were also administered the Woodcock Johnson Quantitative Concepts (18A&B), Working Memory Test Battery for Children (WMTB-c) Digit and Block, Comprehensive Receptive and Expressive Vocabulary Test (CREVT), and NEPSY Arrows, Auditory Attention and Response Set and Memory for Names. IQ was also collected in a subset of FASD participants (n=7) at scan 2 using the Wide Range Intelligence Test (WRIT, Glutting, 2000). One sample t-tests were used to determine if standard score were different from population norms (test-value of 100 for all tests except NEPSY; test value 10). Demographic data were collected via questionnaire completed by parents/caregivers at scan two for the FASD participants, and retrospectively by phone interview for controls (though note only 14 of 21 controls were reached).

5.2.3 Image Acquisition

All data at both time-points were acquired using identical methods on the same 1.5T Siemens Sonata MRI scanner. Scans included diffusion tensor imaging, T1-weighted, T2-weighted, fluid-attenuated inversion recovery (FLAIR), and FLAIR-DTI imaging for a total scan time of ~26 minutes. Head motion was minimized using ear pads. T1-weighted images for

cortical thickness measurements were acquired using a high resolution ($1 \times 1 \times 1 \text{ mm}^3$) MPRAGE sequence with: TR=1870 ms, TE=4.38ms, TI=1100 ms, FOV $220 \times 220 \text{ mm}^2$, flip angle 15° , scan time 4:29 minutes.

5.2.4 Image Processing and Statistics

Images were manually quality checked for gross abnormalities or image artifacts and then processed using the CIVET 1.1.11 pipeline with normalization to the ICBM-152 template to obtain cortical thickness, total brain volume, white matter and grey matter volumes for each scan. Cortical thickness was measured across 40,962 vertices per hemisphere, and smoothed using a kernel of 20 mm full width at half maximum that preserves cortical topology. Cortical surface data were then segmented to 39 areas per hemisphere with an automated anatomical labelling (AAL) template (Tzourio-Mazoyer et al., 2002), averaging all vertices within each region. AAL regions were used for all statistical analysis in order to reduce multiple comparisons and increase signal-to-noise compared to over 80,000 vertices. Statistical analyses were carried out in SurfStat and SPSS 18.0. Change of cortical thickness and volumes with age and by group (FASD versus control), and age-by-group interactions were determined for each AAL region using linear mixed-model: cortical thickness (mm) or volume (cm^3) = intercept + a*age + b*group + c*interaction (age x group) + residual, controlling for sex and handedness. Single time-point group differences in volume and total mean thickness were tested controlling for age, sex and handedness. Mixed models analysis was chosen for its ability to handle longitudinal data sets with varied spacing between measurements. P-values of <0.05 were considered significant.

To investigate the relationship between cognitive ability and cortical development, partial correlations were performed between Δ cognitive score (raw score scan 2 – raw score scan 1) and Δ cortical thickness (thickness at scan 2 – thickness at scan 1) for each AAL region, controlling

for mean age and time between scans. Cognitive scores included WRMT-R Word ID, WJ Quantitative Concepts, WMTB-c (digit and block averaged), and CREVT (receptive and expressive scores averaged). NEPSY and WRIT IQ scores were excluded from correlation analysis due to the small number of subjects with scores at two time points (n=7). Given the large number of correlations performed, p-values were false-discovery-rate (FDR) corrected to correct for multiple comparisons, with significance at $q < 0.05$.

5.2.5 Sub-Sample Comparison

To confirm that results do not stem from power differences between groups (n=11 versus n=21), analysis of age effects and age-by-group interactions were repeated with a subset of 11 controls chosen from the full sample of 21, matched as closely as possible for age, time between scans, and sex (mean age at scan1: 8.9 ± 1.8 for FASD and 8.4 ± 1.6 for Controls; scan 2: 12.0 ± 2.2 for FASD and 12.0 ± 1.6 for Controls; time between scans 3.1 ± 0.9 years for FASD and 3.6 ± 0.8 years for Controls, 4 females and 7 males in each group). Analysis of this sub-sample was carried out using identical statistical methods as described above.

5.3 Results

5.3.1 Demographic and Cognitive Scores

Control and FASD participants did not differ in median household income (\$76-100,000/year) or primary caregiver level of education (over half had some university to graduate degrees), though caregiver status differed between groups with 100% of controls in their biological homes, and 100% of the FASD group in either foster, adoptive, or kinship home placements. Ninety-three percent of the control sample was Caucasian, whereas 46% of the FASD sample was Caucasian (54% were Aboriginal). IQ was only measured in 7 FASD subjects

at scan 2 (none at scan 1 or at either time-point in the control group), yielding a mean score of 94 ± 13 , which was not significantly different from the population norm of 100 (one sample t-test, $p=0.160$) (Table 5.1), though it should be noted that power to detect a difference from the norm is reduced in only 7 subjects. The WRMT-R Word ID test yielded significantly lower standard scores in the FASD than control group at both scans (scan one: FASD 94 ± 9 , Controls 111 ± 14 , $p=0.024$; scan two: FASD 91 ± 14 , Controls 108 ± 12 $p=0.019$), though scores were only significantly different from the population norm (100) at scan 2. Likewise, the FASD group scored significantly below population norms on the WMTB digit and block at both scans, receptive and expressive vocabulary at both scans, WJ Quantitative Concepts (mathematics) at scan 2, NEPSY Auditory Attention and Response Set at scan 1, and NEPSY memory for names at scan 2 (Table 5.1).

Table 5.1: Participant characteristics, demographic information and cognitive scores

Participant Characteristics:			FASD (n=11)	Control (n=21)
Age in years: mean \pm SD (range)	Scan 1:		8.9 \pm 1.8 (6.1-11.8)	8.1 \pm 1.3 (5.7-10.7)
	Scan 2:		12.0 \pm 2.2 (9.1-15.4)	11.8 \pm 1.6 (7.4-14.4)
Time between scans: mean \pm SD (range)			3.1 \pm 0.9 (1.6-3.9)	3.7 \pm 0.7 (1.7-4.2)
N males: n (%)			7 (64%)	11 (52%)
Cognitive Testing:				
Woodcock Reading	Word ID	Scan 1	95 \pm 9	111 \pm 14
Mastery Test-Revised (n=11; 18)		Scan 2	91 \pm 13 [†]	109 \pm 12
Working memory test battery for children (n=10)	Digit	Scan 1	90 \pm 8 [†]	---
		Scan 2	88 \pm 13 [†]	---
	Block	Scan 1	83 \pm 17 [†]	---
		Scan 2	85 \pm 16 [†]	---
Woodcock Johnson Quantitative Concepts (n=10)	18A&B	Scan 1	90 \pm 15	---
		Scan 2	89 \pm 12 [†]	---
Comprehensive Receptive and Expressive Vocabulary Test (n=11)	Receptive	Scan 1	90 \pm 7 [†]	---
		Scan 2	94 \pm 8 [†]	---
	Expressive	Scan 1	85 \pm 16 [†]	---
Scan 2		85 \pm 12 [†]	---	
NEPSY I/II (n=7)	Arrows	Scan 1	8.8 \pm 2.4	---
		Scan 2	10.4 \pm 3.3	---
	Auditory Attention	Scan 1	5.1 \pm 4.1 [†]	---
		Scan 2	7.7 \pm 3.7	---
	Response Set	Scan 1	7.0 \pm 2.5 [†]	---
		Scan 2	8.8 \pm 4.0	---
Memory for Names	Scan 1	8.6 \pm 3.8	---	
		Scan 2	7.0 \pm 3.2 [†]	---
Wide Range Intelligence Test (n=7)	Composite IQ	Scan 1	---	---
		Scan 2	94 \pm 13	---

[†]Significantly different from population norm at p<0.05

5.3.2 Brain Volume and Cortical Thickness Trajectories

Compared to controls, FASD participants had consistently reduced volumes of total brain (-13%, $p < 0.001$ scan 1; -13%, $p < 0.001$ scan 2), white matter (-15%, $p < 0.001$ scan one; -18%, $p < 0.001$ scan two) and grey matter (-11%, $p < 0.001$ scan one; -10%, $p < 0.001$ scan two). Raw volumes are not presented here, but comparable values in our larger cohort can be found in our longitudinal DTI paper (Treit et al., 2013). Longitudinally, mixed-models analysis in each group revealed decreases of grey matter volume and increases of white matter volume with age in both groups ($p < 0.001$ for all) and no significant change with age for total brain volume in either group. Mixed-models analysis with both groups analyzed together did not reveal significant age-by-group interactions for any volumes, suggesting similar volume growth rates between groups.

After correcting for sex and handedness, the FASD group had lower total mean cortical thickness than controls at scan one but not scan two (-3%, $p = 0.026$ scan 1; -0.4%, $p = 0.300$ scan 2). Mixed-models analysis performed separately in each group revealed significant age-related decreases of total mean thickness in the control ($p < 0.001$) but not FASD group, and repeating the analysis across both groups revealed a significant age-by-group interaction for total mean thickness ($p = 0.044$; Figure 1). Figure 5.2 shows example individual cortical thickness maps for one control and one FASD participant, both scanned ~4 years apart (~7 years old at scan 1 and ~11 years old at scan 2). Both maps show similar patterns of cortical thickness, e.g. thicker medial frontal cortex, thinner visual cortex, etc (Figure 5.2A-B, D-E), but the degree of thinning between scans is notably greater in the control subjects (Figure 5.2C). The FASD subject maps show fewer regions with reduced cortical thickness between scans, and many regions that show little change or potentially even increases in thickness (Figure 5.2F).

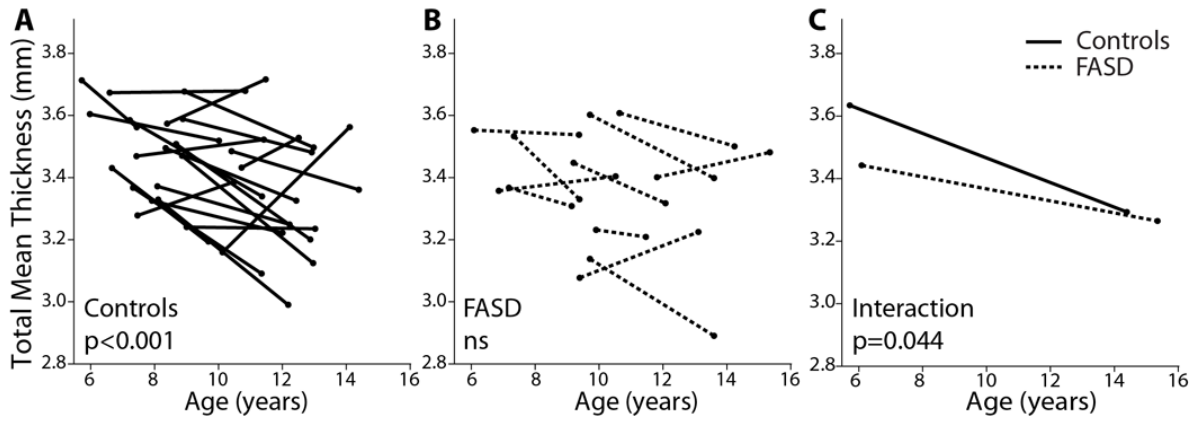


Figure 5.1: Total mean thickness by group. Leftmost plots (A-B) show thinning trajectories of control subjects (solid lines) and FASD subjects (dotted lines) by age. A significant effect of age is found in the controls ($p < 0.001$) but not the FASD group (ns). A significant age-by-group interaction (C) ($p = 0.044$) indicates a difference in the rate of thinning between groups, with controls undergoing steeper rates of age related thinning than FASD participants.

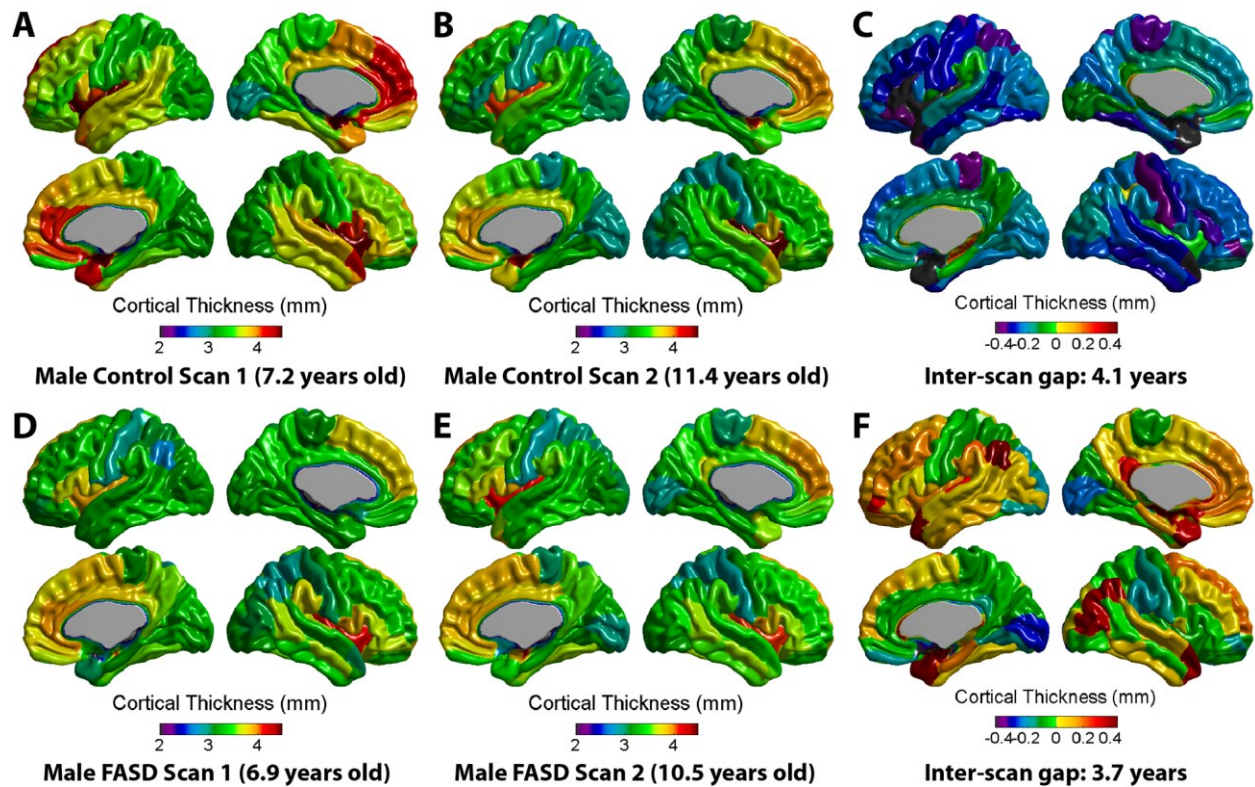


Figure 5.2: Individual subject maps. Examples of individual subject cortical thickness maps. Top panel (A-C) displays cortical thickness maps at scan 1 (7.2 years) and scan 2 (11.4 years) as well as the difference map (scan 2 – scan 1, gap=4.1 years) for a male control participant. Below (D-F) is an example of a male FASD participant aged 6.9 years at first scan and 10.5 years at second scan, (inter-scan gap = 3.7 years). Although general patterns of cortical morphology are similar between these two individuals, the control participant has a thicker cortex in many areas at both scans, and undergoes more thinning (areas in blue, purple or green on far right) between scans. Of note, several areas in the FASD subject appear to lack cortical thinning, but rather show little change or even increases in thickness between scans.

When the cortex was subdivided according to AAL regions within the entire sample, significant age-related thinning was found extensively in 65 of 78 (83%) cortical sub-regions in the control group, but only in 9 of 78 regions (12%) in the FASD group (Figure 5.3). Of the regions with significant age-related thinning in the FASD group, most were in the right temporal and parietal lobes. No regions significantly increased in thickness from scan 1 to scan 2 in either the FASD or control group. Significant age-by-group interactions were found in 16/78 regions (21%), indicating a steeper slope of thinning in controls than in the FASD group (Table 5.2,

Figures 5.3 & 5.4). The majority of age-by-group interactions were found in medial frontal and parietal regions. As seen in Figure 5.4, in addition to steeper decreases in the control group, a greater amount of inter-subject variability can be seen in the FASD group; e.g. in the left medial superior frontal gyrus (Figure 5.4B), where it appears that ~15/21 (71%) of control participants undergo decreases in thickness between scans, 5/21 (24%) stay about the same and 1/21 (5%) show increased thickness, whereas in the FASD group only about 5/11 (45%) decrease and the remaining show no change (2/11, 18%) or increases in thickness between scans (4/11, 36%) in this region.

Table 5.2: AAL regions with significant age-by-group interactions of cortical thickness between controls and FASD

		Age-by-Group Interaction p-values	Slope (mm/year)	
			Controls	FASD
Total Mean Thickness:		0.044	-0.04	-0.02
Frontal:	Right Superior frontal gyrus dorsolateral	0.014	-0.06	-0.01
	Left Superior frontal gyrus medial	0.008	-0.06	0.01
	Right Superior frontal gyrus medial	0.026	-0.06	0.00
	Right Middle frontal gyrus	0.026	-0.04	-0.02
	Left Supplementary motor area	0.004	-0.04	-0.01
	Right Supplementary motor area	0.024	-0.05	-0.03
	Right Inferior frontal gyrus orbital part	0.038	-0.06	-0.01
Parietal:	Left Superior parietal gyrus	0.027	-0.05	-0.04
	Left Precuneus	0.003	-0.04	-0.02
	Left Paracentral lobule	0.017	-0.06	-0.04
	Right Paracentral lobule	0.015	-0.07	-0.05
Occipital:	Left Middle occipital gyrus	0.019	-0.05	-0.02
	Left Superior Occipital Gyrus	0.013	-0.05	-0.03
Limbic:	Right Anterior cingulate & paracingulate gyri	0.016	-0.05	-0.02
	Left Median cingulate & paracingulate gyri	0.029	-0.02	-0.00
	Right Medial cingulate & paracingulate gyri	0.029	-0.03	-0.02

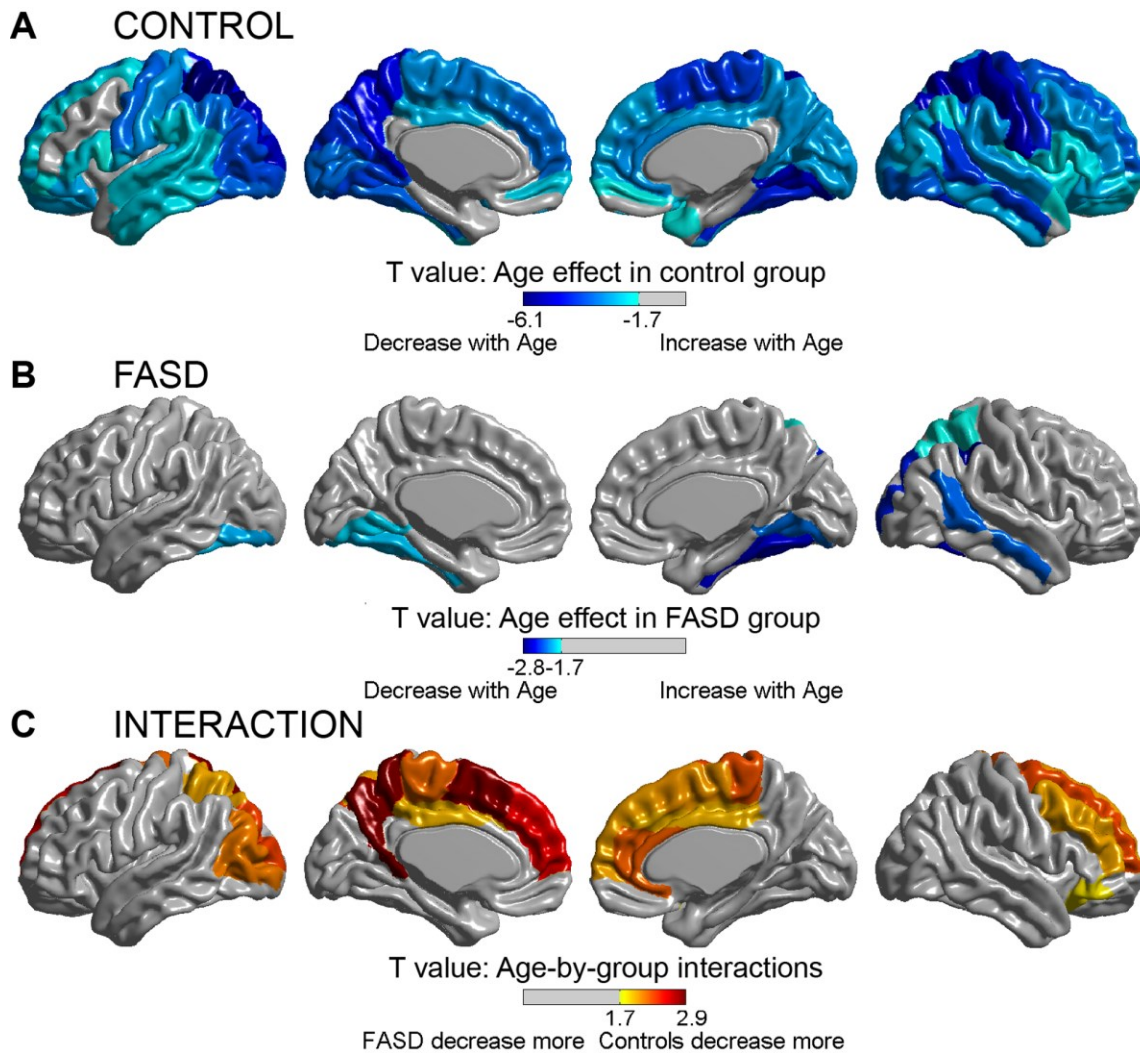


Figure 5.3: Thinning patterns across the cortex. Regional age effects and age-by-group interactions on cortical thinning. The top two panels display AAL regions with significant effects of cortical thickness with age in the control (A) and FASD (B) groups. Significant effects of age (decreasing thickness with increasing age) are seen across most of the cortical mantle in the control group (A), but are limited to discrete temporal and parietal regions, mostly right hemisphere, in the FASD group (B). Likewise, several regions with significant age-by-group interactions are found (C), indicating regional differences in the rate of change with age, with the FASD group undergoing less thinning than controls between scans.

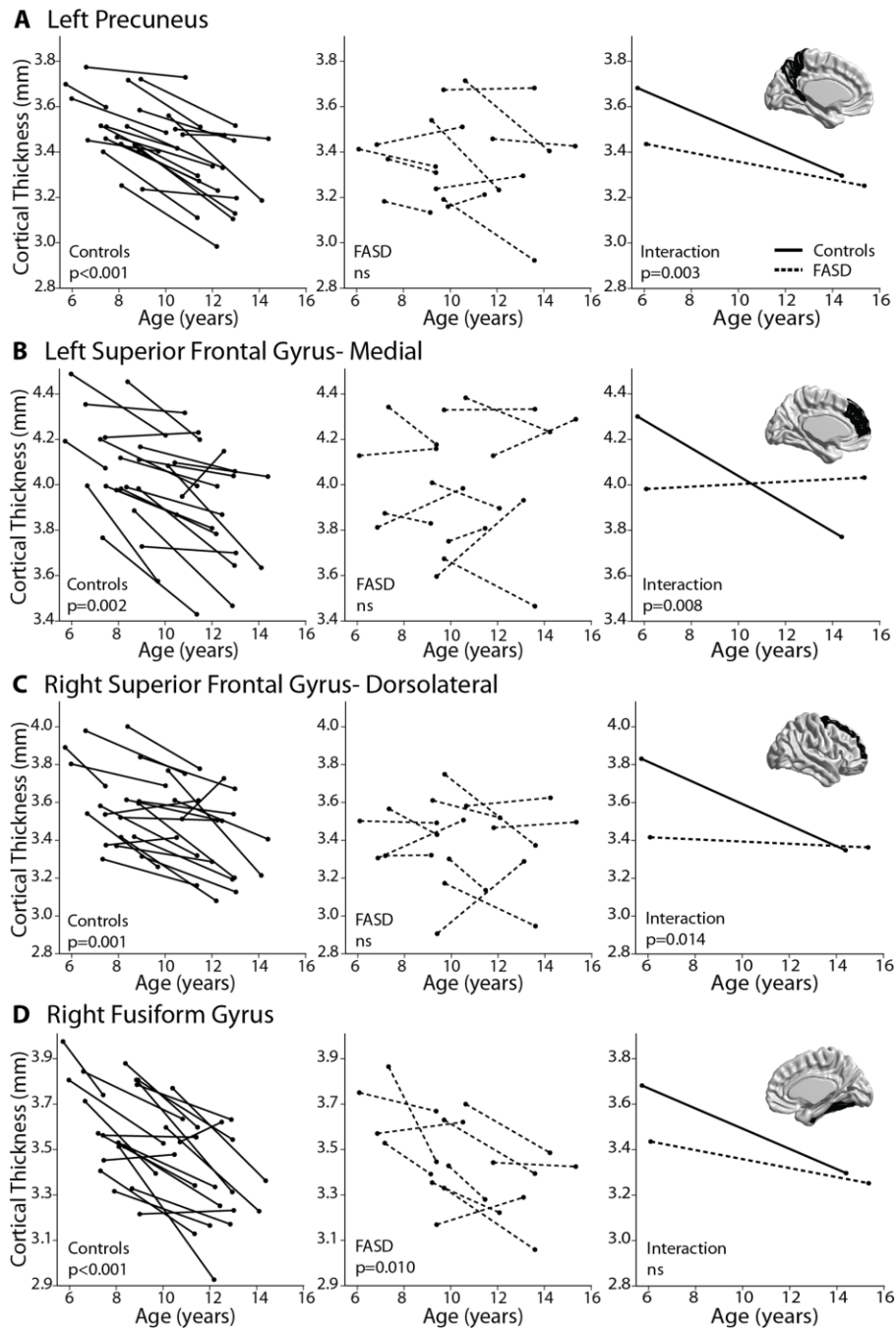


Figure 5.4 Age-by-group interactions: Examples of significant regional age-by-group interactions (A-C) and a contrasting example showing significant thinning in both groups with no significant interaction (D). Age-effects are shown in the first column for controls (solid lines) and second column for FASD participants (dotted lines), followed by age-by-group interactions in the 3rd column. Regions include the left precuneus (A), left superior frontal gyrus medial (B), right superior frontal gyrus dorsolateral (C) and right fusiform gyrus (D). In addition to significant thinning that is found in the control but not FASD group for A-C, individual subject data also provides a visual of the increased variability found in the FASD group relative to the robust cortical thinning between scans seen in controls.

5.3.3 Sub-Sample Comparisons

Sub-sample analysis (11 versus 11) yielded similar findings to Figure 5.3, with near whole brain cortical thinning between scans in controls, and similar patterns of significant age-by-group interactions that spanned 13 of 78 (17%) cortical regions (data not shown).

5.3.4 Relationship between Cortical Thickness and Cognition

There were no significant correlations between change in cognitive score and change in cortical thickness in either group after FDR correction.

5.4 Discussion

This longitudinal study demonstrates an altered trajectory of brain development in individuals diagnosed with an FASD, who are shown here to undergo less developmental cortical thinning than healthy controls in several brain regions during childhood and adolescence. Cortical thinning is an essential developmental process that begins in early childhood and continues into adulthood at varying rates and magnitudes across the cortical mantle (Raznahan et al., 2011; Shaw et al., 2008; Sowell et al., 2004). This process is thought to be primarily driven by synaptic pruning and myelination of underlying white matter, mechanisms that contribute to the refinement of neural networks and specialization of cognitive functions within the cerebral cortices. Abnormal cortical thinning during critical periods of childhood and adolescence may underlie deficits in behaviour and cognition that are commonly observed in those prenatally exposed to alcohol.

Age-by-group interactions indicate that the FASD group underwent less cortical thinning than controls, primarily in frontal, parietal and limbic regions. These areas undergo protracted

thinning trajectories in healthy development (Tamnes et al., 2010), and are commonly associated with higher level aspects of cognition such as emotional regulation and executive functioning. Previous structural MRI studies have uncovered various frontal and limbic abnormalities in FASD (Lebel et al., 2011), including abnormal cortical thickness (Sowell et al., 2008b; Yang et al., 2011), though longitudinal thinning trajectories have not been previously demonstrated in FASD. Slower rates of thinning measured longitudinally in frontal and cingulate gyri have been shown to account for normal variation in Attention Deficit Hyperactivity Disorder (ADHD) symptomatology within typically developing children (Shaw et al., 2011), and may relate to ADHD co-morbidity frequently observed in FASD (note that 10 of 11 FASD subjects here had ADHD). A recent longitudinal study of cortical volume development in FASD demonstrated that change in volume of the left posterior cingulate gyrus, parahippocampal gyrus, and insula negatively correlated with number of drinks per week during pregnancy, varying by trimester of exposure (Lebel et al., 2012b). These findings highlight the impact of quantity and timing of gestational exposure on subsequent development in childhood, which may contribute to contrasting results in previous cross-sectional studies that have included varied clinical severities under the FASD umbrella. Although mean age has been similar across previous cross-sectional cortical thickness studies (Fernandez-Jaen et al., 2011; Sowell et al., 2008b; Yang et al., 2011; Zhou et al., 2011), other differences, such as the proportion of participants with full FAS (ranging from ~10% (Zhou et al., 2011) to 100% (Fernandez-Jaen et al., 2011)), presence of co-morbid ADHD (ranging from ~30% (Yang et al., 2011; Zhou et al., 2011) to 100% (Fernandez-Jaen et al., 2011)) and mean IQ, (65 in (Yang et al., 2011), not reported in others) may also contribute to inconsistent findings.

Age-by-group interactions emphasize the value of longitudinal data in uncovering trajectories that may have been masked in previous cross-sectional studies. Given the interaction of thinning trajectories shown here, further measurements of this sample at older ages may again be expected to diverge, with FASD subjects having thicker cortices than controls in agreement with previous cross-sectional findings by other groups (Fernandez-Jaen et al., 2011; Sowell et al., 2008b; Yang et al., 2011). Thus both longitudinal and cross-sectional findings may reflect impaired cortical thinning. Rates of cortical thinning, rather than absolute thickness values, have been shown to correlate with intellectual ability in healthy development (Shaw et al., 2006a), and have also been valuable for differentiating numerous disorders including ADHD (Shaw et al., 2007) and the emergence of psychopathology (Wood et al., 2008). Together with longitudinal volume findings (Lebel et al., 2012b), our results suggest that reduced cortical change during childhood may be a marker of pathology in alcohol-exposed children.

In our recent longitudinal diffusion tensor imaging (DTI) study (which includes the sample presented here), the FASD group underwent larger decreases of mean diffusivity (MD) between scans than the control group; changes that we attributed to delayed development (Treit et al., 2013). Although cortical thinning and DTI parameters are driven in part by convergent mechanisms (e.g. myelination), they follow distinct trajectories during development (Tamnes et al., 2010). DTI studies have demonstrated non-linear decreases of MD throughout healthy childhood, with an eventual plateau in early adulthood and subsequent increases thereafter (Bava et al., 2010; Lebel and Beaulieu, 2011); whereas cortical thickness is typically shown to plateau or decrease slightly during childhood (Raznahan et al., 2012) and then subsequently undergo accelerated thinning during adolescence (Shaw et al., 2008). In keeping with the model of delayed development proposed in our DTI study, here we find relatively less cortical thinning

during adolescence (patterns typical of early childhood), which we may expect to accelerate during late adolescence /early adulthood after the majority of developmental cortical thinning is complete in the control sample if we were to continue following this FASD group. Age-by-group interactions found here were mostly in medial parietal and frontal regions in proximity to the white matter tracts implicated in our DTI paper (namely, the superior longitudinal fasciculus and the superior and inferior fronto-occipital fasciculus). Thus, although the direction of age-by-group interactions are opposite between these two imaging parameters, we predict that they are in fact complimentary and both reflect underlying delays of cellular brain development. Moreover, the slowed thinning in medial aspects of the cortex fit with many previous reports of midline abnormalities resulting from alcohol exposure (Bookstein et al., 2002a), which are thought to reflect disrupted cellular proliferation and migration patterns during development and may underlie relationships between midline brain abnormalities and facial dysmorphology in FASD (Yang et al., 2011).

Animal models of prenatal ethanol exposure have demonstrated numerous cortical abnormalities that may underlie the thickness reductions observed in cross sectional human studies (Zhou et al., 2011), including decreased cell proliferation rates (Miller, 1989; Miller and Nowakowski, 1991), delayed neuroblast migration (Aronne et al., 2008), apoptosis (Farber et al., 2010; Ikonomidou et al., 2000), altered synaptic architecture (Cui et al., 2010), disruption of laminar organization (Kotkoskie and Norton, 1988), and reductions in overall thickness (Aronne et al., 2008; Aronne et al., 2011; Fakoya and Caxton-Martins, 2006; Norton et al., 1988). Although informative, most animal models have examined the neonatal or early post-natal periods, with less focus on subsequent cortical development. One recent study of cortical development in a rat model of FASD demonstrated reduced cortical thickness in ethanol exposed

rats across developmental periods (Leigland et al., 2013) in support of some human work (Zhou et al., 2011), though imaging was cross-sectional and there were no age-by-alcohol group interactions. Pre-natal ethanol exposure is shown to impair experience-dependent synaptic plasticity in both the cerebellum (Servais et al., 2007) and hippocampus (Puglia and Valenzuela, 2010; Zucca and Valenzuela, 2010), which results in motor and memory impairments in these models. Similar mechanisms may also disrupt synaptic plasticity in the cortex (Medina, 2011), which could underlie both reduced thinning found longitudinally and increased thickness found in some previous cross-sectional studies. The transition from synaptogenesis to synaptic pruning in human cortical development is at least partially mediated by modification of glutamatergic receptors (Stoneham et al., 2010) and GABA signalling (Wu et al., 2012), neurotransmitter systems which are disrupted in FASD (Costa et al., 2000; Cuzon et al., 2008) and thus may mediate cortical thinning abnormalities. Direct experimental models are needed to determine the effects of prenatal ethanol exposure on synaptic pruning during development. MRI measurements of cortical thickness rely on T1-weighted tissue contrast, which is influenced by numerous cellular factors and may not reflect the cortex *per se*, as would be measured directly with histological measurement. However, previous work comparing histological and MRI derived measures of cortical thickness suggest that reduced thickness is found in prenatally exposed rats using both methods (Leigland et al., 2013).

Determining a direct relationship between alcohol-induced prenatal brain damage and subsequent abnormal cortical development during childhood is challenging in humans. Timing and quantity of exposure likely interact with a host of environmental and genetic factors to produce the wide range of phenotypic and neurological outcomes under the FASD umbrella, resulting in considerable heterogeneity within and between FASD samples. Likewise, the

influence of ADHD co-morbidity on cortical development could not be teased apart here, as 10 of 11 FASD participants also had ADHD, in keeping with co-occurrence estimates >70% in FASD samples (Burd et al., 2003; Fryer et al., 2007). Cortical thickness studies in idiopathic ADHD (without prenatal alcohol exposure) have yielded somewhat inconsistent findings (Almeida et al., 2010; Duerden et al., 2012; Montes et al., 2013; Narr et al., 2009; Shaw et al., 2006b; Shaw et al., 2013), and suggest that this complex relationship may be mediated by age, sex, ADHD subtype (Montes et al., 2013; Shaw et al., 2013), IQ (de Zeeuw et al., 2012) and stimulant use (Shaw et al., 2009), among other variables. Studies of children with both FASD and ADHD suggest that prenatal alcohol exposure exerts a greater influence than ADHD on neurocognitive measures (Glass et al., 2013; Mattson et al., 2013) and cortical thickness (Fernandez-Jaen et al., 2011); however, the underlying mechanisms of their co-occurrence remain elusive. Future large longitudinal studies must endeavour to tease apart the influence of co-morbid ADHD on cortical development in alcohol exposed children.

Significant adverse life experiences are common to individuals with FASD (Streissguth et al., 2004), and likely compound deficits from alcohol exposure or even alter brain development through independent mechanisms (McCrorry et al., 2010). Indeed, this study is limited by differences in home placement between control and FASD participants, which may reflect confounding environmental factors such as early life adversity. We found no difference in primary caregiver education or annual household income between our FASD and control groups, indicating no gross disparity in present living situation, but were not able to assess previous placements. Thus, prenatal alcohol exposure is a common denominator of subjects with FASD, but an abundance of environmental influences (both positive and negative) must also be considered. Ethnicity was imbalanced between groups, partly resulting from recruiting our

FASD sample from a hospital diagnostic clinic that serves both urban and rural areas, whereas our control group came from advertising in the community and schools exclusively within the city. Nonetheless, other studies with more ethnically diverse FASD and control samples (Astley et al., 2009a; Lebel et al., 2012b), and more ethnically matched samples (Coles et al., 2011b) have reported reductions in brain volume between FASD and controls on par with those found in this sample. These groups also differ in sex distribution (Table 5.1, 64% male FASD, 52% male controls), which may influence brain development during adolescence, and sample size differed between groups with 21 controls but only 11 FASD participants. These limitations were addressed with the analysis of 11 FASD versus 11 (of the 21) age and sex matched controls (4 females and 7 males in each group), which yielded similar findings to Figure 5.3 with near whole brain cortical thinning between scans in controls, and similar patterns of significant age-by-group interactions in 13 of 78 regions in the mixed models analysis (data not shown). Thus, the sex inequality and sample size (power) differences between groups are not a factor in our results. Here we chose to analyse cortical thickness in AAL regions in order to increase signal-to-noise and reduce multiple comparisons rather than applying FDR correction across 80,000 vertices, which can also be too stringent in small sample sizes. However, if we FDR correct our AAL results, age-effects in the FASD group and age-by-group interactions are no longer significant, while age effects in both our total control group (n=21) and our post-hoc reduced control sample (n=11) remain significant (with the exception of only 2 regions out of 65), further suggesting robust cortical thinning in the control group which is not observed in the FASD group. Given the relatively small sample size of this study, we were limited to the use of a linear model, despite evidence that cortical development is non-linear (Nie et al., 2013; Raznahan et al., 2011; Shaw et

al., 2008). Further longitudinal work is needed to model the developmental trajectories of cortical development in larger samples of FASD participants.

Nonetheless, it remains evident here that children with FASD undergo altered brain development, and that prenatal alcohol exposure itself may result in impaired cortical thinning many years later. This longitudinal study overcomes many of the limitations of previous cross-sectional work by identifying changes within individuals. An understanding of deviations in brain development beyond in-utero insult will provide insight into the lifespan progression of neurological impairment from pre-natal alcohol exposure, and may inform biological and behavioural interventions to improve quality of life and prevent the emergence of secondary deficits in affected individuals.

6 Head Circumference as a Proxy for Brain Volume and Cognition in FASD

Abstract

Head circumference is used together with other measures as a proxy for central nervous system damage in the diagnosis of fetal alcohol spectrum disorders, yet the relationship between head circumference and brain volume has not been investigated in this population. The objective of this study is to characterize the relationship between head circumference, brain volume and cognitive performance in children with prenatal alcohol exposure. Children with prenatal alcohol exposure (n=144) and healthy controls (n=145), ages 5-19 years, underwent magnetic resonance imaging (MRI) of the brain to yield brain volume (cm³) and head circumference (cm), normalized to control for age and sex. Relationships between head circumference, brain volume and 6 cognitive tests were assessed with Pearson's correlations. Head circumference, brain volume, and cognitive scores were all reduced in the prenatal alcohol exposure group compared to controls, albeit with considerable overlap between groups. Microcephaly (head circumference $\leq 3^{\text{rd}}$ percentile) occurred more often in prenatal alcohol exposed participants than controls, but 90% still had head circumference above this clinical cutoff. Normalized head circumference and brain volume were positively correlated in both groups, but this did not hold among prenatal alcohol exposed participants with head circumference more than one standard deviation below the norm. There were no significant correlations were found between head circumference and any cognitive scores. These findings confirm smaller head circumference in children with prenatal alcohol exposure at a group level, but raise concerns about its diagnostic utility as an indicator of central nervous system injury at an individual level.

6.1 Introduction

Head circumference (HC) trajectories are commonly used as a gross measure of neurological development in infancy and early childhood, providing a rapid and cost-effective method to screen for abnormalities such as hydrocephalus or delayed development (Rollins et al., 2010). Although not typically used in routine care beyond 3 years of age, HC is shown to positively correlate with brain volume and intelligence in groups of healthy children and adolescents (Bartholomeusz et al., 2002; Ivanovic et al., 2004), and is often smaller in children with mental retardation (O'Connell et al., 1965). Large deviations from the norm can indicate micro- or macrocephaly associated with a multitude of genetic disorders, perinatal brain injuries, and teratogenic exposures (Von der Hagen et al., 2014; Williams et al., 2008) including prenatal alcohol exposure (PAE).

Neurotoxicity from prenatal alcohol exposure is sometimes observable at birth, as evidenced by reduced birth weight (Little, 1977), lower Apgar scores (Bagheri et al., 1998) and increased rates of microcephaly (low HC) in infants with PAE (Feldman et al., 2012). HC reductions persist throughout childhood and adolescence, and have been shown to correlate with performance IQ in individuals with PAE (Ervalahti et al., 2007). Several studies of PAE suggest that the degree of HC reduction relates to timing (Feldman et al., 2012), amount (Russell et al., 1991; Smith et al., 1986) and pattern (Day et al., 2002; Sampson et al., 1994) of alcohol exposure in utero, though HC reductions are typically modest (e.g. -1.3 to -3.9% in children of heavy drinkers compared to abstainers (Coles et al., 1991; Day et al., 2002; Russell et al., 1991) and are not present in every sample (O'Callaghan et al., 2003).

Nonetheless, HC is used (among other measures) in the diagnosis of fetal alcohol spectrum disorders (FASD) as “evidence of deficient brain growth or abnormal morphogenesis”

(Hoyme et al., 2005), “structural evidence of CNS damage” (Astley, 2004) or “structural CNS dysfunction” (Chudley et al., 2005). However, the relationship between HC and brain volume has not been reported in children with PAE and may differ from observations in typically developing children or children with microcephaly of other etiologies. Further investigation of this relationship is needed to better characterize the clinical significance of microcephaly in children with PAE and to inform the use of HC in FASD diagnostic guidelines.

6.2 Methods

6.2.1 Participants

Participants were 144 individuals with confirmed PAE (5-19 years, mean 12.5 ± 3.3 years; 76 males) and 145 controls (5-19 years, mean 11.9 ± 3.4 years; 69 males). This subject pool includes participants from previous (Lebel et al., 2008a; Nardelli et al., 2011; Zhou et al., 2011) and current FASD studies conducted at the University of Alberta, as well as from a new multi-site MRI study of brain development (Reynolds et al., 2011). The PAE group was recruited through various multi-disciplinary FASD diagnostic clinics across Canada. All PAE participants had confirmed prenatal alcohol exposure and were assessed according to the Canadian Guidelines for the Diagnosis of FASD (Chudley et al., 2005) and the 4-Digit Code (Astley, 2004). Of the 144 participants in the PAE group, 33 (23%) had a dysmorphic diagnosis of fetal alcohol syndrome (FAS) or partial fetal alcohol syndrome (pFAS), 79 (55%) were diagnosed with static encephalopathy: alcohol exposed (SE:AE), neurobehavioural disorder: alcohol exposed (NBD:AE), alcohol related neurodevelopmental disorder (ARND), or FASD that was not further specified, and 32 (22%) had confirmed pre-natal alcohol exposure but did not meet criteria for formal diagnosis or were deferred for re-evaluation. Controls were recruited through advertising and had no self-reported history of neurological, psychiatric, or developmental

disorders. All participants or parents/legal guardians provided written informed consent, and participants were screened for contraindications to MRI.

6.2.2 Image Acquisition and Analysis

Head circumference and brain volumes were calculated from MRI scans (T1-weighted 3D-MPRAGE, $1 \times 1 \times 1 \text{ mm}^3$) collected on 4 scanners across Canada: 3T Philips Intera at University of British Columbia (12 PAE and 16 controls), 1.5T Siemens Sonata at University of Alberta (100 PAE and 106 controls), 3T Siemens Trio at each of University of Manitoba (9 PAE and 8 controls) and Queens University (23 PAE and 15 controls). Total brain volume (excluding brainstem, cerebellum and cerebrospinal fluid) and the volume of the frontal, temporal, parietal and occipital lobes were calculated with Freesurfer v5.1, averaging left and right. HC was manually traced by the same user (ST) on an axial oblique slice aligned with the most prominent parts of the occiput and forehead in OsiriX v5.8.5.

6.2.3 Cognitive Testing

Cognitive testing was performed by a trained research assistant on the same day as each subjects' MRI scan. The test battery included: Woodcock Johnson (WJ) Quantitative Concepts; Woodcock Reading Mastery Test-Revised (WRMT-R) Word ID; Working Memory Test Battery-Children (WMTB-C) Digit and Block recall; NEPSY-II Animal Sorting, Auditory Attention, Inhibition, and Memory for Names; Behavior Rating Inventory of Executive Function (BRIEF) Parent form and the Wide Range Intelligence Test (WRIT) General IQ (Table 1). For a small subset of PAE subjects ($n=12$), Wechsler Intelligence Scale for Children (WISC) full scale IQ was instead collected via chart review.

6.2.4 Normalization of Cognitive scores, HC and Brain Volume

Raw cognitive scores were converted to standard, scaled or t-scores based on the normative sample of each test, according to the procedures outlined by each test manual. Raw HC values were converted to standard deviations (SDs) and percentiles based on a large population based sample (Rollins et al., 2010), in order to control for age and sex. Given that there are no normative standards for brain volume, raw brain volumes were converted to Z scores based on the control group mean and standard deviation, calculated separately in males and females.

6.2.5 Group Differences, Change with Age, and Correlations between HC, Brain Volume and Cognition

Group differences (PAE vs control) in normed cognitive scores, raw HC and raw brain volume were determined with independent sample t-tests (alpha was set at <0.001 to compensate for multiple comparisons). Change with age for raw HC, raw brain volume and IQ standard scores was tested with Pearson's correlations. Relationships between normalized HC (SD), brain volume Z scores, and cognitive test scores were tested with Pearson's correlations, assessed separately for PAE and controls. Correlations between normed HC and brain volume Z scores were repeated including only subjects with HC more than 1 SD below the population norm (~15th percentile) to determine how this relationship holds outside of the normal range. Although a diagnosis of microcephaly is not given unless HC is $\leq 10^{\text{th}}$ percentile (Hoyme et al., 2005) or $\leq 3^{\text{rd}}$ percentile (Astley, 2004; Chudley et al., 2005), this more liberal cut-off was chosen to increase power in a subset of participants on the low end of the HC spectrum, given our limited sample of 22 PAE below the 10th percentile for HC, 14 of whom were below the 3rd percentile. Rates of microcephaly are low even in very large samples, e.g. 64 of 973 (~6.5%) children with

PAE who had HC < 10th percentile (Feldman et al., 2012), so correlation analysis among only children with clinically significant microcephaly would require MRI data (not routinely ordered in diagnosis) from several hundred subjects with PAE and many more controls. As such, here only descriptive statistics are presented for participants with HC < 3rd percentile.

6.3 Results

6.3.1 Group Differences and Changes with Age

Raw HC increased with age in both groups and sexes (male controls $R=0.53$, $p<0.001$; female controls $R=0.51$, $p<0.001$; male PAE $R=0.45$, $p<0.001$; female PAE $R=0.44$, $p<0.001$ - Figure 6.1 A,B), but raw brain volume did not change with age (Figure 1 D,E). Raw HC was lower in males with PAE, but not females, relative to male and female controls ($t=-3.81$, $p<0.001$ and $t=-1.58$, $p=0.117$, respectively - Figure 6.1C). Conversely, raw brain volume was lower in both males and females with PAE ($t=-6.47$, $p<0.001$ and $t=-3.32$, $p=0.001$, respectively - Figure 6.1F), though greater overlap between sexes can be seen in the PAE than control group (Figure 6.1 D,E). IQ did not change with age (as expected for a standard score) and sex differences were not evident in either group (Figure 6.1G-I), though the control group significantly outperformed the PAE group ($t=-8.73$, $p<0.001$ - Table 1, Figure 6.1I). Likewise, the control group had superior scores relative to the PAE group on all other cognitive tests ($t=-4.77-19.19$, $p<0.001$ - Table 6.1), except NEPSY-II Response Set ($t=-2.37$, $p=0.019$).

Table 6.1: Subject Characteristics and Cognitive Test Scores

	Control	PAE ^a	PAE with HC ≤ 3 rd percentile ^b
Sample size	145	144	14
Age (years)	11.9 ± 3.4	12.5 ± 3.3	13.9 ± 3.3
Number of Males	69 (48%)	76 (53%)	8 (57%)
Ethnicity			
Caucasian	126 (87%)	38 (26%)	4 (33%)
Aboriginal	4 (3%)	72 (50%)	7 (50%)
Other/Unknown	15 (10%)	34 (24%)	3 (25%)
Wide Range Intelligence Test/Weschler Intelligence Scale ^c			
General IQ	112 ± 12 (n=66)	88 ± 17** (n=50)	--- ^f
Woodcock Johnson ^c			
Quantitative Concepts 18A&B	106 ± 15 (n=141)	82 ± 19** (n=122)	89 ± 18 (n=11)
Woodcock Reading Mastery Test ^c			
Word ID	106 ± 13 (n=140)	90 ± 15** (n=110)	93 ± 13 (n=10)
BRIEF (parent form) ^d			
Behavioural Regulation Index	48 ± 8 (n=131)	72 ± 12** (n=116)	76 ± 13 (n=11)
Metacognitive Index	51 ± 12 (n=130)	68 ± 10** (n=116)	70 ± 12 (n=11)
Global Executive Composite	49 ± 10 (n=130)	73 ± 10** (n=116)	75 ± 11 (n=11)
Working Memory Test Battery ^c			
Digit	99 ± 16 (n=125)	85 ± 13** (n=108)	88 ± 9 (n=7)
Block	100 ± 16 (n=124)	86 ± 16** (106)	88 ± 15 (n=8)
NEPSY-II ^e			
Animal Sorting	9.4 ± 3.8 (n=129)	7.0 ± 3.4** (n=86)	8.3 ± 5.6 (n=7)
Auditory Attention	10.3 ± 3.1 (n=135)	7.1 ± 4.1** (n=103)	7.9 ± 5.1 (n=9)
Response Set	10.1 ± 3.5 (n=129)	8.9 ± 3.9 (n=101)	10.7 ± 2.8 (n=9)
Inhibition-Naming	9.3 ± 3.5 (n=135)	6.6 ± 4.0** (n=99)	8.4 ± 5.0 (n=8)
Inhibition-Inhibition	9.7 ± 3.8 (n=135)	6.1 ± 3.6** (n=98)	6.4 ± 4.2 (n=8)
Inhibition-Switching	10.2 ± 3.8 (n=129)	6.4 ± 4.1** (n=96)	6.4 ± 6.5 (n=8)
Memory for Names	9.3 ± 2.9 (n= 135)	6.1 ± 3.6** (n=105)	6.7 ± 4.5 (n=9)

^a**p<0.001 on independent sample t-tests (PAE versus Controls)

^bRelative to population norms reported in Rollins et al Journal of Pediatrics, 2010. Significance versus controls not tested for HC ≤ 3rd percentile due to small sample size

^cStandard scores, mean=100, SD=15, higher score indicates better performance

^dT scores, mean=50, SD=10, higher score indicates worse performance

^eScaled scores, mean=10, SD=3, higher score indicates better performance

^fMean ± SD not reported given n=3 with IQ scores in this category

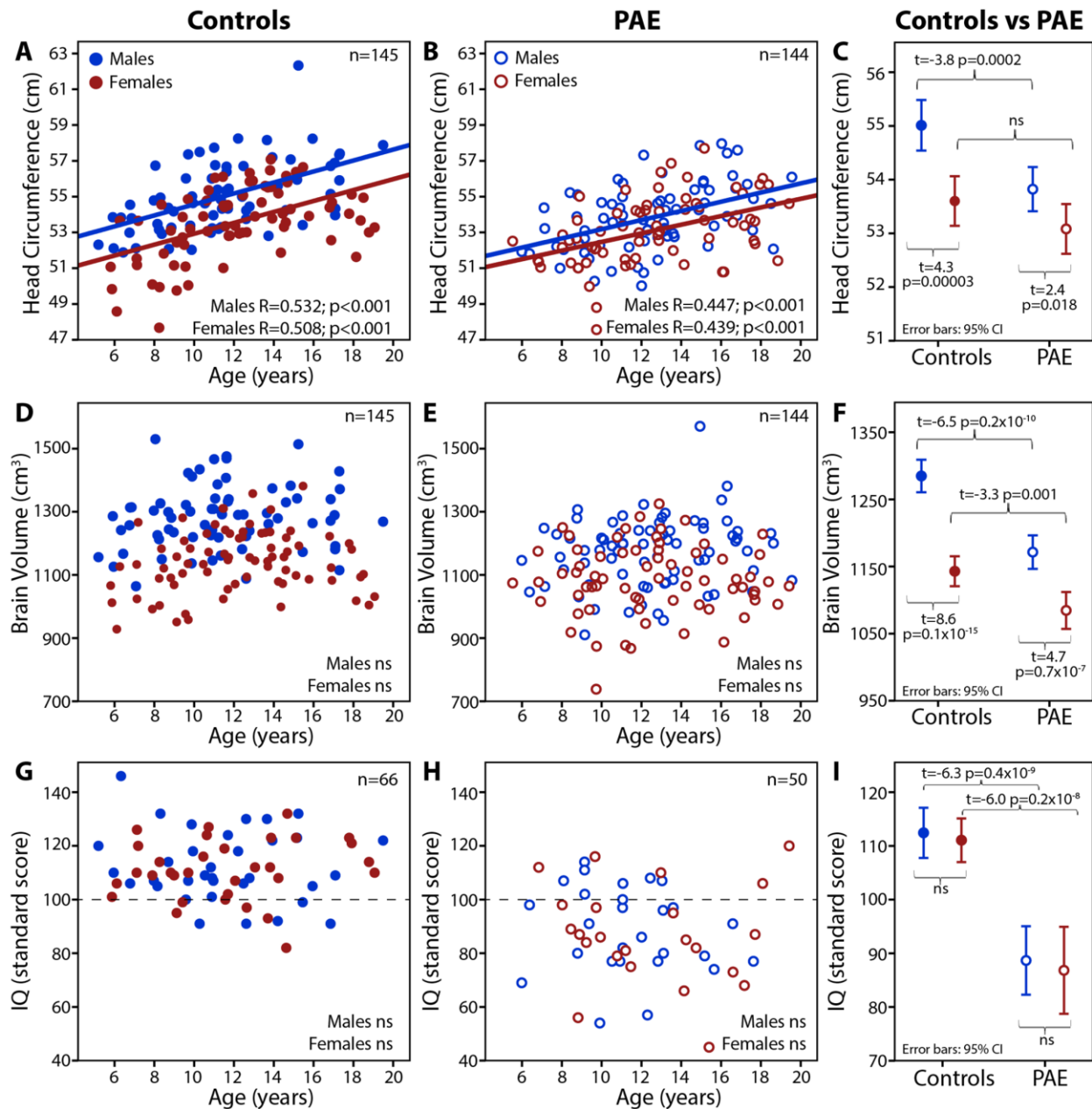


Figure 6.1: Raw head circumference, brain volume and IQ by group and sex. Head circumference increased with age in both groups (A,B) groups, but was consistently lower in the PAE group than controls (C). Brain volume did not change with age in either group (D,E), and was significantly reduced in the PAE group relative to controls (F). IQ standard scores did not change with age in either group (G, H), and were again lower in the PAE group (I). Reductions in brain volume were greater between males (PAE versus control) than females (F), and reductions in HC were only significant in males but not females with PAE (C). Likewise, sex differences within groups were larger in the control group for both HC (C) and brain volume (F).

Normed HC, brain volume and IQ scores showed right-shifted distributions toward higher values in controls and lower values in the PAE group (Figure 6.2A-C). Notably, only 10% of controls had a HC more than 1 SD below the population norm, compared to 24% of the PAE group. The greatest reductions of HC, IQ and brain volume were found in participants with dysmorphic features indicative of FAS/pFAS (data not shown) in keeping with previous literature (Astley et al., 2009a); however, subgroup analysis was not further explored given that IQ and HC are used in the sub-classification of FASD. Despite group differences, substantial overlap between groups is evident for all three metrics (Figures 6.1&2).

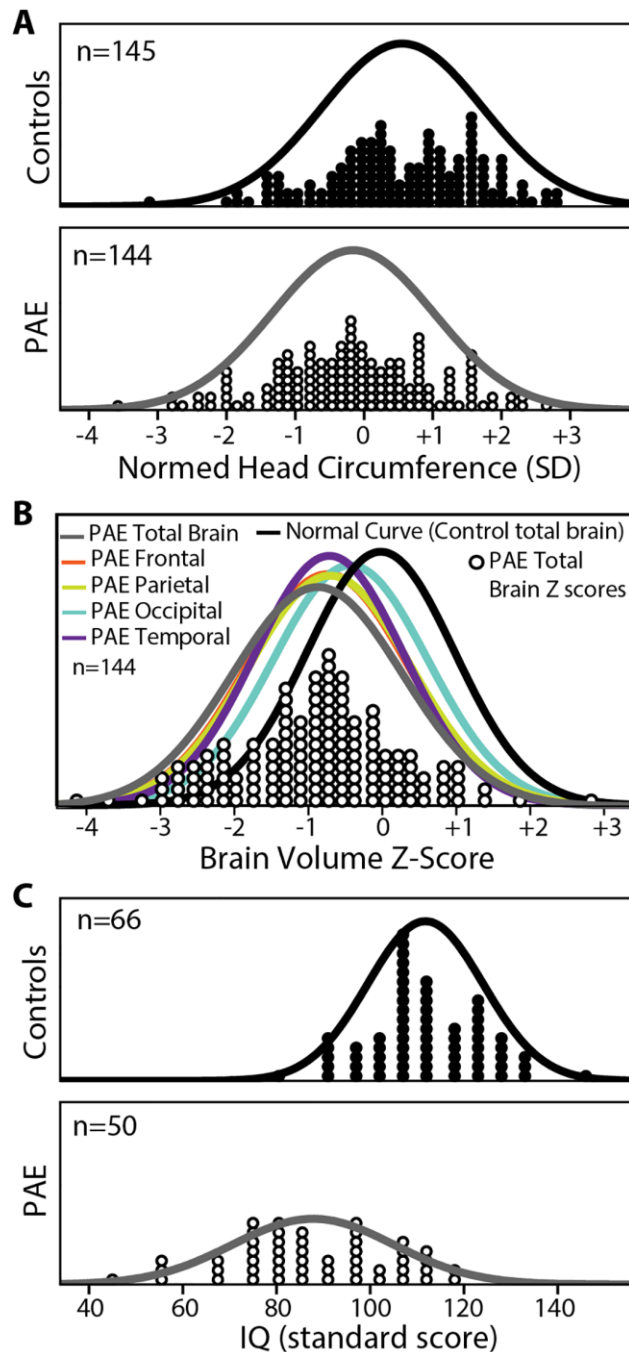


Figure 6.2: Standardized head circumference, brain volume and IQ by group. (A) Head circumference (HC) standard deviation distributions showing a shift towards the number of participants with higher normed HC in controls and lower normed HC in PAE subjects, albeit with substantial overlap between groups. (B) Z score distribution for total brain volume is left-shifted in the PAE group (grey curve) relative to controls (black curve). PAE distribution curves for brain lobe volumes show similar leftward shifts towards negative Z scores. (C) Likewise, IQ score profile is right-shifted in the control group compared to PAE (C), peaking above the population norm of 100 in controls, and below in the PAE group.

6.3.2 HC Correlations

Normed HC and brain volume were positively correlated in both the control ($R=0.66$, $p<0.001$) and PAE groups ($R=0.57$, $p<0.001$), indicating that on the whole, subjects with larger HC for their age/sex have larger brain volumes (Figure 6.3A). However, this correlation did not hold among PAE participants with HC more than 1 SD below the norm ($n=34$). IQ did not significantly correlate with normed HC (controls $R=0.22$, $p=0.080$; PAE $R=0.24$ $p=0.093$), total brain volume Z scores (controls $R=0.09$, $p=0.479$; PAE $R=0.21$, $p=0.146$), or any lobe volume Z scores (controls $R=-0.01-0.16$, $p=0.957-0.202$; PAE $R=0.19-0.26$, $p=0.190-0.072$). IQ was only available in 50 PAE and 66 control participants; however, this subsample had a similar age, sex and diagnostic sub-group distribution as the total sample (Figure 6.1G,H), and demonstrated tight correlations between brain volume Z scores and normed HC (Figure 6.3C,D), indicating that these negative findings (no relationships between HC/brain volume and IQ) are unlikely to stem from sample bias. Likewise, no other cognitive scores correlated with normed HC or total brain volume Z scores in either group (all $p>0.01$), despite larger sample sizes of $n\sim 90-140$ in each group.

6.3.3 PAE Participants with HC under 3rd Percentile

14/144 (10%) of PAE participants met the clinical definition of microcephaly with HC \leq 3rd percentile. Of these subjects, 11 (80%) had brain volume \leq 3rd percentile (Figure 6.3E). Conversely, of the PAE participants with brain volume \leq 3rd percentile ($n=28$), only ~35% had HC \leq 3rd percentile and more than half had HC percentiles in the normal range. However, given that HC and brain volume were normed on different scales (population based sample versus control group, respectively) direct comparison may be confounded by group differences between our controls and the population norm. Nonetheless, only 50% subject overlap was found between

the 14 subjects with HC $\leq 3^{\text{rd}}$ percentiles and the 14 subjects with the lowest brain volume percentiles in the PAE group, again suggesting a disconnect between these metrics. Cognitive test scores of the 10% of PAE participants who had HC $\leq 3^{\text{rd}}$ percentile were not different than the whole PAE group (Table 6.1), suggesting that these participants are not more cognitively impaired than those PAE subjects with normal HC.

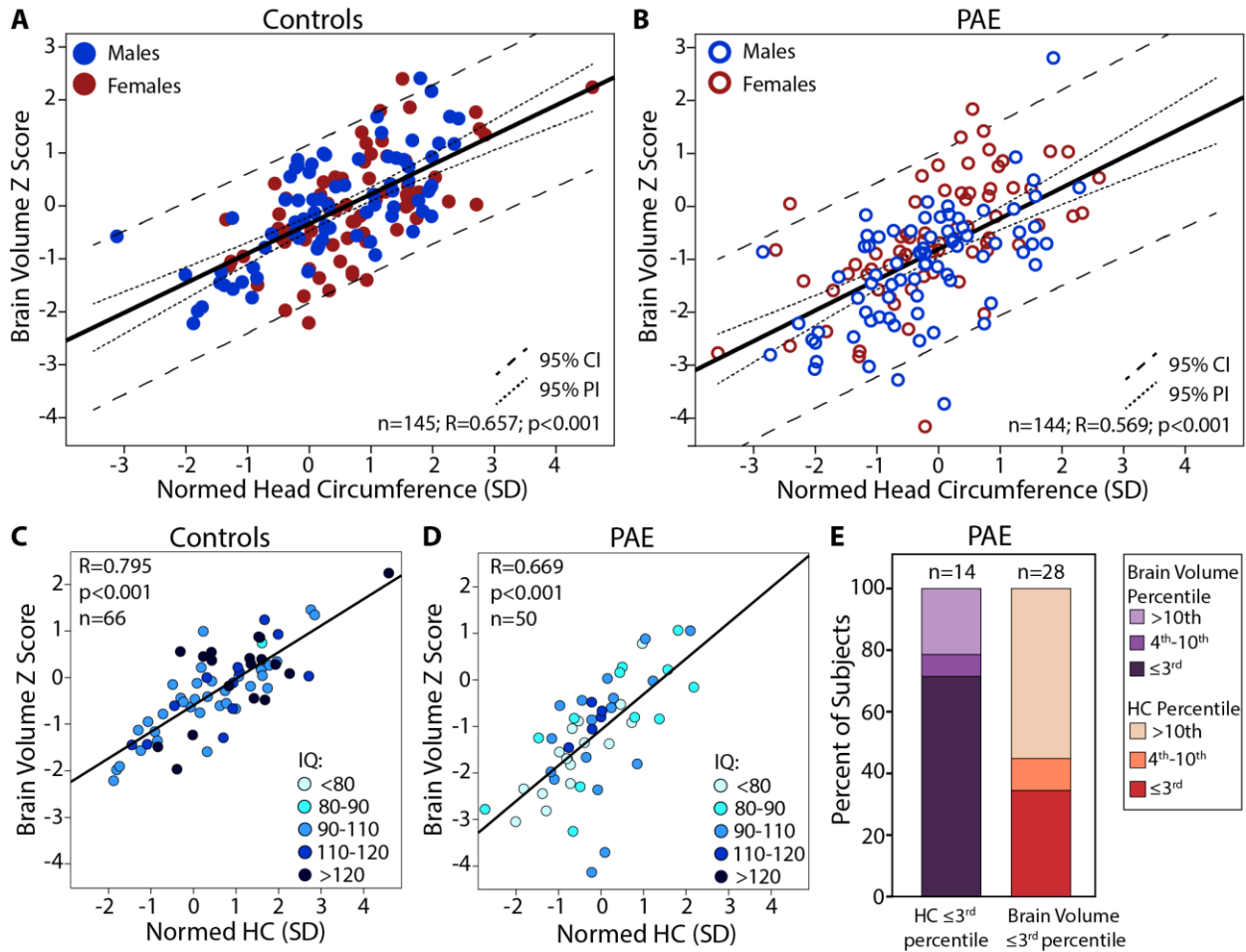


Figure 6.3: Head circumference-brain volume correlations. Brain volume Z scores and head circumference (HC) standard deviations are shown to positively correlate in both the control (A) and prenatal alcohol exposure (PAE) groups (B). Despite significant correlations between brain volume and HC in the subset of participants with IQ scores in both groups, there does not appear to be any systematic pattern/grouping of IQ in controls (C) or PAE (D). In other words, those with the smallest normed HC and brain volume (bottom left of the plots) did not show consistently lower IQ scores. (E) When only including the 14 PAE participants below the clinical cut-off for microcephaly ($HC \leq 3^{\text{rd}}$ percentile), it is notable that 10 (~70%) of the subjects have a brain volume below the 3rd percentile. Conversely, among the 28 PAE participants with total brain volume $\leq 3^{\text{rd}}$ percentile, 15 subjects (~55%) have a head circumference above the 10th percentile.

6.4 Discussion

Here we provide evidence to support previous assertions of reduced head circumference in a group of individuals with prenatal alcohol exposure (Coles et al., 1991; Day et al., 2002; Russell et al., 1991; Sampson et al., 1994; Smith et al., 1986) by demonstrating (i) a 29-point gap in median HC percentile, (ii) a 2-fold increase in the number of subjects with HC more than 1 SD below the population mean, and (iii) a nearly 5-fold increase in the number of subjects with $HC \leq 3^{\text{rd}}$ percentile in our PAE group compared to controls. This sample spans a wide age range from 5 to 19 years old, suggesting that HC deficits persist into young adulthood, in agreement with longitudinal studies of PAE (Carter et al., 2013). Likewise, significant reductions of brain volume, IQ and cognitive performance are demonstrated in the PAE group, in keeping with previous literature in this population (Lebel et al., 2011).

However, these results also highlight several important limitations of HC measurement in children with PAE. Despite group differences, the substantial spread in HC and its overlap between groups suggests that this metric does not discriminate individuals with PAE from healthy controls at a single-subject level. Moreover, although microcephaly ($HC \leq 3^{\text{rd}}$ percentile) occurred at a higher frequency in the PAE than control group, 90% of the PAE group had HC values above this clinical cut-off (others have reported ~94%, Feldman et al., 2012), suggesting that microcephaly is not a sensitive marker of PAE.

HC is shown to positively correlate with brain volume; however, this relationship appears to be driven by the spread and range of these data - it is not surprising that a child with a very low HC has a smaller brain than a child on the high end of the HC range. Increased variability and lack of correlation within subsets of this range (e.g. at -1 SD and below) suggest that HC is a poor predictor of brain volume among groups of children with roughly similar normed HC

values. Furthermore, lack of correlations between HC and cognitive measures suggests that HC does not predict functional impairment. As such, further investigation may be needed to determine if HC deficits are indeed a reflection of CNS impairment rather than overall growth deficiency.

Among PAE participants with clinically significant microcephaly ($HC \leq 3^{\text{rd}}$ percentile), we see no greater impairment in cognition (Table 6.1) and a large spread in brain volume Z scores that span from -3 to just over 0 (the mean of the control group). Nonetheless, most brain volumes in this small HC sub-set fall below the 10th percentile, as expected given that HC (i.e. the skull) poses a physical limitation on brain volume. However, it is important to note that the reverse relationship is not observed: about half of the subjects with very small brain volumes are shown to have ‘normal’ HC values.

Lack of consistent correlation between brain volume and HC may reflect greater variability in the ratio of brain tissue to cerebrospinal fluid in children with PAE, which may explain cases where brain volume is very small but HC is in the normal range. Conversely, reduced bone volume in the skull has been observed with micro computed tomography in a mouse-model of FASD (Shen et al., 2013), and may account for cases where HC was reduced with intact brain volume. The skeletal and nervous systems are each uniquely affected by the toxic effects of alcohol in utero (Dunty et al., 2001; Goodlett et al., 2005; Hernandez-Guerrero et al., 1998) likely adding variability to the relationship between brain volume and HC in children who were exposed to alcohol in varying amounts, frequencies and time-points throughout pregnancy.

Beyond in utero sensitivity, the distinct post-natal trajectories of nervous and skeletal system development may also impact this relationship. HC is shown to increase with age at similar rates in both PAE and control groups, while brain volume does not change significantly in either group from 5-19 years, fitting with previous literature demonstrating that brain volume reaches ~90% of adult maximum at around age 6 years, while skull thickness continues to increase linearly with age into adolescence (Giedd, 2004). In addition, the brain-scalp distance has been shown to increase with age in healthy children, driven primarily by increases in cerebrospinal fluid and cranial thickness (Beauchamp et al., 2011), providing further evidence that HC reflects the composite of multiple systems that each develop at different rates with age. Nonetheless, when assessed separately, the developmental trajectories of HC and brain volume appear to be similar between the PAE and control groups, albeit in cross-sectional cohorts. Longitudinal samples may be better positioned to tease apart the relationship between these trajectories in PAE.

In addition to group differences, sex effects were observed for both brain volume and HC in the control group, as expected (Giedd et al., 2012), but were less so between males and females in the PAE group (Figure 6.1). Likewise, it appears that group differences in both metrics are more pronounced in males than females with PAE, in keeping with previous findings of more substantial brain volume reductions in males with FASD (Chen et al., 2012; Nardelli et al., 2011). Age-by-sex interactions have been observed in PAE studies of longitudinal cortical volume development (Lebel et al., 2012b), though the mechanisms underlying sex effects in PAE are unclear. Greater overlap is observed between males and females in the PAE group for HC (Figure 6.1B) and brain volumes (Figure 6.1E) across the whole age range, with no apparent divergence between sexes during adolescence. However, the effects of puberty were not tested

and cannot be ruled out. Nonetheless, it remains possible that prenatal alcohol exposure has sex-specific impacts on nervous system development, as observed in some animal models of PAE (Sickmann et al., 2014; Uban et al., 2013; Weinberg et al., 2008), and as suggested in developmental programming models of disease (Aiken and Ozanne, 2013).

Several limitations of this study should be acknowledged. First, converting brain volumes to Z scores based on the control group (n=144) may be less generalizable and more sensitive to sample bias than the much larger normative sample on which head circumference norms were validated (n=537; Rollins et al., 2010). However, normative standards do not exist for brain volume, and thus the control sample was used here. Secondly, although weight was routinely collected prior to MRI acquisition, height was not consistently collected, precluding examination of the effects of stature and/or growth deficiency on reduced head circumference in this population. Nonetheless, the key findings here focus on the relationship between head circumference and brain volume, which should be impervious to variations in body size. Lastly, although the lack of correlation between head circumference and brain volume among PAE participants with head circumference more than 1 SD below the population norm is intriguing, it is important to keep in mind that the reduced sample size of this sub-sample (n=34) limits power relative to the larger sample (n=144) across the entire head circumference spectrum. Nonetheless, lack of correlation in this subset underscores the large inter-subject variability in this relationship and provides further caution against application to single-subject data.

Here we confirm previous reports of reduced head circumference, brain volume, and cognitive function in a large cohort of children with PAE relative to age and sex matched controls. Positive correlations are demonstrated between HC and brain volume, but the relationship does not hold among sub-sets outside of the normal range for PAE, which may

reflect the complex interplay between skeletal and neural development, each differentially affected by prenatal alcohol exposure. Further, although microcephaly is clearly more common in the PAE population, our findings suggest that it is only present in a small subset of children with PAE and does not co-occur with greater cognitive impairments in this sample. Thus, the use of head circumference as a proxy for CNS impairment in PAE requires further investigation.

7 Relationships between DTI tractography, volumes and cortical thickness in FASD

Abstract

Advanced MRI has revealed various abnormalities of brain structure in individuals with fetal alcohol spectrum disorders (FASD), including reduced brain volumes, abnormalities of cortical thickness and alterations in white matter microstructure. However, no one study has examined all three modalities in one cohort, needed to determine the degree of coherence between these observations within-subjects. Here we examine 70 individuals with FASD (5-32 years, mean 14 ± 6 years, 40 males) and 73 healthy controls (5-32 years, 13 ± 5 years, 38 males), who all underwent cognitive testing and 1.5 T MRI including T1-weighted MPRAGE and diffusion tensor imaging. T1 data were processed with CIVET and FreeSurfer to calculate cortical thickness and brain volumes (respectively), and an automated tractography pipeline was used to delineate 9 major white matter tracts. Effects of age, sex and group were tested with multivariate analysis of covariance, and variables with significant group differences were converted to *Z* scores (based on control group mean and standard deviations) to permit comparison between variables (fractional anisotropy (FA), mean diffusivity (MD; mm^2/s), cortical thickness (mm), brain volumes (cm^3) and cognitive test scores) on the same scale. This analysis revealed robust volume reductions, smaller but consistent reductions in cortical thickness and few, small differences in diffusion tractography parameters, many of which were significant in males (FASD versus Controls) but not females. In addition, the magnitude of difference relative to controls was larger in males than females with FASD for several volumes,

despite equal impairment on cognitive tests, and fewer brain-behaviour relationships were observed in males than females with FASD. These results may reflect an attenuation of expected sexual dimorphism of brain structure in this population. In addition, few correlations were observed between imaging variables, suggesting that abnormalities in brain volumes, cortical thickness and white matter microstructure may each represent ‘independent’ features of FASD, influenced by unique pre and postnatal factors.

7.1 Introduction

The teratogenic effects of alcohol were first established through a series of seminal case studies in the 1970s (Clarren et al., 1978; Jones and Smith, 1973), and have since been confirmed by a large body of research in both humans and animal models. This work has demonstrated numerous direct and indirect mechanisms by which alcohol acts on the developing nervous system (Goodlett et al., 2005), producing a range of physical, behavioural and cognitive deficits, collectively termed fetal alcohol spectrum disorders (FASD) (Riley and McGee, 2005). However, interactions between exposure, genetics and environmental factors result in enormous variability in both clinical presentation and structural brain damage associated with this common developmental disorder.

Advanced neuroimaging has revealed numerous structural abnormalities associated with FASD, including reductions in total brain, white matter, cortical and deep grey matter volumes (Lebel et al., 2011), as well as abnormalities in cortical thickness (Sowell et al., 2008b; Treit et al., 2014b; Zhou et al., 2011) and white matter microstructure (Wozniak and Muetzel, 2011). However, no study has examined all three modalities together in the same cohort, needed to

determine the relative severity of each finding. Establishing which aspects of brain structure are most robustly affected will help to establish a clearer global picture of brain structure in FASD, as well as the relative utility of each imaging modality for studying this population. Moreover, an understanding of the relationships within and between modalities will help to determine the degree of coherence between structures, needed to establish if previous observations represent ‘independent’ features of FASD.

Lastly, there is a paucity of data on sex differences in brain structure in FASD, likely due to small sample sizes and a focus on other important variables such as diagnostic category. Sex differences in brain structure, function and neurochemistry have been well established in healthy populations, and are proposed to partially underlie sexual dimorphism of neurodevelopmental and degenerative diseases (Cahill, 2006; Cosgrove et al., 2007). Animal models have revealed several sexually-dimorphic neurophysiological and neurochemical abnormalities resulting from prenatal alcohol exposure (Converse et al., 2014; Lan et al., 2009; Sliwowska et al., 2014; Weinberg et al., 2008), but links to human brain structure remain largely understudied.

The purpose of this study is to evaluate diffusion tensor imaging, cortical thickness and brain volume abnormalities in a large (n=70) cohort of individuals with FASD from 5-32 years of age, with the aim of examining: i) sex-differences in abnormalities of brain structure associated with FASD, ii) the relative severity of abnormalities observed with each imaging modality, and iii) the relationship between observed abnormalities.

7.2 Materials and Methods

7.2.1 Subjects

Participants were 70 individuals with FASD (5-32 years, mean 14 ± 6 years, 40 males) and 73 controls (5-32 years, 13 ± 5 years, 38 males). FASD participants were primarily recruited through two FASD diagnostic clinics at the Glenrose Rehabilitation Hospital, and diagnosed according the Canadian Guidelines (Chudley et al., 2005) and the 4 digit code (Astley, 2004). The remaining FASD participants were recruited through school and social work services, and were diagnosed by primary care physicians and practitioners in other developmental disability clinics. Ten had a diagnosis of FAS, 6 pFAS, 13 SE:AE, 7 NBD:AE, 4 ARND and 30 FASD that was not further specified. Of the 70 FASD participants, 20 were included in previous publications (Nardelli et al., 2011; Zhou et al., 2011), and 50 were newly recruited by the author. Controls were recruited with advertising on public bulletin boards in community centres, hospitals, recreation centres etc., through letters sent home from several public schools, and by word of mouth. All 73 controls were newly recruited by the author-- 49/73 were included in a recent publication on healthy development (Treit et al., 2014a), but none have been included in any previous FASD papers. Controls were screened for neurological, psychiatric conditions, head injuries and contraindications to MRI as well as prenatal exposure to alcohol, nicotine, and other drugs. Control subjects with exposure to more than 2 drinks per occasion or more than 6 drinks in total during pregnancy were excluded. Seven controls included here were exposed to alcohol within the threshold for inclusion (average exposure: 3 drinks total), 12 were exposed to nicotine (all via cigarettes in varying frequencies and amounts) and none were exposed to illicit drugs. Written informed consent was obtained from all participants or parents/legal guardians (in

addition to written assent from participants under 18 years of age) prior to study procedures. This study was approved by the Health Research Ethics Board at the University of Alberta.

7.2.2 Demographic and Cognitive Data

All participants underwent approximately 1.5 hours of cognitive testing on the same day as their MRI, administered by a trained research assistant or myself. Participants of all ages were administered the Woodcock Reading Mastery Test Revised (WRMT-R) Word ID; Woodcock Johnson (WJ) Quantitative Concepts; Rey Complex Figure Test (RCFT) and Recognition Trial; Comprehensive Receptive and Expressive Vocabulary Test (CREVT); and the Wide Range Intelligence Test (WRIT). In addition, participants under 15 years of age were administered the Working Memory Test Battery for Children (WMTB-C) Digit and Block recall, and those under 16 years of age were administered either the NEPSY Tower, Auditory Attention/Response Set and Visual Attention, or the NEPSY II Memory for Names, Animal Sorting, Arrows, Auditory Attention and Response Set, Inhibition and Narrative Memory (NEPSY was updated to NEPSY II mid-recruitment). Participants over 16 years of age were administered the Delis-Kaplan Executive Functioning System (D-KEFS) Trail Making, Verbal Fluency and Card Sorting. Given that each subject only had executive functioning measures from one of the NEPSY, NEPSY II or D-KEFS, a “composite” executive function score was calculated from the mean of: NEPSY I Executive Composites (Tower, Auditory Attention and Visual Attention), NEPSY II Response Set, Animal Sorting, Inhibition-Inhibition, and Inhibition-Switching scaled scores, and D-KEFS Verbal Fluency condition 3 (Category Switching), Trail Making condition 4 (Number-Letter Switching), and Card Sorting (Free Sorting and Sort Recognition combined) composite scaled scores. This score is intended to characterize general executive function ability, with the assumption that performance across these tests would be highly correlated. Demographic

information was collected in a subset of participants through questionnaires given to participants or their parents/legal guardians (Table 7.1).

7.2.3 Image Acquisition

Participants were scanned on a 1.5T Siemens Sonata in the Peter S. Allen MR Research Centre at the University of Alberta. Scans included DTI, T1-weighted, T2-weighted, fluid-attenuated inversion recovery (FLAIR), and FLAIR-DTI (not used here) for a total scan time of ~26 minutes. DTI was acquired using a dual spin-echo, single shot echo-planar imaging sequence with: 40 3-mm axial-oblique slices with no inter-slice gap; TR=6400 ms; TE=88 ms; 6 non-collinear diffusion sensitizing gradient directions with $b=1000 \text{ s/mm}^2$; 8 averages; FOV=220x220 mm²; matrix of 128x128 with 75% phase partial Fourier zero-filled to 256x256 for a total acquisition time of 6:06 minutes. T1-weighted images for volume analysis were acquired using a high resolution (1x1x1 mm³) MPRAGE sequence with: TR=1870 ms, TE=4.38 ms, TI=1100 ms for a total acquisition of 4:29 minutes.

7.2.4 DTI Tractography

A semi-automated tractography method (adapted from Lebel et al., 2008b) was used to delineate 9 major white matter tracts for each participant. Subject images were motion/distortion corrected in ExploreDTI v8.3, and then normalized to the ICBM-DTI81 template using a deformable tensor-based registration algorithm in DTI-TK (Zhang et al., 2006; <http://dti-tk.sourceforge.net>), saving warping parameters for each subject. Seed, target and exclusion regions were drawn on the template according to a priori information on tract location (Wakana et al., 2004), and then applied to each subject's native colourmap using an inverse of their normalization parameters, such that the same seed, target and exclusion regions were applied to all subjects. White matter tracts included the genu (gCC), body (bCC), and splenium (sCC) of

the corpus callosum, corticospinal tracts (CST), superior and inferior longitudinal fasciculus (SLF; ILF), inferior fronto-occipital fasciculus (SFO; IFO), cingulum, and uncinate fasciculus (UF). Tractography was carried out in native space for each subject, using a deterministic streamline method in ExploreDTI (Leemans et al., 2009), and fibres in the left and right hemisphere were measured separately for all tracts except the corpus callosum. A minimum FA threshold of 0.25 was used to initiate and continue tracking, and an angle threshold of 60° was set for the UF and SLF and 30° for all other tracts. All tracts were manually inspected for consistency with known anatomy and additional exclusions of spurious fibres were made as necessary. Fractional anisotropy (FA) and mean diffusivity (MD) were measured for each tract counting each voxel only once.

7.2.5 Cortical Thickness

T1-weighted MRPAGE images were processed in CBrain using the CIVET 1.1.11 pipeline, with normalization to the ICBM-152 template. Cortical thickness was measured across 40,962 vertices per hemisphere, and smoothed using a kernel of 20 mm full width at half maximum that preserves cortical topology. Cortical surface data were then segmented to 39 areas per hemisphere with an automated anatomical labelling (AAL) template (Tzourio-Mazoyer et al., 2002), averaging all vertices within each region. AAL regions were used for all statistical analysis in order to reduce multiple comparisons and increase signal-to-noise compared to over 80,000 vertices.

7.2.6 Brain Volumes

T1-weighted MRPAGE images were processed using Freesurfer v 5.1 (Anthinoula A Martinos Centre for Biomedical Imaging, Charlestown M.A.), according to a previously described segmentation algorithm (Fischl et al., 2002). Intracranial, total brain (excluding

cerebrospinal fluid and cerebellum), white matter, cortical grey matter, bilateral thalamus, caudate, putamen, globus pallidus, hippocampus and amygdala volumes were calculated.

7.2.7 Statistical Analysis

Statistical analysis was carried out in IBM SPSS 22.0, and is outlined in Figure 7.1. First, multivariate analysis of covariance (MANCOVA) was used to test for effects of age and sex on each variable (FA, MD, cortical thickness, brain volumes and cognitive scores) separately in FASD and Control groups (at $p < 0.05$), in order to confirm expected sex differences and developmental changes across this wide age span. Next, MANCOVA was used to test for group differences (FASD versus Controls) controlling for age and sex where significant in either group. This was repeated separately in males (FASD versus Controls) and females (FASD versus Controls), controlling for age where significant in either group (Tables 7.3-7.10). Z scores were then calculated for the FASD group (using the control mean and standard deviation) for variables with a significant effect of group in any comparison. FASD Z scores were calculated separately in males and females (using male and female control means and standard deviations) for variables with group differences and a significant effect of sex in the control group.

Hemispheric differences in FASD Z scores of bilateral structures were then tested with paired t-tests, performed separately in males and females. Bilateral structures with significant left-right differences ($p < 0.05$) in either males or females were kept separate, and averaged when non-significant in order to reduce multiple comparisons. Note that this approach only identifies asymmetries in the FASD group that differ from those observed in the control group: lateralization of structure that is equivalent in both groups would produce non-significant paired t-tests here.

A stepwise approach was then used to identify variables presumed to represent the most robust differences in the FASD group relative to controls. First, Z scores of all variables with significant group differences in MANCOVA analysis were plotted on the same scale for both males and females. Next, FASD Z scores greater than ± 0.5 standard deviations from the control mean were ranked according to their magnitude, separately in males and females. Sex differences in the magnitude of these Z scores were tested with independent sample t-test (males versus females in FASD group). Lastly, correlations within and between the FASD Z scores $> \pm 0.5$ were tested using partial correlations, controlling for age (assessed separately in males and females) and false-discovery-rate (FDR) corrected for multiple comparisons.

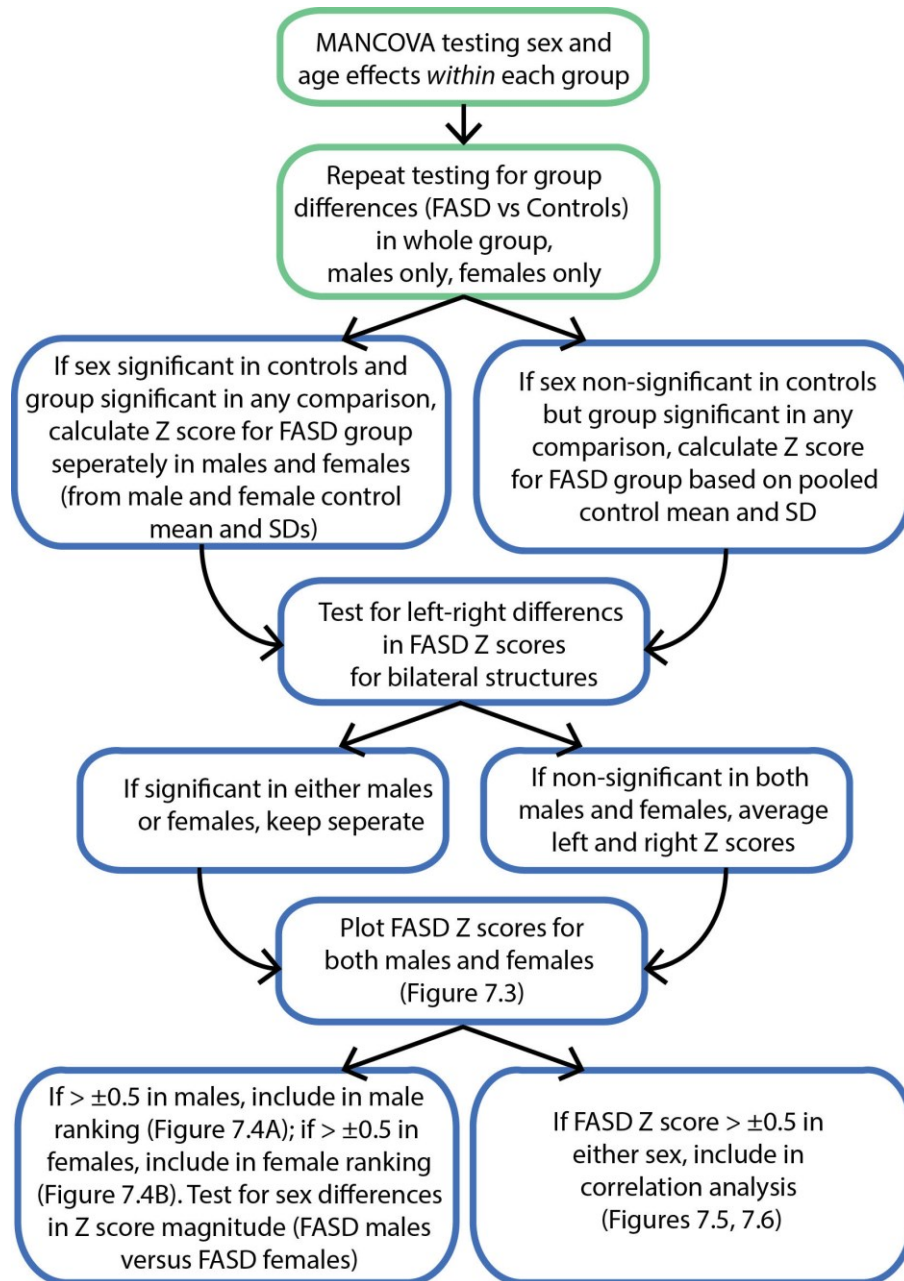


Figure 7.1: Flowchart outlining statistical analysis plan. Green box used to signify analysis done on raw data in both groups; blue boxes for analysis done on FASD group Z scores.

7.3 Results

7.3.1 Cognitive and Demographic Data

Demographic data was collected for 72 controls and 44 FASD participants, presented in Table 7.1. Demographic information was not collected in the 20 previously recruited FASD participants, and collection was initiated part-way through recruitment of the remaining 50 FASD participants. In the subset of participants for which demographic information was collected, notable differences in ethnicity, living situation, co-morbidities and medication use are seen.

FASD participants scored significantly lower than controls on all cognitive tests except RCFT Recognition (Table 7.2). Z score analysis suggests that IQ, reading (Word ID), mathematics (WJ Quantitative Concepts) and vocabulary (CREVT) were more impaired relative to visual memory and integration (RCFT), executive function and working memory (Figure 7.3); however, differences in the magnitude of these impairments were not statistically tested. Impairments were similar between males and females, and no significant sex differences in cognitive test Z score magnitude were found.

Table 7.1: Participant Demographic and Clinical Information

	Control (n=74)	FASD (n=70)
Age	13.2 ± 6.0	14.2 ± 6.3
N males (%)	40 (57%)	38 (51%)
Demographic Information:	N=72	N=44
Ethnicity		
Caucasian	58 (81%)	18 (41%)
Aboriginal	4 (6%)	21 (48%)
Other	10 (14%)	5 (11%)
Living situation		
Biological parent(s)	62 (86%)	5 (11%)
Adopted/Biological Relative	1 (1%)	21 (48%)
Foster Care	0 (0%)	12 (27%)
Group home	0 (0%)	2 (5%)
Independent	9 (13%)	4 (9%)
Foster care placements per person (mean, range)	0 (0-0)	1.5 (0-5)
Annual Household income	\$51,000-75,000	\$76,000-100,000
Basic needs not met at any time ^a	1 (1%)	24 (55%)
Psychiatric Co-Morbidities ^a		
ADHD	0 (0%)	38 (87%)
Reactive Attachment Disorder	0 (0%)	10 (23%)
Anxiety	3 (4%) ^b	12 (27%)
Other ^c	0 (0%)	15 (34%)
Psychiatric medications ^a		
Atypical Antipsychotics	0 (0%)	24 (55%)
Stimulants	0 (0%)	20 (45%)
Antidepressants	0 (0%)	12 (27%)
Other	0 (0%)	3 (7%)
Number of psychiatric meds per person (mean, range)	0 (0-0)	1.7 (0-4)

^aSelf/parent reported

^bSelf or parent reported anxiety for which medical attention/counselling was sought. None were taking anxiolytic medication or had a formal diagnosis.

^cNumber of subjects with at least one other comorbidity

Table 7.2: Cognitive Test Scores in FASD and Controls

Test		Control		FASD		Group difference p-value
		Mean ± SD	Sex	Mean ± SD	Sex	
WRIT ^a (age 4+)	General IQ	112 ± 13 (n=74)	ns	87 ± 18 (n=45)	ns	<0.001
WRMT-R ^a (age 5+)	Word ID	107 ± 13 (n=74)	0.034; boys> girls	88 ± 16 (n=69)	ns	<0.001
WJ ^a (age 5+)	Quantitative Concepts	108 ± 13 (n=74)	ns	83 ± 14 (n=65)	ns	<0.001
CREVT ^a (age 5+)	Receptive & Expressive Composite	102 ± 10 (n=74)	ns	84 ± 12 (n=50)	ns	<0.001
NEPSY/ DKEFS ^b (age 5+)	Executive Function Composite	10.2 ± 2.2 (n=74)	ns	7.3 ± 3.0 (n=66)	ns	<0.001
RCFT ^c (age 6+)	Immediate Recall	47 ± 12 (n=71)	ns	36 ± 14 (n=33)	ns	<0.001
	Delayed recall	47 ± 11 (n=71)	ns	36 ± 15 (n=33)	ns	<0.001
	Recognition	51 ± 13 (n=71)	ns	48 ± 15 (n=33)	ns	ns
BRIEF ^d (5-18 years)	BRI	48 ± 7 (n=61)	0.026; boys> girls	76 ± 12 (n=57)	ns	<0.001
	MI	48 ± 8 (n=60)	ns	72 ± 8 (n=57)	ns	<0.001
	GEC	48 ± 7 (n=60)	ns	75 ± 8 (n=57)	ns	<0.001
WMTB-C ^a (5-15 years)	Digit	98 ± 16 (n=59)	ns	86 ± 13 (n=43)	ns	<0.001
	Block	98 ± 16 (n=59)	ns	83 ± 15 (n=41)	ns	<0.001

^aStandard score, population mean=100 ± 15 (higher score= better performance)

^bScaled score, population mean = 10 ± 3 (higher score=better performance)

^cT score, population mean= 50 ± 10 (higher score= better performance)

^dT score, population mean 50 ± 10 (higher score = worse behaviour)

7.3.2 Age Effects on FA, MD, Brain Volumes and Cortical Thickness

FA increased significantly with age in all tracts in the control group ($p < 0.001-0.027$), except for the genu and splenium of the corpus callosum. In the FASD group, however, FA increased significantly with age in the body of the corpus callosum, bilateral cingulum, right CST, bilateral IFO, and right UF ($p < 0.001-0.034$; Table 7.3, Figure 7.2A,B) but did not change in any of the remaining 8 tracts. MD decreased significantly with age for all tracts in both the control ($p < 0.001$ in all) and FASD group ($p < 0.001-0.007$; Table 7.4, Figure 7.2C,D).

In the control group, white matter volume increased with age ($p = 0.002$), and cortical grey matter and right globus pallidus volumes decreasing with age ($p < 0.001$ and 0.025 , respectively; Table 7.5, Figure 7.2E,F). Likewise, white matter volume increasing with age ($p = 0.014$), and cortical grey matter ($p < 0.001$) and bilateral globus pallidus volumes decreased with age in the FASD group (left $p = 0.002$, right $p < 0.001$), but in addition left ($p = 0.004$) and right putamen volumes also decreased with age ($p = 0.007$). Significant change with age was not observed for any other structures in either group.

Cortical thickness decreased significantly with age in 60/78 cortical regions in the control group ($p < 0.001-0.029$) and 51/78 regions in the FASD group ($p < 0.001-0.048$; Tables 7.6-7.10, Figure 7.3I-L). The effect of age appeared to vary regionally, e.g. both groups showed decreases in 14/14 parietal regions (Table 7.7), but in only 5/16 and 11/16 temporal regions in the FASD and control groups, respectively (Table 7.8).

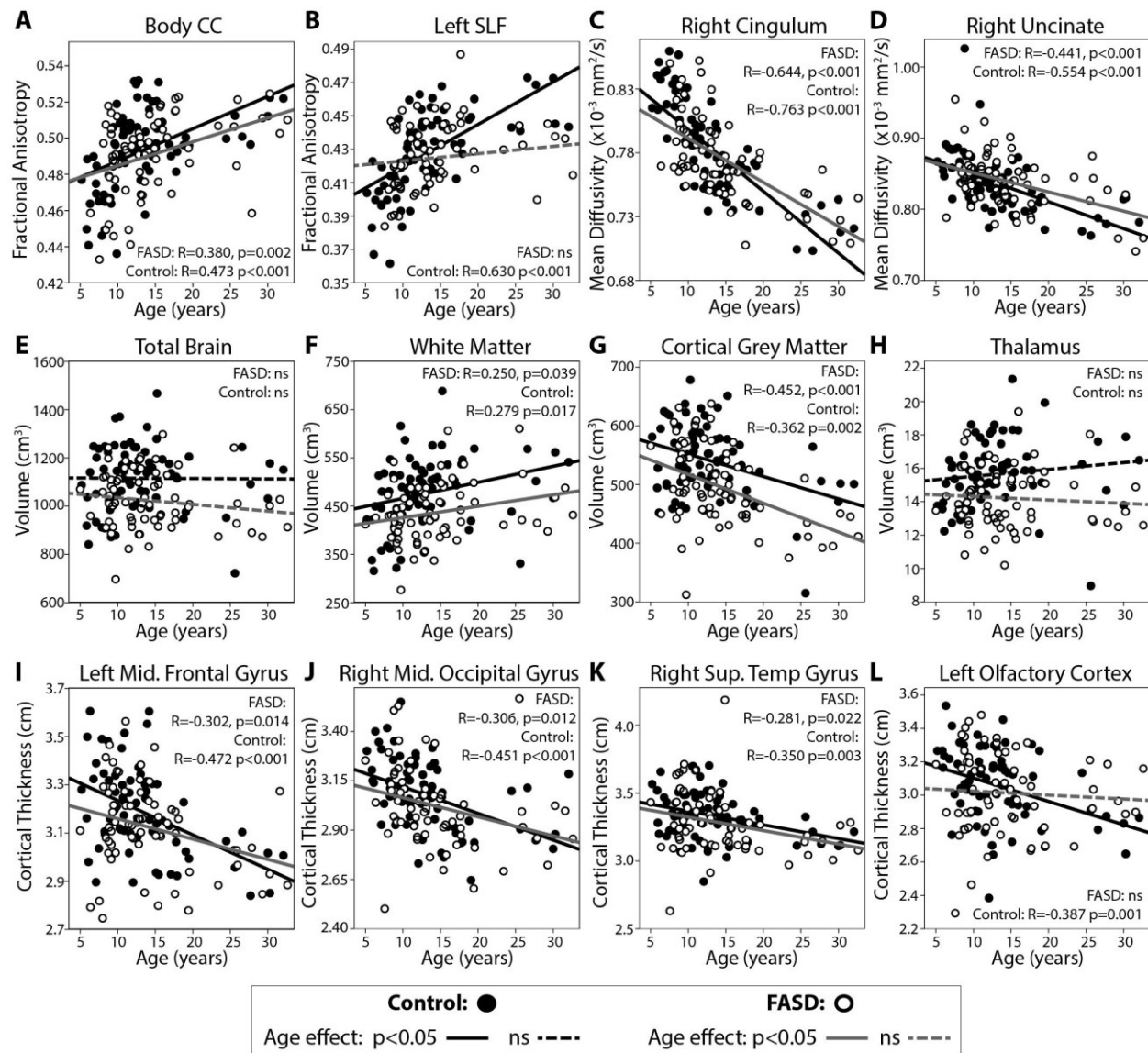


Figure 7.2: Examples of correlations with age for diffusion parameters (A-D), brain volumes (E-H) and cortical thickness (I-J). A general trend of increasing FA and decreasing MD with age was observed in both groups, though several tracts showed weaker or non-significant correlations in the FASD group (e.g. FA of the left SLF, B). Changes with age were similar between groups for most volumes, despite overall reductions in the FASD group (e.g. white matter, F). Cortical thinning with age was observed in 60 of 78 cortical regions in controls and 51 regions in the FASD group, though correlations were often weaker in the FASD group (e.g. left middle frontal gyrus, I).

7.3.3 Sex Effects on FA, MD, Brain Volumes and Cortical Thickness

Sex differences were observed in the BRIEF Behavioural Regulation Index ($t=2.176$; $p=0.034$, worse performance in males) and WRMT Word ID ($t=2.269$, $p=0.026$, worse performance in females) in the control group. No other cognitive test scores were significantly different between males and females.

Significant sex differences in FA were found for 6/15 white matter tracts in the control group (gCC, bCC, left cingulum, bilateral CST and right SLF), and 8/15 tracts in the FASD group (bCC, bilateral cingulum, left IFO, bilateral SLF, bilateral UF) (Table 7.3); in all cases FA was higher in males than females. No significant effects of sex were found for MD of any tract in the control group. Conversely, sex differences in MD were found in the bilateral ILF and bilateral UF in the FASD group; with higher MD in females than males (Table 7.4).

Brain volumes were significantly larger in males than females for 16/16 structures in the control group ($p<0.001$ for all except right hippocampus, $p=0.001$). In the FASD group, volumes were larger in males than females for 12/16 structures ($p<0.001-0.036$), but were not significantly different between males and females for bilateral caudate, right putamen or right globus pallidus (Table 7.5).

Significant sex differences in cortical thickness were found in 19/78 cortical regions in controls (1 frontal, 6 temporal, 9 occipital, 3 limbic, $p<0.001-0.049$; all thicker in males) and 8/78 cortical regions in the FASD group (3 temporal, 5 occipital, $p=0.002-0.047$; all thicker in males) (Tables 7.6-7.10).

7.3.4 Group Differences and FASD Group Z-Score Calculation

MANCOVA analysis revealed group differences (FASD versus controls) in FA of the gCC (lower in male FASD than male control participants) and right UF (lower in female FASD than female control), and in MD of the right and left UF (higher in female FASD than female control participants) (Tables 7.3, 7.4). Significant group differences (FASD versus controls) in brain volumes were found in 16/16 structures in males, and in 10/16 structures in females (all smaller in the FASD group; Table 7.5). Group differences in cortical thickness were significant in 15/78 cortical regions in males (5 frontal, 1 parietal, 2 temporal, 6 occipital, 1 limbic; all thinner in FASD) and 1/78 regions in females (1 occipital; thinner in FASD) (Tables 7.6-7.10).

Including cognitive, DTI, volume and cortical thickness data, significant group differences (FASD versus Controls) were found in 41 variables in males and 22 variables in females. Nineteen of these variables were overlapping (i.e. significant in both males and females), yielding a total of 45 unique variables with significant group differences in males, females or both. Z scores were then calculated in the FASD group for these 45 variables, as described in the methods.

7.3.5 Hemispheric Asymmetry of FASD Z Scores

Differences between left and right Z scores of bilateral structures were tested with paired sample t-test to permit averaging of bilateral structure Z scores in structures with no hemispheric differences, in order to reduce multiple comparisons in subsequent analysis. Paired sample t-test of bilateral structure Z scores (tested separately in males and females) revealed significant left-right differences in: caudate ($t=-2.687$, $p=0.011$ right>left in males), putamen ($t=3.064$, $p=0.004$ left>right in males), hippocampus ($t=-3.805$, $p<0.001$ right>left in males) amygdala ($t=2.338$, $p=0.027$, left>right in females), inferior parietal supramarginal and angular ($t=2.395$, $p=0.022$

left>right in males), middle temporal ($t=3.81$ $p=0.001$ left>right in males), middle frontal ($t=2.48$ $p=0.019$ left>right in females), superior frontal gyrus medial ($t=2.277$ $p=0.031$ left>right in females), angular ($t=3.042$, $p=0.005$ left>right in females), inferior occipital ($t=-2.147$, $p=0.041$, right>left in females) and fusiform gyri ($t=-5.013$, $p<0.001$, right>left in females). Z scores of all other structures were not different between left and right in either sex, and were therefore averaged to reduce multiple comparisons in subsequent analysis.

Table 7.3: Effects of Age, Sex and Group on Fractional Anisotropy

	Control			FASD			Group Difference (FASD vs Controls)		
	Mean ± SD	Age ^a	Sex ^a	Mean ± SD	Age ^a	Sex ^a	All ^b	Males ^c	Females ^c
gCC	0.52 ± 0.02	---	0.003	0.51 ± 0.03	---	---	0.004	0.030	---
bCC	0.49 ± 0.02	<0.001	0.033	0.49 ± 0.02	0.001	0.018	---	---	---
sCC	0.52 ± 0.02	---	---	0.52 ± 0.02	---	---	---	---	---
L Cing	0.45 ± 0.03	<0.001	0.017	0.45 ± 0.02	0.034	0.011	---	---	---
R Cing	0.44 ± 0.02	<0.001	---	0.44 ± 0.02	0.002	0.007	---	---	---
L CST	0.50 ± 0.03	<0.001	0.047	0.50 ± 0.05	---	---	---	---	---
R CST	0.50 ± 0.02	<0.001	0.022	0.50 ± 0.03	0.017	---	---	---	---
L IFO	0.45 ± 0.03	<0.001	---	0.46 ± 0.02	<0.001	0.024	---	---	---
R IFO	0.46 ± 0.03	<0.001	---	0.46 ± 0.02	0.004	---	---	---	---
L ILF	0.43 ± 0.02	0.027	---	0.42 ± 0.02	---	---	---	---	---
R ILF	0.43 ± 0.02	0.003	---	0.42 ± 0.02	---	---	---	---	---
L SLF	0.43 ± 0.02	<0.001	---	0.42 ± 0.02	---	0.030	---	---	---
R SLF	0.42 ± 0.02	<0.001	0.022	0.41 ± 0.02	---	0.029	---	---	---
L UF	0.38 ± 0.02	<0.001	---	0.38 ± 0.02	---	0.028	---	---	---
R UF	0.38 ± 0.02	<0.001	---	0.38 ± 0.02	0.015	0.001	---	---	0.021

^ap-values, shown if <0.05

^bControlling for age and sex if significant in either FASD or Controls

^cControlling for age if significant in either FASD or Controls

gCC=genu; bCC=body; sCC=splenium of the corpus callosum; L=left; R=right; Cing=cingulum; CST=corticospinal tract; IFO=inferior fronto-occipital fasciculus; ILF=inferior longitudinal fasciculus; SLF=superior longitudinal fasciculus; UF=uncinated fasciculus

Table 7.4: Effects of Age, Sex and Group on Mean Diffusivity

	Controls			FASD			Group Difference (FASD vs Control)		
	Mean ± SD	Age ^a	Sex ^a	Mean ± SD	Age ^a	Sex ^a	All ^b	Males ^c	Females ^c
gCC	0.81 ± 0.04	<0.001	---	0.80 ± 0.04	0.004	---	---	---	---
bCC	0.86 ± 0.05	<0.001	---	0.86 ± 0.05	<0.001	---	---	---	---
sCC	0.89 ± 0.05	<0.001	---	0.87 ± 0.04	0.001	---	---	---	---
L Cing	0.78 ± 0.04	<0.001	---	0.77 ± 0.03	<0.001	---	---	---	---
R Cing	0.78 ± 0.04	<0.001	---	0.78 ± 0.03	<0.001	---	---	---	---
L CST	0.81 ± 0.04	<0.001	---	0.80 ± 0.03	0.001	---	---	---	---
R CST	0.81 ± 0.04	<0.001	---	0.81 ± 0.03	0.007	---	---	---	---
L IFO	0.81 ± 0.04	<0.001	---	0.81 ± 0.03	<0.001	---	---	---	---
R IFO	0.81 ± 0.03	<0.001	---	0.81 ± 0.03	<0.001	---	---	---	---
L ILF	0.86 ± 0.04	<0.001	---	0.85 ± 0.04	<0.001	0.029	---	---	---
R ILF	0.85 ± 0.04	<0.001	---	0.84 ± 0.03	<0.001	0.046	---	---	---
L SLF	0.79 ± 0.05	<0.001	---	0.78 ± 0.03	<0.001	---	---	---	---
R SLF	0.79 ± 0.04	<0.001	---	0.77 ± 0.04	<0.001	---	---	---	---
L UF	0.84 ± 0.04	<0.001	---	0.84 ± 0.04	0.001	0.038	---	---	0.046
R UF	0.84 ± 0.04	<0.001	---	0.84 ± 0.04	<0.001	0.010	---	---	0.017

^ap-values, shown if <0.05

^bControlling for age and sex if significant in either FASD or Controls

^cControlling for age if significant in either FASD or Controls

gCC=genu; bCC=body; sCC=splenium of the corpus callosum; L=left; R=right; Cing=cingulum; CST=corticospinal tract; IFO=inferior fronto-occipital fasciculus; ILF=inferior longitudinal fasciculus; SLF=superior longitudinal fasciculus; UF=uncinated fasciculus

Table 7.5: Effects of Age, Sex and Group on Brain Volumes

	Control			FASD			Group Difference (FASD vs Control) ^a		
	Mean ± SD	Age ^a	Sex ^a	Mean ± SD	Age ^a	Sex ^a	All ^b	Males ^c	Females ^c
ICV	1450 ± 164	---	<0.001	1390 ± 126	---	0.001	0.001	<0.001	---
Total Brain	1115 ± 133	---	<0.001	1020 ± 117	---	<0.001	<0.001	<0.001	0.013
Cortical GM	540 ± 63	<0.001	<0.001	496 ± 68	<0.001	<0.001	<0.001	<0.001	0.028
White Matter	477 ± 71	0.002	<0.001	435 ± 60	0.014	<0.001	<0.001	<0.001	0.027
L Thal	7.8 ± 1.0	---	<0.001	7.1 ± 0.9	---	0.024	<0.001	<0.001	0.014
L Caud	4.0 ± 0.6	---	<0.001	3.4 ± 0.6	---	---	<0.001	<0.001	0.001
L Put	6.1 ± 0.8	---	<0.001	5.6 ± 0.7	0.044	0.036	<0.001	<0.001	0.044
L GP	1.9 ± 0.3	---	<0.001	1.8 ± 0.3	0.002	0.004	<0.001	<0.001	0.038
L Hipp.	4.3 ± 0.5	---	<0.001	4.0 ± 0.5	---	0.020	<0.001	<0.001	---
L Amyg	1.5 ± 0.2	---	<0.001	1.5 ± 0.2	---	0.008	---	0.010	---
R Thal	7.9 ± 1.0	---	<0.001	7.2 ± 0.9	---	0.015	<0.001	<0.001	0.013
R Caud	4.0 ± 0.6	---	<0.001	3.4 ± 0.6	---	---	<0.001	<0.001	0.003
R Put	6.0 ± 0.8	---	<0.001	5.4 ± 0.7	0.007	---	<0.001	<0.001	---
R GP	1.7 ± 0.3	0.025	<0.001	1.6 ± 0.3	<0.001	---	<0.001	<0.001	---
R Hipp	4.3 ± 0.6	---	0.001	4.0 ± 0.5	---	0.001	<0.001	0.002	0.023
R Amyg	1.6 ± 0.2	---	<0.001	1.5 ± 0.2	---	0.002	0.008	0.013	---

^ap-values, shown if <0.05

^bControlling for age and sex if significant in either FASD or Controls

^cControlling for age if significant in either FASD or Controls

ICV= Intracranial Volume; GM=Grey Matter; L=Left; R=Right; Thal=Thalamus; Caud=Caudate; Put=Putamen; GP=Globus Pallidus; Hipp=Hippocampus; Amyg=Amygdala

Table 7.6: Effects of Age, Sex and Group on Cortical Thickness in Frontal Regions

	Control			FASD			Group Difference (FASD vs Control)		
	Mean ± SD	Age ^a	Sex ^a	Mean ± SD	Age ^a	Sex ^a	Both ^b	Males ^c	Females ^c
L Gyrus Rectus	3.17 ± 0.2	.006	---	3.19 ± 0.2	---	---	---	---	---
L SFG orbital	3.19 ± 0.2	.000	---	3.18 ± 0.2	.025	---	---	---	---
L SFG medialorbital	3.42 ± 0.2	.000	---	3.37 ± 0.3	---	---	---	---	---
L MFG orbital	3.22 ± 0.2	.000	---	3.17 ± 0.2	.027	---	---	---	---
L IFG orbital	3.41 ± 0.2	.000	---	3.39 ± 0.2	.015	---	---	---	---
L SFG dorsolateral	3.21 ± 0.2	.000	---	3.14 ± 0.2	.007	---	---	.040	---
L MFG	3.19 ± 0.2	.000	.022	3.12 ± 0.2	.015	---	.039	.022	---
L IFG opercular	3.40 ± 0.2	.001	---	3.38 ± 0.2	.002	---	---	---	---
L IFG triangular	3.26 ± 0.2	.000	---	3.22 ± 0.2	.000	---	---	---	---
L SFG medial	3.59 ± 0.2	.000	---	3.53 ± 0.2	.014	---	---	---	---
L sup. motor	3.51 ± 0.2	.000	---	3.45 ± 0.2	.010	---	---	---	---
L precentral	2.99 ± 0.2	.029	---	2.96 ± 0.2	.013	---	---	---	---
R Gyrus Rectus	3.15 ± 0.2	.001	---	3.18 ± 0.2	---	---	---	---	---
R SFG orbital	3.23 ± 0.2	.000	---	3.22 ± 0.2	.009	---	---	---	---
R SFG medialorbital	3.40 ± 0.3	.000	---	3.37 ± 0.2	.005	---	---	---	---
R MFG orbital	3.32 ± 0.2	.000	---	3.26 ± 0.2	.005	---	---	---	---
R IFG orbital	3.55 ± 0.2	.000	---	3.51 ± 0.2	---	---	---	---	---
R SFG dorsolateral	3.21 ± 0.2	.000	---	3.15 ± 0.2	.000	---	---	---	---
R MFG	3.21 ± 0.2	.000	---	3.14 ± 0.2	.003	---	.029	.032	---
R IFG opercular	3.39 ± 0.2	.002	---	3.38 ± 0.2	.010	---	---	---	---
R IFG triangular	3.32 ± 0.2	.000	---	3.26 ± 0.2	.007	---	---	---	---
R SFG medial	3.51 ± 0.2	.000	---	3.42 ± 0.2	.003	---	.026	.040	---
R sup. motor	3.43 ± 0.2	.000	---	3.40 ± 0.2	.001	---	---	---	---
R precentral	3.00 ± 0.2	---	---	2.93 ± 0.2	.025	---	.041	.038	---

^ap-values, shown if <0.05

^bControlling for age and sex if significant in either FASD or Controls

^cControlling for age if significant in either FASD or Controls

L=Left; R=Right; SFG=superior frontal gyrus; MFG=middle frontal gyrus; sup. motor= supplementary motor area; IFG=inferior frontal gyrus

Table 7.7: Effects of Age, Sex and Group on Cortical Thickness in Parietal Regions

	Control			FASD			Group Difference (FASD vs Control)		
	Mean ± SD	Age ^a	Sex ^a	Mean ± SD	Age ^a	Sex ^a	Both ^b	Males ^c	Females ^c
L paracentral lobule	3.03 ± 0.2	.000	---	2.99 ± 0.2	.001	---	---	---	---
L postcentral	2.70 ± 0.2	.002	---	2.66 ± 0.2	.003	---	---	---	---
L Superior Parietal	2.76 ± 0.2	.000	---	2.72 ± 0.2	.000	---	---	---	---
L Inferior parietal supramarginal angular	2.89 ± 0.2	.000	---	2.86 ± 0.2	.000	---	---	---	---
L supramarginal	3.18 ± 0.2	.011	---	3.15 ± 0.2	.001	---	---	---	---
L angular	3.13 ± 0.2	.000	---	3.10 ± 0.2	.001	---	---	---	---
L precuneous	3.03 ± 0.2	.000	---	2.99 ± 0.2	.000	---	---	---	---
R paracentral lobule	2.93 ± 0.2	.001	---	2.92 ± 0.2	.000	---	---	---	---
R postcentral	2.67 ± 0.2	.003	---	2.61 ± 0.2	.000	---	---	---	---
R Superior Parietal	2.76 ± 0.2	.000	---	2.68 ± 0.2	.000	---	---	---	---
R Inferior parietal but supramarginal and angular	2.88 ± 0.2	.000	---	2.80 ± 0.2	.000	---	.024	.043	---
R supramarginal	3.07 ± 0.2	.000	---	3.05 ± 0.2	.000	---	---	---	---
R angular	3.08 ± 0.2	.000	---	2.99 ± 0.2	.000	---	.020	---	---
R precuneous	3.09 ± 0.2	.000	---	3.05 ± 0.2	.000	---	---	---	---

^ap-values, shown if <0.05

^bControlling for age and sex if significant in either FASD or Controls

^cControlling for age if significant in either FASD or Controls

L=left; R=right

Table 7.8 Effect of Age, Sex and Group on Cortical Thickness in Temporal Regions

	Control			FASD			Group Difference (FASD vs Control)		
	Mean ± SD	Age ^a	Sex ^a	Mean ± SD	Age ^a	Sex ^a	Both ^b	Males ^c	Females ^c
L Olfactory	3.06 ± 0.2	.001	---	3.01 ± 0.2	---	---	---	---	---
L Rolandic operculum	3.35 ± 0.2	.005	---	3.35 ± 0.2	.021	---	---	---	---
L Heschl	3.14 ± 0.2	---	---	3.12 ± 0.2	---	---	---	---	---
L STG	3.31 ± 0.2	.020	---	3.27 ± 0.2	---	---	---	---	---
L MTG	3.32 ± 0.2	.000	---	3.26 ± 0.2	.003	---	---	---	---
L ITG	3.58 ± 0.2	.011	.001	3.50 ± 0.3	---	.022	---	---	---
L Temporal pole STG	3.77 ± 0.3	---	.025	3.73 ± 0.4	---	---	---	---	---
L Temporal pole MTG	3.91 ± 0.3	---	.007	3.86 ± 0.4	---	.043	---	---	---
R Olfactory Cortex	3.04 ± 0.2	.002	---	3.05 ± 0.2	---	---	---	---	---
R Rolandic operculum	3.32 ± 0.2	.000	---	3.32 ± 0.2	.006	---	---	---	---
R Heschl	3.19 ± 0.2	.026	---	3.18 ± 0.2	---	---	---	---	---
R STG	3.33 ± 0.2	.003	---	3.28 ± 0.2	.026	---	---	---	---
R MTG	3.39 ± 0.2	.000	.010	3.31 ± 0.2	.002	---	.013	.041	---
R ITG	3.59 ± 0.2	.002	.000	3.50 ± 0.3	---	.015	.017	.018	---
R Temporal pole STG	3.81 ± 0.2	---	---	3.75 ± 0.4	---	---	---	---	---
R Temporal pole MTG	3.94 ± 0.2	---	.049	3.86 ± 0.4	---	---	---	---	---

^ap-values, shown if <0.05

^bControlling for age and sex if significant in either FASD or Controls

^cControlling for age if significant in either FASD or Controls

L=left; R=right; STG=superior temporal gyrus; MTG=middle temporal gyrus; ITG=inferior temporal gyrus

Table 7.9: Effects of Age, Sex and Group on Cortical Thickness of Occipital Regions

	Control			FASD			Group Difference (FASD vs Control)		
	Mean ± SD	Age ^a	Sex ^a	Mean ± SD	Age ^a	Sex ^a	Both ^b	Males ^c	Females ^c
L superior occipital	2.75 ± 0.2	.013	.043	2.75 ± 0.2	---	---	---	---	---
L middle occipital	3.06 ± 0.2	.000	---	3.01 ± 0.2	.001	---	---	---	---
L inferior occipital	3.23 ± 0.2	---	.009	3.13 ± 0.2	.046	.043	.005	.010	---
L calcarine fissure and surrounding cortex	2.73 ± 0.2	---	---	2.68 ± 0.2	---	.047	---	---	---
L cuneus	2.71 ± 0.1	---	---	2.73 ± 0.1	.029	---	---	---	---
L lingual	2.99 ± 0.3	---	.001	2.88 ± 0.2	---	.042	.003	.005	---
L fusiform	3.40 ± 0.3	---	.002	3.26 ± 0.2	.006	.002	.000	.002	.032
R superior occipital	2.75 ± 0.2	.025	.004	2.76 ± 0.2	---	---	---	---	---
R middle occipital	3.08 ± 0.2	.000	---	3.02 ± 0.2	.014	.031	---	---	---
R inferior occipital	3.14 ± 0.2	---	.000	3.06 ± 0.2	---	---	.042	.017	---
R calcarine fissure and surrounding cortex	2.79 ± 0.2	---	.004	2.76 ± 0.2	.048	---	---	---	---
R cuneus	2.81 ± 0.2	.009	---	2.82 ± 0.2	.012	---	---	---	---
R lingual	2.97 ± 0.2	---	.004	2.92 ± 0.2	---	---	---	.029	---
R fusiform	3.37 ± 0.2	---	.000	3.30 ± 0.2	.007	---	.031	.002	---

^ap-values, shown if <0.05

^bControlling for age and sex if significant in either FASD or Controls

^cControlling for age if significant in either FASD or Controls

L=left; R=right

Table 7.10: Effect of Age, Sex and Group on Cortical Thickness of Limbic Areas

	Control			FASD			Group Difference (FASD vs Control)		
	Mean ± SD	Age ^a	Sex ^a	Mean ± SD	Age ^a	Sex ^a	Both ^b	Males ^c	Females ^c
L parahippocampal	3.24 ± 0.2	.002	.006	3.21 ± 0.2	---	---	---	---	---
L Anterior cingulate and paracingulate	3.57 ± 0.2	.000	---	3.56 ± 0.2	---	---	---	---	---
L Median cingulate and paracingulate	3.22 ± 0.2	.000	---	3.21 ± 0.2	.000	---	---	---	---
L Posterior Cingulate	2.84 ± 0.2	---	---	2.82 ± 0.2	.030	---	---	---	---
L Insula	3.83 ± 0.3	---	.032	3.77 ± 0.3	---	---	---	---	---
R parahippocampal	3.24 ± 0.2	.013	.035	3.19 ± 0.2	---	---	---	.042	---
R Anterior cingulate and paracingulate	3.58 ± 0.2	.000	---	3.54 ± 0.2	.002	---	---	---	---
R Median cingulate and paracingulate	3.31 ± 0.2	.000	---	3.32 ± 0.2	.000	---	---	---	---
R Posterior Cingulate	2.82 ± 0.2	.009	---	2.82 ± 0.1	---	---	---	---	---
R Insula	3.85 ± 0.2	---	---	3.84 ± 0.2	---	---	---	---	---

^ap-values, shown if <0.05

^bControlling for age and sex if significant in either FASD or Controls

^cControlling for age if significant in either FASD or Controls

L=left; R=right

7.3.6 FASD group Z Score Rankings

After averaging left and right where appropriate, Z scores of 41 variables in the FASD group (9 cognitive, 3 DTI, 14 volumes, 15 cortical thickness regions) were plotted on the same scale in males and females in order to compare the magnitude of difference relative to the control mean (Figure 7.3). The largest Z scores were observed for cognitive tests and volumes, followed by cortical thickness and DTI parameters. This plot also indicates that males with FASD have larger Z scores than females for brain volumes and select cortical regions, indicating greater reductions relative to controls (Figure 7.3).

To further test sex differences, variables with Z scores $> \pm 0.5$ were ranked separately in males and females according to their magnitude (Figure 7.4) for a total of 32 variables in males and 20 variables in females. In both males and females, cognitive testing variables were among the largest absolute Z scores, though note that diagnosis of FASD requires cognitive impairment. In addition to males having a greater number of variables with Z scores more than ± 0.5 SD from the control mean, males also had significantly larger magnitudes of Z scores than females for ICV ($t=4.261$, $p<0.001$), total brain ($t=-3.112$, $p=0.003$), white matter ($t=-2.934$, $p=0.005$), cortical grey matter ($t=-2.084$, $p=0.041$), left and right putamen ($t=-3.103$, $p=0.003$ and $t=-4.488$, $p<0.001$, respectively), globus pallidus ($t=-2.201$, $p=0.031$), left hippocampus ($t=-2.279$, $p=0.026$), left amygdala ($t=-2.589$, $p=0.012$) and right fusiform gyrus ($t=-3.478$, $p<0.001$) (indicated with asterisks in Figure 7.4). No variables were observed to have larger Z scores in females, and no sex differences were found in the Z scores of any cognitive tests.

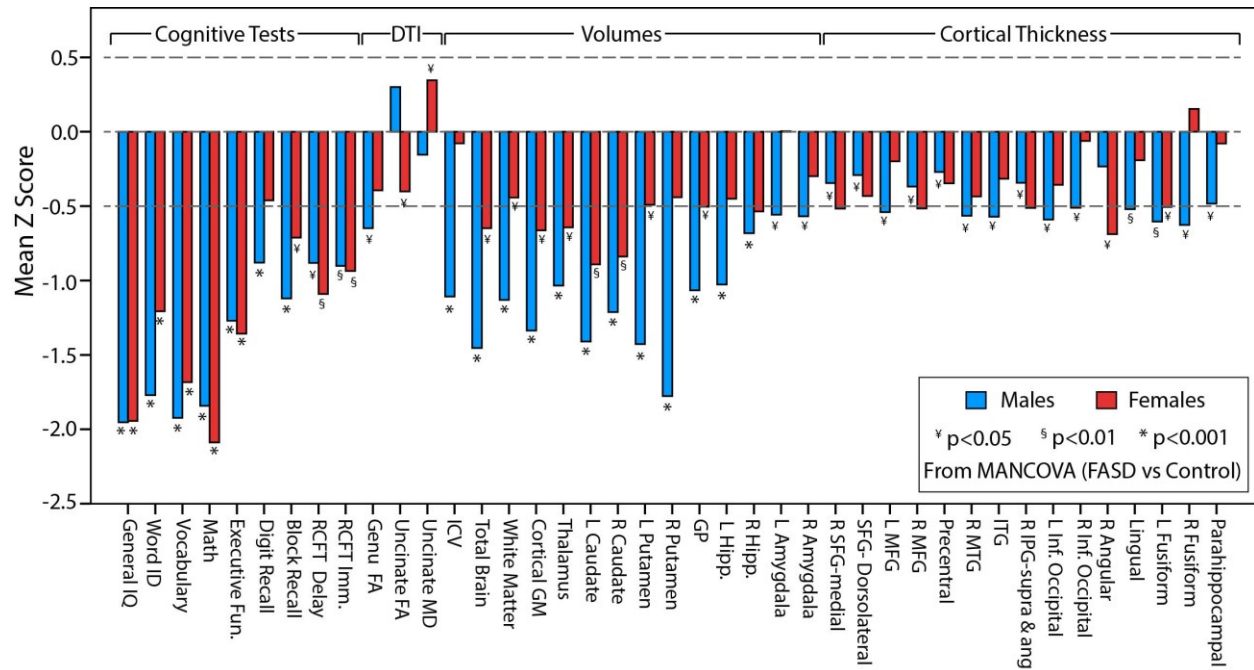


Figure 7.3: Z scores in the FASD group. Z scores are shown for variables with significant group differences (FASD versus controls) in either males or females in MANCOVA analysis. The largest magnitude differences are observed for cognitive tests and brain volumes relative to tractography and cortical thickness. Of note, Z score magnitude appears to be larger in males (blue) relative to females (red) for several volumes and cortical thickness regions, but not cognitive tests.

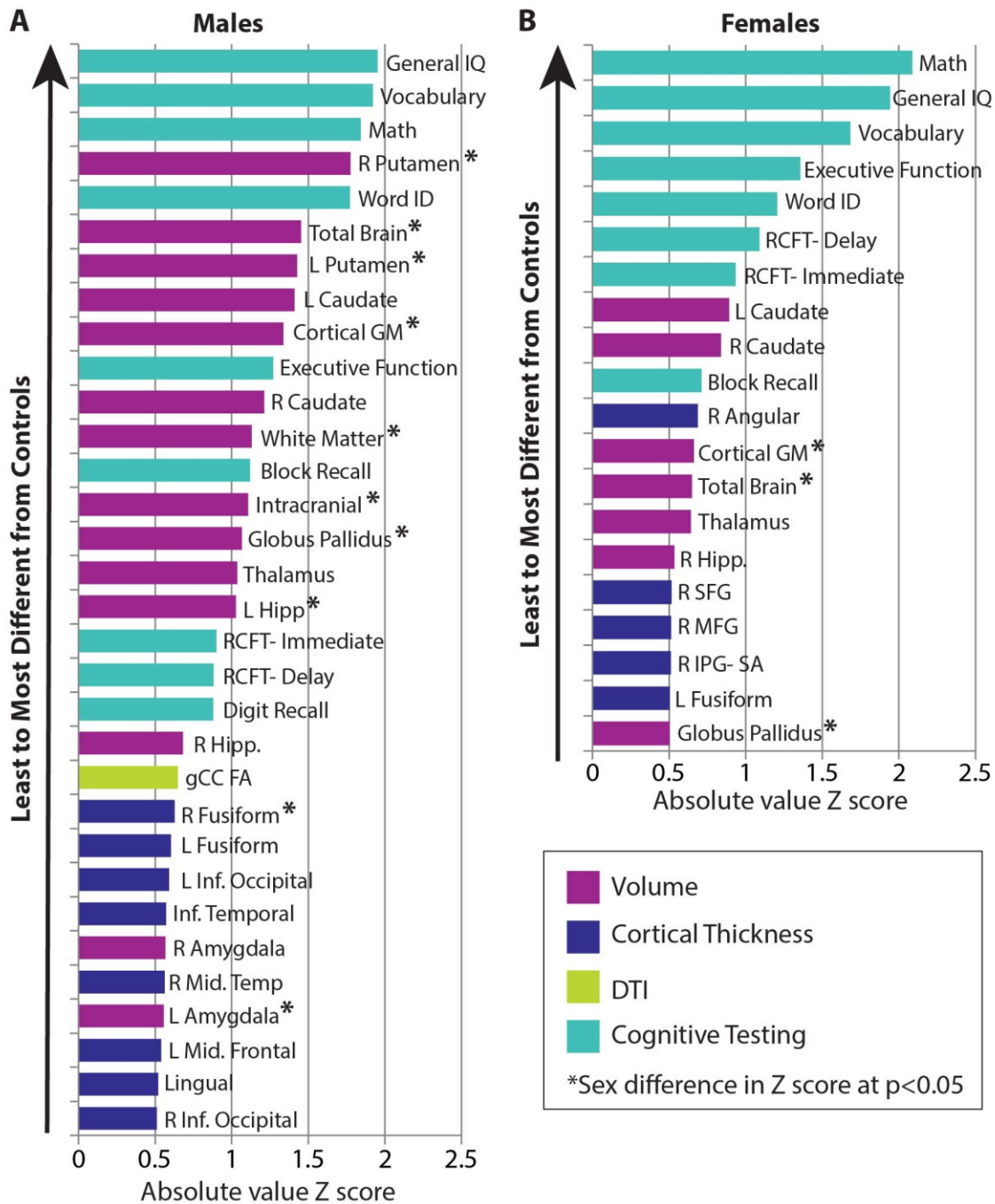


Figure 7.4: Rank ordered FASD group Z scores in male (A) and females (B). Only variables with Z scores $> \pm 0.5$ are included here. More variables meet these criteria in males than females (32 versus 20). In addition, larger magnitude Z scores can also be seen in males relative to females (e.g. right putamen is almost 2 standard deviations below the control norm in males, and only about 0.5 standard deviations below in females). Variables with significantly different Z score magnitudes between males and females are indicated with asterisks. Cognitive scores are shown to have the largest absolute volume Z scores in both males and females, though it should be noted that all participants have a diagnosis which requires significant cognitive impairment.

7.3.7 FASD Z-Score Correlation Analysis

Partial correlations (controlling for age) were performed between Z scores $> \pm 0.5$ standard deviations from the control norm in either males or females (36 variables total), and FDR corrected for multiple comparisons. This analysis revealed several significant correlations between cognitive scores (e.g. between IQ and math) in both males and females, as expected, though a greater number of correlations reached significance in females (Figure 7.5). Likewise, significant correlations were observed between several volumes in both males and females (e.g. total brain and cortical grey matter volume), though in this case more correlations reached significance in males. Cortical thickness correlations were similar in both males and females.

Several significant correlations were found between cognitive scores and volumes in females but not males, including: RCFT immediate recall and right hippocampus volume ($r=0.674$, $p=0.004$); RCFT delay and both left ($r=0.631$, $p=0.009$) and right hippocampus volumes ($r=0.704$, $p=0.002$; Figure 7.6A); executive function composite and thalamus ($r=0.616$, $p=0.001$), left caudate ($r=0.517$, $p=0.006$), right caudate ($r=0.573$, $p=0.002$; Figure 7.6B) and globus pallidus volume ($r=0.569$, $p=0.002$); WRIT IQ and thalamus ($r=0.703$, $p=0.001$; Figure 7.6C), left caudate ($r=0.518$, $p=0.028$), right caudate ($r=0.509$, $p=0.031$) and globus pallidus volumes ($r=0.738$, $p<0.001$); Word ID and FA of the genu ($r=0.594$, $p=0.001$; Figure 7.6D); and digit recall and left and right putamen volume ($r=-0.685$, $p=0.007$ and $r=-0.716$, $p=0.004$, respectively). No correlation between brain structure and cognitive scores survived FDR correction in males.

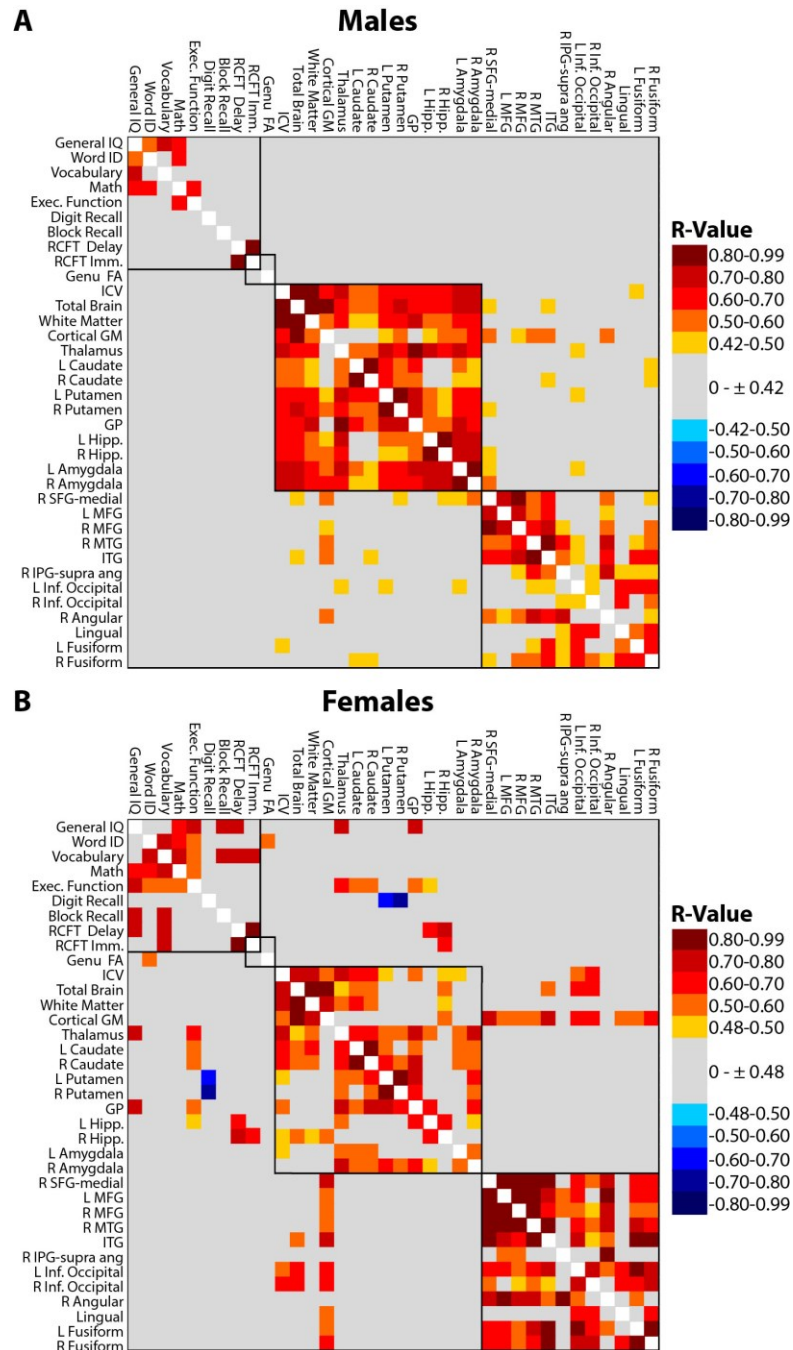


Figure 7.5: FASD group Z score correlation matrix. Includes all variables with Z scores $> \pm 0.5$ in either males or females (36 variables total). Significant correlations are observed between the various cognitive scores in both sexes (upper left box), though a greater number are seen in females. Correlations within volumes are observed within both sexes (middle box), but with slightly more in males. Conversely, a greater number of correlations within cortical thickness areas are seen in females (bottom right box). Interestingly, no correlations are observed between volumes or cortical thickness Z scores and cognitive scores in males, but several significant correlations are observed in females (upper middle).

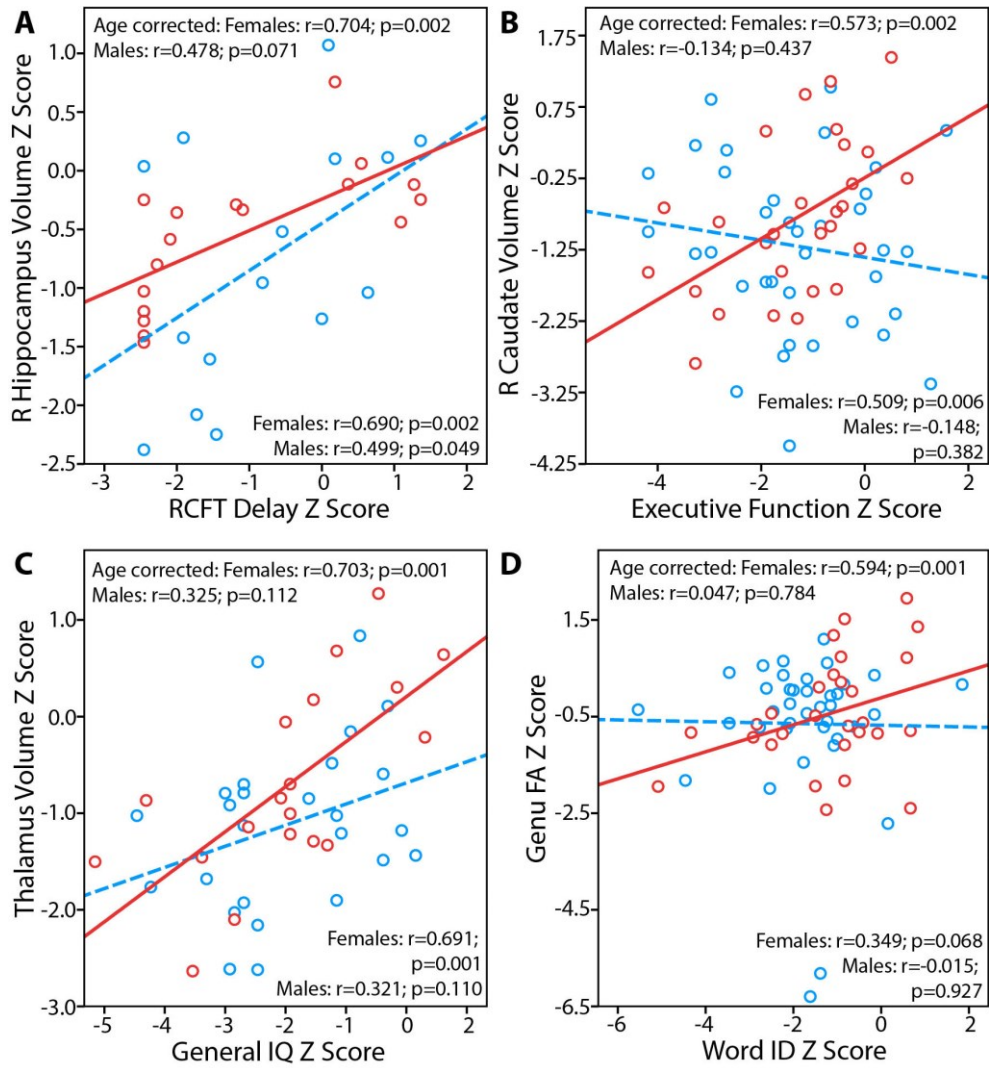


Figure 7.6: Examples of partial correlations controlling for age. All four plots (A-D) show examples of significant positive correlations between MRI metrics and cognitive tests in females but not males. In A-C, correlations indicate that larger volumes are associated with better cognitive performance (hippocampus and visual memory, caudate and executive function, and thalamus and IQ); D indicates that higher FA of the genu is associated with better reading scores in females but not males. Age corrected partial correlation r and p -values are shown in the upper left corner of each plot, Pearson correlation r and p -values are shown in the bottom right corner of each plot.

7.4 Discussion

This large cross-sectional study of children, adolescents and young adults with fetal alcohol spectrum disorders demonstrates robust reductions of cortical and subcortical volumes and cognitive scores, relatively smaller magnitude but consistent reductions of cortical thickness, and fewer, small abnormalities of white matter microstructure. Many previous studies have reported reduced brain volumes in this population (e.g. Archibald et al., 2001; Astley et al., 2009a; Roussotte et al., 2011), suggesting that volume reductions are a robust finding among individuals with prenatal alcohol exposure and possibly reflecting alcohol-induced alterations in neuronal proliferation, migration and cell death in utero (Goodlett et al., 2005). Conversely, cortical thickness studies have been less conclusive, which may stem in part from the robust developmental effects of age on this measure. Nonetheless, here we see reduced cortical thickness in several regions, in keeping with our previous work (Zhou et al., 2011). Likewise, we find reduced fractional anisotropy in the genu of the corpus callosum and the uncinate fasciculus, in keeping with previous studies (Fryer et al., 2009; Ma et al., 2005) as well as elevated mean diffusivity of the uncinate; albeit with fewer group differences than previous work with similar methods (Lebel et al., 2008a). Unlike previous literature, this study allowed for comparison of the relative magnitude of groups differences between imaging methods within the same sample, suggesting that volume and cortical thickness analysis yields more robust group differences than diffusion imaging in individuals with FASD.

In addition to replicating previous literature, these data also demonstrate striking sex differences in the number and magnitude of structural abnormalities (but not cognitive performance) in the FASD group relative to controls, and may suggest that prenatal alcohol exposure is associated with abnormal development of sexual dimorphism in brain structure.

Greater magnitude differences were observed in males (FASD versus Controls) than females for several structures, reaching statistical significance in all volumes except bilateral caudate and thalamus, right hippocampus and right amygdala, which were all equally reduced in males and females with FASD. Only a handful of imaging studies of FASD have examined sex-differences in brain structure, likely due to sample size limitations and interest in sub-grouping based on other important variables (e.g. symptom severity). Nonetheless, there is emerging evidence that brain structure may be more affected by prenatal alcohol exposure in males than females, as evidenced by greater relative reductions in regional cortical (Chen et al., 2012) and deep grey matter volumes (Dudek et al., 2014; Nardelli et al., 2011) in male than female humans with FASD, and greater abnormalities in the corpus callosum in male than female rats with prenatal alcohol exposure (Zimmerberg and Mickus, 1990; Zimmerberg and Reuter, 1989; Zimmerberg and Scalzi, 1989). Moreover, a recent longitudinal study demonstrated greater differences in cortical growth trajectories between males (prenatal alcohol exposure versus controls) than females (Lebel et al., 2012b), suggesting that prenatal alcohol may also influence postnatal developmental trajectories of brain structure in a sexually dimorphic manner. Of note, caudate volume was one of the few structures that was significantly reduced in both males and females with no sex differences in magnitude. The ‘coherence’ of reduction here may underlie consistent observations of disproportionately reduced caudate volume observed in previous studies that have pooled males and females (e.g. up to 20% reductions; Astley et al., 2009a) and confirms the vulnerability of this structure to damage from prenatal alcohol exposure in an independent sample.

Robust sex differences in brain volumes are observed in healthy populations, and may partially explain greater relative impairment observed in male FASD participants if this expected

process of sexual differentiation in brain structure is disrupted by prenatal alcohol exposure. A recent study of over 1000 healthy adults demonstrated disproportionately larger putamen and globus pallidus (but not caudate) volumes in males than females, even after controlling for increased total grey and white matter volumes (Rijkema et al., 2012). Likewise, higher percentage of white matter (Cosgrove et al., 2007) and larger amygdala volume relative to total brain volume has been demonstrated in healthy males relative to females (Cahill, 2006; Goldstein et al., 2001). Here we see significantly larger Z scores for putamen, globus pallidus, white matter and amygdala volumes in males relative to females with FASD. Absence of expected sex differences in these structures would further widen the gap between male FASD participants and male controls in these structures, compared to females who do not typically show this disproportionate increase. Indeed, fewer and smaller sex differences are seen raw volumes in the FASD than control group (Table 7.5), suggesting that sexual dimorphism of brain structure may be attenuated in the FASD group.

Basal ganglia structures (including the putamen and globus pallidus) have been implicated in numerous psychiatric and developmental disorders that have higher prevalence in males than females (e.g. Parkinson's disease, Autism, ADHD) as well as with disorders that differ phenotypically between males and females (e.g. obsessive compulsive disorder) (Rijkema et al., 2012), which may stem in part from their neurochemical properties or density of sex steroid receptors. For example, females have higher presynaptic dopaminergic tone in the striatum (Cosgrove et al., 2007), which has been proposed as a protective factor against the development of schizophrenia, alcoholism and other disorders that are both more common in men and are associated with disturbed dopamine function (Cahill, 2006). A recent study has demonstrated that prenatal alcohol exposure induces increased dopamine receptor D₁ receptor

binding in rhesus macaques (Converse et al., 2014), providing a possible mechanism through which alcohol may induce the male brain to become morphologically more similar to the ‘female’ brain (though notably without offering neuroprotection in this context). Links between neurotransmitter dysfunction and structural variables such as volume are not straightforward, though there is emerging evidence that pharmacologically manipulation of dopamine receptors can induce transient changes in striatal volume (Tost et al., 2010). Although intriguing, further work is needed to tease apart the influence of prenatal alcohol exposure-induced changes in the dopamine system on long-term sex specific striatal volume deficits, particularly in the context of other confounding factors such as antipsychotic medication use (which also act on the dopamine system).

Alterations in androgens may also influence sex-specific effects of prenatal alcohol exposure on the brain. Testosterone is converted to estradiol during early development in a process that enhances neuronal density and size, maturation, migration and synaptogenesis, and is thought to ‘masculinize’ the brain (Goldstein et al., 2001; McCarthy, 2008). Interestingly, decreased systemic tissue responsiveness to testosterone (despite increased levels) has recently been observed in males and female adolescents with prenatal alcohol exposure (Carter et al., 2014), in keeping with animal models demonstrating reduced sensitivity to neurophysiological effects of testosterone in male rats with prenatal alcohol exposure (Lan et al., 2009). As such, reduced responsiveness to testosterone may confer another mechanism by which males with prenatal alcohol exposure show greater relative reductions in structures highly innervated with sex steroids, though further work is needed to investigate the influence of prenatal alcohol exposure on testosterone bioavailability and responsiveness in the brain. Sexually dimorphic effects of prenatal alcohol exposure have been observed in other systems, including long-term

potentiation (LTP) in the hippocampus, whereby prenatal alcohol exposure lead to 40% reductions of LTP in male but not female rats (Sickmann et al., 2014), and sex-specific alterations in the hypothalamic-pituitary axis (Weinberg et al., 2008), which may also play influence sex-dependent differences in brain structure observed in humans with FASD.

In addition to static effects, it is important to consider sex-differences in the developmental trajectories of brain structure that have been established in healthy populations (Lenroot et al., 2007). In addition to age, effects of puberty (which differs in onset between males and females) have been shown to better model development than age in some structures (Goddings et al., 2014), and may well influence group differences observed in FASD. With males and females grouped together we observed expected patterns of change in DTI parameters with age in the majority of white matter tracts (i.e. increasing FA, decreasing MD) in both groups, though in some cases weaker and non-significant changes of FA were observed in the FASD group. Likewise, volume changes with age were similar between groups, with the exception decreasing putamen volume in the FASD group. Cortical thickness decreased with age across more than 80% of the cortex in controls, as expected (Zhou et al., 2015), reaching significance in fewer regions in the FASD group and with generally weaker correlations in keeping with recent longitudinal work (Treit et al., 2014b). However, as a post-hoc analysis, correlations between age-by-group terms and volumes were tested separately in males and females, revealed age-by-group interactions in intracranial, total brain, white matter, left and right thalamus, left caudate, left and right hippocampus and amygdala, and right putamen ($R=0.227-0.515$, $p=0.02 \times 10^{-4}$ to 0.047) in males, but only white matter in females ($R=0.382$, $p=0.002$). Indeed this suggests that postnatal developmental trajectories are more different in males with FASD (versus male controls) than between females, in keeping with a recent

longitudinal study of cortical volume development (Lebel et al., 2012b). Large longitudinal studies of FASD are needed to tease apart the effects of age and puberty on reduced sexual dimorphism of the brain in FASD.

Despite sex-specific effects on brain structure, we did not observe sex differences in cognitive deficits in this FASD sample. However, this may not be surprising given that healthy males and females typically perform similarly in many cognitive domains, despite robust differences in brain volumes, suggesting a complex relationship between sexual dimorphism of brain structure and function. In addition, the majority of cognitive tests employed here focus on academic or basic cognitive skills, so it remains possible that sex differences would be revealed by querying other aspects of cognition (e.g. ‘hot’ executive functions or emotional regulation skills). We did however find several significant brain-behaviour correlations in females with FASD that were absent in males, e.g. thalamus volume and general IQ (Figures 7.4 & 7.5), suggesting that brain-behaviour relationships may also differ between males and females with prenatal alcohol exposure. Other studies have demonstrated sex differences in impairment associated with prenatal alcohol exposure, including affective (depression and anxiety) behaviours in rats (Hellemans et al., 2010; Osborn et al., 1998) and in eye tracking in humans (e.g. Paolozza et al., 2015). Interestingly, IQ, mathematics and vocabulary were among the most impaired domains in both males and females, in keeping with many previous reports of impaired intellectual function, language and numerical processing in this population (Kodituwakku, 2007).

Overall very few correlations were observed between the most significant imaging variables identified here (Figure 7.4), suggesting that a child with well below average volume of a given structure does not necessarily also have well below average cortical thickness or white matter microstructure. This lack of cohesion may suggest that these are ‘independent’

abnormalities arising from a confluence of unique factors, perhaps influenced by timing of exposure and the developmental trajectories of each variable. This may partially explain the challenges that have thus been observed in establishing a common set of neurobehavioural and structural features that would serve as a biomarker for FASD. Future work should strive to collect large longitudinal FASD samples where the effects of postnatal development on both the relationship between observed abnormalities and the relative difference between sexes can be further investigated.

Summary and Conclusions

The work presented in this thesis demonstrates that children with fetal alcohol spectrum disorders experience both abnormal brain structure and altered developmental trajectories of brain development during childhood and adolescence. In addition, this work also provides independent confirmation of neurological deficit FASD, beyond the tools used in diagnosis.

Chapters 4 and 5 present data suggesting abnormal brain development beyond in utero insult. Specifically, when scanned several years apart, children with FASD are found to undergo greater rates of change in white matter microstructure, and slower rates of cortical thinning. Although seemingly counter-intuitive, the expected developmental trajectories of these processes, which undergo the greatest change in childhood and adolescence, respectively, suggest that children with FASD are experiencing delayed development. Interestingly, trajectories of volume change were not different from controls in any structure, despite having the most robust absolute differences at each scan. Further longitudinal work in older samples, and samples followed for multiple time points will help to determine if older adolescents/young adults with FASD experience developmental changes typically observed in healthy teenagers, as may be expected by our findings. Future directions in this field should also include the study of aging populations with FASD, which may be expected to begin undergoing degenerative processes earlier despite delayed childhood development, particularly in light of already reduced brain volumes.

Chapter 6 examines the use of head circumference as a proxy for brain volume in prenatal alcohol exposure, given its widespread use in the diagnostic process. Head circumference and brain volume are found to correlate in both FASD and control subjects. This

is not surprising—a child with a very small head should necessarily have a smaller brain than a child with a very large head. However, within sub-groups (e.g. those children with head circumference values that are more than a standard deviation below the population norm), this relationship begins to fall apart. Lack of correlation among children with similar head circumferences may stem from increased variability in CSF and skull thickness in FASD. Although head circumference is a fast and cost effective measure, caution must be applied in interpreting the relevance of a given measurement; this sample would suggest that it is only a moderate predictor of brain volume and a poor predictor of cognitive function.

Finally, chapter 7 examines a large cross sectional study of children, adolescents and adults with FASD, with the goal of comparing and correlating abnormalities identified with diffusion tensor imaging tractography, cortical thickness and brain volumes in the same sample. Importantly, this work also sought to explore sex differences in these measures, which have been consistently under-studied in the literature. This study confirmed that volume reductions are the most robust abnormality, followed by smaller magnitude but consistent reductions of cortical thickness, whereas DTI parameters only differed between groups in two white matter tracts. Interestingly, although volume difference were the most robust at a single time point, developmental change in volume with age was the least different from controls, in contrast to DTI and cortical thickness which both showed age-by-group interactions in Chapters 4 and 5.

Chapter 7 also uncovers several significant sex differences in the magnitude of volume and cortical thickness reductions relative to controls, with males showing greater relative impairment than females, despite equally impaired performance on cognitive testing. In both males and females, putamen and caudate volumes were the most reduced, in keeping with many previous studies finding disproportionate reductions of the basal ganglia. Correlation analysis of

variables with the greatest group differences revealed very few significant relationships between imaging variables, suggesting that even the most robust abnormalities may represent unique or independent features of FASD that vary between subjects as a result of timing, genetics etc. Interestingly, several brain-behaviour relationships were found in females but not males, again suggesting sexual dimorphism of structural impairment in FASD. Future work should further investigate sex effects in even younger children (as sexual dimorphisms emerge) as well as in animal models of brain structure. It is possible that the normal processes of sexual dimorphism in the brain are attenuated in children with prenatal alcohol exposure, or that males are more susceptible to the teratogenic effects of alcohol due to neurochemical, hormonal or genetic factors.

Several limitations of this work should be noted. FASD studies face many challenges, the most important of which is that human studies do not directly measure the effects of prenatal alcohol exposure. Many environmental variables have the potential to confound observations made many years after the prenatal insult, so we have tried to be careful to suggest that prenatal alcohol exposure is a common factor in our FASD group rather than a definitive cause of our findings. Many children with FASD experience the ‘double jeopardy’ of prenatal alcohol exposure combined with early life adversity, economic disparity and poor quality home environments (Olson et al., 2009). These factors likely compound deficits from alcohol exposure and may even alter brain development through independent mechanisms (McCrorry et al., 2010). For example, impaired language and social development is often observed in children of substance abusing parents, and is proposed to stem from difficulties with attachment, poor care, and other post-natal factors (K et al., 2014). However, not all children with FASD experience

early childhood adversity, creating a very heterogeneous group that's only common denominator is prenatal alcohol exposure.

Unfortunately we are unable to obtain accurate or detailed information on our sample's early life experiences needed to properly quantify or control for these variables. We did collect annual household income and primary caregiver level of education, though it is important to keep in mind that socio-economic status is challenging to measure in children who have experienced multiple home placements, given that indicators at the time of study participation may not accurately reflect their past socioeconomic environments. Indeed, in most of our sample we find no difference in primary caregiver education or annual household income between our FASD and control groups, indicating no gross disparity in present living situation, but are not able to assess previous placements (nor is there a standardized method for integrating this information even if it were available). This at least crudely controls for some potential environmental differences (e.g. current poverty), but also limits the generalizability of the results by potentially underestimating the degree of altered development that may characterize the general population of individuals with FASD, who may typically live in more tumultuous environments. Nonetheless, it is very likely that prenatal alcohol exposure imposes greater magnitude effects on brain structure than socioeconomic status.

Many of the cognitive measures discussed in this thesis examine academic and cognitive skills, which although impaired, may still over-estimate the adaptive capacity of many of the individuals included here. Anecdotally, we know that many of the adults with FASD in this sample continue to experience adversities that are not measured here, including having been incarcerated, experienced tumultuous family relationships including apprehension of their own children, struggled with addictions, and experienced mental health crises including suicide

attempts. Future work should attempt to better capture these types of data to provide a more complete picture of “impairment”.

Research studies that place significant demands on participants (e.g. staying still in an MRI scanner for ~20 minutes) have the potential to include less impaired clinical populations, as may be the case in our FASD samples, which typically include fewer participants with FAS than other studies in the literature. In addition, control participants typically represent children of families with an interest in research, and are often members of the broader University community, recruited through word-of-mouth. We attempted to overcome this by recruiting with a variety of methods and advertising in a wide range of neighborhoods. Nonetheless, these recruitment methods may introduce systematic differences in the socio-economic status and other geographical factors between groups here. Moreover, differences in ethnicity between groups have been observed in our previous samples (with a greater proportion of aboriginal participants in the FASD than control group). We attempted to overcome this by specifically recruiting aboriginal controls through various outreach resources in Edmonton, but were still unable to match the proportions in our FASD sample. Nonetheless, aboriginal representation in our control sample roughly matches the demographic distribution of Edmonton.

Lastly, even though many significant group differences have been identified throughout this thesis, all have been of relatively small magnitude, with substantial overlap between groups. Thus, none of the findings here (or in much of the neuroimaging literature in FASD), have provided evidence of discriminatory or ‘diagnostic’ structural abnormalities. Future work will likely need to move toward multi-site imaging, which has the advantage of increased power through large subject numbers and improved generalizability of patient populations. With large samples from pooled datasets, future work will be able to further investigate sex, age and

diagnosis related differences in FASD, as well as apply more sophisticated data analysis methods to determine if a combination of features can be used to identify an imaging ‘biomarker’ for FASD.

Despite these important limitations, this work has advanced the field of neuroimaging in FASD in several ways. The data presented include the first ever longitudinal DTI and cortical thickness studies of FASD, the first investigation of head circumference-brain volume correlations in this population, the first simultaneous report of white matter tractography, cortical thickness and brain volume in the same sample, and one of only a handful of studies to investigate sexual dimorphism of structural abnormalities in FASD. Together, this work has uncovered differences the trajectory of brain development and the relative magnitude of impairments between males and females with FASD, needed to develop FASD-specific medical and behavioural interventions. As with all pursuits in science, this work has probably led to more questions than it has answered, but nonetheless it has also contributed to a greater collective effort aimed at identifying, understanding and ultimately preventing neurodevelopmental impairments from prenatal alcohol exposure.

References

- Aiken, C.E., Ozanne, S.E., 2013. Sex differences in developmental programming models. *Reproduction* 145, R1-R13.
- Almeida, L.G., Ricardo-Garcell, J., Prado, H., Barajas, L., Fernandez-Bouzas, A., Avila, D., Martinez, R.B., 2010. Reduced right frontal cortical thickness in children, adolescents and adults with ADHD and its correlation to clinical variables: A cross-sectional study. *Journal of Psychiatric Research* 44, 1214-1223.
- Archibald, S.L., Fennema-Notestine, C., Gamst, A., Riley, E.P., Mattson, S.N., Jernigan, T.L., 2001. Brain dysmorphology in individuals with severe prenatal alcohol exposure. *Developmental Medicine and Child Neurology* 43, 148-154.
- Aronne, M.P., Evrard, S.G., Mirochnic, S., Brusco, A., 2008. Prenatal ethanol exposure reduces the expression of the transcriptional factor Pax6 in the developing rat brain. *Ann N Y Acad Sci* 1139, 478-498.
- Aronne, M.P., Guadagnoli, T., Fontanet, P., Evrard, S.G., Brusco, A., 2011. Effects of prenatal ethanol exposure on rat brain radial glia and neuroblast migration. *Experimental Neurology* 229, 364-371.
- Astley, S., 2004. Diagnostic Guide for Fetal Alcohol Spectrum Disorders: The 4-Digit Diagnostic Code. Fetal Alcohol Syndrome Diagnostic and Prevention Network, University of Washington, Seattle USA.
- Astley, S.J., 2006. Comparison of the 4-digit diagnostic code and the Hoyme diagnostic guidelines for fetal alcohol spectrum disorders. *Pediatrics* 118, 1532-1545.
- Astley, S.J., Aylward, E.H., Olson, H.C., Kerns, K., Brooks, A., Coggins, T.E., Davies, J., Dorn, S., Gendler, B., Jirikowic, T., Kraegel, P., Maravilla, K., Richards, T., 2009a. Magnetic Resonance Imaging Outcomes From a Comprehensive Magnetic Resonance Study of Children With Fetal Alcohol Spectrum Disorders. *Alcoholism-Clinical and Experimental Research* 33, 1671-1689.
- Astley, S.J., Clarren, S.K., 2000. Diagnosing the full spectrum of fetal alcohol-exposed individuals: Introducing the 4-Digit Diagnostic Code. *Alcohol and Alcoholism* 35, 400-410.
- Astley, S.J., Olson, H.C., Kerns, K., Brooks, A., Aylward, E.H., Coggins, T.E., Davies, J., Dorn, S., Gendler, B., Jirikowic, T., Kraegel, P., Maravilla, K., Richards, T., 2009b. Neuropsychological and behavioral outcomes from a comprehensive magnetic resonance study of children with fetal alcohol spectrum disorders. *The Canadian Journal of Clinical Pharmacology* 16, e178-201.

- Autti-Ramo, I., Autti, T., Korkman, M., Kettunen, S., Salonen, O., Valanne, L., 2002. MRI findings in children with school problems who had been exposed prenatally to alcohol. *Developmental Medicine and Child Neurology* 44, 98-106.
- Bagheri, M.M., Burd, L., Martsolf, J.T., Klug, M.G., 1998. Fetal alcohol syndrome: maternal and neonatal characteristics. *Journal of Perinatal Medicine* 26, 263-269.
- Bartholomeusz, H.H., Courchesne, E., Karns, C.M., 2002. Relationship between head circumference and brain volume in healthy normal toddlers, children, and adults. *Neuropediatrics* 33, 239-241.
- Basser, P.J., Mattiello, J., Lebihan, D., 1994. MR diffusion tensor spectroscopy and imaging. *Biophysical Journal* 66, 259-267.
- Bava, S., Thayer, R., Jacobus, J., Ward, M., Jernigan, T.L., Tapert, S.F., 2010. Longitudinal characterization of white matter maturation during adolescence. *Brain Research* 1327, 38-46.
- Bayer, S.A., Altman, J., Russo, R.J., Zhang, X., 1993. Timetables Of Neurogenesis In The Human Brain Based On Experimentally Determined Patterns In The Rat. *Neurotoxicology* 14, 83-144.
- Beauchamp, M.S., Beurlot, M.R., Fava, E., Nath, A.R., Parikh, N.A., Saad, Z.S., Bortfeld, H., Oghalai, J.S., 2011. The Developmental Trajectory of Brain-Scalp Distance from Birth through Childhood: Implications for Functional Neuroimaging. *Plos One* 6.
- Beaulieu, C., Allen, P.S., 1994. Determinants of anisotropic water diffusion in nerves. *Magnetic Resonance in Medicine* 31, 394-400.
- Beaulieu, C., Does, M.D., Snyder, R.E., Allen, P.S., 1996. Changes in water diffusion due to wallerian degeneration in peripheral nerve. *Magnetic Resonance in Medicine* 36, 627-631.
- Bishop, K.M., Goudreau, G., O'Leary, D.D.M., 2000. Regulation of area identity in the mammalian neocortex by *Emx2* and *Pax6*. *Science* 288, 344-349.
- Bjorkquist, O.A., Fryer, S.L., Reiss, A.L., Mattson, S.N., Riley, E.P., 2010. Cingulate gyrus morphology in children and adolescents with fetal alcohol spectrum disorders. *Psychiatry Research-Neuroimaging* 181, 101-107.
- Bonthius, D.J., West, J.R., 1990. Alcohol-induced neuronal loss in developing rats - increased brain-damage with binge exposure. *Alcoholism-Clinical and Experimental Research* 14, 107-118.
- Bookstein, F.L., Sampson, P.D., Connor, P.D., Streissguth, A.P., 2002a. Midline corpus callosum is a neuroanatomical focus of fetal alcohol damage. *Anatomical Record* 269, 162-174.

- Bookstein, F.L., Sampson, P.D., Streissguth, A.P., Connor, P.D., 2001. Geometric morphometrics of corpus callosum and subcortical structures in the fetal-alcohol-affected brain. *Teratology* 64, 4-32.
- Bookstein, F.L., Streissguth, A.P., Connor, P.D., Sampson, P.D., 2006. Damage to the human cerebellum from prenatal alcohol exposure: The anatomy of a simple biometrical explanation. *Anatomical Record Part B: The New Anatomist* 289, 195-209.
- Bookstein, F.L., Streissguth, A.P., Sampson, P.D., Connor, P.D., Barr, H.M., 2002b. Corpus callosum shape and neuropsychological deficits in adult males with heavy fetal alcohol exposure. *Neuroimage* 15, 233-251.
- Brain Development Cooperative Group, 2011. Total and Regional Brain Volumes in a Population-Based Normative Sample from 4 to 18 Years: The NIH MRI Study of Normal Brain Development. *Cerebral Cortex* 22, 1-12.
- Brauer, J., Anwander, A., Friederici, A.D., 2011. Neuroanatomical Prerequisites for Language Functions in the Maturing Brain. *Cerebral Cortex* 21, 459-466.
- Brown, R., 1828. A brief account of microscopic observations made in the months of June, July and August, 1827, on the particles contained in the pollen of plants; and on the general existence of active molecules in 14, organic and inorganic bodies. *Annals of Physics* 14, 294-313.
- Burd, L., Klug, M.G., Martsof, J.T., Kerbeshian, J., 2003. Fetal alcohol syndrome: neuropsychiatric phenomics. *Neurotoxicology and Teratology* 25, 697-705.
- Buss, R.R., Oppenheim, R.W., 2004. Role of programmed cell death in normal neuronal development and function. *Anatomical Science International* 79, 191-197.
- Cahill, L., 2006. Why sex matters for neuroscience. *Nature Reviews Neuroscience* 7, 477-484.
- Canada, H., 2006.
- Carter, R.C., Jacobson, J.L., Dodge, N.C., Granger, D.A., Jacobson, S.W., 2014. Effects of Prenatal Alcohol Exposure on Testosterone and Pubertal Development. *Alcoholism-Clinical and Experimental Research* 38, 1671-1679.
- Carter, R.C., Jacobson, J.L., Sokol, R.J., Avison, M.J., Jacobson, S.W., 2013. Fetal Alcohol-Related Growth Restriction from Birth through Young Adulthood and Moderating Effects of Maternal Prepregnancy Weight. *Alcoholism-Clinical and Experimental Research* 37, 452-462.
- Catani, M., Thiebaut de Schotten, M., 2008. A diffusion tensor imaging tractography atlas for virtual in vivo dissections. *Cortex* 44, 1105-1132.

- Chen, X.C., Coles, C.D., Lynch, M.E., Hu, X.P., 2012. Understanding specific effects of prenatal alcohol exposure on brain structure in young adults. *Human Brain Mapping* 33, 1663-1676.
- Chen, Y., Ozturk, N.C., Ni, L., Goodlett, C., Zhou, F.C., 2011. Strain Differences in Developmental Vulnerability to Alcohol Exposure via Embryo Culture in Mice. *Alcoholism-Clinical and Experimental Research* 35, 1293-1304.
- Christoffel, K.K., Salafsky, I., 1975. Fetal Alcohol Syndrome in Dizygotic Twins. *Journal of Pediatrics* 87, 963-967.
- Chudley, A.E., Conry, J., Cook, L.L., Looock, C., Rosales, T., LeBlanc, N., 2005. Fetal alcohol spectrum disorder: Canadian guidelines for diagnosis. *Canadian Medical Association Journal* 172, S1-S21.
- Clark, C.M., Li, D., Conry, J., Conry, R., Looock, C., 2000. Structural and functional brain integrity of fetal alcohol syndrome in nonretarded cases. *Pediatrics* 105, 1096-1099.
- Clarren, S.K., Alvord, E.C., Sumi, S.M., Streissguth, A.P., Smith, D.W., 1978. Brain malformations related to prenatal exposure to ethanol. *Journal of Pediatrics* 92, 64-67.
- Coles, C.D., Brown, R.T., Smith, I.E., Platzman, K.A., Erickson, S., Falek, A., 1991. Effects of Prenatal Alcohol Exposure at School Age .1. Physical and Cognitive-Development. *Neurotoxicology and Teratology* 13, 357-367.
- Coles, C.D., Goldstein, F.C., Lynch, M.E., Chen, X., Kable, J.A., Johnson, K.C., Hu, X., 2011a. Memory and brain volume in adults prenatally exposed to alcohol. *Brain and Cognition* 75, 67-77.
- Coles, C.D., Goldstein, F.C., Lynch, M.E., Chen, X.C., Kable, J.A., Johnson, K.C., Hu, X.P., 2011b. Memory and brain volume in adults prenatally exposed to alcohol. *Brain and Cognition* 75, 67-77.
- Converse, A.K., Moore, C.F., Holden, J.E., Ahlers, E.O., Moirano, J.M., Larson, J.A., Resch, L.M., DeJesus, O.T., Barnhart, T.E., Nickles, R.J., Murali, D., Christian, B.T., Schneider, M.L., 2014. Moderate-Level Prenatal Alcohol Exposure Induces Sex Differences in Dopamine D-1 Receptor Binding in Adult Rhesus Monkeys. *Alcoholism-Clinical and Experimental Research* 38, 2934-2943.
- Cortese, B.M., Moore, G.J., Bailey, B.A., Jacobson, S.W., Delaney-Black, V., Hannigan, J.H., 2006. Magnetic resonance and spectroscopic imaging in prenatal alcohol-exposed children: Preliminary findings in the caudate nucleus. *Neurotoxicology and Teratology* 28, 597-606.
- Cosgrove, K.P., Mazure, C.M., Staley, J.K., 2007. Evolving knowledge of sex differences in brain structure, function, and chemistry. *Biol Psychiatry* 62, 847-855.

- Costa, E.T., Savage, D.D., Valenzuela, C.F., 2000. A review of the effects of prenatal or early postnatal ethanol exposure on brain ligand-gated ion channels. *Alcoholism-Clinical and Experimental Research* 24, 706-715.
- Cui, Z.J., Zhao, K.B., Zhao, H.J., Yu, D.M., Niu, Y.L., Zhang, J.S., Deng, J.B., 2010. Prenatal Alcohol Exposure Induces Long-Term Changes in Dendritic Spines and Synapses in the Mouse Visual Cortex. *Alcohol and Alcoholism* 45, 312-319.
- Cuzon, V.C., Yeh, P.W.L., Yanagawa, Y., Obata, K., Yeh, H.H., 2008. Ethanol consumption during early pregnancy alters the disposition of tangentially migrating GABAergic interneurons in the fetal cortex. *Journal of Neuroscience* 28, 1854-1864.
- Day, N.L., Leech, S.L., Richardson, G.A., Cornelius, M.D., Robles, N., Larkby, C., 2002. Prenatal alcohol exposure predicts continued deficits in offspring size at 14 years of age. *Alcoholism-Clinical and Experimental Research* 26, 1584-1591.
- De Guio, F., Mangin, J.-F., Riviere, D., Perrot, M., Molteno, C.D., Jacobson, S.W., Meintjes, E.M., Jacobson, J.L., 2014. A study of cortical morphology in children with fetal alcohol spectrum disorders. *Human Brain Mapping* 35, 2285-2296.
- de Zeeuw, P., Schnack, H.G., van Belle, J., Weusten, J., van Dijk, S., Langen, M., Brouwer, R.M., van Engeland, H., Durston, S., 2012. Differential Brain Development with Low and High IQ in Attention-Deficit/Hyperactivity Disorder. *Plos One* 7.
- Detrait, E.R., George, T.M., Etchevers, H.C., Glibert, J.R., Vekemans, M., Speer, M.C., 2005. Human neural tube defects: Developmental biology, epidemiology, and genetics. *Neurotoxicology and Teratology* 27, 515-524.
- Dougherty, R.F., Ben-Shachar, M., Deutsch, G.K., Hernandez, A., Fox, G.R., Wandell, B.A., 2007. Temporal-callosal pathway diffusivity predicts phonological skills in children. *Proceedings of the National Academy of Sciences of the United States of America* 104, 8556-8561.
- Dudek, J., Skocic, J., Sheard, E., Rovet, J., 2014. Hippocampal Abnormalities in Youth with Alcohol-Related Neurodevelopmental Disorder. *Journal of the International Neuropsychological Society* 20, 181-191.
- Duerden, E.G., Tannock, R., Dockstader, C., 2012. Altered cortical morphology in sensorimotor processing regions in adolescents and adults with attention-deficit/hyperactivity disorder. *Brain Research* 1445, 82-91.
- Dunty, W.C., Chen, S.Y., Zucker, R.M., Dehart, D.B., Sulik, K.K., 2001. Selective vulnerability of embryonic cell populations to ethanol-induced apoptosis: Implications for alcohol-related birth defects and neurodevelopmental disorder. *Alcoholism-Clinical and Experimental Research* 25, 1523-1535.
- Eckstrand, K.L., Ding, Z.H., Dodge, N.C., Cowan, R.L., Jacobson, J.L., Jacobson, S.W., Avison, M.J., 2012. Persistent Dose-Dependent Changes in Brain Structure in Young Adults with

Low-to-Moderate Alcohol Exposure In Utero. *Alcoholism-Clinical and Experimental Research* 36, 1892-1902.

- Einstein, A., 1905. The motion of elements suspended in static liquids as claimed in the molecular kinetic theory of heat. *Annalen Der Physik* 17, 549-560.
- Eervalahi, N., Korkman, M., Fagerlund, A., Autti-Ramo, I., Loimu, L., Hoyme, H.E., 2007. Relationship between dysmorphic features and general cognitive function in children with fetal alcohol spectrum disorders. *American Journal of Medical Genetics Part A* 143A, 2916-2923.
- Fakoya, F.A., Caxton-Martins, E.A., 2006. Neocortical neurodegeneration in young adult Wistar rats prenatally exposed to ethanol. *Neurotoxicology and Teratology* 28, 229-237.
- Farber, N.B., Creeley, C.E., Olney, J.W., 2010. Alcohol-induced neuroapoptosis in the fetal macaque brain. *Neurobiology of Disease* 40, 200-206.
- Feldman, H.S., Jones, K.L., Lindsay, S., Slymen, D., Klonoff-Cohen, H., Kao, K., Rao, S., Chambers, C., 2012. Prenatal Alcohol Exposure Patterns and Alcohol-Related Birth Defects and Growth Deficiencies: A Prospective Study. *Alcoholism-Clinical and Experimental Research* 36, 670-676.
- Feng, M.J., Yan, S.E., Yan, Q.S., 2005. Effects of prenatal alcohol exposure on brain-derived neurotrophic factor and its receptor tyrosine kinase B in offspring. *Brain Research* 1042, 125-132.
- Fernandez-Jaen, A., Fernandez-Mayoralas, D.M., Quinones Tapia, D., Calleja-Perez, B., Garcia-Segura, J.M., Arribas, S.L., Munoz Jareno, N., 2011. Cortical thickness in fetal alcohol syndrome and attention deficit disorder. *Pediatr Neurol* 45, 387-391.
- Fischl, B., Dale, A.M., 2000. Measuring the thickness of the human cerebral cortex from magnetic resonance images. *Proceedings of the National Academy of Sciences of the United States of America* 97, 11050-11055.
- Fischl, B., Salat, D.H., Busa, E., Albert, M., Dieterich, M., Haselgrove, C., van der Kouwe, A., Killiany, R., Kennedy, D., Klaveness, S., Montillo, A., Makris, N., Rosen, B., Dale, A.M., 2002. Whole brain segmentation: Automated labeling of neuroanatomical structures in the human brain. *Neuron* 33, 341-355.
- Forkel, S.J., de Schotten, M.T., Kawadler, J.M., Dell'Acqua, F., Danek, A., Catani, M., 2014. The anatomy of fronto-occipital connections from early blunt dissections to contemporary tractography. *Cortex* 56, 73-84.
- Fryer, S.L., Mattson, S.N., Jernigan, T.L., Archibald, S.L., Jones, K.L., Riley, E.P., 2012. Caudate Volume Predicts Neurocognitive Performance in Youth with Heavy Prenatal Alcohol Exposure. *Alcoholism-Clinical and Experimental Research* 36, 1932-1941.

- Fryer, S.L., McGee, C.L., Matt, G.E., Mattson, S.N., 2007. Evaluation of psychopathological conditions in children with heavy prenatal alcohol exposure. *Pediatrics* 119, E733-E741.
- Fryer, S.L., Schweinsburg, B.C., Bjorkquist, O.A., Frank, L.R., Mattson, S.N., Spadoni, A.D., Riley, E.P., 2009. Characterization of White Matter Microstructure in Fetal Alcohol Spectrum Disorders. *Alcoholism-Clinical and Experimental Research* 33, 514-521.
- Gautam, P., Nunez, S.C., Narr, K.L., Kan, E.C., Sowell, E.R., 2014. Effects of prenatal alcohol exposure on the development of white matter volume and change in executive function. *Neuroimage-Clinical* 5, 19-27.
- Giedd, J.N., 2004. Structural magnetic resonance imaging of the adolescent brain. In: Dahl, R.E., Spear, L.P. (Eds.), *Adolescent Brain Development: Vulnerabilities and Opportunities*, pp. 77-85.
- Giedd, J.N., Blumenthal, J., Jeffries, N.O., Castellanos, F.X., Liu, H., Zijdenbos, A., Paus, T., Evans, A.C., Rapoport, J.L., 1999. Brain development during childhood and adolescence: a longitudinal MRI study. *Nature Neuroscience* 2, 861-863.
- Giedd, J.N., Castellanos, F.X., Rajapakse, J.C., Vaituzis, A.C., Rapoport, J.L., 1997. Sexual dimorphism of the developing human brain. *Progress in Neuro-Psychopharmacology & Biological Psychiatry* 21, 1185-1201.
- Giedd, J.N., Raznahan, A., Mills, K.L., Lenroot, R.K., 2012. Review: magnetic resonance imaging of male/female differences in human adolescent brain anatomy. *Biology of Sex Differences* 3.
- Giorgio, A., Watkins, K.E., Chadwick, M., James, S., Winmill, L., Douaud, G., De Stefano, N., Matthews, P.M., Smith, S.M., Johansen-Berg, H., James, A.C., 2010. Longitudinal changes in grey and white matter during adolescence. *Neuroimage* 49, 94-103.
- Glass, L., Ware, A.L., Crocker, N., Dewese, B.N., Coles, C.D., Kable, J.A., May, P.A., Kalberg, W.O., Sowell, E.R., Jones, K.L., Riley, E.P., Mattson, S.N., 2013. Neuropsychological deficits associated with heavy prenatal alcohol exposure are not exacerbated by ADHD. *Neuropsychology* 27, 713-724.
- Glavas, M.M., Ellis, L., Yu, W.K., Weinberg, J., 2007. Effects of prenatal ethanol exposure on basal limbic-hypothalamic-pituitary-adrenal regulation: Role of corticosterone. *Alcoholism-Clinical and Experimental Research* 31, 1598-1610.
- Glutting, J., Adams, W., & Sheslow, D., 2000. *Wide Range Intelligence Test*. Wilmington, DE.
- Goddings, A.-L., Mills, K.L., Clasen, L.S., Giedd, J.N., Viner, R.M., Blakemore, S.-J., 2014. The influence of puberty on subcortical brain development. *Neuroimage* 88, 242-251.
- Gogtay, N., Giedd, J.N., Lusk, L., Hayashi, K.M., Greenstein, D., Vaituzis, A.C., Nugent, T.F., Herman, D.H., Clasen, L.S., Toga, A.W., Rapoport, J.L., Thompson, P.M., 2004. Dynamic mapping of human cortical development during childhood through early

- adulthood. *Proceedings of the National Academy of Sciences of the United States of America* 101, 8174-8179.
- Goldstein, J.M., Seidman, L.J., Horton, N.J., Makris, N., Kennedy, D.N., Caviness, V.S., Faraone, S.V., Tsuang, M.T., 2001. Normal sexual dimorphism of the adult human brain assessed by in vivo magnetic resonance imaging. *Cerebral Cortex* 11, 490-497.
- Goodlett, C.R., Horn, K.H., Zhou, F.C., 2005. Alcohol teratogenesis: Mechanisms of damage and strategies for intervention. *Experimental Biology and Medicine* 230, 394-406.
- Gordon, N., 1995. Apoptosis (Programmed Cell-Death) And Other Reasons For Elimination Of Neurons And Axons. *Brain & Development* 17, 73-77.
- Green, C.R., Lebel, C., Rasmussen, C., Beaulieu, C., Reynolds, J.N., 2013. Diffusion Tensor Imaging Correlates of Saccadic Reaction Time in Children with Fetal Alcohol Spectrum Disorder. *Alcoholism-Clinical and Experimental Research* 37, 1499-1507.
- Guerri, C., Bazinet, A., Riley, E.P., 2009. Foetal Alcohol Spectrum Disorders and Alterations in Brain and Behaviour. *Alcohol and Alcoholism* 44, 108-114.
- Guo, W.X., Crossey, E.L., Zhang, L., Zucca, S., George, O.L., Valenzuela, C.F., Zhao, X.Y., 2011. Alcohol Exposure Decreases CREB Binding Protein Expression and Histone Acetylation in the Developing Cerebellum. *Plos One* 6.
- Haydon, P.G., 2001. Glia: Listening and talking to the synapse. *Nature Reviews Neuroscience* 2, 185-193.
- Hellemans, K.G.C., Verma, P., Yoon, E., Yu, W.K., Young, A.H., Weinberg, J., 2010. Prenatal Alcohol Exposure and Chronic Mild Stress Differentially Alter Depressive- and Anxiety-Like Behaviors in Male and Female Offspring. *Alcoholism-Clinical and Experimental Research* 34, 633-645.
- Herculano-Houzel, S., 2009. The human brain in numbers: a linearly scaled-up primate brain. *Frontiers in Human Neuroscience* 3, 11.
- Hernandez-Guerrero, J.C., Ledesma-Montes, C., Loyola-Rodriguez, J.P., 1998. Effects of maternal ethanol intake on second alcoholic generation murine skull and mandibular size. *Archives of Medical Research* 29, 297-302.
- Hildebrand, C., Remahl, S., Persson, H., Bjartmar, C., 1993. Myelinated nerve-fibers in the CNS. *Progress in Neurobiology* 40, 319-384.
- Hoefl, F., Barnea-Goraly, N., Haas, B.W., Golarai, G., Ng, D., Mills, D., Korenberg, J., Bellugi, U., Galaburda, A., Reiss, A.L., 2007. More is not always better: Increased fractional Anisotropy of superior longitudinal fasciculus associated with poor Visuospatial abilities in Williams syndrome. *Journal of Neuroscience* 27, 11960-11965.

- Hoefl, F., McCandliss, B.D., Black, J.M., Gantman, A., Zakerani, N., Hulme, C., Lyytinen, H., Whitfield-Gabrieli, S., Glover, G.H., Reiss, A.L., Gabrieli, J.D.E., 2011. Neural systems predicting long-term outcome in dyslexia. *Proceedings of the National Academy of Sciences of the United States of America* 108, 361-366.
- Honse, Y., Nixon, K.M., Browning, M.D., Leslie, S.W., 2003. Cell surface expression of NR1 splice variants and NR2 subunits is modified by prenatal ethanol exposure. *Neuroscience* 122, 689-698.
- Hoyme, H.E., May, P.A., Kalberg, W.O., Kodituwakku, P., Gossage, J.P., Trujillo, P.M., Buckley, D.G., Miller, J.H., Aragon, A.S., Khaole, N., Viljoen, D.L., Jones, K.L., Robinson, L.K., 2005. A practical clinical approach to diagnosis of fetal alcohol spectrum disorders: Clarification of the 1996 Institute of Medicine Criteria. *Pediatrics* 115, 39-47.
- Hughes, P.D., Wilson, W.R., Leslie, S.W., 2001. Effect of gestational ethanol exposure on the NMDA receptor complex in rat forebrain: from gene transcription to cell surface. *Developmental Brain Research* 129, 135-145.
- Huppi, P.S., Maier, S.E., Peled, S., Zientara, G.P., Barnes, P.D., Jolesz, F.A., Volpe, J.J., 1998. Microstructural development of human newborn cerebral white matter assessed in vivo by diffusion tensor magnetic resonance imaging. *Pediatric Research* 44, 584-590.
- Huttenlocher, P.R., 1979. Synaptic density in human frontal-cortex - developmental-changes and effects of aging. *Brain Research* 163, 195-205.
- Huttenlocher, P.R., Decourten, C., Garey, L.J., Vanderloos, H., 1982. Synaptogenesis In Human Visual-Cortex - Evidence For Synapse Elimination During Normal Development. *Neuroscience Letters* 33, 247-252.
- Idrus, N.M., Napper, R.M., 2012. Acute and long-term Purkinje cell loss following a single ethanol binge during the early third trimester equivalent in the rat. *Alcohol Clin Exp Res* 36, 1365-1373.
- Ikonomidou, C., Bittigau, P., Ishimaru, M.J., Wozniak, D.F., Koch, C., Genz, K., Price, M.T., Stefovskaja, V., Horster, F., Tenkova, T., Dikranian, K., Olney, J.W., 2000. Ethanol-induced apoptotic neurodegeneration and fetal alcohol syndrome. *Science* 287, 1056-1060.
- Innocenti, G.M., Clarke, S., Koppel, H., 1983. Transitory Macrophages In The White Matter Of The Developing Visual-Cortex .2. Development And Relations With Axonal Pathways. *Developmental Brain Research* 11, 55-66.
- Innocenti, G.M., Price, D.J., 2005. Exuberance in the development of cortical networks. *Nature Reviews Neuroscience* 6, 955-965.
- Ivanovic, D.M., Leiva, B.P., Perez, H.T., Olivares, M.G., Diaz, N.S., Urrutia, M.S.C., Almagia, A.F., Toro, T.D., Miller, P.T., Bosch, E.O., Larrain, C.G., 2004. Head size and

- intelligence, learning, nutritional status and brain development Head, IQ, learning, nutrition and brain. *Neuropsychologia* 42, 1118-1131.
- Jacobson, J.L., Jacobson, S.W., 1996. Prospective, longitudinal assessment of developmental neurotoxicity. *Environ Health Perspect* 104 Suppl 2, 275-283.
- Jernigan, T.L., Tallal, P., 1990. Late childhood changes in brain morphology observable with MRI. *Developmental Medicine and Child Neurology* 32, 379-385.
- Johnson, V.P., Swayze, V.W., Sato, Y., Andreasen, N.C., 1996. Fetal alcohol syndrome: Craniofacial and central nervous system manifestations. *American Journal of Medical Genetics* 61, 329-339.
- Jones, K.L., Smith, D.W., 1973. Recognition of fetal alcohol syndrome in early infancy. *Lancet* 2, 999-1001.
- Joseph, J., Warton, C., Jacobson, S.W., Jacobson, J.L., Molteno, C.D., Eicher, A., Marais, P., Phillips, O.R., Narr, K.L., Meintjes, E.M., 2014. Three-Dimensional Surface Deformation-Based Shape Analysis of Hippocampus and Caudate Nucleus in Children with Fetal Alcohol Spectrum Disorders. *Human Brain Mapping* 35, 659-672.
- K, J.H., Siqueland, T., Smith, L., Wentzel-Larsen, T., Walhovd, K.B., Moe, V., 2014. Mother-Child Interaction and Early Language Skills in Children Born to Mothers with Substance Abuse and Psychiatric Problems. *Child Psychiatry Hum Dev* 10, 10.
- Kasprian, G., Brugger, P.C., Weber, M., Krssak, M., Krampl, E., Herold, C., Prayer, D., 2008. In utero tractography of fetal white matter development. *Neuroimage* 43, 213-224.
- Kilb, W., 2012. Development of the GABAergic System from Birth to Adolescence. *Neuroscientist* 18, 613-630.
- Kim, J.S., Singh, V., Lee, J.K., Lerch, J., Ad-Dab'bagh, Y., MacDonald, D., Lee, J.M., Kim, S.I., Evans, A.C., 2005. Automated 3-D extraction and evaluation of the inner and outer cortical surfaces using a Laplacian map and partial volume effect classification. *Neuroimage* 27, 210-221.
- Kodituwakku, P.W., 2007. Defining the behavioral phenotype in children with fetal alcohol spectrum disorders: A review. *Neuroscience and Biobehavioral Reviews* 31, 192-201.
- Kotkoskie, L.A., Norton, S., 1988. Prenatal brain malformations following acute ethanol exposure in the rat. *Alcohol Clin Exp Res* 12, 831-836.
- Lamantia, A.S., Rakic, P., 1990. Axon overproduction and elimination in the corpus-callosum of the developing rhesus-monkey. *Journal of Neuroscience* 10, 2156-2175.
- Lan, N., Helleman, K.G.C., Ellis, L., Viau, V., Weinberg, J., 2009. Role of testosterone in mediating prenatal ethanol effects on hypothalamic-pituitary-adrenal activity in male rats. *Psychoneuroendocrinology* 34, 1314-1328.

- Laule, C., Vavasour, I.M., Kolind, S.H., Li, D.K.B., Traboulsee, T.L., Moore, G.R.W., MacKay, A.L., 2007. Magnetic resonance imaging of myelin. *Neurotherapeutics* 4, 460-484.
- Lebel, C., Beaulieu, C., 2011. Longitudinal Development of Human Brain Wiring Continues from Childhood into Adulthood. *Journal of Neuroscience* 31, 10937-10947.
- Lebel, C., Gee, M., Camicioli, R., Wieler, M., Martin, W., Beaulieu, C., 2012a. Diffusion tensor imaging of white matter tract evolution over the lifespan. *Neuroimage* 60, 340-352.
- Lebel, C., Mattson, S.N., Riley, E.P., Jones, K.L., Adnams, C.M., May, P.A., Bookheimer, S.Y., O'Connor, M.J., Narr, K.L., Kan, E., Abaryan, Z., Sowell, E.R., 2012b. A Longitudinal Study of the Long-Term Consequences of Drinking during Pregnancy: Heavy In Utero Alcohol Exposure Disrupts the Normal Processes of Brain Development. *Journal of Neuroscience* 32, 15243-15251.
- Lebel, C., Rasmussen, C., Wyper, K., Andrew, G., Beaulieu, C., 2010. Brain Microstructure Is Related to Math Ability in Children With Fetal Alcohol Spectrum Disorder. *Alcoholism-Clinical and Experimental Research* 34, 354-363.
- Lebel, C., Rasmussen, C., Wyper, K., Walker, L., Andrew, G., Yager, J., Beaulieu, C., 2008a. Brain diffusion abnormalities in children with fetal alcohol spectrum disorder. *Alcoholism-Clinical and Experimental Research* 32, 1732-1740.
- Lebel, C., Roussotte, F., Sowell, E.R., 2011. Imaging the Impact of Prenatal Alcohol Exposure on the Structure of the Developing Human Brain. *Neuropsychology Review* 21, 102-118.
- Lebel, C., Walker, L., Leemans, A., Phillips, L., Beaulieu, C., 2008b. Microstructural maturation of the human brain from childhood to adulthood. *Neuroimage* 40, 1044-1055.
- Leemans, A., Jeurissen, B., Sijbers, J., Jones, D., 2009. ExploreDTI: a graphical toolbox for processing, analyzing, and visualizing diffusion MR data. 17th Annual Meeting of International Society of Magnetic Resonance Medicine, Hawaii, USA, 2009, p. 3537.
- Leigland, L.A., Ford, M.M., Lerch, J.P., Kroenke, C.D., 2013. The Influence of Fetal Ethanol Exposure on Subsequent Development of the Cerebral Cortex as Revealed by Magnetic Resonance Imaging. *Alcoholism-Clinical and Experimental Research* 37, 924-932.
- Lenroot, R.K., Gogtay, N., Greenstein, D.K., Wells, E.M., Wallace, G.L., Clasen, L.S., Blumenthal, J.D., Lerch, J., Zijdenbos, A.P., Evans, A.C., Thompson, P.M., Giedd, J.N., 2007. Sexual dimorphism of brain developmental trajectories during childhood and adolescence. *Neuroimage* 36, 1065-1073.
- Li, L.C., Coles, C.D., Lynch, M.E., Hu, X.P., 2009. Voxelwise and Skeleton-Based Region of Interest Analysis of Fetal Alcohol Syndrome and Fetal Alcohol Spectrum Disorders in Young Adults. *Human Brain Mapping* 30, 3265-3274.
- Lidow, M.S., Goldmanrakic, P.S., Rakic, P., 1991. Synchronized Overproduction Of Neurotransmitter Receptors In Diverse Regions Of The Primate Cerebral-Cortex.

- Proceedings of the National Academy of Sciences of the United States of America 88, 10218-10221.
- Little, R.E., 1977. Moderate Alcohol use During Pregnancy and Decreased Infant Birth-Weight. *American Journal of Public Health* 67, 1154-1156.
- Ma, X.Y., Coles, C.D., Lynch, M.E., LaConte, S.M., Zurkiya, O., Wang, D.L., Hu, X.P., 2005. Evaluation of corpus callosum Anisotropy in young adults with fetal alcohol syndrome according to diffusion tensor imaging. *Alcoholism-Clinical and Experimental Research* 29, 1214-1222.
- Marsh, R., Gerber, A.J., Peterson, B.S., 2008. Neuroimaging Studies of Normal Brain Development and Their Relevance for Understanding Childhood Neuropsychiatric Disorders. *Journal of the American Academy of Child and Adolescent Psychiatry* 47, 1233-1251.
- Martin, L.J., Cork, L.C., 2014. The non-human primate striatum undergoes marked prolonged remodeling during postnatal development. *Frontiers in Cellular Neuroscience* 8, 15.
- Mattson, S.N., Riley, E.P., Gramling, L., Delis, D.C., Jones, K.L., 1998. Neuropsychological comparison of alcohol-exposed children with or without physical features of fetal alcohol syndrome. *Neuropsychology* 12, 146-153.
- Mattson, S.N., Roesch, S.C., Glass, L., Deweese, B.N., Coles, C.D., Kable, J.A., May, P.A., Kalberg, W.O., Sowell, E.R., Adnams, C.M., Jones, K.L., Riley, E.P., Cifas, 2013. Further Development of a Neurobehavioral Profile of Fetal Alcohol Spectrum Disorders. *Alcoholism-Clinical and Experimental Research* 37, 517-528.
- May, P.A., Gossage, J.P., 2001. Estimating the Prevalence of Fetal Alcohol Syndrome - A Summary. *Alcohol Research & Health* 25, 159-167.
- May, P.A., Gossage, J.P., Kalberg, W.O., Robinson, L.K., Buckley, D., Manning, M., Hoyme, H.E., 2009. Prevalence and epidemiologic characteristics of FASD from various research methods with an emphasis on recent in-school studies. *Developmental Disabilities Research Reviews* 15, 176-192.
- McCarthy, M.M., 2008. Estradiol and the developing brain. *Physiological Reviews* 88, 91-124.
- McCrary, E., De Brito, S.A., Viding, E., 2010. Research Review: The neurobiology and genetics of maltreatment and adversity. *Journal of Child Psychology and Psychiatry* 51, 1079-1095.
- McTigue, D.M., Tripathi, R.B., 2008. The life, death, and replacement of oligodendrocytes in the adult CNS. *Journal of Neurochemistry* 107, 1-19.
- Medina, A.E., 2011. Fetal Alcohol Spectrum Disorders and Abnormal Neuronal Plasticity. *Neuroscientist* 17, 274-287.

- Miller, M.W., 1986. Effects of alcohol on the generation and migration of cerebral cortical-neurons. *Science* 233, 1308-1311.
- Miller, M.W., 1989. Effects of prenatal exposure to ethanol on neocortical development: II. Cell proliferation in the ventricular and subventricular zones of the rat. *J Comp Neurol* 287, 326-338.
- Miller, M.W., 2003. Expression of transforming growth factor-beta in developing rat cerebral cortex: Effects of prenatal exposure to ethanol. *Journal of Comparative Neurology* 460, 410-424.
- Miller, M.W., Nowakowski, R.S., 1991. Effect of prenatal exposure to ethanol on the cell cycle kinetics and growth fraction in the proliferative zones of fetal rat cerebral cortex. *Alcohol Clin Exp Res* 15, 229-232.
- Miller, M.W., Robertson, S., 1993. Prenatal exposure to ethanol alters the postnatal-development and transformation of radial glia to astrocytes in the cortex. *Journal of Comparative Neurology* 337, 253-266.
- Mitchell, J.J., Paiva, M., Moore, D.B., Walker, D.W., Heaton, M.B., 1998. A comparative study of ethanol, hypoglycemia, hypoxia and neurotrophic factor interactions with fetal rat hippocampal neurons: a multi-factor in vitro model for developmental ethanol effects. *Developmental Brain Research* 105, 241-250.
- Montague, D.M., Lawler, C.P., Mailman, R.B., Gilmore, J.H., 1999. Developmental regulation of the dopamine D-1 receptor in human caudate and putamen. *Neuropsychopharmacology* 21, 641-649.
- Montes, L.G.A., Alcantara, H.P., Garcia, R.B.M., De La Torre, L.B., Acosta, D.A., Duarte, M.G., 2013. Brain Cortical Thickness in ADHD: Age, Sex, and Clinical Correlations. *Journal of Attention Disorders* 17, 641-654.
- Nair, G., Tanahashi, Y., Low, H.P., Billings-Gagliardi, S., Schwartz, W.J., Duong, T.Q., 2005. Myelination and long diffusion times alter diffusion-tensor-imaging contrast in myelin-deficient shiverer mice. *Neuroimage* 28, 165-174.
- Narberhaus, A., Segarra, D., Gimenez, M., Caldu, X., Junque, C., Bargallo, N., Botet, F., 2004. Differential cerebral and neuropsychological consequences in dizygotic twins with prenatal alcohol exposure. *Alcohol and Alcoholism* 39, 321-324.
- Nardelli, A., Lebel, C., Rasmussen, C., Andrew, G., Beaulieu, C., 2011. Extensive Deep Gray Matter Volume Reductions in Children and Adolescents with Fetal Alcohol Spectrum Disorders. *Alcoholism-Clinical and Experimental Research* 35, 1404-1417.
- Narr, K.L., Woods, R.P., Lin, J., Kim, J., Phillips, O.R., Del'Homme, M., Caplan, R., Toga, A.W., McCracken, J.T., Levitt, J.G., 2009. Widespread Cortical Thinning Is a Robust Anatomical Marker for Attention-Deficit/Hyperactivity Disorder. *Journal of the American Academy of Child and Adolescent Psychiatry* 48, 1014-1022.

- Nie, J.X., Li, G., Shen, D.G., 2013. Development of cortical anatomical properties from early childhood to early adulthood. *Neuroimage* 76, 216-224.
- Norman, A.L., Crocker, N., Mattson, S.N., Riley, E.P., 2009. Neuroimaging and Fetal Alcohol Spectrum Disorders. *Developmental Disabilities Research Reviews* 15, 209-217.
- Norton, S., Terranova, P., Na, J.Y., Sanchotello, M., 1988. Early Motor Development and Cerebral Cortical Morphology in Rats Exposed Perinatally to Alcohol. *Alcoholism-Clinical and Experimental Research* 12, 130-136.
- Nowinski, W.L., Chua, B.C., Yang, G.L., Qian, G.Y., 2012. Three-Dimensional Interactive and Stereotactic Human Brain Atlas of White Matter Tracts. *Neuroinformatics* 10, 33-55.
- Nunez, S.C., Roussotte, F., Sowell, E.R., 2011. Focus On: Structural and Functional Brain Abnormalities in Fetal Alcohol Spectrum Disorders. *Alcohol Research & Health* 34, 121-131.
- O'Callaghan, F.V., O'Callaghan, M., Najman, J.M., Williams, G.M., Bor, W., 2003. Maternal alcohol consumption during pregnancy and physical outcomes up to 5 years of age: a longitudinal study. *Early Human Development* 71, 137-148.
- O'Connell, E.J., Feldt, R.H., Stickler, G.B., 1965. Head Circumference Mental Retardation and Growth Failure. *Pediatrics* 36, 62-&.
- O'Hare, E.D., Kan, E., Yoshii, J., Mattson, S.N., Riley, E.P., Thompson, P.M., Toga, A.W., Sowell, E.R., 2005. Mapping cerebellar vermal morphology and cognitive correlates in prenatal alcohol exposure. *Neuroreport* 16, 1285-1290.
- Oishi, K., Zilles, K., Amunts, K., Faria, A., Jiang, H., Li, X., Akhter, K., Hua, K., Woods, R., Toga, A.W., Pike, G.B., Rosa-Neto, P., Evans, A., Zhang, J., Huang, H., Miller, M.I., van Zijl, P.C.M., Mazziotta, J., Mori, S., 2008. Human brain white matter atlas: Identification and assignment of common anatomical structures in superficial white matter. *Neuroimage* 43, 447-457.
- Olney, J.W., Ishimaru, M.J., Bittigau, P., Ikonomidou, C., 2000. Ethanol-induced apoptotic neurodegeneration in the developing brain. *Apoptosis* 5, 515-521.
- Olson, H.C., Oti, R., Gelo, J., Beck, S., 2009. "Family Matters:" Fetal Alcohol Spectrum Disorders And The Family. *Developmental Disabilities Research Reviews* 15, 235-249.
- Ornoy, A., 2007. Embryonic oxidative stress as a mechanism of teratogenesis with special emphasis on diabetic embryopathy. *Reproductive Toxicology* 24, 31-41.
- Osborn, J.A., Kim, C.K., Steiger, J., Weinberg, J., 1998. Prenatal ethanol exposure differentially alters behavior in males and females on the elevated plus maze. *Alcoholism-Clinical and Experimental Research* 22, 685-696.

- Ozer, E., Sarioglu, S., Gure, A., 2000. Effects of prenatal ethanol exposure on neuronal migration, neuronogenesis and brain myelination in the mice brain. *Clinical Neuropathology* 19, 21-25.
- Paolozza, A., Munn, R., Munoz, D.P., Reynolds, J.N., 2015. Eye movements reveal sexually dimorphic deficits in children with fetal alcohol spectrum disorder. *Frontiers in neuroscience* 9, 76-76.
- Paolozza, A., Treit, S., Beaulieu, C., Reynolds, J.N., 2014. Response inhibition deficits in children with Fetal Alcohol Spectrum Disorder: Relationship between diffusion tensor imaging of the corpus callosum and eye movement control. *Neuroimage-Clinical* 5, 53-61.
- Peiffer, J., Majewski, F., Fischbach, H., Bierich, J.R., Volk, B., 1979. Alcohol embryopathy and fetopathy - neuropathology of 3 children and 3 fetuses. *Journal of the Neurological Sciences* 41, 125-137.
- Perea, G., Araque, A., 2005. Glial calcium signaling and neuron-glia communication. *Cell Calcium* 38, 375-382.
- Pfefferbaum, A., Mathalon, D.H., Sullivan, E.V., Rawles, J.M., Zipursky, R.B., Lim, K.O., 1994. A quantitative magnetic-resonance-imaging study of changes in brain morphology from infancy to late adulthood. *Archives of Neurology* 51, 874-887.
- Phillips, D.E., 1989. Effects of limited postnatal ethanol exposure on the development of myelin and nerve-fibres in rat optic-nerve. *Experimental Neurology* 103, 90-100.
- Pollard, I., 2007. Neuropharmacology of drugs and alcohol in mother and fetus. *Seminars in Fetal & Neonatal Medicine* 12, 106-113.
- Puglia, M.P., Valenzuela, C.F., 2010. Repeated third trimester-equivalent ethanol exposure inhibits long-term potentiation in the hippocampal CA1 region of neonatal rats. *Alcohol* 44, 283-290.
- Rajaprakash, M., Chakravarty, M.M., Lerch, J.P., Rovet, J., 2014. Cortical morphology in children with alcohol-related neurodevelopmental disorder. *Brain and behavior* 4, 41-50.
- Rakic, P., 1995. A Small Step for the Cell, A Giant Leap for Mankind - A Hypothesis of Neocortical Expansion During Evolution. *Trends in Neurosciences* 18, 383-388.
- Raznahan, A., Greenstein, D., Lee, N.R., Clasen, L.S., Giedd, J.N., 2012. Prenatal growth in humans and postnatal brain maturation into late adolescence. *Proceedings of the National Academy of Sciences of the United States of America* 109, 11366-11371.
- Raznahan, A., Shaw, P., Lalonde, F., Stockman, M., Wallace, G.L., Greenstein, D., Clasen, L., Gogtay, N., Giedd, J.N., 2011. How Does Your Cortex Grow? *Journal of Neuroscience* 31, 7174-7177.

- Redila, V.A., Olson, A.K., Swann, S.E., Mohades, G., Webber, A.J., Weinberg, J., Christie, B.R., 2006. Hippocampal cell proliferation is reduced following prenatal ethanol exposure but can be rescued with voluntary exercise. *Hippocampus* 16, 305-311.
- Reinhardt, K., Mohr, A., Gartner, J., Spohr, H.L., Brockmann, K., 2010. Polymicrogyria in Fetal Alcohol Syndrome. *Birth Defects Research Part a-Clinical and Molecular Teratology* 88, 128-131.
- Reiss, A.L., Abrams, M.T., Singer, H.S., Ross, J.L., Denckla, M.B., 1996. Brain development, gender and IQ in children - A volumetric imaging study. *Brain* 119, 1763-1774.
- Reynolds, J.N., Weinberg, J., Clarren, S., Beaulieu, C., Rasmussen, C., Kobor, M., Dube, M.-P., Goldowitz, D., 2011. Fetal Alcohol Spectrum Disorders: Gene-Environment Interactions, Predictive Biomarkers, and the Relationship Between Structural Alterations in the Brain and Functional Outcomes. *Seminars in Pediatric Neurology* 18, 49-55.
- Rice, D., Barone, S., 2000. Critical periods of vulnerability for the developing nervous system: Evidence from humans and animal models. *Environmental Health Perspectives* 108, 511-533.
- Riikonen, R., Salonen, I., Partanen, K., Verho, S., 1999. Brain perfusion SPECT and MRI in foetal alcohol syndrome. *Developmental Medicine and Child Neurology* 41, 652-659.
- Rijkema, M., Everaerd, D., van der Pol, C., Franke, B., Tendolkar, I., Fernandez, G., 2012. Normal sexual dimorphism in the human basal ganglia. *Human Brain Mapping* 33, 1246-1252.
- Riley, E.P., Mattson, S.N., Sowell, E.R., Jernigan, T.L., Sobel, D.F., Jones, K.L., 1995. Abnormalities of the corpus-callosum in children prenatally exposed to alcohol. *Alcoholism-Clinical and Experimental Research* 19, 1198-1202.
- Riley, E.P., McGee, C.L., 2005. Fetal alcohol spectrum disorders: An overview with emphasis on changes in brain and behavior. *Experimental Biology and Medicine* 230, 357-365.
- Rollins, J.D., Collins, J.S., Holden, K.R., 2010. United States Head Circumference Growth Reference Charts: Birth to 21 Years. *Journal of Pediatrics* 156, 907-U977.
- Roussotte, F., Soderberg, L., Sowell, E., 2010. Structural, Metabolic, and Functional Brain Abnormalities as a Result of Prenatal Exposure to Drugs of Abuse: Evidence from Neuroimaging. *Neuropsychology Review* 20, 376-397.
- Roussotte, F.F., Sulik, K.K., Mattson, S.N., Riley, E.P., Jones, K.L., Adnams, C.M., May, P.A., O'Connor, M.J., Narr, K.L., Sowell, E.R., 2011. Regional brain volume reductions relate to facial dysmorphology and neurocognitive function in fetal alcohol spectrum disorders. *Human Brain Mapping* 33, 920-937.

- Russell, M., Czarnecki, D.M., Cowan, R., McPherson, E., Mudar, P.J., 1991. Measures of Maternal Alcohol-Use as Predictors of Development in Early-Childhood. *Alcoholism-Clinical and Experimental Research* 15, 991-1000.
- Sampson, P.D., Bookstein, F.L., Barr, H.M., Streissguth, A.P., 1994. Prenatal Alcohol Exposure, Birth-Weight, and Measures of Child Size from Birth to Age 14 Years. *American Journal of Public Health* 84, 1421-1428.
- Schmahmann, J.D., Pandya, D.N., 2007. The complex history of the fronto-occipital fasciculus. *Journal of the History of the Neurosciences* 16, 362-377.
- Servais, L., Hourez, R., Bearzatto, B., Gall, D., Schiffmann, S.N., Cheron, G., 2007. Purkinje cell dysfunction and alteration of long-term synaptic plasticity in fetal alcohol syndrome. *Proceedings of the National Academy of Sciences of the United States of America* 104, 9858-9863.
- Shaw, P., Eckstrand, K., Sharp, W., Blumenthal, J., Lerch, J.P., Greenstein, D., Clasen, L., Evans, A., Giedd, J., Rapoport, J.L., 2007. Attention-deficit/hyperactivity disorder is characterized by a delay in cortical maturation. *Proceedings of the National Academy of Sciences of the United States of America* 104, 19649-19654.
- Shaw, P., Gilliam, M., Liverpool, M., Weddle, C., Malek, M., Sharp, W., Greenstein, D., Evans, A., Rapoport, J., Giedd, J., 2011. Cortical Development in Typically Developing Children With Symptoms of Hyperactivity and Impulsivity: Support for a Dimensional View of Attention Deficit Hyperactivity Disorder. *American Journal of Psychiatry* 168, 143-151.
- Shaw, P., Greenstein, D., Lerch, J., Clasen, L., Lenroot, R., Gogtay, N., Evans, A., Rapoport, J., Giedd, J., 2006a. Intellectual ability and cortical development in children and adolescents. *Nature* 440, 676-679.
- Shaw, P., Kabani, N.J., Lerch, J.P., Eckstrand, K., Lenroot, R., Gogtay, N., Greenstein, D., Clasen, L., Evans, A., Rapoport, J.L., Giedd, J.N., Wise, S.P., 2008. Neurodevelopmental trajectories of the human cerebral cortex. *Journal of Neuroscience* 28, 3586-3594.
- Shaw, P., Lerch, J., Greenstein, D., Sharp, W., Clasen, L., Evans, A., Giedd, J., Castellanos, F.X., Rapoport, J., 2006b. Longitudinal mapping of cortical thickness and clinical outcome in children and adolescents with attention-deficit/hyperactivity disorder. *Archives of General Psychiatry* 63, 540-549.
- Shaw, P., Malek, M., Watson, B., Greenstein, D., de Rossi, P., Sharp, W., 2013. Trajectories of Cerebral Cortical Development in Childhood and Adolescence and Adult Attention-Deficit/Hyperactivity Disorder. *Biological Psychiatry* 74, 599-606.
- Shaw, P., Sharp, W.S., Morrison, M., Eckstrand, K., Greenstein, D.K., Clasen, L.S., Evans, A.C., Rapoport, J.L., 2009. Psychostimulant Treatment and the Developing Cortex in Attention Deficit Hyperactivity Disorder. *American Journal of Psychiatry* 166, 58-63.

- Shen, L., Ai, H., Liang, Y., Ren, X., Anthony, C.B., Goodlett, C.R., Ward, R., Zhou, F.C., 2013. Effect of prenatal alcohol exposure on bony craniofacial development: A mouse MicroCT study. *Alcohol* 47, 405-415.
- Shetty, A.K., Phillips, D.E., 1992. Effects of prenatal ethanol exposure on the development of bergmann glia and astrocytes in the rat cerebellum - an immunohistochemical study. *Journal of Comparative Neurology* 321, 19-32.
- Sickmann, H.M., Patten, A.R., Morch, K., Sawchuk, S., Zhang, C., Parton, R., Szlavik, L., Christie, B.R., 2014. Prenatal Ethanol Exposure has Sex-Specific Effects on Hippocampal Long-Term Potentiation. *Hippocampus* 24, 54-64.
- Sisk, C.L., Zehr, J.L., 2005. Pubertal hormones organize the adolescent brain and behavior. *Frontiers in Neuroendocrinology* 26, 163-174.
- Sliwowska, J.H., Song, H.J., Bodnar, T., Weinberg, J., 2014. Prenatal Alcohol Exposure Results in Long-Term Serotonin Neuron Deficits in Female Rats: Modulatory Role of Ovarian Steroids. *Alcoholism-Clinical and Experimental Research* 38, 152-160.
- Smith, I.E., Coles, C.D., Lancaster, J., Fernhoff, P.M., Falek, A., 1986. The Effect of Volume and Duration of Prenatal Ethanol Exposure on Neonatal Physical and Behavioral-Development. *Neurobehavioral Toxicology and Teratology* 8, 375-381.
- Society, C.P., 2002.
- Song, S.K., Sun, S.W., Ju, W.K., Lin, S.J., Cross, A.H., Neufeld, A.H., 2003. Diffusion tensor imaging detects and differentiates axon and myelin degeneration in mouse optic nerve after retinal ischemia. *Neuroimage* 20, 1714-1722.
- Song, S.K., Sun, S.W., Ramsbottom, M.J., Chang, C., Russell, J., Cross, A.H., 2002. Dysmyelination revealed through MRI as increased radial (but unchanged axial) diffusion of water. *Neuroimage* 17, 1429-1436.
- Sowell, E.R., Johnson, A., Kan, E., Lu, L.H., Van Horn, J.D., Toga, A.W., O'Connor, M.J., Bookheimer, S.Y., 2008a. Mapping white matter integrity and neurobehavioral correlates in children with fetal alcohol spectrum disorders. *Journal of Neuroscience* 28, 1313-1319.
- Sowell, E.R., Mattson, S.N., Kan, E., Thompson, P.M., Riley, E.P., Toga, A.W., 2008b. Abnormal cortical thickness and brain-behavior correlation patterns in individuals with heavy prenatal alcohol exposure. *Cerebral Cortex* 18, 136-144.
- Sowell, E.R., Mattson, S.N., Thompson, P.M., Jernigan, T.L., Riley, E.P., Toga, A.W., 2001. Mapping callosal morphology and cognitive correlates - Effects of heavy prenatal alcohol exposure. *Neurology* 57, 235-244.
- Sowell, E.R., Thompson, P.M., Leonard, C.M., Welcome, S.E., Kan, E., Toga, A.W., 2004. Longitudinal mapping of cortical thickness and brain growth in normal children. *Journal of Neuroscience* 24, 8223-8231.

- Sowell, E.R., Thompson, P.M., Mattson, S.N., Tessner, K.D., Jernigan, T.L., Riley, E.P., Toga, A.W., 2002a. Regional brain shape abnormalities persist into adolescence after heavy prenatal alcohol exposure. *Cerebral Cortex* 12, 856-865.
- Sowell, E.R., Thompson, P.M., Peterson, B.S., Mattson, S.N., Welcome, S.E., Henkenius, A.L., Riley, E.P., Jernigan, T.L., Toga, A.W., 2002b. Mapping cortical gray matter asymmetry patterns in adolescents with heavy prenatal alcohol exposure. *Neuroimage* 17, 1807-1819.
- Spottiswoode, B.S., Meintjes, E.M., Anderson, A.W., Molteno, C.D., Stanton, M.E., Dodge, N.C., Gore, J.C., Peterson, B.S., Jacobson, J.L., Jacobson, S.W., 2011. Diffusion Tensor Imaging of the Cerebellum and Eyeblink Conditioning in Fetal Alcohol Spectrum Disorder. *Alcoholism-Clinical and Experimental Research* 35, 2174-2183.
- Steinbrink, C., Vogt, K., Kastrup, A., Muller, H.P., Juengling, F.D., Kassubeek, J., Riecker, A., 2008. The contribution of white and gray matter differences to developmental dyslexia: Insights from DTI and VBM at 3.0 T. *Neuropsychologia* 46, 3170-3178.
- Stejskal, E.O., Tanner, J.E., 1965. Spin Diffusion Measurements: Spin Echoes In The Presence Of A Time-Dependent Field Gradient. *Journal of Chemical Physics* 42, 288-+.
- Stiles, J., 2008. *The Fundamentals of Brain Development: Integrating Nature and Nurture*. Harvard University Press.
- Stoneham, E.T., Sanders, E.M., Sanyal, M., Dumas, T.C., 2010. Rules of Engagement: Factors That Regulate Activity-Dependent Synaptic Plasticity During Neural Network Development. *Biological Bulletin* 219, 81-99.
- Streissguth, A.P., Aase, J.M., Clarren, S.K., Randels, S.P., Ladue, R.A., Smith, D.F., 1991. Fetal Alcohol Syndrome in Adolescents and Adults. *Journal of the American Medical Association* 265, 1961-1967.
- Streissguth, A.P., Bookstein, F.L., Barr, H.M., Sampson, P.D., O'Malley, K., Young, J.K., 2004. Risk factors for adverse life outcomes in fetal alcohol syndrome and fetal alcohol effects. *Journal of Developmental and Behavioral Pediatrics* 25, 228-238.
- Streissguth, A.P., Dehaene, P., 1993. Fetal Alcohol Syndrome in Twins of Alcoholic Mothers - Concordance of Diagnosis and IQ. *American Journal of Medical Genetics* 47, 857-861.
- Sulik, K.K., 2005. Genesis of alcohol-induced craniofacial dysmorphism. *Experimental Biology and Medicine* 230, 366-375.
- Sulik, K.K., Cook, C.S., Webster, W.S., 1988. Teratogens And Craniofacial Malformations - Relationships To Cell-Death. *Development* 103, 213-&.
- Sulik, K.K., Johnston, M.C., Webb, M.A., 1981. Fetal Alcohol Syndrome - Embryogenesis in a Mouse Model. *Science* 214, 936-938.

- Swayze, V.W., Johnson, V.P., Hanson, J.W., Piven, J., Sato, Y., Giedd, J.N., Mosnik, D., Andreasen, N.C., 1997. Magnetic resonance imaging of brain anomalies in fetal alcohol syndrome. *Pediatrics* 99, 232-240.
- Tamnes, C.K., Ostby, Y., Fjell, A.M., Westlye, L.T., Due-Tonnessen, P., Walhovd, K.B., 2010. Brain Maturation in Adolescence and Young Adulthood: Regional Age-Related Changes in Cortical Thickness and White Matter Volume and Microstructure. *Cerebral Cortex* 20, 534-548.
- Taylor, P.A., Jacobson, S.W., van der Kouwe, A., Molteno, C.D., Chen, G., Wintermark, P., Alhamud, A., Jacobson, J.L., Meintjes, E.M., 2015. A DTI-Based Tractography Study of Effects on Brain Structure Associated with Prenatal Alcohol Exposure in Newborns. *Human Brain Mapping* 36, 170-186.
- Theodosis, D.T., Poulain, D.A., Oliet, S.H.R., 2008. Activity-dependent structural and functional plasticity of astrocyte-neuron interactions. *Physiological Reviews* 88, 983-1008.
- Toga, A.W., Thompson, P.M., Sowell, E.R., 2006. Mapping brain maturation. *Trends in Neurosciences* 29, 148-159.
- Tost, H., Braus, D.F., Hakimi, S., Ruf, M., Vollmert, C., Hohn, F., Meyer-Lindenberg, A., 2010. Acute D-2 receptor blockade induces rapid, reversible remodeling in human cortical-striatal circuits. *Nature Neuroscience* 13, 920-922.
- Treit, S., Chen, Z., Rasmussen, C., Beaulieu, C., 2014a. White Matter Correlates Of Cognitive Inhibition During Development: A Diffusion Tensor Imaging Study. *Neuroscience* 276, 87-97.
- Treit, S., Lebel, C., Baugh, L., Rasmussen, C., Andrew, G., Beaulieu, C., 2013. Longitudinal MRI Reveals Altered Trajectory of Brain Development during Childhood and Adolescence in Fetal Alcohol Spectrum Disorders. *Journal of Neuroscience* 33, 10098-10109.
- Treit, S., Zhou, D., Lebel, C., Rasmussen, C., Andrew, G., Beaulieu, C., 2014b. Longitudinal MRI reveals impaired cortical thinning in children and adolescents prenatally exposed to alcohol. *Hum Brain Mapp*.
- Tzourio-Mazoyer, N., Landeau, B., Papathanassiou, D., Crivello, F., Etard, O., Delcroix, N., Mazoyer, B., Joliot, M., 2002. Automated anatomical labeling of activations in SPM using a macroscopic anatomical parcellation of the MNI MRI single-subject brain. *Neuroimage* 15, 273-289.
- Uban, K.A., Comeau, W.L., Ellis, L.A., Galea, L.A.M., Weinberg, J., 2013. Basal regulation of HPA and dopamine systems is altered differentially in males and females by prenatal alcohol exposure and chronic variable stress. *Psychoneuroendocrinology* 38, 1953-1966.

- van Soelen, I.L.C., Brouwer, R.M., van Baal, G.C.M., Schnack, H.G., Peper, J.S., Collins, D.L., Evans, A.C., Kahn, R.S., Boomsma, D.I., Pol, H.E.H., 2012. Genetic influences on thinning of the cerebral cortex during development. *Neuroimage* 59, 3871-3880.
- Von der Hagen, M., Pivarsci, M., Liebe, J., Von Bernuth, H., Didonato, N., Hennermann, J.B., Buhrer, C., Wiczorek, D., Kaindl, A.M., 2014. Diagnostic approach to microcephaly in childhood: a two-center study and review of the literature. *Developmental Medicine and Child Neurology* 56, 732-741.
- Wakana, S., Jiang, H.Y., Nagae-Poetscher, L.M., van Zijl, P.C.M., Mori, S., 2004. Fiber tract-based atlas of human white matter anatomy. *Radiology* 230, 77-87.
- Wake, H., Lee, P.R., Fields, D., 2011. Control of Local Protein Synthesis and Initial Events in Myelination by Action Potentials. *Science* 333, 1647-1651.
- Warren, K.R., Li, T.K., 2005. Genetic polymorphisms: Impact on the risk of fetal alcohol spectrum disorders. *Birth Defects Research Part a-Clinical and Molecular Teratology* 73, 195-203.
- Weinberg, J., Sliwowska, J.H., Lan, N., Hellemans, K.G.C., 2008. Prenatal alcohol exposure: Foetal programming, the hypothalamic-pituitary-adrenal axis and sex differences in outcome. *Journal of Neuroendocrinology* 20, 470-488.
- White, T., Su, S., Schmidt, M., Kao, C.-Y., Sapiro, G., 2010. The development of gyrification in childhood and adolescence. *Brain and Cognition* 72, 36-45.
- Williams, C.A., Dagi, A., Battaglia, A., 2008. Genetic disorders associated with macrocephaly. *American Journal of Medical Genetics Part A* 146A, 2023-2037.
- Witelson, S.F., Beresh, H., Kigar, D.L., 2006. Intelligence and brain size in 100 postmortem brains: sex, lateralization and age factors. *Brain* 129, 386-398.
- Wodarz, A., Huttner, W.B., 2003. Asymmetric cell division during neurogenesis in *Drosophila* and vertebrates. *Mechanisms of Development* 120, 1297-1309.
- Wood, S.J., Pantelis, C., Velakoulis, D., Yuecel, M., Fornito, A., McGorry, P.D., 2008. Progressive changes in the development toward schizophrenia: Studies in subjects at increased symptomatic risk. *Schizophrenia Bulletin* 34, 322-329.
- Wozniak, J.R., Mueller, B.A., Bell, C.J., Muetzel, R.L., Hoecker, H.L., Boys, C.J., Lim, K.O., 2013. Global Functional Connectivity Abnormalities in Children with Fetal Alcohol Spectrum Disorders. *Alcoholism-Clinical and Experimental Research* 37, 748-756.
- Wozniak, J.R., Mueller, B.A., Chang, P.N., Muetzel, R.L., Caros, L., Lim, K.O., 2006. Diffusion tensor imaging in children with fetal alcohol spectrum disorders. *Alcoholism-Clinical and Experimental Research* 30, 1799-1806.

- Wozniak, J.R., Muetzel, R.L., 2011. What Does Diffusion Tensor Imaging Reveal About the Brain and Cognition in Fetal Alcohol Spectrum Disorders? *Neuropsychology Review* 21, 133-147.
- Wozniak, J.R., Muetzel, R.L., Mueller, B.A., McGee, C.L., Freerks, M.A., Ward, E.E., Nelson, M.L., Chang, P.N., Lim, K.O., 2009. Microstructural Corpus Callosum Anomalies in Children With Prenatal Alcohol Exposure: An Extension of Previous Diffusion Tensor Imaging Findings. *Alcoholism-Clinical and Experimental Research* 33, 1825-1835.
- Wu, X.Y., Fu, Y., Knott, G., Lu, J.T., Di Cristo, G., Huang, Z.J., 2012. GABA Signaling Promotes Synapse Elimination and Axon Pruning in Developing Cortical Inhibitory Interneurons. *Journal of Neuroscience* 32, 331-343.
- Yakovlev, P.I., Lecours, A.-R., 1967. The myelogenetic cycles of regional maturation of the brain man.
- Yang, Y., Roussotte, F., Kan, E., Sulik, K.K., Mattson, S.N., Riley, E.P., Jones, K.L., Adnams, C.M., May, P.A., O'Connor, M.J., Narr, K.L., Sowell, E.R., 2011. Abnormal Cortical Thickness Alterations in Fetal Alcohol Spectrum Disorders and Their Relationships with Facial Dysmorphology. *Cereb Cortex*.
- Zhang, H., Yushkevich, P.A., Alexander, D.C., Gee, J.C., 2006. Deformable registration of diffusion tensor MR images with explicit orientation optimization. *Medical Image Analysis* 10, 764-785.
- Zhou, D., Lebel, C., Evans, A., Beaulieu, C., 2013. Cortical thickness asymmetry from childhood to older adulthood. *Neuroimage* 83, 66-74.
- Zhou, D., Lebel, C., Lepage, C., Rasmussen, C., Evans, A., Wyper, K., Pei, J., Andrew, G., Massey, A., Massey, D., Beaulieu, C., 2011. Developmental cortical thinning in fetal alcohol spectrum disorders. *Neuroimage* 58, 16-25.
- Zhou, D., Lebel, C., Treit, S., Evans, A., Beaulieu, C., 2015. Accelerated longitudinal cortical thinning in adolescence. *Neuroimage* 104, 138-145.
- Zimmerberg, B., Mickus, L.A., 1990. Sex-Differences in Corpus-Callosum - Influence of Prenatal Alcohol Exposure and Maternal Undernutrition. *Brain Research* 537, 115-122.
- Zimmerberg, B., Reuter, J.M., 1989. Sexually Dimorphic Behavioral and Brain Asymmetries in Neonatal Rats - Effects of Prenatal Alcohol Exposure. *Developmental Brain Research* 46, 281-290.
- Zimmerberg, B., Scalzi, L.V., 1989. Commissural Size in Neonatal Rats - Effects of Sex and Prenatal Alcohol Exposure. *International Journal of Developmental Neuroscience* 7, 81-86.

Zucca, S., Valenzuela, C.F., 2010. Low Concentrations of Alcohol Inhibit BDNF-Dependent GABAergic Plasticity via L-type Ca(2+) Channel Inhibition in Developing CA3 Hippocampal Pyramidal Neurons. *Journal of Neuroscience* 30, 6776-6781.

Appendix A: Diagnostic Terms under the FASD Umbrella

Name	Abbreviation	Diagnosis Requirements
Fetal Alcohol Syndrome	FAS	<ul style="list-style-type: none"> History of exposure Characteristic facial anomalies 1) short palpebral fissures, 2) thin upper lip, and 3) smooth philtrum Growth retardation CNS abnormalities (e.g. microcephaly, hard neurological signs, neurobehavioural impairment)
Partial Fetal Alcohol Syndrome	pFAS	<ul style="list-style-type: none"> History of exposure At least one characteristic facial anomaly Growth retardation and/or CNS abnormalities and/or behavioural/developmental delay
¹ Static Encephalopathy Alcohol Exposed	SE:AE	<ul style="list-style-type: none"> History of exposure “Probable or Definite Brain Damage” as defined by Microcephaly/abnormal imaging/neurological hard signs OR three or more abnormalities in cognition, achievement, adaptation, neurological soft signs, or language.
¹ Neurobehavioural Disorder Alcohol Exposed	NBD:AE	<ul style="list-style-type: none"> History of exposure “Possible Brain Damage” as defined by historical information or observation strongly suggesting the possibility of brain damage (but not meeting criteria of static encephalopathy)
² Alcohol Related Birth Defects	ARBD	<ul style="list-style-type: none"> History of exposure Congenital anomalies, including malformations or dysplasia
² Alcohol Related Neurobehavioural Disorder	ARND	<ul style="list-style-type: none"> History of exposure Evidence of CNS abnormalities and/or behavioural/developmental delay
Fetal Alcohol Spectrum Disorder Unspecified	FASD Unspecified	<ul style="list-style-type: none"> History of exposure Neurocognitive delay but insufficient information/evidence for a specific diagnosis

¹From the 4-digit diagnostic code

²From the Canadian Guidelines for FASD Diagnosis

It is important to note that under the Canadian Guidelines, individuals with both SE:AE and NBD:AE would fall under the diagnosis of ARND. ARBD and ARND can be given concurrently.

Appendix B: Studies of DTI in FASD

1 st Author Journal Year	N	Age (yrs)	Method	Corpus Callosum									Other
				Ant.	Mid.	Post.	Cing	CST	IFO	ILF	SLF	UF	
Ma ACER 2005	9 FASD 7 Ctrl	18-25	ROI	↓ FA ↑ MD	--	↓ FA ↑ MD	--	--	--	--	--	--	---
Wozniak ACER 2006	14 FASD 13 Ctrl	10-13	ROI	X	X	↑ MD	--	--	--	--	--	--	---
Sowell J Neurosci 2008	17 FASD 19 Ctrl	7-15	VBA; ROI	X	X	↓ FA	↓ FA	X	↓ FA	↓ FA	X	X	↓ FA brainstem, internal capsule
Lebel 2008 ACER	24 FASD 95 Ctrl	5-13	WM Tractography; GM ROIs	↓ MD	X	↓ FA	↓ FA	↑ MD	↑ MD	↓ FA ↑ MD	↓ FA	X	↓ FA thalamus, GP ↑ MD GP, thalamus, putamen
Fryer ACER 2009	15 PAE 12 Ctrl	8-18	TBSS ROI	X	↓ FA	↓ FA	↑ FA	X	X	X	↓ FA	↓ FA	↓ FA SFO and ant/sup corona radiata, post. corona radiata, ↑ FA PLIC
Li HBM 2009	57 FASD 25 Ctrl	19-27	TBSS ^b ROI	X	X	↓ FA ↑ MD	X	--	---	---	X	---	---
Wozniak 2009 ACER	33 FASD 19 Ctrl	10-17	Tractography	X	X	↓ FA	--	--	--	--	--	--	---
Spottiswood ACER 2011	13 FASD 12 Ctrl	9-13	VBA ^d	---	---	---	---	---	---	---	---	---	↓ FA and ↑λ ₁ in MCP
Paolozza NI: Clinical 2014	47 FASD 41 Ctrl	7-18	Tractography	X	X	↑ MD	---	---	---	---	---	---	---
Taylor HBM 2015	11 PAE 9 Ctrl	Infants	Tractography ^c	↓ λ ₁	---								

Anterior CC= genu, anterior midbody; Middle CC=Body; Posterior CC= Isthmus, Genu, ROI=region of interest; VBA=voxel based analysis; TBSS=tract based spatial statistics; MCP=Middle cerebellar peduncle; PLIC=posterior limb of the internal capsule

↑=higher in FASD group than controls; ↓=lower in FASD group than controls; X=not significant; --=not tested; ↗=positive correlation; ↘=negative correlation;

Table excludes DTI studies that do not test for group differences: e.g. Lebel 2010 ACER; Wozniak 2011 ACER; Green 2013 ACER

Only Li, Wozniak 2011 and Spottiswood tested for sex effects of group-sex interactions; none found in any.

--- Start of thesis program (2010)

--- Publication of Chapter 2

^a FAS, mental retardation and microcephaly excluded

^b 64 mm coverage in middle of brain so assumed to not include IFO, UF, ILF

^c Same cohort as Lebel 2008 ACER

^d Only examined cerebellum and brainstem

^e 5 networks delineated: R and L projection networks, R and L association networks, Callosal network—probable overlap with tracts assumed here.

Appendix C: Studies of Brain Volume in FASD

Author Journal Year	N	Age	CC ^b	CB ^b	ICV	TBV	WM	Cort. GM	Thal	Caud	Put	GP	Hipp	Am	Other
Mattson ACER 1992	2 FAS 9 Ctrl	13 & 14	---	---	↓	---	↓	---	↓*	↓*	↓*	↓*	---	---	---
Mattson Neurotox & Teratol 1994	2 FASD 20 Ctrl	16	---	---	↓	---	---	--- ^b	--- ^b	↓*	↓*	↓*	--- ^b	--- ^b	---
Riley ACER 1995	13 FASD 12 Ctrl	8-19	↓	---	---	---	---	---	---	---	---	---	---	---	---
Mattson ACER 1996	6 FASD 7 Ctrl	8-19	---	---	↓	---	---	---	↓	↓*	↓	↓	---	---	---
Sowell ACER 1996	9 FASD 22 Ctrl	8-24	---	↓	---	---	---	---	---	---	---	---	---	---	---
Archibald DMCN 2001	26 FASD 41 Ctrl		---	---	↓	---	↓*	↓	↓	↓*	↓	↓	X/↑*	↓	↓* parietal lobe
Sowell Neuroreport 2001a	21 FASD 21 Ctrl	8-22	---	---	↓	---	↓	↓ ↑*	---	---	---	---	---	---	---
Sowell Neurology 2001b	21 FASD 21 Ctrl	8-22	↓	---	---	---	---	---	---	---	---	---	---	---	---
Roebuck ACER 2002	22 FASD 20 Ctrl	9-14	↓	---	---	---	---	---	---	---	---	---	---	---	---

Author Journal Year	N	Age	CC ^b	CB ^b	ICV	TBV	WM	Cort. GM	Thal	Caud	Put	GP	Hipp	Am	Other
Autti-Ramo DMCN 2002	17 FASD 17 Controls	Mean 13	---	---	---	↓	---	---	---	---	---	---	---	---	---
Riikonen Biol Psychiatry 2005	12 FASD and 12 Ctrl%		---	---	---	↓	---	---	---	↓X	↓X	---	↓X	↓X	---
Cortese Neurotox & Teratol 2006	11 FASD 4 Ctrl	9-12	---	---	↓	---	---	---	---	↓X	---	---	---	---	---
Wozniak ACER 2006	14 FASD 13 HC	10- 13	---	---	---	X	X	↓	---	---	---	---	---	---	---
Li Brain Imag & Behav 2008	7 FASD 7 Ctrl	18- 24	---	---	---	↓	↓*tem p- occipi tal and CC region s	↓* temp- occipital and CC regions	---	---	---	---	---	---	---
Lebel ACER 2008	24 FASD 95 Ctrl	5-13	---	---	---	↓	↓	↓	---	---	---	---	---	---	---
Willoughby JINS 2008	19 FASD 18 Ctrl	9-15	---	---	↓	---	---	---	---	---	---	---	↓*	---	---
Dodge ACER 2009	7 FASD 7 Ctrl	---	↓	---	---	---	---	---	---	---	---	---	---	---	---
Astley ACER 2009	65 FASD 16 Ctrl	12 +/- 2	↓	↓	---	↓	↓ (front al lobe)	↓ (frontal lobe)	---	↓*	↓	---	↓	---	---

Author Journal Year	N	Age	CC ^b	CB ^b	ICV	TBV	WM	Cort. GM	Thal	Caud	Put	GP	Hipp	Am	Other
Bjorkquist Psych Res- Neuroimag 2010	21 FASD 10 Ctrl	8-16	---	---	↓	↓	↓	↓	---	---	---	---	---	---	↓* Cingul ate gyrus gray and white matter
Willford Neurotox & Teratol 2010	25 FASD 20 Ctrl	8-22	---	---	---	X	---	---	---	X	---	---	---	---	---
Coles Brain & Cognition 2011	66 FASD 26 Ctrl		---	---	---	↓	---	↓ (lateral frontal lobes and temporal)	---	---	---	---	↓	---	---
Nardelli ACER 2011	28 FASD 56 Ctrl	6-17	---	---	↓	---	↓	↓	↓*	↓*	↓*	↓*	↓*	↓	---
Roussotte HBM 2012	56 FASD 43 Ctrl	8-16	---	---	↓	---	↓	↓*	↓	↓	↓*	↓*	↓	↓	---
Lebel J Neurosci 2012	70 FASD 63 Ctrl	5-15	---	---	---	Diff traje ctory	↓ but same traject ory	Different trajectory	---	---	---	---	---	---	---
Eckstrand ACER 2012	11 FASD 9 Ctrl	18- 20	---	---	---	X	X	X Overall ↓ Regional	---	---	---	---	---	---	---
Rajaprakash Brain & Behaviour 2014	36 FASD 52 Ctrl	8-15	---	---	---	↓	---	↓	---	---	---	---	---	---	---

Author Journal Year	N	Age	CC ^b	CB ^b	ICV	TBV	WM	Cort. GM	Thal	Caud	Put	GP	Hipp	Am	Other
Cardenas NI: Clinical 2014	11 FASD 9 Ctrl	10- 18	---	↓	--	---	---	---	---	---	---	---	---	---	---
Meintjes NI: Clinical 2014	39 FASD 16 Controls	9-11	---	---	↓	---	---	---	---	---	---	---	---	---	TBM volume reducti on in several broad areas
Guatam NI: Clinical 2014	27 FASD 42 Ctrl	6-17	↓	---	↓	---	↓ region al ↓*CC, mid.fr ontal, supra mar., inf. pariet al	---	---	---	---	---	---	---	---
Joseph HBM 2014	12 FAS 19 Ctrl	10- 13	---	---	---	---	---	---	---	X	---	---	X	---	---
Dudek JINS 2014	18 FASD 17 Ctrl	11- 14	---	---	↓	---	---	---	---	---	---	---	↓*	---	---

Excludes case studies and qualitative studies where brain volume is not statistically compared (i.e. excludes reports of microencephaly on radiological review)

CC=corpus callosum; CB=cerebellum; Ctrl=control subjects; ICV=intracranial volume; WM=white matter; Cort. GM=cortical grey matter; Thal=thalamus; Caud=caudate; Put=putamen; GP=globus pallidus; Hipp=hippocampus; Amyg=amygdala;

↓ Reduced in FASD relative to Control group; ↑ Elevated in FASD relative to Control group

*Remains significant after controlling for total brain volume or ICV; X No difference between groups; --- Not tested or not reported

^a Volume or mid-sagittal area ; ^b Only tested proportional volume, not raw volume.; ^{%%} Not healthy controls—all had clinical reasons for scans, mostly motor deficits, etc but no PAE.

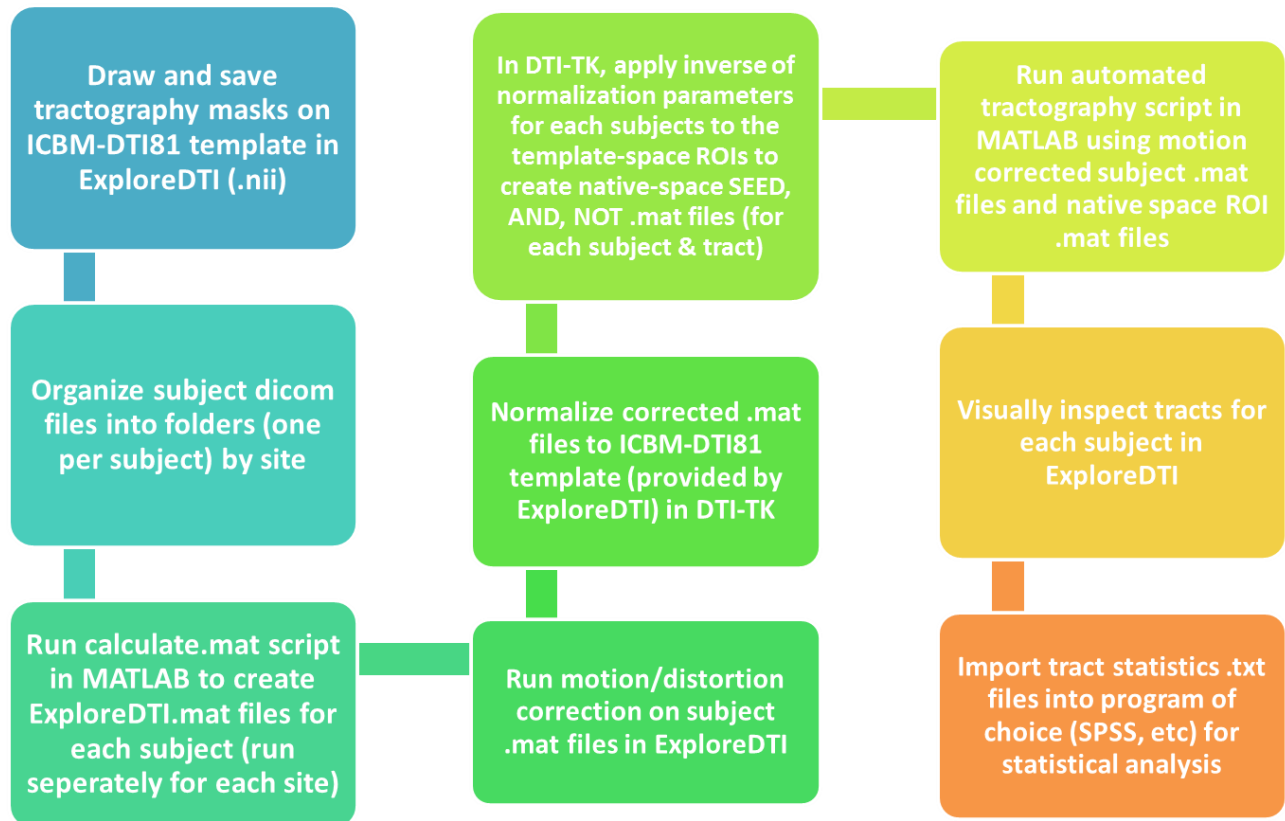
Appendix D: Studies of Cortical Thickness in FASD

1 st Author Journal Year	N	Age Range (years)	Pipeline	Controlled for Total Brain Vol	Frontal (Lobe or Regions)	Parietal (Lobe or Regions)	Temporal (Lobe or Regions)	Occipital (Lobe or Regions)
Sowell Cereb Cortex 2008	21 FASD 21 Ctrls	8-22	Custom made pipeline	No	↑	↑	↑	↑
Yang Cereb Cortex 2011	69 FASD 58 Ctrls	8-16	Freesurfer	Yes	↑	↑	↑	↑
Zhou Neuroimage 2011	33 FASD 33 Ctrls	6-30	CIVET	Yes	↓	↓	↓	↓
Fernandez-Jean Pediatric Neurology 2011	20 FASD* 20 Ctrls	7-16	Brain Voyager	No	↑	X	↑	X
Wozniak ACER 2013	32 FASD 33 Ctrls	10-17	Freesurfer	No	X	X	X	X
Rajaprakash Brain & Behaviour 2014	36 FASD 52 Ctrls	8-15	CIVET	No	X	X	X	X
Guatam Dev. Cog. Neurosci 2015	27 Prenatal drug exposure* 15 Ctrls	14-16	FreeSurfer	No	↓ (negative correlation with alcohol exposure)	↓ (negative correlation with alcohol exposure)	↓ (negative correlation with alcohol exposure)	X

*FASD diagnosed according to family history and physical phenotype. This paper also included a 3rd group diagnosed with ADHD (but not FASD), omitted here.

** Primary focus of this paper was on prenatal cocaine exposure, but interactions between cocaine, alcohol and tobacco were found for cortical thickness, whereby greater PAE was associated with lower cortical thickness, though all were prenatally exposed to cocaine. Also note that children with exposure to more than 1.5 ounces of alcohol per day were excluded.

Appendix E: Automated DTI Tractography Pipeline



Appendix F: Cognitive Testing 'Bloopers'

One of the best parts of getting to do some of the cognitive testing for this thesis was not only getting to know the kids in my study, but also hearing the hilarious ways they attempted to answer some of the tougher questions. For the most part, cognitive testing was a neat and educational process for me, but it was also filled with lots of cute misunderstandings and creative answers from kids in both groups. Here are a few of my favourites:

Mathematics (WJ Quantitative Concepts)

What is this formula used for (πr^2)

“Shampoo”

What are the four basic arithmetic operations?

“Plus, Minus, Times... Shapes, and I don't remember the last one”

Verbal Analogies (WRIT)

Irrigation is to water, as ventilation is to: _____

“Hot tub.”

Vocabulary (WRIT and CREVT):

Janitor:

“It's someone who is like a king, but doesn't sit in a chair like a king”

Reputation:

“Something that goes over and over again”

Apprentice:

“Someone who helps a wizard.”

“takes over someone's job and it's what they were taught for a long time. For example a princess would be a Queen's apprentice”

Testify:

“I think I’m testifying right now”

Cider:

“Something at a restaurant when there’s your actual meal like if you have meat, meat could be your cider and then you could have a salad”

“A person that isn’t in your tribe.”

Gasoline:

“I don’t know, but I do know what Vasoline is.”

Kettle:

“Like a hurd of sheep and farmers. Can also be corn, like kettle corn, and that’s it.”

Dog:

“A dog is a big puppy that you can ride like a tiger.”

Narrative Memory (NEPSY-II)-- After being read this passage about the brain and then asked the following questions:

“Two types of tissue are found in the brain and are named for their color. These tissues are called gray matter and white matter. The gray matter, made up of neurons, becomes folded as it develops. These folds give the brain a wrinkled appearance. The folding maximizes the amount of gray matter that can grow within in our heads. The white matter lies below the gray matter. It is made up of fibres that connect different parts of the brain in addition to connecting the brain to other parts of the body.”

What happens to the grey matter when it grows?

“It rots”

Where is the white matter located?

“Right here.” (points to forehead)

What is white matter made up of?

“Plastic”